Removal of Adsorbing Estrogenic Micropollutants by Nanofiltration Membranes in Cross-Flow – Experiments and Model Development

Andrea Joana Correia Semião

A thesis submitted for the degree of Doctor of Philosophy

University of Edinburgh

School of Engineering

August 2011

For my Mum

For my Dad

For Colin

"It was the best of times, it was the worst of times, it was the age of wisdom, it was the age of foolishness, it was the epoch of belief, it was the epoch of incredulity, it was the season of Light, it was the season of Darkness, it was the spring of hope, it was the winter of despair, we had everything before us, we had nothing before us, we were all going direct to Heaven, we were all going direct the other way- in short, the period was so far like the present period, that some of its noisiest authorities insisted on its being received, for good or for evil, in the superlative degree of comparison only."

Charles Dickens – A Tale of Two Cities

Declaration

I declare that the thesis has been composed by myself and the work contained in it is my own, except where stated otherwise. Further, this work has not been submitted for any other degree or professional qualification except as specified.

Andrea Joana Correia Semião
August 2011

Thesis Supervisors

Professor Andrea Schäfer, University of Edinburgh, School of Engineering, Edinburgh, United Kingdom

Dr. Donald Glass, University of Edinburgh, School of Engineering, Edinburgh, United Kingdom

Thesis Examiners

Dr. Pierre Aimar, Université de Toulouse, Toulouse, France

Dr. Martin Crapper, University of Edinburgh, School of Engineering, Edinburgh, United Kingdom

ABSTRACT

Nanofiltration (NF) can be used in water and wastewater treatment as well as water recycling applications, removing micropollutants such as hormones. Due to their potential health risk it is vital to understand their removal mechanisms by NF membranes aiming at improving and developing more effective and efficient treatment processes.

Although NF should be effective and efficient in removing small molecular sized compounds such as hormones, the occurrence of adsorption onto polymeric membranes results in performances difficult to predict and with reduced effectiveness and efficiency. This study aims firstly at defining, understanding and quantifying the relevant filtration operation parameters and, secondly, in identifying the physical mechanisms of momentum and mass transfer controlling the adsorption and transport of hormones onto polymeric NF membranes in cross-flow mode. The hormones estrone (E1) and 17-β-estradiol (E2) were chosen as they have very high endocrine disrupting potency. The NF membranes used and tested were the NF 270, NF 90, BW30, TFC-SR2 and TFC-SR3 since they have a wide span of pore sizes.

The first step is to experimentally acquire the knowledge of how fluid flow hydrodynamics and mass transfer close to the membrane affect hormone adsorption. The focus will be particularly on the effect of operating pressure, circulating Reynolds numbers (based on channel height, Re_h) and hormone feed concentration. These hydrodynamic parameters play an important role in concentration polarisation development at the membrane surface.

A Re_h increase from 400 to 1400 for the NF 270 membrane caused the total mass adsorbed of E1 and E2 to decrease from 1.5 to 1.3 $ng.cm^{-2}$ and 0.7 to 0.5 $ng.cm^{-2}$, respectively. In contrast, a pressure increase from 5 to 15 bar yielded an increase in the adsorbed mass of E1 and E2 from 1.0 to 1.8 $ng.cm^{-2}$ and 0.5 to 0.7 $ng.cm^{-2}$, respectively. Moreover, increasing hormone feed concentration caused an increase in the mass adsorbed for both hormones. These observations led to the conclusion that adsorption is governed by the initial concentration at the membrane surface which, in turn, depends on the hormone feed concentration, operating Re_h and pressure. Membrane retention, however, depends on the initial polarisation

modulus, defined as the ratio between the initial concentration at the membrane surface and the initial feed concentration.

The same trends were obtained for the TFC-SR2 membrane. However, this membrane has a much lower permeability compared to the NF 270 one (7.2 vs 17 $L.h^{-1}.m^{-2}.bar^{-1}$, respectively) and concentration polarisation is less severe. The experimental variations in mass adsorbed and retention as a function of the operating filtration parameters (Re_h and pressure) were therefore lower.

Based on these experimental results, a sorption model was developed. This model predicts well both feed and permeate transient concentrations for both hormones and membranes (NF 270 and TFC-SR2) in the common range of operating pressures and Re_h of spiral-wound membrane modules. The model was further applied for E2 in the presence of background electrolyte, yielding good predictions. These findings are an important advancement in determining which membrane would be more suitable to effectively remove hormones with a substantial reduction of experimental work.

The above-mentioned developed model does not give insight into the phenomena occurring inside the membrane since it focuses on the feed conditions. However, membrane characteristics, such as material and pore radius were found to have an impact in adsorption and retention of hormones. It was found experimentally that polyamide, from which the active layer of the NF membranes is made, adsorbs three times more mass of hormone than any other polymers constituting the membranes. Since this active layer is the membrane selective barrier of the membrane that is in contact with the largest hormone concentration (due to concentration polarization in the feed solution) it is concluded that the active layer adsorbs most of the hormones. Further experimental work carried out in this thesis showed that increasing the pore radius from 0.32 nm to 0.52 nm increased the E2 mass adsorbed from 0.17 $ng.cm^{-2}$ to 1.1 $ng.cm^{-2}$ and decreased the retention from 88% to 34%. These results show that the wider the pore, the larger the quantity of hormone that penetrates (*i.e.* partitions) inside the membrane and, therefore, the more the membrane adsorbs the hormone. For membranes of similar pore radius, the membrane with larger internal surface area was found to adsorb more.

All the previous results led to the establishment of a new model for the hormone transport inside the membrane pore taking convection, diffusion and adsorption into account. Since the differential equation describing the transport with adsorption inside the pore has no analytical solution, a numerical model based on the finite-difference approach was applied. With such a model, its validation against experiments and parametric studies it was possible to understand the transport mechanisms of adsorbing hormones through NF membranes. The results show that for low pressures the hormone transport is diffusion dominated. In contrast, for higher pressures (above 11 bar) the transport is convection dominated, showing that a purely diffusion transport model does not describe well the actual transport phenomena of hormones in NF membranes.

Furthermore, it was found that two similar molecules can behave very differently in terms of adsorption on the membrane. E1, which adsorbs 20% more than E2 in static mode, being slightly smaller than E2, partitions more inside the membrane pore and adsorbs double under filtration conditions.

This study contributes to illuminating the adsorption mechanisms of hormones onto NF membranes by understanding what parameters control adsorption such as hydrodynamics, materials, structure, etc. This not only identifies a potential problem in large scale applications, but it also provides an understanding of the mechanisms involved in the removal of these hormones and a tool that can be used to design future membranes for the improvement of micropollutant removal.

ACKNOWLEDGEMENTS

I would like to thank Professor Andrea Schäfer for giving me the opportunity to do a PhD and the conditions to have the financial support for it. Her support, constructive criticism, ability to make me think and perseverance were essential to the success of this work. The difficult moments also turned out to be helpful and a valuable contribution to my personal and scientific maturity.

I would like to express my deepest gratitude to Dr. Don Glass, my second supervisor, for his unconditional support, kind words and constructive feedback.

I would also like to express my deepest gratitude to Dr. Don Glass, Katherine Moore, Bridgeen McCloskey, Steven Gourlay and Bobby Hogg for their help in my most difficult times, particularly when acquiring new pumps and backpressure regulators, without which I would not have been able to do the work in this thesis. Thank you.

Professor David Ingram and Professor Jose Torero are acknowledged for their support, help and advice.

The University of Edinburgh, School of Engineering, is also acknowledged for providing all the necessary conditions to carry out this work. I had a brilliant time there during my PhD.

Dr. Alan Simm, Dr. Peter Anderson, Derek Jardine and Douglas Carmichael are acknowledged for their help in the lab; Jef Karn (Hydracell) for the diaphragm pump modifications; Annalisa De Munari, Dr. Alexander Bismarck and Dr. Kingsley Ho (Imperial College, UK) for the zeta potential and contact angle measurements (Chapter 3); Ime Akanyeti for arranging AFM measurements with Dr. Nhan T. Pham (Center for Systems Biology, University of Edinburgh) and for the TEM pictures with Dr. Chris Jeffree (University of Edinburgh, UK) (Chapter 3); Professor Howard Colquhoun (University of Reading), Dr. Arno Kraft (Heriot-Watt University) and Dr. Nuno Maulide (Max-Planck-Institut für Kohlenforschung, Germany) have

contributed with useful discussions on polymer – micropollutant interactions and supramolecular chemistry; Professor Bart van der Bruggen (KU Leuven) and Rudolf Graf (Berghof) have supplied membrane polymers; Nigel Staples from Retsch assisted with the loan of the Ultra Centrifugal Mill; Annalisa De Munari, Helfrid Rossiter and Laura Richards for some of the membrane pore characterisation (Chapter 6); Ime Akanyeti for sharing the work of grinding the polymers and some hormone-polymer sorption results (Chapter 6). That certainly was good fun, especially because the polymers you were interested in were so painful to grind and mine only took 5 seconds…!; Florian Chaumeil for his help in the RTD code writing; Matthieu Foucher for his help in the code writing of the transport in a NF pore model (Chapter 7); Dow Filmtec and Koch membranes for providing the membranes; Gary Cuthbertson (Fujifilm, Scotland) for lending me a pump; Henry Seah, Hilda Lie and John Poon for providing so diligently NEWater plant pictures (Chapter 2); Helfrid Rossiter for sharing the work of uranium removal by submerged UF membranes (we truly are lab twins!) and David Stewart and Joan Birse (University of Edinburgh, UK) for the support.

A very special thank to Prof. Stefano Polizzi and Dr. Davide Cristofori (Department of Molecular and Nanosystem Science, University of Ca' Foscari Venezia, Italy) for providing the TEM pictures of the NF 90 and the NF 270 membranes.

Numerous people have provided helpful advice and discussions during my PhD, including: Dr. Chris McDermott and Dr. Prashant Valluri (University of Edinburgh, UK), Dr. Ben Corry (University of Western Australia, Australia), Professor Elimelech and his group (Yale University, USA) who have received me so warmly in New Haven, Professor Melin (Aachen Unversity, Germany), Dr. Freger and Dr. Bernstein (Ben Gurion University of the Negev, Israel) and Professor Crespo (Universidade Nova de Lisboa, Portugal) for their useful discussions in GRC 2010 conference. Finally I would like to thank Professor Maria Norberta de Pinho (Instituto Superior Tecnico, Lisboa) for all her support and advice before, during and after my PhD.

A special thank to everybody in the Edinburgh University Membrane group for the camaraderie, daily support and for sharing unforgettable moments.

Thank you to Peta Neale, Laura Banasiak and Helfrid Rossiter. We were the Fantastic Four! I will never forget the moments we spent setting up a whole lab from scratch, the daily stories we had from our housemates in our first year, our trip to France with a flat tire in the first day and a car crash in the last day and many other leisurely events!

Peta thanks for receiving me so well in the first days in Edinburgh and for the lunch and jam donut on my birthday. I had just arrived in Edinburgh and was quite home sick!

Laura thanks for moving in with me in the second year. You gave me peace of mind and quiet nights, which I was not getting in Newington! It was so nice to get home everyday, cook dinner and eat it together. Our dinner discussions also helped me keep a semblance of sanity, believe me!

Helfrid, thank you for being my lab, office and art painting Siamese twin. We started and finished at the same time in what was a long and treacherous journey at times, but the support you gave me helped me go through it. Your sweet and calm Swedish character always helped balancing my typical Portuguese Latin one!

Annalisa De Munari, Ime Akanyeti and Helen Cope: thank you for all the laughs, whisky drinking and tears we shared together. Your friendship was essential in helping me through my PhD. Thank you girls!

Laura Richards, Payam Malek and Than Hieu: thanks for sharing so many laughs with me.

Molly Patrick, a million thanks for letting me stay with you in Boston when I went for a conference. It was such a warm welcome when I was by myself and did not know anyone!

My love and thirst for knowledge started forming very early on in my life thanks to my parents, Viriato and Margarida, who have constantly encouraged me and taught me how to become an independent thinker. Thank you for believing so much in me and for encouraging me to fly as high as possible, even if that takes me away from you. Without your constant support, advice, guidance, sacrifice and especially love I

would not stand where I am now. You have made me what I am today and I hope I have made you proud. You are the best parents anyone could have.

Colin McGill, your love, constant support and belief in me made me happier than I ever thought I could be, especially during the toughest phases of my PhD. You brought me peace, laughter, joy and love, and you taught me that life is so precious that every moment needs to be enjoyed. Thank you for making me complete.

LIST OF PUBLICATIONS

1. Semião, A.J.C.; Rossiter, H.M.A.; Schäfer, A.I. (2010) **Impact of organic matter and pH on the removal of uranium by submerged ultrafiltration**, Journal of Membrane Science, 348, 1-2, 174–180

2. Semião, A.J.C.; Schäfer, A.I. (2010) **Xenobiotics removal by membrane technology: An overview**, Xenobiotics in the Urban Water Cycle: Mass Flows, Environmental Processes and Mitigation Strategies, Bester, K.; Kümmerer, K.; Fatta-Kassinos, D. (Eds) (Springer Environmental Book Series, Environmental Pollution, Vol. 16), Springer

3. Schäfer, A.I., Akanyeti, I. Semião, A.J.C. (2010) **Micropollutant sorption to membrane polymers: a review of mechanisms for estrogens**, Advances in Colloid and Interface Science – Colloid Science and Membrane Separation, 164, 1-2, 100-117

4. Semião, A.J.C., Schäfer, A.I. (2011) **Estrogenic micropollutant adsorption dynamics onto nanofiltration membranes**, Journal of Membrane Science – *accepted* - doi:10.1016/j.memsci.2011.07.031

IN PREPARATION

5. **Estrogenic micropollutant removal by nanofiltration membranes. Part A - experimental evidence** (2011) Journal of Membrane Science – *in preparation*

6. **Estrogenic micropollutant removal by nanofiltration membranes. Part B - modelling** (2011) Journal of Membrane Science – *in preparation*

TABLE OF CONTENTS

1 Introduction

The presence of organic trace contaminants in potable water sources has been the focus of much attention in the last two decades as it became an environmental concern [1, 2]. High loads of these contaminants are present in waste water treatment influents with concentrations up to the level of $\mu g.L^{-1}$ [3-5]. These organic trace contaminants may originate from different sources like human and animal medicine consumption (*e.g.* antibiotics) [6-9], human daily consumption (surfactants in detergents, personal care products and plasticizers) [10-12], agriculture (pesticides) [13-15] and human and animal excretion (hormones) [16].

These contaminants are not totally removed by the established wastewater treatment processes (WWTP), and concentrations in their effluents up to the level of $\mu g.L^{-1}$ have been measured on a global scale [17, 18]. WWTP rely on the degradation and adsorption of these compounds by the sludge, which depends on the temperature and sludge retention time, amongst other parameters. If the necessary requirements to degrade these contaminants are not met in the process their removal is incomplete. WWTP effluents are then discharged into surface waters, where a clear relation between the trace contaminant effluent and stream concentrations has been established [2].

Such discharges into surface waters pose a health risk to the flora and fauna that depend on them leading to reported reproductive abnormalities [19, 20]. These trace contaminants, which have possible negative impact on human health [21, 22], further threaten to contaminate potable water sources.

Membrane technology was originally developed for desalination (reverse osmosis, RO) and water softening (nanofiltration, NF). Due to the high water quality obtained, this technology quickly found a widespread application in water treatment, where microfiltration (MF) and ultrafiltration (UF) are used as pre-treatment processes, performing both as filters for particulate matter and virus and bacteria (disinfection), and NF and RO are used to remove dissolved salts, organic matter and

small organic contaminants. This technology has several advantages over the conventional water treatment processes: its low chemical consumption, small area foot-print and superior water quality produced. Furthermore, since it is based on a physical removal mechanism of size exclusion it is simpler than biological treatment used in WWTP.

However, trace contaminants retention by NF and RO membranes is not well understood [23]. Retention results from bench-scale studies vary significantly for organic contaminants of similar molecular weight, with retention values ranging from less than 10% to 100% [24-31]. Some trace contaminants, including hormones, pesticides and pharmaceuticals, adsorb onto NF and RO membranes [23, 24, 26, 28, 29, 32-36]. Such adsorption onto the membrane is strongly dependent on the membrane used [29, 37] and on the trace contaminant properties such as size, hydrophobicity, acid dissociation constant (pK_a), aptitude for hydrogen bonding and other possible interaction mechanisms [29, 38-40]. The adsorption phenomenon results in a feed concentration decrease and permeate concentration increase with time, until the membrane is saturated and steady state is reached [23]. This translates into a decrease in the contaminant retention with time until steady-state is reached, where a lower retention is obtained compared to the theoretical retention based on size exclusion only [23]. In fact, due to the occurrence of adsorption, opposite results have been obtained [32, 41].

Due to the clear gap in the understanding of which parameters affect adsorption and retention of trace contaminants by NF membranes, the main objective of this work is to identify and quantify the fundamental mechanisms involved in the removal of adsorbing estrone (E1) and 17-β estradiol (E2) by NF membranes. These are two of the most potent endocrine disrupting contaminants [42]. Understanding the fundamental mechanisms involved in the removal of trace contaminants by NF membranes can lead to the development of new membrane designs capable of avoiding the occurrence of adsorption and further improve the performance of these processes in order to obtain higher water quality compliant with the increasingly strict water quality regulations.

In order to identify and quantify the fundamental mechanisms involved in the removal of adsorbing hormones by NF membranes, the main objective of this thesis was divided into three objectives:

- Understand how hydrodynamics affect adsorption and retention of hormones by NF membranes. Several radiolabelled hormones (E1 and E2) and membranes (NF 270 and TFC-SR2) were used in a cross-flow system with a slit channel. The hydrodynamic effect on the adsorption and retention of hormones was studied by varying pressure, Reynolds numbers (based on channel height Re_h) and hormone feed concentration.

- Understand how membrane and solute characteristics affect adsorption and retention of hormones by NF membranes. The effect of membrane pore radius and internal surface area was tested in the cross-flow system for the above mentioned hormones, whilst the preferential adsorption of hormones onto different polymeric materials was carried out in a shaker for ground polymers and in a diffusion cell for the case of the NF 270 membrane.

- Develop a new transport model for the removal of adsorbing trace contaminants by NF membranes. The hydrodynamic model [43] was modified by taking hormone adsorption into account. This model was numerically solved in Matlab by using a tridiagonal matrix algorithm allowing the determination of which transport mechanisms contribute to the removal of hormones by NF membranes.

Following these objectives, the structure of the dissertation is shown in Figure 1.1. The body of the dissertation consists of 7 chapters. A comprehensive up-to-date literature review on the removal of trace contaminants by membrane separation processes is presented in Chapter 2. This allows the identification of the gaps in the knowledge of this subject. Chapter 3 is divided into two main sections. The first main section encompasses a detailed description of the physical changes carried out for 1.5 years in a cross-flow apparatus unsuitable for a bench-scale study of hormone filtration with NF and RO membranes. Besides the already serious problem of oil leakage from the pump, the flow rates delivered by the pump were abnormally high (Reynolds numbers based on hydraulic diameter above 10,000).

This created much too large shear stresses at the membrane surface causing the active layer to be ripped off from the support layer during operation. The unsuitability of the application of this apparatus is illustrated by comparing a few hormone filtration experiments with this system and the final modified cross-flow apparatus used for the chapters that will follow. The second part of Chapter 3 includes a detailed description of the several membranes, filtration systems, analytical equipment and chemicals used to perform experiments aimed towards the improvement of knowledge in the mechanisms governing the removal of hormones by NF membranes.

The following chapters are organised as to show what parameters affect the adsorption and retention of hormones by NF membranes at different levels. In Chapter 4, the effect of operational filtration parameters such as pressure, Re_h numbers and feed concentration on hormone adsorption and retention in NF membranes is carried out. This allowed the determination of the role that hydrodynamics on the membrane surface have in the removal of adsorbing hormones by NF membranes. The understanding in Chapter 4 of the mechanisms involved in the removal of hormones by NF membranes, as far as hydrodynamics and mass transfer are concerned, allowed the development of a new sorption model in Chapter 5. This model predicts the feed and permeate transient concentrations for several hormones and membranes when subjected to different experimental conditions. Since in Chapter 4 and 5 the membranes had been treated as a black box, in Chapter 6 the effect of several membrane characteristics such as material and pore radius on the hormone adsorption and retention were studied to relate this adsorption phenomenon to the physical characteristics of the membranes. The affinity of the hormones to different polymers was tested in order to determine where these adsorb the most in thin film composite (TFC) NF membranes. The effect of the membrane pore radius and internal surface area were further studied. Finally, the results of these three chapters were applied in Chapter 7 to the development of a new pore transport model for hormones by NF membranes, taking adsorption into account. This allowed clarification of what transport mechanisms dominate the removal of adsorbing contaminants in NF membranes, since much debate exists as to whether convection

plays a role in it. In Chapter 8 the conclusions of this study and future work suggestions are then delineated.

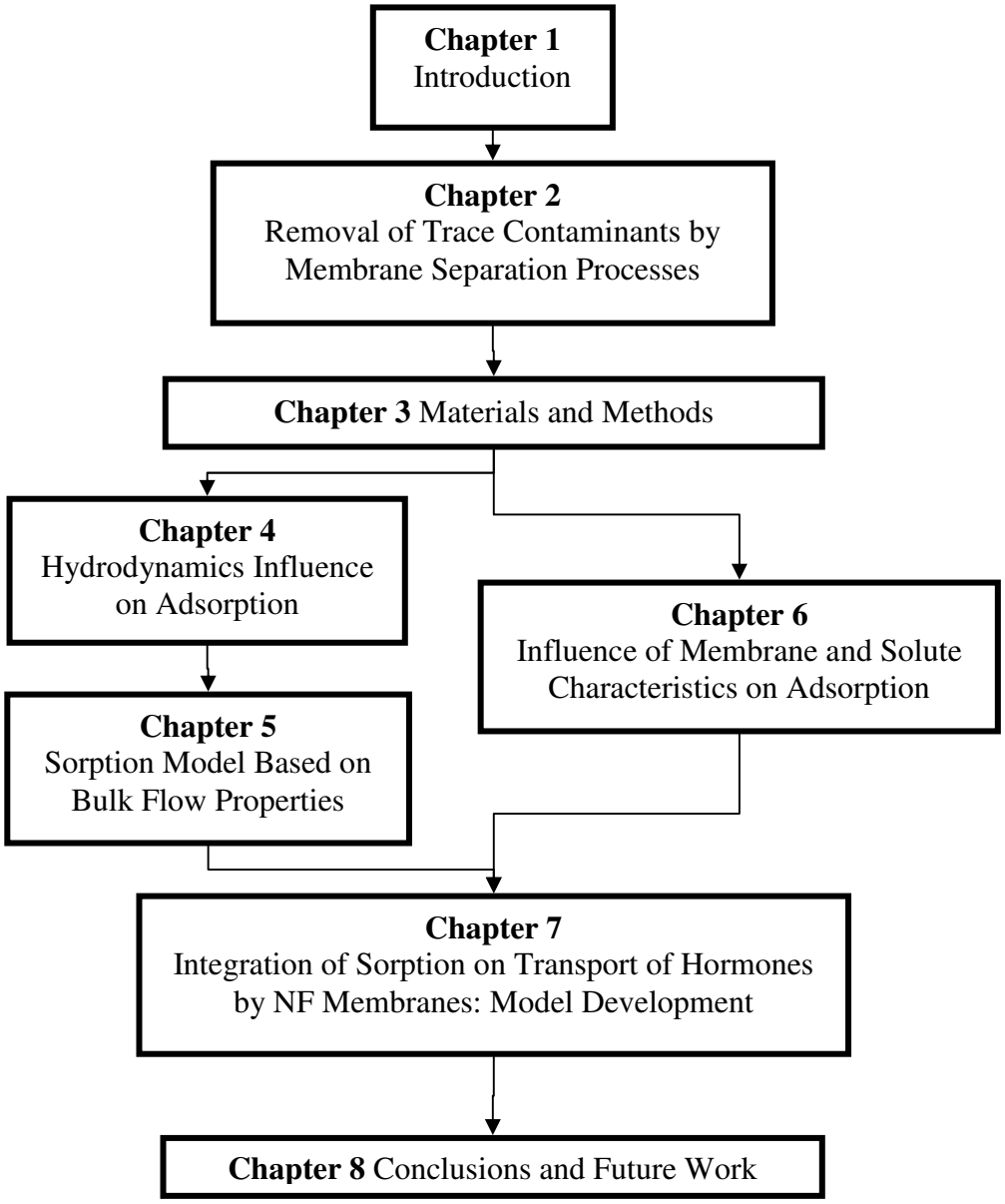

Figure 1.1 Removal of adsorbing estrogenic micropollutants by nanofiltration membranes in cross-flow – experiments and model development

2 Removal of Trace Contaminants by Membrane Filtration Processes

2.1. Introduction

Trace contaminants have been the focus of much attention in the last couple of decades. They are considered to be compounds of concern due to the negative impact they have on the environment and possibly to public health due to their physicochemical and toxicological properties.

They include many different families of compounds that can either occur naturally or be of anthropogenic source. These include steroids, pharmaceuticals (*e.g.* antibiotics, pain relief medication, anti-anxiety and stimulant drugs), pesticides and herbicides, fire retardants, polycyclic aromatic hydrocarbons (by-products of fuel burning), fragrances and many others. Some of these compounds are further classified as endocrine disruptors since they interfere with the natural cycle of the hormones found in the body, which are in turn responsible for reproduction, development and other functions.

Despite usually occurring at trace concentrations in the aquatic environment, they pose an environmental and health risk to the species that depend on these waters and should therefore be removed.

This chapter describes the current state of art in the occurrence of trace contaminants in the environment, the reported negative health effects they pose and provides an extensive literature review on the removal of these by NF and RO membranes when found in aqueous solutions.

2.2. Trace Contaminant Occurrence and Health Effects

2.2.1 Removal of Trace Contaminants in Wastewater Treatment Plants

Trace contaminants are not completely removed in conventional water treatment plants WTP (*i.e.* wastewater treatment plants) and concentrations up to the $\mu g.L^{-1}$ level have been measured in their influents [3-5] and effluents all over the world [1, 2, 44-48].

Pharmaceuticals, which have a high human consumption, are found at higher concentrations in these effluents compared to other trace contaminants showing an incomplete degradation [4, 17, 45]. Some are more persistent than others, such as carbamazepine, sulfamethoxazole, ibuprofen and paracetamol [3, 17, 18, 49-51]. Concentrations of paracetamol as high as 11.3 $\mu g.L^{-1}$ were measured in the Hérault area, France [18]. Heberer [4] showed a carbamazepine removal of 8% in a Berlin treatment plant with effluent concentrations of 1.63 $\mu g.L^{-1}$.

However, pharmaceuticals are not the only trace contaminants found in these effluents. Pesticides [52], estrogens [53-57], surfactants and fragrances [49] are also measured in these effluents. In fact, in the treatment process, effluent concentrations can be higher than influent concentrations, such as the case of estrone [50], where the process degrades the molecules into more persistent and toxic ones [58, 59]. In general estrone is the estrogen with lowest removal rates in WTP [47, 55].

These effluents are discharged into surface water and groundwaters, contaminating possible potable water sources.

2.2.2 Natural Water Contamination

Water treatment effluents are discharged into surface and groundwaters where concentrations up to the $\mu g.L^{-1}$ level have been measured for pharmaceuticals, anti-depressants and hormones [17, 60]. Rabiet *et al.* [18] showed that drinking water wells in the vicinity of WTPs had concentrations of pharmaceuticals up to 300 $ng.L^{-1}$ compared to other wells with less than 50 $ng.L^{-1}$ upstream the plant. The same

phenomenon was found with surface waters downstream a WTP in the Berlin area [4].

In a UK survey on two rivers in the southeast of England an increase in estrone concentration was observed caused by a WTP discharge [2]. In fact, the estrone concentration profile in the river followed the same profile as the estrone concentration in the effluent. Despite hormones being usually measured at trace level concentrations in WTP effluents [61, 62] and natural waters [47, 63-66], in a Canadian river a concentration of 38 $ng.L^{-1}$ of estradiol [67] was measured. The most worrying levels of trace contaminants in natural waters come from the study in USA streams by Kolpin *et al.* [1] where concentrations as high as 831 $ng.L^{-1}$ for ethinylestradiol and 100 $ng.L^{-1}$ for estradiol, estrone, progesterone and testosterone have been measured.

WTP are not the only possible source of trace contaminants in natural waters. Contamination of soils and sediments with trace contaminants such as pesticides from agriculture [68-70] can lead to further contamination of groundwaters [71, 72]. Levels of pesticides higher than 500 $ng.L^{-1}$ have been measured in rivers [73, 74]. Animal waste from dairy, swine and poultry is another source of estrogens [75], where the main estrogens excreted through urine and faeces are estrone and estradiol [76, 77]. Concentrations of hormones up to 4500 $ng.L^{-1}$ have been measured in dairy and aquaculture effluents [78, 79].

In Figure 2.2 are represented countries in the world where organic trace contaminants have been reported in WTP effluents, natural waters and sediments. Due to the global widespread contamination of water sources, several studies on the impact of these micopollutants in living species have been carried out.

2.2.3 Trace Contaminants Health Effects

Trace contaminants can accumulate in living species [67]. There has been much debate on the health effect of these such as the disrupting effect on the endocrine system [80-83]. Several reviews [20-22] thoroughly describe studies that show a correlation between immunological deficiencies and exposure to endocrine disruptors. Wildlife animals such as birds [19], dolphins, molluscs, fish [83, 84],

alligators [85] and panthers showed immunity abnormalities when exposed to waters with these chemicals, such as pesticides and PCBs. Similar results were obtained with laboratory tests on mice and fish [86], and of humans overexposed to these chemicals by accident (pesticides in agriculture or contaminated food with PCBs) [21]. In a study on Japanese fish, it was shown that exposure to estrogens in the $ng.L^{-1}$ concentrations caused intersex and altered sex [42]. The growth of human embryonic cells was found to be inhibited when exposed to pharmaceuticals commonly present in WTP effluents in the $ng.L^{-1}$ concentrations [87].

Estrogens, such as estrone and 17-β estradiol are two of the most potent endocrine disrupting contaminants when compared to other trace contaminants such as pesticides and plasticizers (Table 2.1), representing a higher risk to any living species. Endocrine disrupting chemicals are substances that disrupt the physiological function of endogenous hormones by acting like hormones in the endocrine system. Potency is a measure of drug activity expressed in terms of the amount required to produce an effect of given intensity. Trace contaminants with a low relative estrogenic potency require much higher concentrations than 17-β estradiol to produce an equivalent biological response.

Table 2.1 Estrogenic potency relative to 17-β estradiol (E2) of some trace contaminants (estrogenic potency is expressed as the ratio of the activity of a test compound relative to that of E2)

Compound	**Relative Estrogenic Potency**
17-β estradiol	1
Bisphenol A	0.0001 [88]
Diethylstylbestrol	0.045-2.5 [88]
Nonylphenol	0.00000072- 0.00041 [89]
Ethinylestradiol	0.19-1.9 [89]
Estrone	0.019-0.3 [89, 90]
Estriol	0.037 [42]
Methoxychlor	0.0025 [90]

Due to their poor removal with established standard water treatment processes and their widespread occurrence in potable water sources, new

technologies have emerged as a possible answer to this problem. Membrane technology is one of these processes.

2.3. Membrane Processes

Membranes work as a physical barrier to the passage of contaminants, with pores or molecular channels incorporated into a polymeric material. The most common membrane processes for water treatment applications are pressure driven. Exerting pressure perpendicularly to the membrane yields a transmembrane pressure gradient through it (driving force) and allows the passage of water through, the permeate, and the retention of solutes and contaminants, the concentrate, from a feed solution that circulates tangentially to the membrane surface (Figure 2.1).

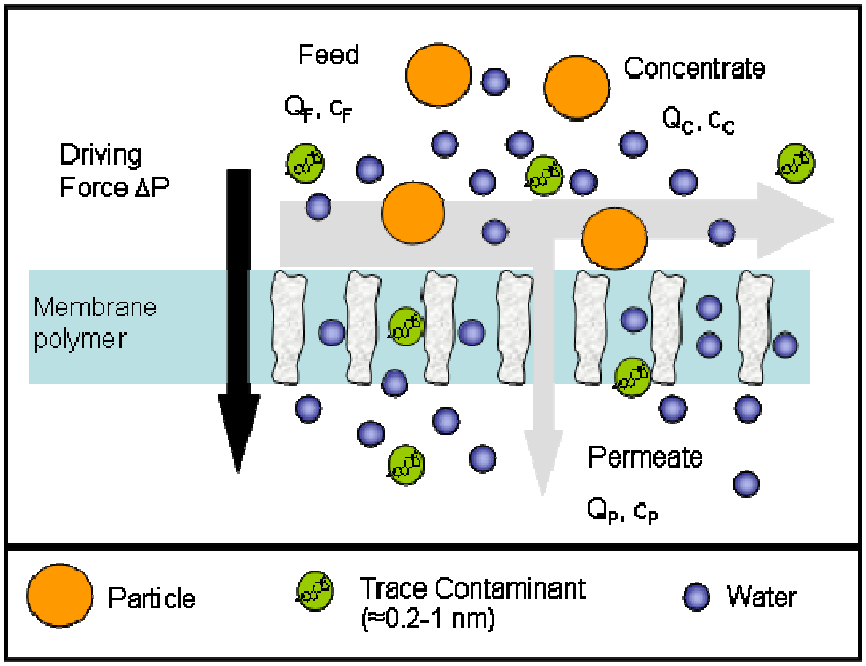

Figure 2.1 Pressure driven membrane process (microfiltration, ultrafiltration, nanofiltration and reverse osmosis)

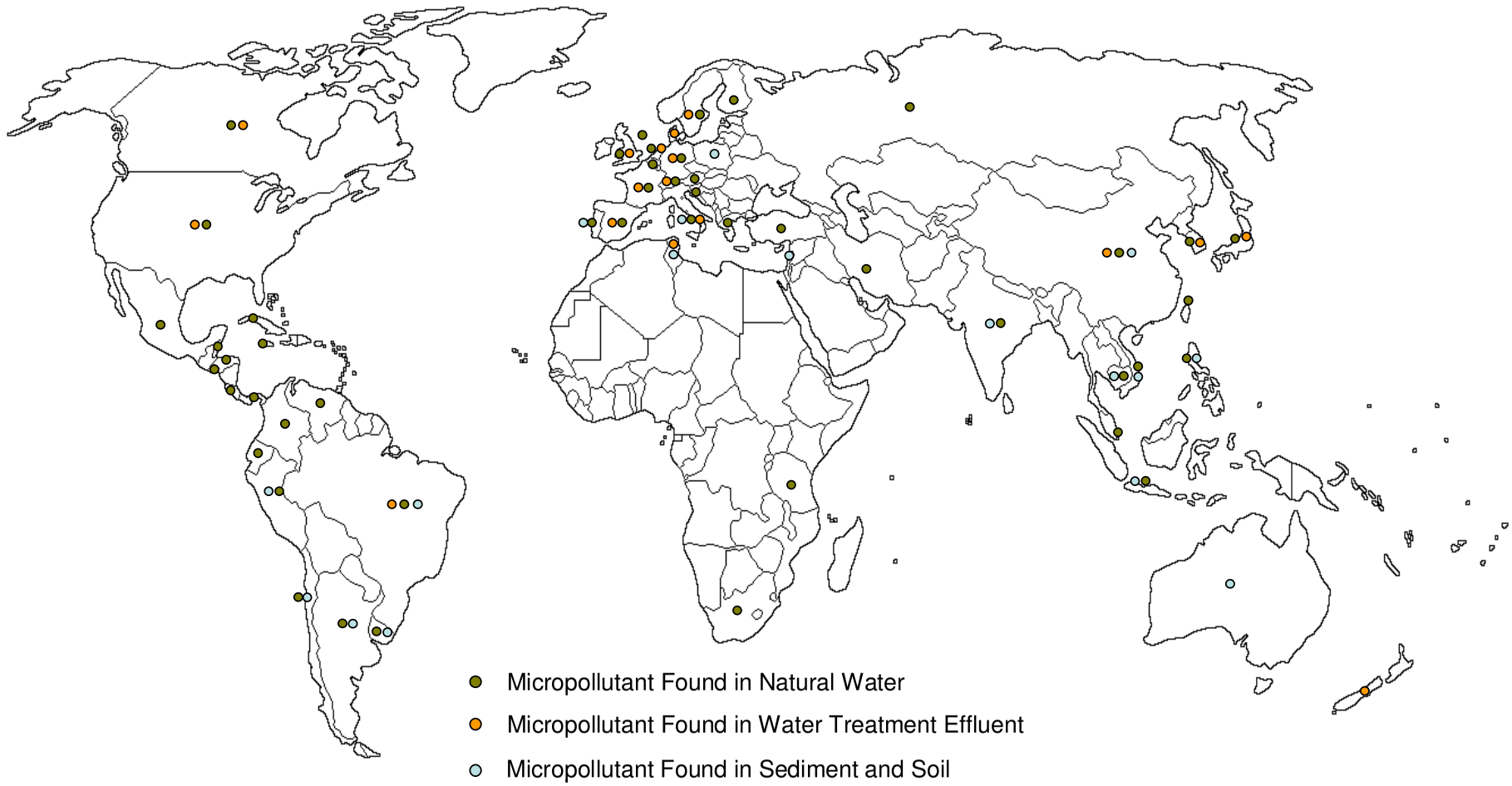

Figure 2.2 Organic contaminants measured all over the world both in natural water (surface water, groundwater, lakes, sea, etc.), WTP effluents, and soils [1, 4, 5, 44, 46, 57, 60, 61, 68, 70-72, 79, 91-126]

Membranes are either porous (ultrafiltration (UF), microfiltration (MF) and membrane bio-reactor (MBR)), or dense (reverse osmosis (RO)). Nanofiltration (NF) membranes are considered to be between porous and dense [127]. These differences dictate how the contaminant is transported through the membrane.

MF and UF membranes are characterised by the molecular weight cut-off (MWCO). The membrane MWCO corresponds to the solute molecular weight (MW) the membrane removes with 90% rejection [128]. NF can be either characterised by MWCO or ionic retention of salts such as NaCl or $CaCl_2$. RO membranes being dense are characterised by salt rejection, although some researchers have determined a corresponding MWCO [24].

Retention of a contaminant is defined as:

$$R\,(\%) = 100 \times (1 - \frac{c_P}{c_F}) \tag{2.1}$$

where c_P and c_F are the permeate and feed concentrations, respectively.

Other common performance parameters for membrane processes are:

$$Q_F = Q_C + Q_P \tag{2.2}$$

$$\text{Recovery} = \frac{Q_P}{Q_F} \tag{2.3}$$

$$J = \frac{1}{A}\frac{dV}{dt} = L_P(\Delta P - \Delta\pi) \tag{2.4}$$

where Q_F, Q_C and Q_P are feed, concentrate and permeate flow rates, recovery is the amount of clean water produced per feed water treated, A is the membrane area, V is the permeate volume, t is time, L_P is the membrane permeability, ΔP is the applied transmembrane pressure and $\Delta\pi$ is the osmotic pressure difference between feed and permeate.

Besides pressure-driven membrane processes, other membrane processes are available for water treatment depending on their separation principle, pore size (pore radius r_p) and driving-force. The different membrane processes found are electrical potential driven (electrodialysis ED), thermally driven (membrane distillation MD) and due to vapour pressure differences between feed and permeate (pervaporation PV). A comparison between different membrane separation processes and solutes they remove is presented in Figure 2.3. The MW range of the compounds and membrane pore sizes or particle sizes are also presented.

Membrane separation processes are in principle able to remove from contaminants as big as bacteria (*e.g.* MF, UF, MBR, NF and RO) to small contaminants such as trace contaminants and metal ions (*e.g.* NF, RO and ED).

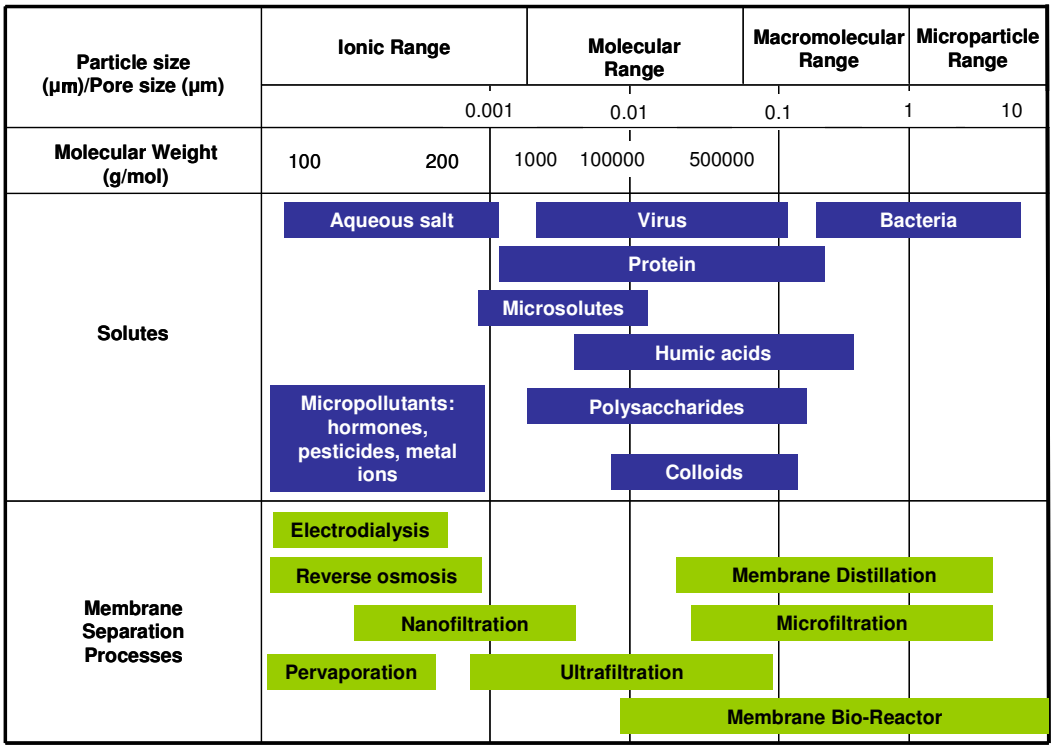

Figure 2.3 Overview of membrane processes available for water and wastewater treatment [128-132]

For the removal of neutral organic trace contaminants, NF and RO are the most widely applied and studied processes. However, a few studies on the

application of pervaporation and membrane distillation, for example, can be found [133-137].

2.4. Removal of Trace Contaminants by MF and UF: the Occurrence of Adsorption

Trace contaminants, generally of MW lower than 400 $g.mol^{-1}$, are not retained by MF and UF membranes due to their large pore sizes [39, 138, 139]. However, studies show the occurrence of adsorption by the membrane polymers [140] leading to apparent high retention.

Chang *et al.* [141] obtained 100% removal of estrone in a MF dead-end process due to adsorption on the membrane. A sieving effect was discarded since the membrane pores are much larger than the estrone molecule. This occurred due to low estrone feed concentration, where the amount of sites available on the membrane allowed for adsorption of almost all the contaminant. High adsorption of trace contaminants has also been reported in several UF studies [38, 39, 142]. These apparent high retentions are related to adsorption on the membrane surface. Once adsorption sites saturate, retention is low and these processes are not effective in removing contaminants sustainably.

Adsorption onto polymeric membranes can however be affected by solution characteristics such as pH. Lyko *et al.* [143] and Schäfer *et al.* [144] obtained UF retentions of BPA around 30% at pH 5 and none at alkaline pH. BPA is neutral at pH 5 adsorbing onto the membrane. Once BPA dissociates and becomes negatively charged at alkaline pH it does not adsorb onto the membrane due to charge repulsion and no retention is obtained.

2.5. Removal of Trace Contaminants by NF and RO Processes

The most commonly applied membrane processes in the removal of trace contaminants are NF and RO. As can be seen in Figure 2.3, NF and RO are effective in the removal of solutes as small as dissolved ions, where NF is effective in

removing divalent ions and RO is effective in removing both divalent and monovalent ions.

The three removal mechanisms (steric exclusion, charge repulsion and adsorption) playing a role in the removal of trace contaminants by NF and RO membranes are described next.

2.5.1 Steric Exclusion

The steric exclusion mechanism is directly related to the contaminant molecular size. Retention generally increases with increase of compound molecular weight [25, 27, 28, 145] and retentions are usually higher than 90% [60, 146-149] for compounds with MW higher than the MWCO of the membrane [25, 26, 150]. MW has been shown to be a good indicator of the retention trend obtained by NF and RO membranes compared to other molecular sizes, such as the Stokes diameter [150].

However, this trend is not always obeyed and deviations occur in NF and RO (Figure 2.4 A and B). For NF this happens especially when the contaminant size is of the same order as the membrane pores [24], where retention can vary from less than 10% and be as high as 100% (Figure 2.4 A).

In the particular case of hormones, which have similar molecular weights (from 268 to 314 $g.mol^{-1}$), retention by NF and RO membranes can vary from 10% to 100% (Figure 2.5). Removal of trace contaminants by NF and RO is not based solely on size, and other mechanisms contribute to their removal.

In fact, trace contaminant retention has been found to be affected by charge interactions between the contaminant and the membrane material, the occurrence of the adsorption phenomenon on the membrane and the presence of a third component in solution such as natural organic matter (NOM) or salts.

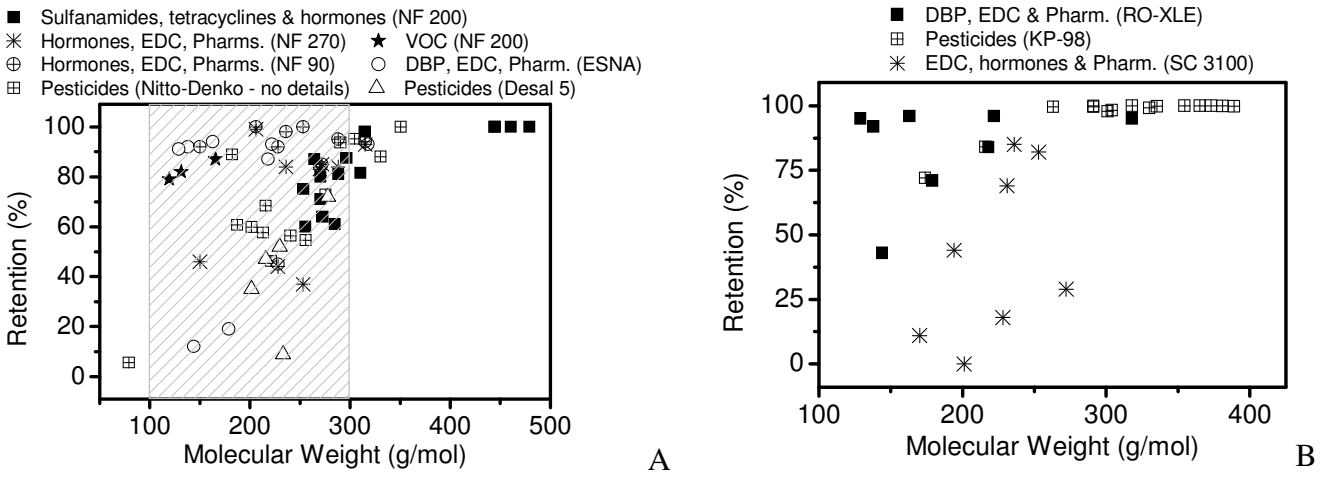

Figure 2.4 Organic trace contaminant retention by **(A)** NF and **(B)** RO membranes as a function of MW – the shaded area corresponds to the MWCO of the NF membranes [24-31] with EDC: Endocrine Disrupting Chemicals, Pharm: Pharmaceuticals, VOC: Volatile Organic Carbon, DBP: Disinfection By-Products and the membranes specified in ( ).

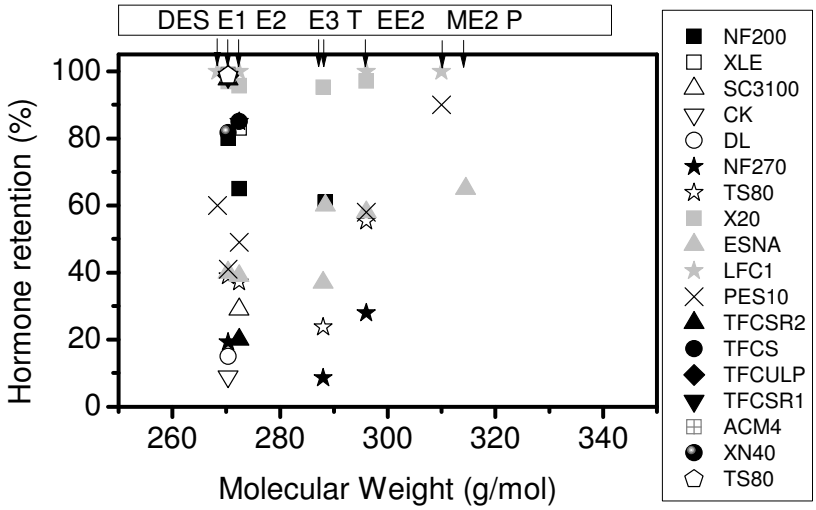

Figure 2.5 Steroid retention by different NF and RO membranes. The hormones represented are: estradiol E2 (272.4 $g.mol^{-1}$), estrone E1 (270.4 $g.mol^{-1}$), estriol E3 (288 $g.mol^{-1}$), ethinylestradiol EE2 (296 $g.mol^{-1}$), progesterone P (314.5 $g.mol^{-1}$), testosterone T (MW=288.4 $g.mol^{-1}$), mestranol ME2 (MW=310 $g.mol^{-1}$) and diethylstilbestrol DES (MW=268.4 $g.mol^{-1}$). The MWCO of the membranes varied between 100 and 560 [24, 26, 41, 138, 148, 151-156]

2.5.2 Charge Interaction

Commercial membranes' surface charge becomes more negative with an increase of pH [32, 41, 157-159]. Some trace contaminants dissociate at the pH corresponding to their pK_a (*e.g.* estrone at pH>10.3). When this occurs, charge repulsion between the membrane and the dissociated compound occurs enhancing the retention. As can be seen in Figure 2.6, sulphametoxazole (SMX), estrone (E1) and bisphenol-A (BPA) retention increase dramatically at a pH above their pK_a, *i.e.* once they dissociate. Carbamazepine (CBZ), however is neutral above pH 3 and has a constant retention over the pH range shown [28, 37, 40, 150, 152, 159-162]. This effect is especially pronounced with molecules smaller than the membrane pore size. For example, Berg *et al.* [25] obtained an increase in the pesticide mecoprop rejection from 10% to 90% when increasing the pH from 3 to 7. Nghiem *et al.* [160] showed an increase of BPA retention with pH from 40% to almost 100%, following the same trend as SMX [159] (Figure 2.6).

The increase of the solution pH is known to increase the membrane negative surface charge. An increased negative surface charge will further enhance the retention of the charged contaminant due to an increased charge repulsion [159, 163], as illustrated in Figure 2.6 for SMX. SMX retention gradually increases from 20% at pH4, to 80% at pH 7 and finally reaches 100% at pH 10. This trend is especially pronounced for charged inorganics [164].

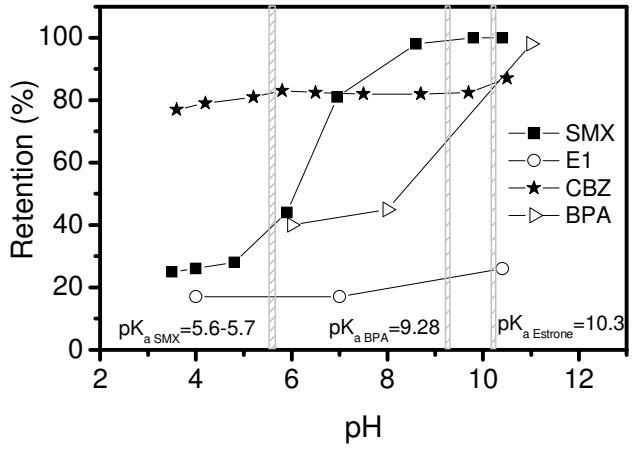

Figure 2.6 Sulphametoxazole (SMX), estrone (E1), bisphenol-A (BPA) and carbamazepine (CBZ) retention as a function of pH [33, 41, 159, 160]

Solution pH can also affect pore size due to repulsion of negatively charged groups on the membrane polymer or due to membrane structural changes, which in turn affect the rejection of trace contaminants [25, 165].

The increase of ionic strength in solution decreases membrane rejection of charged compounds due to charge shielding between the membrane and the contaminant [40, 164, 166, 167], with calcium ions shielding more effectively than sodium ions [40]. Zhang *et al.* [35] also showed a decrease in neutral BPA rejection with increase of ionic strength due to swelling of the membrane pores or due to a decrease in the BPA hydrodynamic radius.

Although most studies are focused on contaminants that become negatively charged and are repelled by the membrane, Heijman *et al.* [168] and Pronk *et al.* [34] showed that attraction between the negative membrane and positively charged contaminants translates into lower retentions. Radjenovic *et al.* [169], however obtained rejections higher than 90% for positively charged pharmaceuticals in a Spanish drinking water treatment plant.

Dipole moment plays a further role in the removal of trace contaminants. As argued by several authors, compounds with higher dipole moment are less retained compared to compounds with lower dipole moments [30, 39, 40, 150, 159, 170, 171]. Molecules with high dipole moment are directed towards the pore with the side of the dipole with opposite charge closer to the membrane pore, entering more easily into the membrane [30]. Kimura *et al.* [24] however found that a higher dipole moment enhances retention when a cellulose acetate membrane is used instead of a polyamide membrane [150]. Retention of polar and non-polar compounds is therefore affected by the membrane material used.

It was previously indicated that negatively charged compounds will suffer charge repulsion from the membrane and be better retained. However, it was shown in several studies [154, 156, 172], that despite E1 and E2 being dissociated and therefore negatively charged at high pH, retention decreased dramatically from higher than 90% to 50% (Figure 2.7 A for the TFC-SR2, TFC-S and X20 membranes). These results seem to contradict what Hu *et al.* [41] obtained, where estrone retention increased from 15% to 25% with increase of pH (Figure 2.7 A, DL

membrane). This discrepancy is explained because in the first case the membranes were not saturated with the hormones. At pH<pK_a, the neutral hormones adsorb on the membrane and give an apparent high rejection (Figure 2.7 B). At higher pH when the molecules dissociate, charge repulsion occurs, decreasing adsorption and, consequently, giving a lower retention (Figure 2.7 B). In the latter case however, when the membrane was saturated with estrone the real retention was measured and shown to increase with pH. Another possible explanation for this discrepancy lies in the different membranes used. Although both polyamide they can have different properties, which are not made public by the manufacturer.

The occurrence of adsorption might lead to the erroneous conclusion that the membrane effectively removes a contaminant by giving an apparent high retention while adsorption occurs. These results show the importance that adsorption can play in the removal mechanisms of trace contaminants by NF and RO membranes.

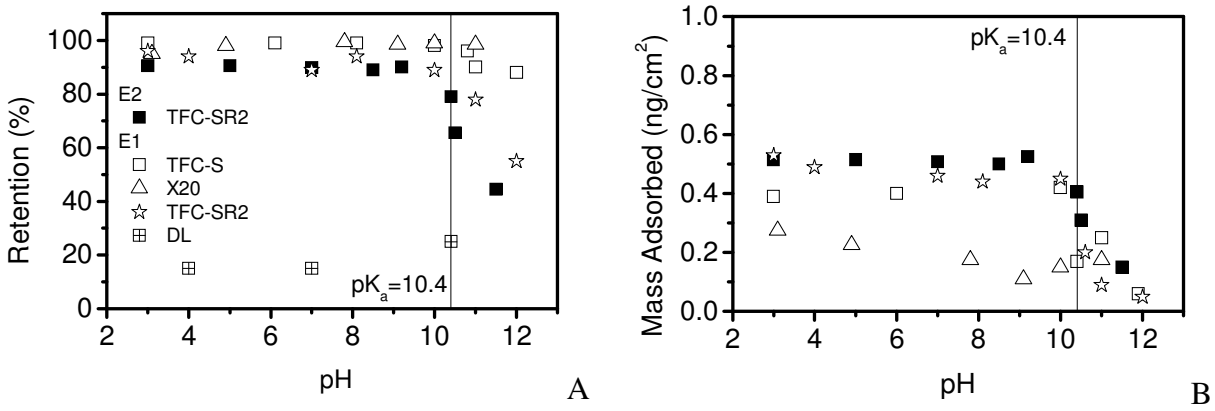

Figure 2.7 Estrone (E1) and estradiol (E2) **(A)** retention and **(B)** sorption for several NF membranes as a function of pH. Membranes were not saturated prior to experiments [41, 154, 156, 172]

2.5.3 Adsorption

Many polymeric membranes have been found to adsorb trace contaminants. Adsorptions of pesticides, steroid hormones, volatile organic carbon (VOCs) and pharmaceuticals of up to 100% are obtained [24, 26-30, 32-36, 142, 155, 160, 173].

Adsorption plays an important role in membrane retention. Until saturation of the membrane sites is achieved the real retention is overestimated [28, 37, 153]. While adsorption occurs, the apparent retention is often higher than 90% but once the membrane becomes saturated this latter decreases drastically, sometimes to less than 10% [28, 37, 41, 152, 173]. The permeate concentration shows a breakthrough curve similar to an activated carbon process, with a slow increase in the initial phase until it reaches equilibrium expressed by a constant permeate concentration with time. This is accompanied by a feed concentration decrease until saturation occurs. This adsorption causes lower retentions than expected for membranes with smaller pores than the compound [28].

However some contaminants such as SMX and CBZ that do not adsorb on the membranes do not show any breakthrough curve during filtration [159]. Retention is mainly governed by size exclusion and charge interactions, as previously shown in Figure 2.6.

Despite adsorption occurring only in the initial stages of filtration, this has repercussions during the whole operation time. The occurrence of adsorption lowers substantially the retention expected if only steric interactions are considered [23, 160], showing that membrane retention is adsorption dependent. Despite a clear connection between adsorption and lowered retention, studies of adsorbing compounds are usually carried out once the membrane has been pre-saturated with the contaminant [24, 174].

Adsorption of trace contaminants occurring in lab-scale and full-scale applications has several negative implications showing the need to understand the fundamentals of this phenomenon. At both lab scale and full scale applications, if the study is carried out in a period of time shorter than the required one, erroneous conclusions can be drawn from the results. In fact, contradictory results have been obtained in the literature in lab-scale experiments due to the short experimental time used [32, 41]. Whilst a membrane is saturating, the permeate concentration can be very low, which could lead to the erroneous conclusion that the membrane performs well, both in lab-scale [175] and full-scale [176] applications. Lab-scale membrane saturation usually takes a few hours [23, 152] whilst full modules can take more than 4 days [162, 176, 177]. Cornelissen *et al.* [176] did not detect xeno-estrogens in the

permeate after 5 days of filtration due to the continuous adsorption onto the membrane module. In the lab-scale study by Steinle-Darling *et al.* [175], no contaminant was detected for 8 hours in the permeate due to adsorption.

Besides giving apparently high retention values at initial stages of filtration, adsorption also causes the accumulation of important amounts of contaminants on the membrane polymers which can be of significant risk in water treatment. The contaminants can desorb from the membrane during operation or cleaning and contaminate the permeate line or the cleaning solution [152, 178, 179]. Moreover, a continuous adsorption-desorption phenomenon can occur during operation caused by fluctuations in feed concentration [152, 178]. For example, if the feed concentration increases, due to fluctuations in the membrane plant inlet, this causes the contaminant to adsorb, permeate through the membrane and contaminate the permeate line [152]. Adsorption can therefore be the source of unpredictable behaviour in contaminant removal, showing the absolute need in understanding what parameters affect it.

Adsorption on the membrane is strongly dependent on the membrane material used [29, 37], the contaminant and their properties. The solution chemistry, such as pH and ionic strength, also affects adsorption on the membranes. Analysing the removal of contaminants with different chemical properties as the ones presented in Table 2.2 by NF membranes illustrates the different mechanisms involved.

The pK_a corresponds to the pH at which the contaminant dissociates and becomes negatively charged. The log K_{ow} is a measure of the hydrophobicity of the contaminant. The higher it is, the more hydrophobic the contaminant is.

When adsorption of sulphametoxazole (SMX), carbamazepine (CBZ), estrone (E1), bisphenol-A (BPA) and fluoranthene are compared the latter three adsorb on NF and RO membranes at neutral pH [38, 39, 142].

At neutral pH SMX and the membrane are both negatively charged and no adsorption occurs due to charge repulsion (Figure 2.8). Moreover SMX is more hydrophilic compared to other contaminants (Table 2.2) so sorptive interactions are not favoured [159].

CBZ adsorbs less [38] or not at all [159] when compared to estrone and BPA (Figure 2.8 and Figure 2.9). CBZ is neutral so charge repulsion does not play

any role. Like SMX, CBZ is more hydrophilic (Table 2.2) which might explain the lower interaction with the membrane [159].

Table 2.2 Selected trace contaminant chemical properties

Compound	**Molecular Formula**	**Molecular Structure**	**MW (g/mol)**	**pK_a**	**Log K_{ow}**	**Dipole moment (Debye)**
Bisphenol A (Endocrine Disruptor)	$C_{15}H_{16}O_2$	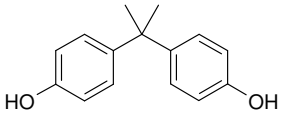	228	9.28 [c]	3.32 [d]	1 -1.4 [a,b,e]
Estradiol (Natural Steroidal Hormone)	$C_{18}H_{24}O_2$	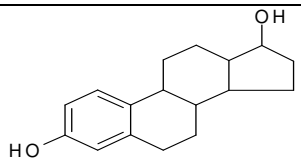	272	10.23 [c]	4.01 [g]	2.2 [h]
Estrone (Natural Steroidal Hormone)	$C_{18}H_{22}O_2$	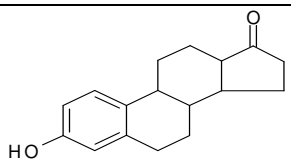	270	10.34 [c]	3.13 [g]	2.1 [h]
Fluoranthene (Polycyclic Aromatic Hydrocarbon)	$C_{16}H_{10}$	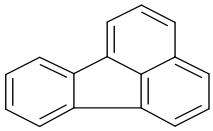	202.3	NA	5.2 [j]	NA
Carbamazepine (Antiepileptic)	$C_{15}H_{12}N_2O$	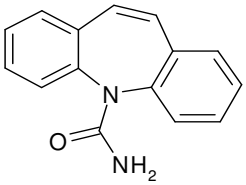	236	<1 [d]	2.45 [d]	3.2-3.6 [b,k]
Sulfamethoxazole (Sulfonamide antibiotic)	$C_{10}H_{11}N_3O_3S$	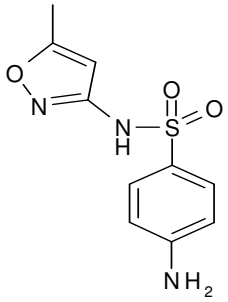	253	1.8, 5.7 [d,k]	0.89 [b,d,k]	5.4 -6.3 [b,k]

[a] [160], [b] [24], [c] [180], [d] [181], [e] [31], [g] [182], [h] [183], [j] [142] , [k] [159].

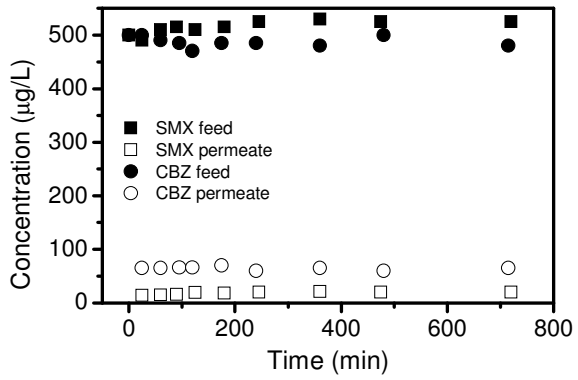

Figure 2.8 Sulphametoxazole (SMX) and carbamazepine (CBZ) feed and permeate concentrations progress with time in NF [159]

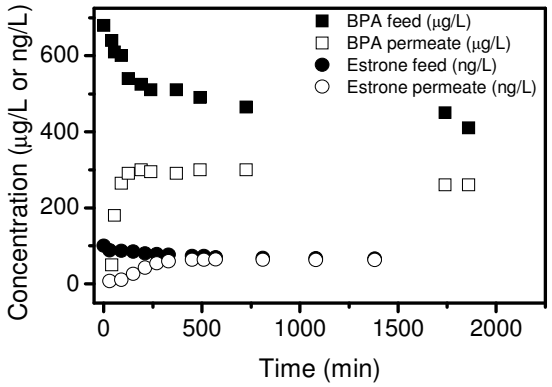

Figure 2.9 Bisphenol-A (BPA) and estrone (E1) feed and permeate concentrations progress with time in NF [160, 173]

E1 and BPA have similar size, Log K_{ow} and pK_a and both readily adsorb on the membrane (Figure 2.9) although E1 has higher adsorption (% wise and under the same filtration conditions [31]). It is argued that one of the mechanisms at play in sorption interactions between the membrane and trace contaminants occurs through H-bonding and/or hydrophobic interactions.

When comparing E1 and BPA the main difference is in their molecular structure, since other properties are very similar (Table 2.2). E1 and BPA are both bipolar, *i.e.* they can be both H donor and receiver. However, E1 has one ketone group which is a strong H receiver and one phenol group which is both H donor and receiver. BPA on the other hand has only two phenol groups. The ketone group is known to form stronger H-bonds than the phenol group explaining the higher adsorption of E1 compared to BPA. This was shown by Neale *et al.* [184] when studying the interaction between hormones and organic matter. Estrone and progesterone bind more to organic matter than estradiol and testosterone due to their ketone groups in the molecule, which are very strong H-acceptors.

As previously discussed, SMX does not adsorb at neutral pH when dissociated. However, when SMX dissociates it does not lose its full H-bonding capacity at neutral pH. Charge repulsion and hydrophilicity overcome the H-bonding capacity and SMX does not adsorb when compared to estrone for example [26]. Adsorption between the membrane and SMX could occur at low pH, when the

compound is neutral and charge repulsion does not take place. However, SMX adsorption is negligible at pH 4, as is CBZ adsorption [40]. It is striking that compared to other bipolar molecules, SMX and CBZ although capable, do not form H-bonding with the membrane material. Being highly hydrophilic they do not need to bind with a hydrophobic membrane to be stable in solution.

Fluoranthene readily adsorbs on the membrane when compared to estradiol [142] despite not possessing any strong H-bonding groups. However, fluoranthene is the most hydrophobic of the studied contaminants with a Log K_{ow} of 5.2 (Table 2.2), and adsorbs therefore on the membrane showing the influence of hydrophobic interactions on adsorption [185]. This was also shown in the study by Chang *et al.* [141] where high adsorption of estrone is obtained on a polypropylene membrane, which is not capable of forming H-bond. As a general trend, the more hydrophobic the compound is the more it will adsorb on the membrane [29, 38-40, 138, 142, 160, 186] since this requires less free energy compared to forming a "cavity" in the water phase [187]. However, this trend is not always met, as can be seen for the case of hormone adsorption onto polyacrylate fibre and the NF 270 membrane in Figure 2.10. Dudziak and Bodzek [188] showed that adsorption and retention was not related with hydrophobicity for two different NF membranes (polyamide and cellulose acetate). Diethylstilbestrol (DES), the most hydrophobic hormone (log K_{OW} 5.07) adsorbed the least for both membranes studied, while the cellulose acetate membrane adsorbed less than the polyamide membrane. This can be explained by the fact that cellulose has practically no binding capacity for steroids [189, 190].

These results show that trace contaminants with different properties will behave differently when treated by NF and RO membranes and no clear explanation has been so far provided. Since contaminant chemical properties affect the extent to which adsorption occurs, it can be expected that different membrane materials will also have an impact in the removal of trace contaminants.

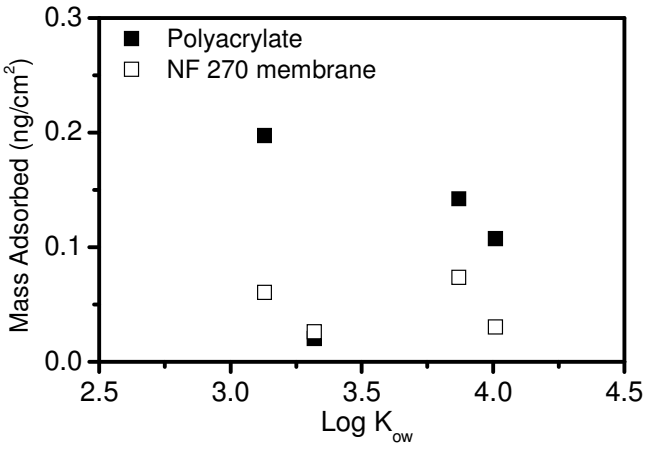

Figure 2.10 Adsorption of estrone (E1), estradiol (E2), progesterone (P) and testosterone (T) onto a polyacrylate fibre and a NF 270 membrane in filtration mode as a function of hormone Log K_{OW} (data adapted from [23, 191])

A high adsorptive interaction between BPA and a polyethersulphone UF membrane was noticed by Lyko *et al.* [143]. Adsorption of 100 ng.L^{-1} estrone to two NF membranes made of cellulose acetate and polyamide resulted in a decrease in feed concentration due to sorption of 20% and 65%, respectively [173]. Adsorption of estrone by a polypropylene MF membrane and estradiol in a UF polyimide membrane has been obtained [141, 142].

Commercial NF and RO membranes are usually thin film composite membranes (TFC) with a very thin active layer and two support layers made of different materials. The active layer is the selective one with pores in the nm level and the support layer, with wider pores, does not give any resistance to flux. Most commercial NF and RO membranes have a polyamide (PA) active layer and a polysulphone (PSu) support layer, followed by a polyester (PE) support layer. No comprehensive study has been made on what material adsorption occurs onto since they cannot be separated and are a property of the manufacturer. According to McCallum *et al.* [152] adsorption of E2 occurs both on the PSu and the PA layer. Williams *et al.* [192] and Steinle-Darling *et al.* [175] obtained higher adsorption of organic contaminants onto the PA layer compared to the other layers.

Despite the numerous studies found in the literature about trace contaminant removal by NF and RO membranes, it is clear from the above discussion that comparison between these studies, and therefore withdrawing a clear conclusion

from them, is very difficult. Trace contaminant removal is achieved by three different mechanisms that not only affect each other, *e.g.* the extent of adsorption is affected by charge interactions, but each of them is also affected by the different trace contaminant and membrane properties.

The lack of fully understanding what affects these different mechanisms has an obvious impact in the models used to describe the removal and transport of trace contaminants by NF membranes.

2.6. Modelling the Removal of Organic Contaminants by NF Membranes

2.6.1 Modelling Non-Adsorbing Contaminants

Descriptions of solute transport in RO membranes were originally given by the irreversible thermodynamic (IT) model [193, 194]. The membrane was treated as a black box, no membrane structural or electrical parameters were acquired and little information about the transport mechanisms inside the membrane could be obtained [195].

The solution-diffusion model was proposed, considering that each permeant dissolves in the membrane and is transported by diffusion due to its gradient in chemical potential through a non-porous membrane [195]. The solute flux is independent of permeation pressure while the solvent flux increases proportionally to it.

For NF membranes, there is some debate about the existence of discrete pores. In this case the solution-diffusion model is incomplete and a convection term should be included in order to take into account the solute transport through membrane pores. The retention of uncharged solutes in NF membranes can be described by the hydrodynamic model [43]. The transport takes into account diffusion and hindered convection, caused by the difference between solute size and pore size. For charged solutes such as ions or organic acids, the addition of the membrane and ion electrochemical potentials derives in the extended Nernst-Planck equation [196]. This last model not only allows determining the same parameters as the hydrodynamic model but also allows for the determination of the effective membrane charge density [23, 197, 198].

Both the solution diffusion model and the hydrodynamic model describe an increase of retention for solutes with pressure. This has been confirmed for metals, ions and some organics (*e.g.* pesticides, pharmaceuticals) [164, 167, 196, 199-201].

2.6.2 Removal of Adsorbing Trace Contaminants

In the previous section it was indicated that the retention of solutes by NF membranes increases with increase of pressure or flux. However, for some contaminants the opposite trend is observed, *e.g.* with hormones [148, 153], pesticides [25, 162], volatile organic carbon (VOC such as chloroform) [27], endocrine disrupting chemicals (EDCs) such as nonylphenol (NP) [171] and pharmaceuticals [162] where retention decreases with pressure.

This phenomenon is not directly linked with the ratio between the solute and pore radius ($\lambda=r_{solute}/r_{pore}$). It could be argued that for $\lambda<1$, the solutes can penetrate the membrane and be less retained. However, for nanofiltration of Na_2SO_4, glycerine and glucose as examples of non-adsorbing compounds with $\lambda<1$, retention increases with increase of pressure [196, 202]. This trend is not verified for adsorbing contaminants with $\lambda<1$ [153]. It is thought that the interaction of contaminants with the membrane polymer plays an important role [23] and contributes to the reduced retention with increase of pressure.

Adsorbing solute retention seems to not only depend on steric exclusion but also on adsorption and chemical organic characteristics such as hydrophobicity, as well as convection and diffusion mechanisms [203]. Whilst some studies show that competition for adsorption sites decreases retention compared to a single contaminant solution [29, 204], others show that retention of these adsorbing compounds is enhanced when their adsorption is decreased due to preferential adsorption of another contaminant on the membrane [205]. This shows the close relationship between adsorption phenomena and retention of contaminants.

Despite the clear relation between adsorption and trace contaminant retention, adsorption of contaminants to the membrane polymer is usually not taken into account in contaminant retention models [23, 159, 160, 176]. In consequence,

retention and permeate concentration are often wrongly determined. Retention, in particular, is commonly overestimated when based solely on size [23].

2.6.3 Removal of Adsorbing Contaminants in Complex Water Matrix

A further complexity that is not yet theoretically predictable is the behaviour of mixtures. In actual waters many contaminants are found together with other organics, such as natural organic matter (NOM) or salts that can result in solute-solute interactions [184]. When organic matter is present in solution enhanced retention is generally obtained for contaminants [26, 139, 153, 160, 162, 169, 173, 179, 206] due to partitioning of the contaminants into the retained organics [34, 204]. Higher adsorption is obtained, possibly on both membrane and organic matter layer that is formed on the membrane surface [41, 155, 161, 173, 179]. In contrast, a decrease in contaminant adsorption may occur when natural organics and contaminants compete for sorption sites [33, 35, 39, 142, 152, 185, 204]. Several models to predict the mass adsorbed on a membrane for mixtures based on the mass adsorbed with only one compound has been developed [207].

Figure 2.11 shows an overview of the retention mechanisms of trace contaminants by NF and RO membranes.

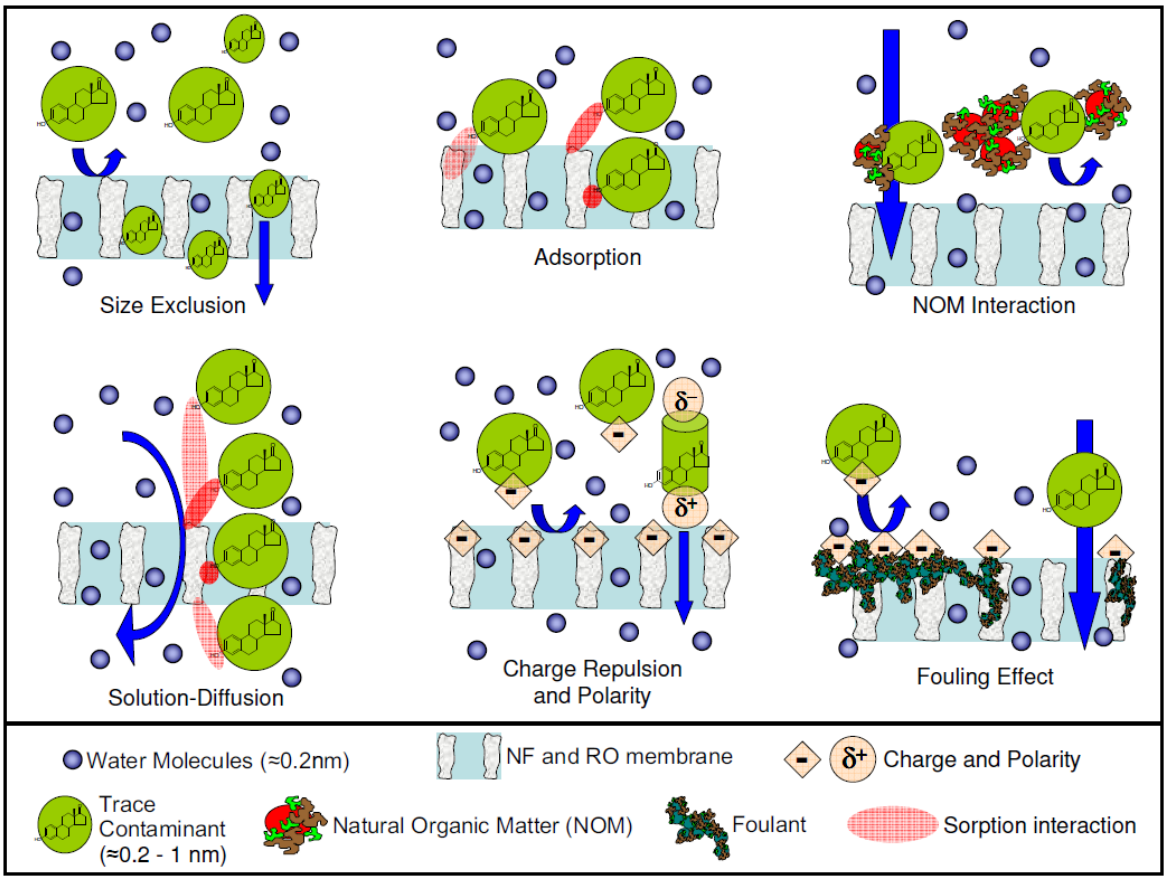

Figure 2.11 Retention mechanisms by NF and RO membranes

2.7. Large Scale Application

Despite the difficulty in predicting the performance previously described by NF and RO membranes in the removal of trace contaminants in lab scale studies, large scale applications have shown good performance with high water quality obtained. These applications are motivated by the need to remove contaminants for water treatment where the water supply is contaminated, or for water recycling where wastewater is treated to a potable water standard. Increasing water pollution awareness combined with increased water demand and water scarcity is rapidly expanding the number of large scale plants. A number of such applications are shown in Table 2.3, as an illustration.

The Méry-sur-Oise water purification plant in Paris, France, treats water for potable usage directly from the river Oise to 650,000 people. The majority of the treated water produced (80%) originates from MF pre-treatment followed by NF

treatment, while the remaining (20%) originates from conventional biological treatment. The choice of the membrane technology was due to its high removal of organic carbon and pesticides when compared to conventional processes [208, 209]. The river Oise has generally very high concentrations of pesticides (*e.g.* >1.6 $\mu g.L^{-1}$ in May, June and August of 2007 [210]) with the highest individual pesticide concentrations measured for glyphosate and aminomethyl-phosphonic acid (AMPA) (ranging from 0.2 $\mu g.L^{-1}$ to 0.9 $\mu g.L^{-1}$).

The NEWater facilities in Singapore (Figure 2.12) are advanced water reclamation plants. The water influent originates from a clarified secondary effluent with conventional activated sludge process (CASP). This treated water can be further reused as high grade industrial water (*e.g.* microelectronics industry) or for indirect potable reuse applications.

Figure 2.12 NEWater potable water recycling plant in Singapore (*photo courtesy PUB Singapore,* [211]). On the left is the Kranji NEWater Plant and on the right the Kranji RO modules

Water Factory 21 (WF21) in California, USA, was built to treat and purify wastewater from the Orange County District to drinking water standards. This treated water was then injected into the groundwater basin [212] that supplies drinking water to a population of more than 2 million people. Groundwater is protected from seawater intrusion by injecting treated reclaimed water to be blended with deep-well water into coastal aquifers. Disinfection by-products (DBP) such as N-Nitrosodimethylamine (NDMA) were detected in several drinking water wells in California [213]. The presence of this compound in the injected water from WF21

forced the interruption of the plant operation in 2000-2001, reducing water treatment by more than 85% [59]. The levels of NDMA in the discharged water were higher than 20 $ng.L^{-1}$ [58, 213]. A UV treatment was subsequently installed to remove the NDMA. According to a study by Plumlee *et al.* [214], the RO process in WF21 removes NDMA between 24-56%, depending on the sampling season. With the addition of UV treatment the overall removal increases up to 75%. As expected, MF does not remove any of the NDMA. On the contrary, due to chlorination pre-treatment to avoid MF fouling the NDMA concentration increases in the MF influent. WF21 has stopped working since 2007 to be replaced by an improved and larger water purification plant [215, 216].

Table 2.3 Water treatment plants with NF and RO membrane technology

Location	**Membranes Used**	**Maximum Capacity ($m^3.d^{-1}$)**	**TOC in treated water (year)**	**Trace Contaminant in treated water (year)**
Méry-sur-Oise (France) [217]	MF followed by NF (NF 200 Dow Filmtech)	340,000	2 $mg.L^{-1}$	<0.1 $\mu g.L^{-1}$ for single pesticide <0.5 $\mu g.L^{-1}$ for total pesticide <50 $ng.L^{-1}$ for atrazine and desethylatrazine (2007) DBP <90 $\mu g.L^{-1}$
NeWater (Singapore) [211]	MF followed by RO and UV disinfection	252,000 -Bedok 28,000 -Seletar 23,000 -Kranji 55,000 -Ulu Pandan 146,000	0.5 $mg.L^{-1}$ (2008)	Pesticide <0.1 $\mu g.L^{-1}$ DBP<75.9 $\mu g.L^{-1}$ (2000-2002) THM <0.08 $mg.L^{-1}$ 2008
Water Factory 21, (USA) [218]	MF followed by RO (ESPA 2 Hydranautics)	19,000	<0.7 $mg.L^{-1}$ (2003)	THM <2.7 $\mu g.L^{-1}$ (2003)
Beckton, (UK)	RO	140,000		

2.8. Conclusions

The need to remove trace contaminants such as hormones from possible potable sources was evidenced above. Their occurrence in water sources and possible health effects in humans and animals urges the development of technologies that allow for their efficient removal in a sustainable way.

Nanofiltration and reverse osmosis are possible technologies as they represent a physical barrier for the removal of trace contaminants without involving chemical additives or excessive energy consumption compared to other technologies such as distillation. As previously mentioned, this technology is being implemented all over the world for water, wastewater and water recycling applications.

Membrane retention, however, was found not to be dependent only on steric exclusion: charge effects, adsorption and membrane affinity contribute further for the removal mechanisms of trace contaminants. These mechanisms, in turn, are dependent on many parameters, such as filtration conditions, solution, solute and membrane characteristics translating into a very complex system.

The above description of the current state of the art illustrates this complexity. The variety of operational parameters and media used in the different studies limits the conclusive understanding of the removal mechanisms of trace contaminants by NF membranes. It is clear that further fundamental research and applied research work is necessary to identify and characterise the mechanisms involved in the removal of these contaminants. This will make possible the development of fully predictive models that can be used for new membrane designs.

Despite its being well established that charge repulsion between a negatively charged organic trace contaminant and a negatively charged membrane will enhance retention, few studies have modelled the removal of these by NF and RO membranes [150, 219, 220]. This mechanism does not often have a high contribution in the removal of trace contaminants since these usually dissociate at very basic or alkaline pH (*e.g.* hormones and BPA), whilst standard water treatment processes work at neutral pH (pH 5-8). However, some trace contaminants have lower pK_a (*e.g.* diclofenac, dichloroacetic and trichloroacetic acid [28]) and

understanding how charge interactions affect their transport in NF and RO would be valuable in order to predict their removal.

Contrary to charge interactions, trace contaminant adsorption occurs in the whole pH range, even when the trace contaminant is dissociated and charge repulsion by the NF and RO membrane occurs. As previously discussed, the occurrence of adsorption affects the overall membrane performance by decreasing the expected retention based solely on size exclusion mechanism. This phenomenon is far from being well understood, and contradictory results have been obtained and reported in the literature [41, 154, 156, 172]. Because of that, predictive models that describe the transport of adsorbing contaminants are scarce. To fully understand and predict the removal of adsorbing trace contaminants by NF and RO membranes it is imperative to understand the contribution each operating parameter involved in the filtration process has on the adsorption of those contaminants. These parameters include solute characteristics, filtration conditions that govern the feed hydrodynamics and membrane characteristics such as different materials, pore size and membrane thickness. Once it is well established how these parameters contribute to the removal of adsorbing trace contaminants then new transport models taking adsorption into account can be developed. Knowledge of the contribution the operating parameters make to the removal of trace contaminants by NF and RO, together with understanding of the fundamental mechanisms involved in such membrane separation processes, with adsorption playing an important role, is certainly a first step to the development of predictive transport models. This is of importance because it may contribute to the design of new membrane modules and new membranes, both chemically (different polymeric materials) and physically (different characteristics such as thickness and pore radius), in order to avoid the occurrence of adsorption. Moreover, adsorption could be combined with NF/RO processes to enhance trace contaminant removal through the design of new hybrid NF/RO-adsorptive processes.

3 Materials and Methods

3.1. Introduction

In order to carry out the work focused in understanding the removal mechanisms of hormones by NF membranes, several types of membranes, analytical instruments and filtration equipment were used. The Materials and Methods chapter describes all the different instrumentation used to achieve this goal.

This chapter however has two main objectives. The first one is to describe the development of a cross-flow system suitable to study the fundamentals of hormone removal by NF membranes, by mimicking the hydrodynamics in spiral-wound modules with no oil leakage from the pump. Several examples comparing the results of an ill-designed system with a well-designed one are provided in order to illustrate the effect that an ill-designed system can have in the fundamental study of the removal mechanisms of hormones by NF membranes. In fact, an oil leakage has been previously reported in the literature in a study on the removal of iron by reverse osmosis membranes in 1973 [221]. In this study the authors state "*The first few fouling experiments performed at different flow velocities showed a wide scattering of results. Each of these experiments had been performed with a new membrane and with new feed brine. Since equipment corrosion […] had been largely avoided, it was felt that the observed irreproducibility might have been caused by oil leakage from a booster pump used during precompaction or from the high pressure pump due to deterioration of the piston packings.*" In their study, the effect of oil on iron hydroxide deposits was checked, and deposits on the membrane were two to almost four times higher in the presence of oil. The results presented here also show a scatter of results of the removal of hormones by NF membranes with the ill-designed system.

Once the well-designed cross-flow system was developed, the second objective of the Materials and Methods chapter is to describe and characterise the

materials (membranes, chemicals, etc.), the instruments used (filtration and analytical equipment, amongst others) and the protocols adopted to study the removal mechanisms of hormones by NF membranes.

Two types of membrane characterization were carried out for the NF and RO membranes used in this study: a physical characterization including the hydrophobicity, active layer thickness and roughness determination for example, and a performance characterisation, including permeability, molecular weight cut-off, NaCl retention and pore radius. Once the membranes are characterised, the chemicals and reagents are described, including hormone and organic tracers characteristics. Finally, the analytical instruments used to measure concentrations, the filtration systems used and the different protocols followed are described.

3.2. The Importance of a Well-Designed Cross-Flow Membrane System

3.2.1 Introduction

Spiral-wound modules are the most common membrane separation technologies used in water treatment, due to their compact geometry and high surface area [208, 218, 222].

Cross-flow systems with a slit channel cell are commonly used in membrane water treatment research, especially when studying the removal of trace contaminants [23, 28, 41, 152, 175, 223-225]. This cell geometry constitutes a model at laboratory scale of spiral-wound modules allowing for the study of the fundamentals of mass and momentum transport in the feed channel by controlling its hydrodynamics. Because of this it is crucial to maintain similar hydrodynamic conditions at both scales.

It should be mentioned that cross-flow systems produce experimental results that may be different from those obtained with other membrane devices. In fact, a study of the removal of hormones by NF membranes showed that different results are obtained between a cross-flow system and a dead-end system [153]. The previous reasoning led to the choice of a cross-flow slit channel membrane geometry to perform the experimental work in this thesis as it mimics large-scale applications.

3.2.2 Original MMS System Set-Up

The cross flow filtration system from MMS (Switzerland) displayed in Figure 3.1, with its P&I diagram shown in Figure 3.2, was originally acquired to carry out the hormone filtration experiments.

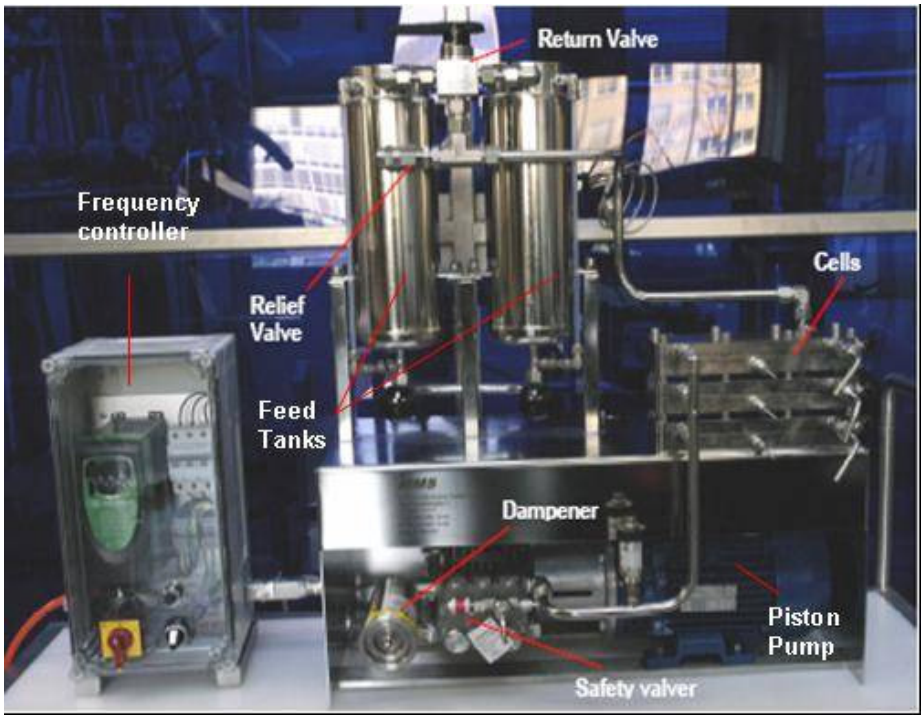

Figure 3.1 Set-up of the original MMS cross-flow system

As can be seen from Figure 3.1 and Figure 3.2 two 2.5 L tanks are connected to a high pressure pump M1 (Speck 10/15-140 RE, 0.75 kW motor, Germany). A controller is set up to control the pump frequency, which is proportional to the feed flow rate. For each experiment only one tank feeds the system with the solution to be permeated, the other tank being at rest. The pump can feed one, two or three rectangular flat sheet membrane cells, and the retentate is recirculated back to the feed tank. Permeate samples are collected in the permeate line, operating at atmospheric pressure. The permeate line can also be recirculated back to the feed tank through a 3 way valve.

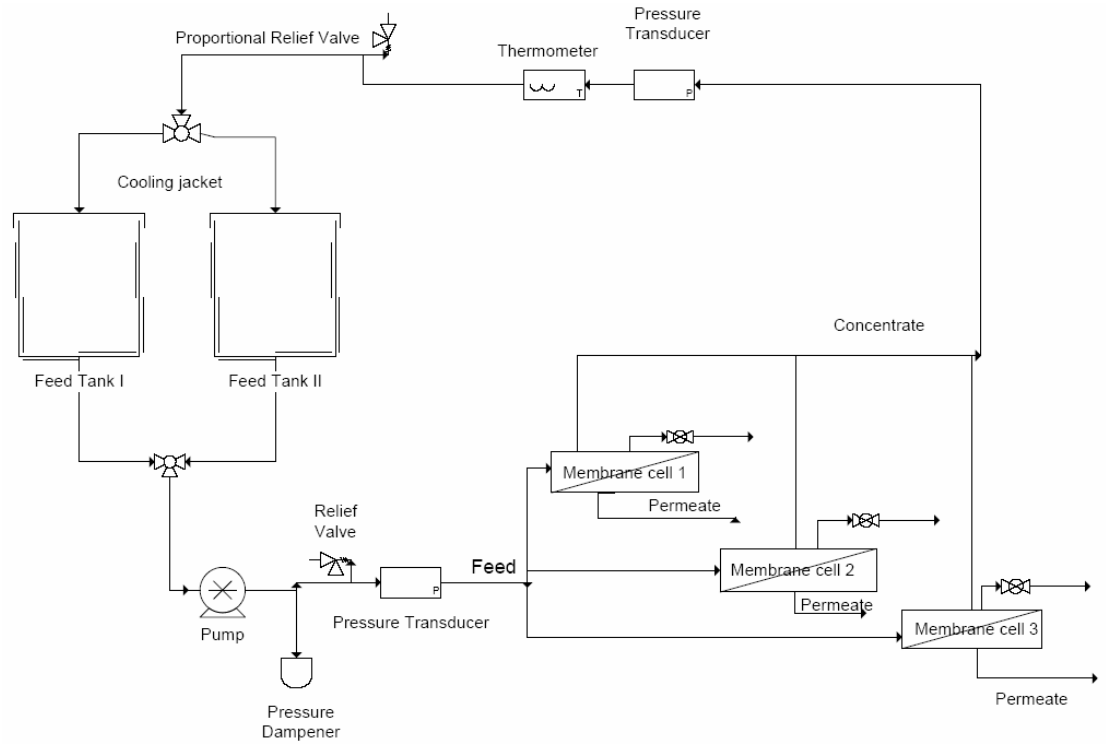

Figure 3.2 Schematic of the MMS cross-flow filtration system

The feed tanks have a cooling jacket of 0.09 m^2 that allows for the temperature control through its monitoring in the retentate line with a thermometer. The cooling jacket is connected to a temperature controlled bath (WK 700, Lauda). The temperature in the system is measured with a thermometer WTM Pt 100-0-6 from Condustrie-Metag, Germany, directly connected to the datalogger for data recording.

A proportional relief valve R4A from Swagelok allows the pressurization of the system up to 50 bar. The pressure is monitored both in the feed and the retentate lines of the membrane cell with two pressure transducers (S model from Swagelok), allowing for the quantification of the pressure drop across the membrane cell.

A pressure dampener (MS160C from Speck, Germany) is inserted downstream the pump to avoid undesirable oscillations in pressure, flow rate and other related operation conditions and system vibrations. The system is made of 316 stainless steel or PTFE to avoid adsorption of solutes used in the study.

The membrane cells shown in Figure 3.3 are slits characterized by a height (1 mm) much smaller than the other two dimensions (25 mm width and 191 mm long). These cells can incorporate membranes with areas of 46 cm^2.

A pressure relief valve is inserted in the system after the pump (R3A from Swagelok), to avoid overpressure. Datalogging was set-up allowing for the control of membrane cell inlet and outlet pressure and temperature. A DAQ 55 Omega datalogger is used (Omega, UK).

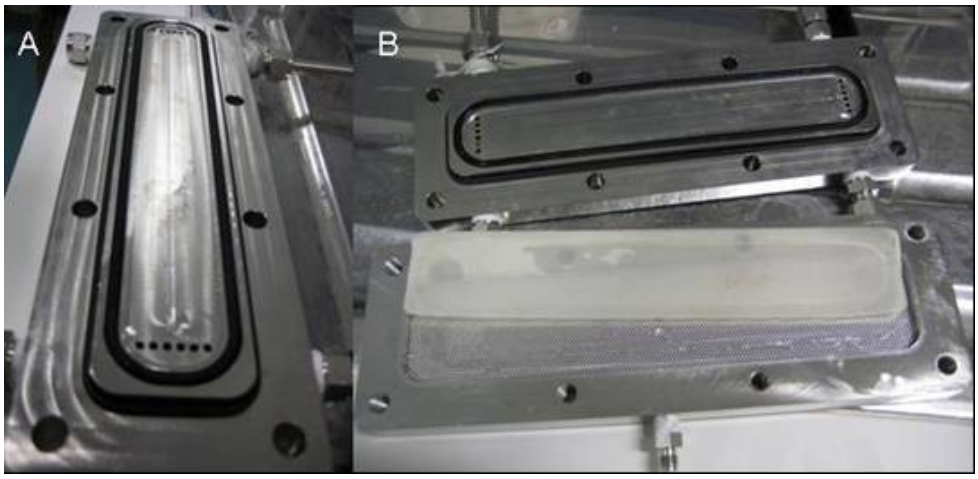

Figure 3.3 Membrane cell: **(A)** membrane cell top part with 1 mm height channel, **(B)** membrane cell bottom (with stainless steel and polysulphone support) and top part

3.2.3 MMS System Operating Re_{dh} Numbers

The MMS system operating conditions (circulating flow rates as a function of the frequency in the control box) were calibrated as described in Appendix A, section A.1. This procedure allowed for the definition of the circulating Reynolds number in the cell (based on the hydraulic diameter – Re_{dh}), which characterises the flow regime in the feed channel, as it is the ratio of inertial to viscous forces, and is a measure of the circulating flow rate for a defined geometry and fluid. This Re_{dh} number is defined as:

$$Re_{dh} = \frac{\rho v d_h}{\mu} \qquad (3.1)$$

where d_h is the hydraulic diameter (m), ρ is the density of the circulating fluid ($kg.m^{-3}$), v is the average velocity ($m.s^{-1}$) and μ is the fluid viscosity (Pa.s) [226].

The results of the calculated Re_{dh} are presented in Table 3.1.

Table 3.1 Reynolds number (Re_{dh}) of the SPECK pump for several frequencies of the pump control box and of spiral-wound modules in industrial applications

Re_{dh} in industrial applications	Re_{dh} in one membrane cell with the Speck pump		Frequency (Hz) in the pump control box
	Single cell fitted	Three cells fitted	
100-1000	6484.6	2161.5	14
	7488.8	2496.3	16
	9468.6	3156.2	20
	12,051.0	4017.0	25

As can be seen in Table 3.1 the lowest value of the Re_{dh} number for one membrane cell fitted is around 6500. The transition regime from laminar to turbulent corresponds to a critical Re_{dh} of 2300 [227]. Moreover Table 3.1 clearly shows that with the Speck pump, the regime with one membrane cell fitted was turbulent with Reynolds numbers quite above the one established in the literature for completely turbulent flows in slits (Re_{dh}=4000) [226]. If three membrane cells are fitted the velocities correspond to the laminar-to-turbulent transition regime (Re_{dh} >2500) – for details, refer to Appendix A, section A.1.

3.2.4 Re_{dh} Numbers in Spiral-Wound Industrial Applications

In industry, spiral-wound and plate and frame modules are frequently used, but due to their channel configuration, characterised by a smaller height compared to the other channel dimensions, flow rates are restricted to typical laminar flows [228]. According to Schock and Miquel [229] the Re_{dh} range used in spiral-wound modules systems in industry for aqueous solutions ranges from 100 to 1000. This Reynolds number is a function of the average velocity in the feed channel and the hydraulic diameter, the characteristic length of the channel. The hydraulic diameter is itself a function of the channel height and feed spacer characteristics – for more details refer to Appendix A, section A.2.

When comparing these Re_{dh} numbers with the ones calculated in Table 3.1 the conclusion is obvious: the Speck pump flow regime is characterised by a far too high Re_{dh} number to be comparable with the hydrodynamic conditions found in spiral-wound membrane modules, thus not reflecting industrial applications.

3.2.5 Consequences of MMS Delivered Re_{dh} Numbers

The regime of the circulating flow delivered by the Speck piston pump operation was not comparable with the hydrodynamic regime occurring in actual industrial applications with spiral-wound membranes, as previously discussed. This means that a single membrane cell could not be fitted and used since the velocities and, consequently, the shear stresses at the membrane surface were much above the value admissible. Even for three membrane cells, the flow rates were far too high compared to actual flows inside spiral-wound modules.

At a frequency of 30 Hz, for example, corresponding to a cross-flow velocity of about 7 $m.s^{-1}$ and a Re_{dh} of 14,346, the shear stress on the membrane surface was so high that the membrane active layer was ripped off or cracked, as can be seen in the photos displayed in Figure 3.4. Unfortunately, the minimum frequency to be used, as advised by the pump manufacturer, was 20 Hz (equivalent to 6.6 $L.min^{-1}$, 4.4 $m.s^{-1}$ or a Re_{dh} number of 9500) to make sure that the pump pistons were not damaged. This flow rate is still higher than that admissible for the membrane and used in real life spiral-wound modules.

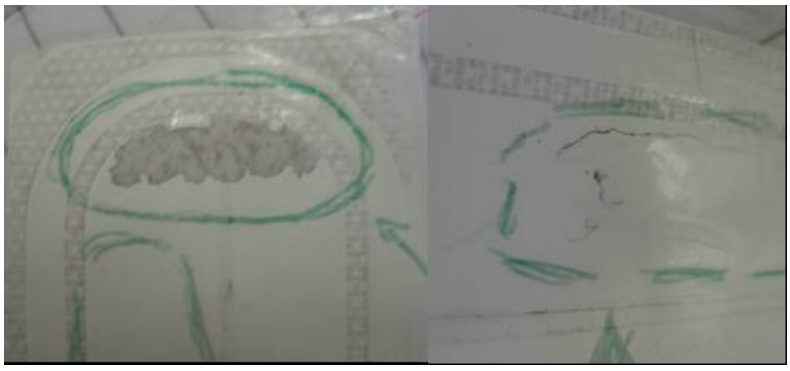

Figure 3.4 NF 270 membrane with active layer ripped off due to the experience of much too high shear stresses at experiments with Re_{dh} above 14,000.

To illustrate the undesirable and detrimental effect of the high feed flow rates (*i.e.* high Re_{dh} numbers) delivered by the pump a comparison between two runs is performed, one with a well-designed and the other with the ill-designed cross-flow system previously described, and the results are shown in Figure 3.5 and Figure 3.6.

In Figure 3.5, the results of a repeated experiment of 300 $ng.L^{-1}$ of E2 carried out with the Speck pump are displayed. The permeate concentrations are far too high in the case where the Speck pump was fitted, and this is mainly caused by the damage on the membrane active layer surface similar to the one showed in Figure 3.4. The final retention obtained by the NF 270 membrane was less than 15%.

In Figure 3.6 is represented a comparison between two runs, one with the Speck pump fitted in the system and one with a well-designed cross-flow system. As can be seen, once again, the permeate concentration is far too high, giving a very low retention at steady-state compared to the retentions obtained in the literature [23]. Furthermore, at the operation conditions delivered by the Speck pump a pressure drop of 16.3 $bar.m^{-1}$ was obtained in the slit cross-flow cell showed in Figure 3.3, compared to a pressure drop of 0.2 $bar.m^{-1}$ obtained in full spiral-wound modules [229].

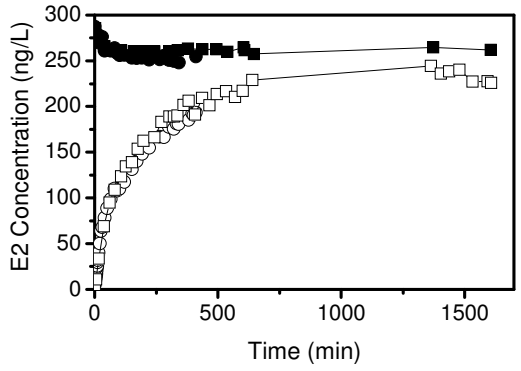

Figure 3.5 Repeat for feed (filled symbols) and permeate (hollow symbols) concentrations variation with time for estradiol (E2) (C_{feed} E2=300 $ng.L^{-1}$, 10 bar, 1mM $NaHCO_3$ and 20 mM of NaCl, SPECK pump: Re_{dh}=12,051, NF 270)

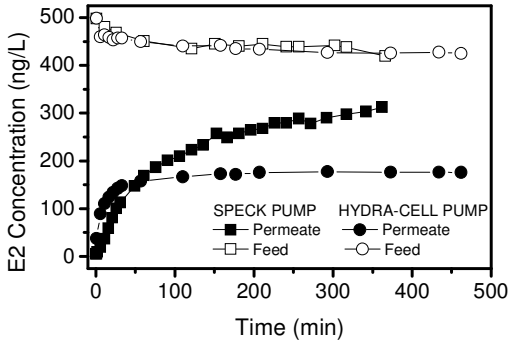

Figure 3.6 Feed and permeate concentration variation with time for estradiol (E2) (C_{feed} E2=500 $ng.L^{-1}$, 11 bar, 1 mM $NaHCO_3$ and 20 mM of NaCl, SPECK pump: Re_{dh}=12,051, Hydra-cell Pump: Re_{dh}=900, NF 270)

As will be seen in Chapter 4, the higher the Re_{dh} number is, the higher the hormone retention should be, which is not the case presented in Figure 3.6. These results show the detrimental effect that high shear stresses have on the membrane surface (*i.e.* for higher Re_{dh} numbers).

To allow for lower flow rates delivered to the membrane cell and overcome the previous problems, a bypass was designed and inserted in the system.

3.2.6 Bypass Insertion and Problems

To avoid the excess flow rate delivered by the Speck pump that circulates tangentially to the membrane, a bypass to the cells was inserted connecting the pump exit to the feed tank (see Figure 3.7), where a high flow rate needle valve (201061, Isis-Fluid Control, Italy) would allow a fine control of the flow rate in the bypass side and would also allow the system to be maintained under pressure, avoiding all the fluid to flow through the bypass and none through the membrane cell. Another needle valve of low flow rate (ss-4L2-MH, Swagelock, UK) was inserted in the membrane cell entrance to finely control the flow rate of the fluid circulating on the membrane cell side as can be seen in Figure 3.7 and Figure 3.8.

This new set up design allowed diverting the excess flow rate delivered by the pump to the feed tank directly without passing by the membrane cell.

Finally, a flow meter (M2SSPI from Hydrasun, UK) was inserted at the membrane cells entrance to measure the flow rate delivered to the cells.

As described in detail in Appendix A, section A.3, the use of this upgraded system brought about a few problems:

1. Impossibility to control simultaneously and independently the operating pressure and the flow rate;
2. Vibrational and noise problems in the experimental set-up caused by the proportional relief valve;
3. Incapacity of the pump to maintain a constant operating pressure and flow rate during the entire experiment;

4. Difficulty of the pump in delivering low flow rates at high pressures as required for the experiments mimicking industrial conditions.

All these problems started to point out for the need of replacement of the pumping device.

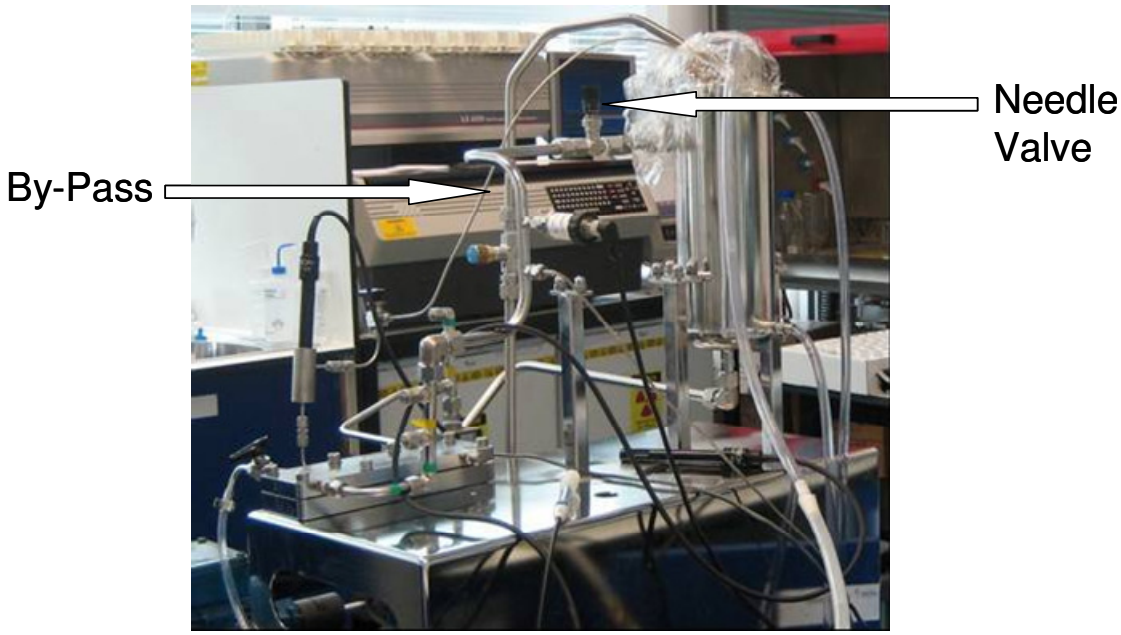

Figure 3.7 Bypass inserted and needle valve replacing pressure relief valve

In fact, from the above reasoning it can be inferred that these pumps had clearly not been designed for a membrane cross-flow application, and particularly not to mimic a spiral-wound membrane.

Besides the obvious problems of the pump performance, another serious problem arose: a contamination emerged in the system and deposited on the membrane surface as described in the next section.

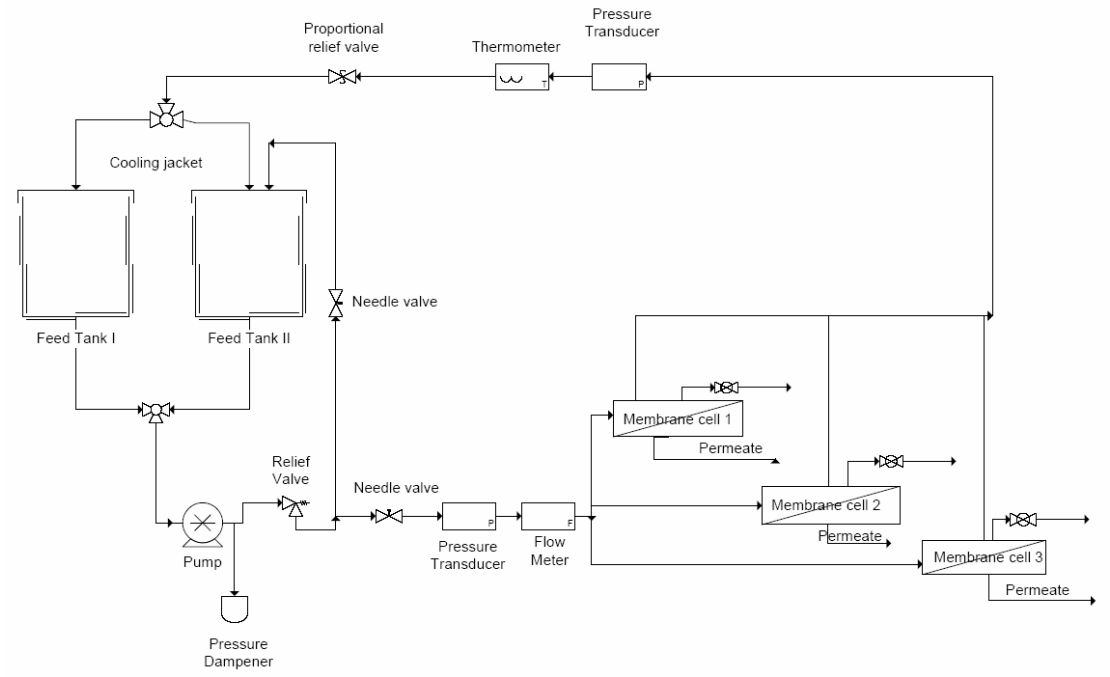

Figure 3.8 Schematic representation of the cross-flow filtration system with a bypass inserted

3.2.7 Oil Contamination with the Piston Pump

After a few experiments carried out with hormone solution (100 ng.L^{-1} of radiolabeled E2, 1mM $NaHCO_3$ and 20 mM of NaCl), and running the system for more than 12 hours, which is the average time for one experiment, a brown dark substance was found to be deposited on the membrane surface, as can be seen in the photo displayed in Figure 3.9, which was easily removable with a cotton bud. This contamination problem persisted in the following experiments and the deposit amount increased with the experimental time. Until 4 hours of experiment were completed visible traces of deposit were obtained. After 4 hours, the deposit on the membrane surface started to build up in a notorious persistent way.

Several procedures were adapted to track the deposit origin, as described in detail in Appendix A, section A.4. However, as clearly demonstrated in the Appendix, the problem persisted and, moreover, a strong sulphur smell started to emanate from the feed tank after a few hours of operation.

Figure 3.9 Membrane NF 270 with oil deposits all over the membranes

Table 3.2 Procedure adopted to find contamination source

Instrument	**Substantial Deposit**	**Some Deposit**	**Almost No deposit**
All the instruments fitted	X		
Without Dampener	X		
Without Bypass with needle valve	X		
Without Flow meter	X		
Without Flow cell and Conductivity meter in permeate		X	
With Flow cell and Conductivity meter in permeate after washed physically			X
With Flow cell and Conductivity meter in permeate	X		

The persistence of the deposits and the sulphur smell led to the conclusion that one of the experimental set up equipments might be leaking oil into the circulating fluid, the pump being the most probable source. Hence, all the

equipments and instruments of the system were checked as described in detail in Appendix A, section A.4 and the results are summarised in Table 3.2.

From all the mentioned tests and results analyses it was concluded that the contamination was an oil leak from the pump due to the following evidences:

- A golden deposit on the membrane surface (Figure 3.10);
- A TOC increase during an experiment with MilliQ water of at least 7 $mg.L^{-1}$ (Figure 3.9);
- An intense sulphuric smell (oil);
- Every other single instrument was ruled out as a contaminant source (Table 3.2).

In addition, there was also confirmation from Speck pumps that these particular piston pumps can leak oil. They are usually used for car wash systems and, therefore, are certainly not appropriate for clean applications where a constant and controllable pressure and flow rate are necessary.

The oil leak was originated from the oil case used to lubricate the pistons, as clearly shown in this work. More details and illustrations can be found in Appendix A, section A.4.

A few experimental results are presented below to demonstrate how oil leakages affect the membrane performance as far as hormones permeation is concerned.

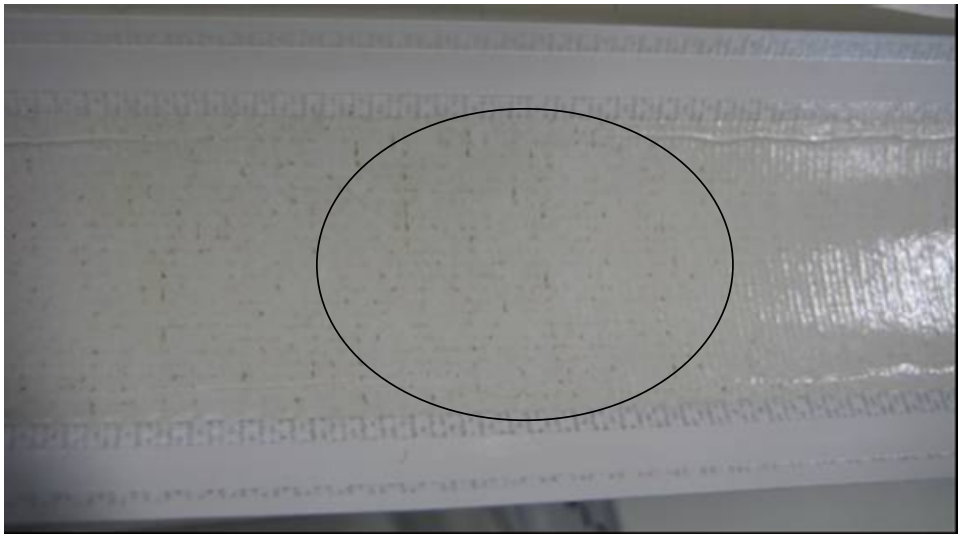

Figure 3.10 Gold shade of deposit on the membrane surface (deposit circled)

The results of two experiments of E2 filtration for the same hydrodynamic conditions with and without oil (that is, with an ill-designed and a well-designed system) are shown in Figure 3.11 for comparison. As can be seen, the deposition of oil causes the membrane to permeate higher amounts of E2, affecting the membrane performance and rendering impossible the fundamental study of hormone removal mechanisms by NF membranes.

Whilst for the experiment with the ill-designed system the permeate flow rate decreases by 20% compared to the pure water flux measured before spiking the hormones showing fouling caused by the contaminant, in a well-designed system, the permeate flux is constant with time.

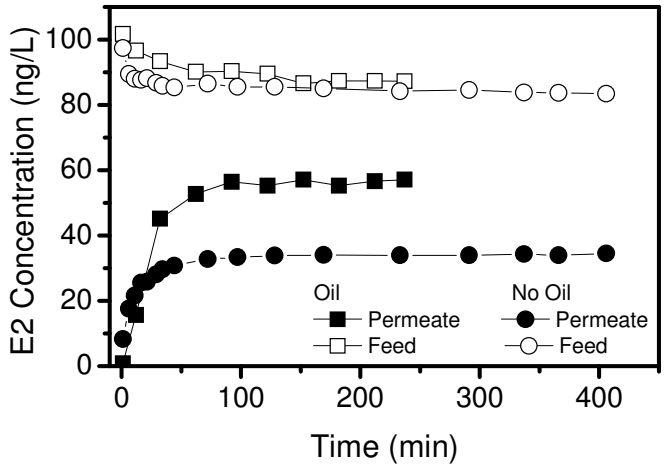

Figure 3.11 Estradiol (E2) feed and permeate concentrations in the presence and absence of SPECK pump oil deposits on the membrane surface (C_{feed} E2=100 ng.L^{-1}, P=11 bar, 1mM $NaHCO_3$ and 20 mM of NaCl, Re_h=427, NF 270)

The serious problems described above made necessary the fitting of an appropriate pump that did not leak oil and would simultaneously allow to control and maintain a fixed pressure and flow rate with values typical of those appearing in industrial applications.

3.3. New Well-Designed System

3.3.1 New Pump and Back-Pressure Regulator

The new pump chosen to replace the ill-designed one was a Hydra-Cell high-pressure metering diaphragm pump (P200 from Hydra-Cell, UK) with PTFE diaphragms to avoid hormone adsorption, which are commonly used in membrane cross-flow systems in research. A Swagelok back pressure regulator (KPB1N0A415P60000, Swagelok, UK) was also fitted in as can be seen in Figure 3.12. A back pressure regulator, commonly used in cross-flow filtration systems, allows the pressurisation of the system without changing the flow rate.

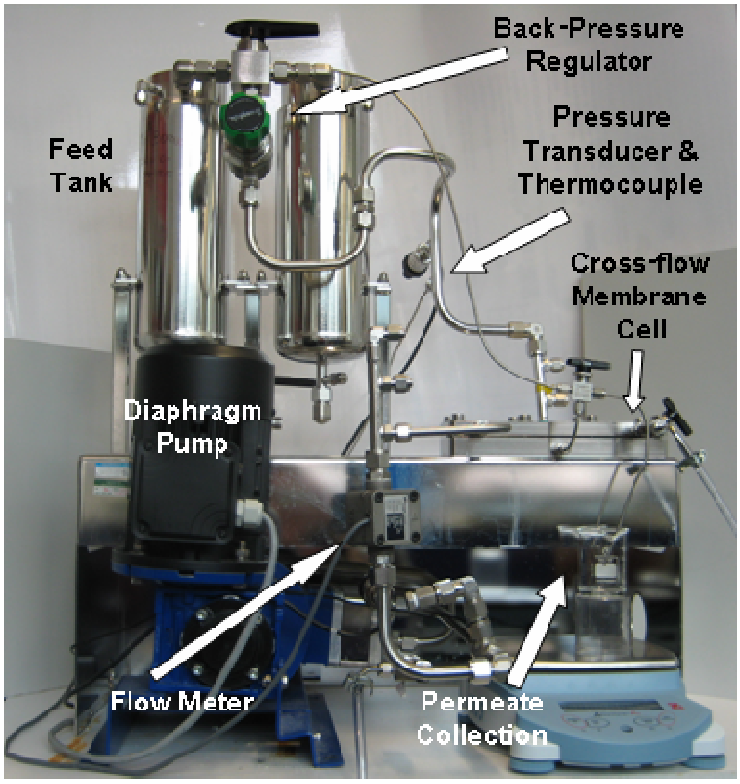

Figure 3.12 Last version of the cross-flow system

3.3.2 Problems Encountered With the New Set Up: Contamination Issue

After running the system for more than four hours, a source of yellow contamination on the membrane surface was observed with the new set-up, as can be seen in the photo shown in Figure 3.13. This deposit was not removable with a cotton

bud (in opposition to what occurred previously) and it seemed adsorbed into the interior of the membrane. Comparing Figure 3.14 (membrane deposits with the Speck pump) and Figure 3.13 (membrane deposits with the Hydra-Cell pump) it can be seen that the nature of the deposits is different.

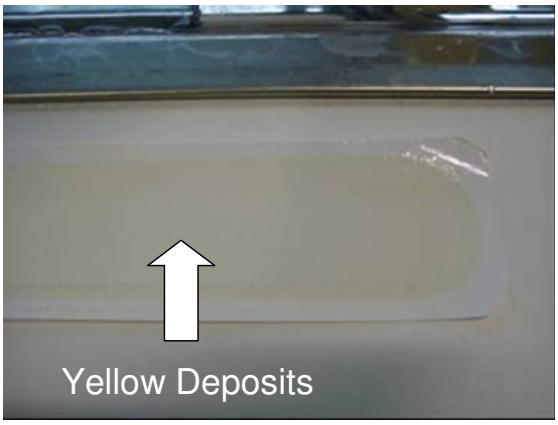

Figure 3.13 Membrane yellow deposits with Hydra-Cell pump

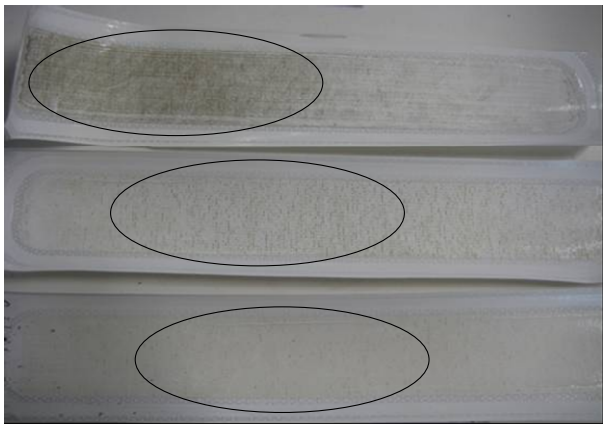

Figure 3.14 Membrane deposits with Speck pump (circled)

The same protocol as before was followed to find the source of the contamination. The yellow deposit, however, persisted after all the described steps were followed (see Figure 3.15):

1. Several washes were performed (as described in appendix A.4);
2. Use of other 2 identical diaphragm pumps in the same MMS system;
3. Use of two other identical MMS systems with the 3 pumps fitted;
4. Use of different types of membranes;
5. Experiment with and without dampener;
6. Removal of a yellow lubricant (NSL 1073 TORQUE TIGHT A/G) used to seal the pumps inlet and outlet that are not being used and that it was in contact with the circulating fluid;
7. The TOC levels between the initial feed and the final feed concentration after reciculating MilliQ water for a few hours increased by a minimum of 2.3 $mgC.L^{-1}$;

In the absence of the dampener, however, the deposits decreased due to the pressure pulsation of ±2.5 bar and on the cross flow velocity of ±0.012 $m.s^{-1}$,

corresponding to a variation of feed flow rate of ±0.018 $L.min^{-1}$, a known technique to avoid membrane fouling [230-232].

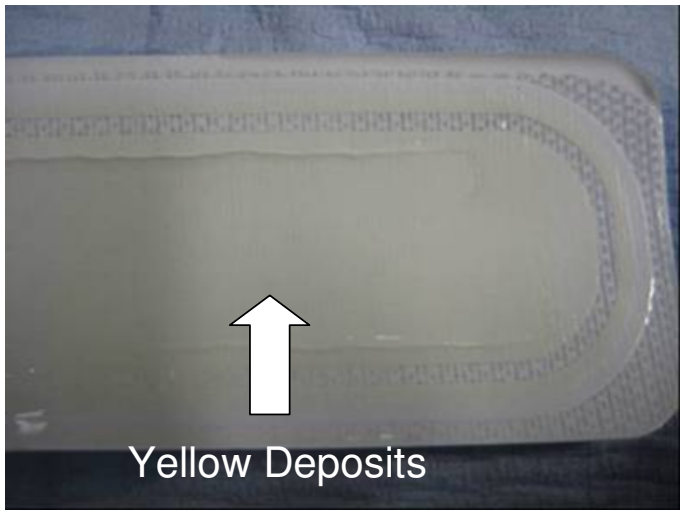

Figure 3.15 Membrane deposit

Experiments with this new pump performed by the manufacturer (see Appendix A, section A.5 for details) clearly demonstrated that the new Hydra-Cell pump also leaked oil into the system.

Finally, to make sure that the pressure dampener had no influence in this problem, this equipment was opened to confirm that the contamination did not originate from inside it. Photographs of the open dampener are displayed in Figure 3.16.

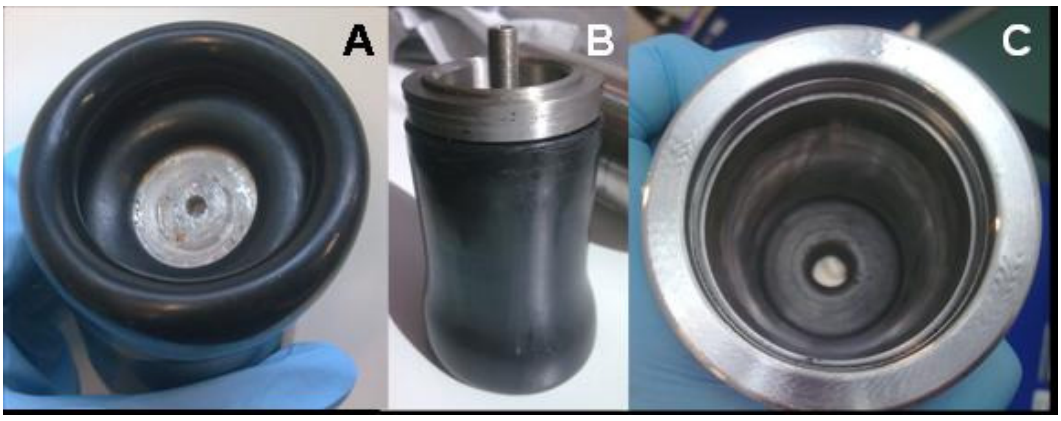

Figure 3.16 Opened dampener

The circulating fluid enters the bottom part of the dampener (opened hole at the bottom in Figure 3.16 C) and is in contact with the bottom part of the dampener in Figure 3.16 B, shown in Figure 3.16 A. The dampener, when full of nitrogen gas, swells up and is compressed against the metallic walls in Figure 3.16 C. As can be seen, both the dampener and the metallic case were clean and intact, with no visible source of the deposits. The fact that the dampener was not the source of the contamination was confirmed in the protocols described by removing it from the system and checking that the deposits persisted, as previously mentioned.

3.3.3 Redesign of the System

The tests performed at the manufacturer of the Hydra-Cell pump clearly indicated that the pump head required an improvement in order to prevent oil from leaking.

The pump head was hence modified by the manufacturer by inserting a new inlay in the metal surface where the diaphragm is inserted and also by modifying the diaphragm geometry. As can be seen in Figure 3.17 the resistance to the oil passage around the diaphragm was substantially increased with the inserted recesses and the new diaphragm design, compared to the old design (see Appendix A, section A.5 for details).

After these modifications and using Viton diaphragms the membrane contamination disappeared, i.e. no deposits on the membrane or measurable TOC in the solution were obtained. Contrary to the Speck pump, this pump allows for a pressure and flow rate variation of less than 2%, which allowed the removal of the pressure dampener from the system.

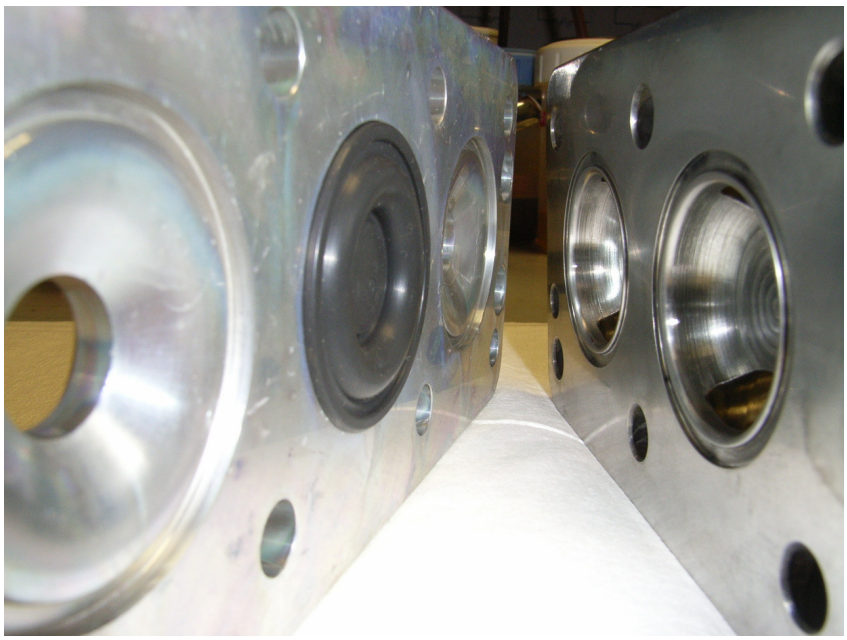

Figure 3.17 Modifications on the pump head

The presence of large amounts of contamination had a clear impact on the membrane performance in the removal of radiolabelled E2. The effect of oil in the removal of E2 is shown in Figure 3.18. For the case of contamination, and after 4 hours of recirculation the hormone feed concentration decreases drastically, showing a high adsorption of the hormone onto the membrane, as previously reported for the adsorption of iron hydroxides in reverse osmosis membranes fouled with oil from a pump [221]. Any decrease in the feed concentration is caused by adsorption of estradiol in the membrane. Estradiol adsorption in the system without a membrane was carried out with a variation in the feed concentration of less than 5%. Adsorption in the system is therefore negligible. Total adsorption at the end of the experiment was found to be 77 ng of estradiol with contamination *vs* 30 ng in a clean experiment. The retention was also substantially different with 18% retention with the contamination *vs* 50% retention in the clean system.

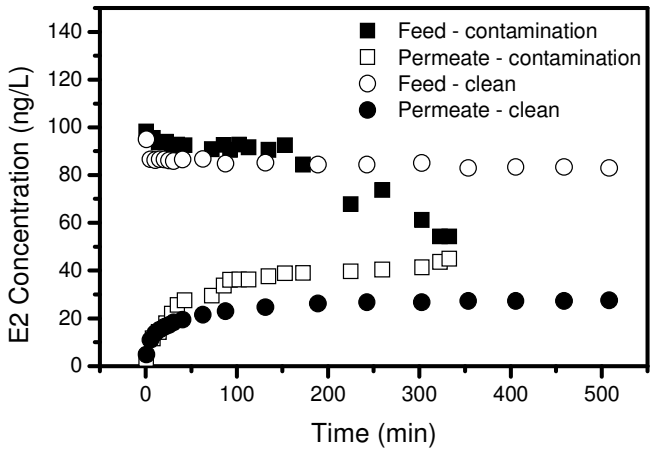

Figure 3.18 Estradiol (E2) feed and permeate concentrations as a function of time in a cross-flow system with and without Hydra-Cell contamination ($C_{feed\ E2}$=100 ng/L, 1 mM of $NaHCO_3$, 10 mM of NaCl, 5 bar and Re_h=427, NF 270)

The present section extensively describes the consequences of an ill-designed cross-flow system for the research study of removal of hormones by NF membranes. Firstly, the poor performance of the pump caused the membrane active layer to be ripped from the support layer and the E2 retention by the membrane being less than 15% compared to an expected value above 80% (Chapter 4). This was caused by the delivery of high feed flow rates to the membrane cell causing high shear stresses at the membrane surface. Secondly, the presence of oil contamination from the pump affected the membrane performance and gave different results compared to results in the absence of oil. This did not allow the fundamental study of the removal of hormones by NF membranes due to the unpredictability and lack of control in the system performance. Furthermore, the lack of control on how much oil was inserted in the system rendered the study of the influence of oil in the removal of hormones impossible, as results would not be comparable.

3.4. Final and Well-Designed Filtration Set-Up

The final cross-flow stainless steel system used, presented in Figure 3.19, is the result of several modifications carried out in the original system bought (MMS, Switzerland). The system has a 2.5 L feed tank with a cooling jacket and a high

pressure pump (P200 from Hydra-Cell, UK) was used. The system was connected to a flat sheet membrane cell (MMS, Switzerland) with a slit type channel height of 1 mm, width of 25 mm and length of 191 mm (Figure 3.3). Temperature was monitored in the retentate by a temperature indicator (WTM Pt 100-0-6 from Condustrie-Metag, Germany) and maintained at 24ºC ± 0.5ºC using a cooling jacket with a surface of 0.09 m^2 connected to a temperature controlled water bath (WK 700, Lauda). A back pressure regulator (KPB1N0A415P60000, Swagelok, UK) allows the pressurization of the system up to 130 bar. The pressure was monitored in both feed and retentate side of the membrane cell with two pressure transducers (S model, Swagelok, UK). The membrane cell holds a membrane of 46 cm^2. The feed flow was measured using a flow meter (M2SSPI from Hydrasun, UK). Datalogging was set-up allowing for data collection of membrane cell inlet and outlet pressure, feed flow rate and temperature (DAQ 55 Omega, UK). The permeate mass was measured using an Ohaus Adventurer Pro electronic balance (Leicester, UK). The P&ID of the cross-flow filtration system is depicted in Figure 3.19.

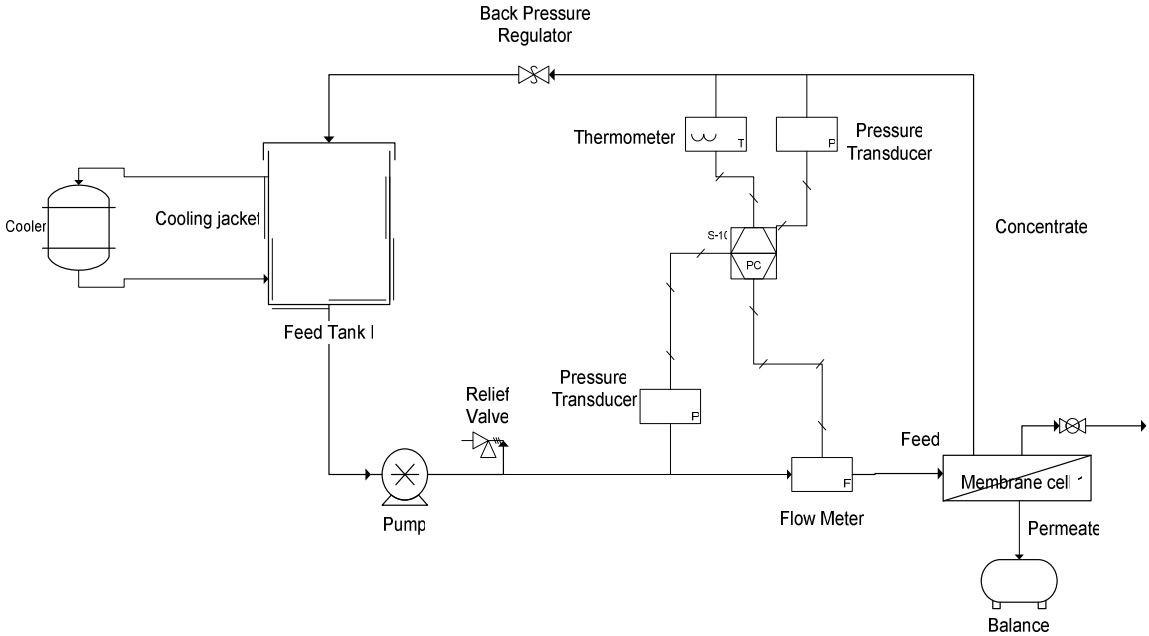

Figure 3.19 P&ID of the cross-flow filtration system

Once the cross-flow system was modified in order to allow the mimicking of spiral-wound modules (*i.e.* similar hydrodynamic conditions), and in the absence

of oil contamination from the pump, this allowed carrying out the work focused in understanding the fundamentals of the removal mechanisms of hormones by NF membranes. The following sections describe the equipment and chemicals used.

3.5. NF Membranes

Five different commercial thin film composite (TFC) membranes were chosen to study the removal mechanisms of hormones by NF membranes: the NF 270, NF 90 and BW 30 (FilmTec Corp., MN, USA) and the TFC-SR2 and TFC-SR3 (Koch membranes). Their characteristics can be found in Table 3.3. In the cases of the NF 270 and the TFC SR2 two batches with different permeabilities were used as will be discussed in the next sections.

Table 3.3 Membranes manufacturers and materials (as indicated by manufacturers)

Membrane	**Type**	**Manufacturer**	**Material**
BW30	NF/RO	Dow Filmtec	Aromatic Polyamide on Polysulphone
NF 90	NF		
NF 270			Polypiperazine Polyamide on Polysulphone
TFC-SR2		Koch Membrane	Aromatic Polyamide on Polysulphone
TFC-SR3			

The membranes span a wide spectrum of pore size, molecular weight cut off (MWCO) or sodium chloride (NaCl) rejection, from the tight NF/RO BW30 to the loose NF TFC-SR2. Besides these characteristics, which are directly related to solute rejection, other membrane characteristics such as roughness and surface charge play an important role in solute removal.

The next section presents membrane characteristics measured, such as the MWCO, hydrophobicity and roughness.

3.5.1 Membrane Molecular Weight Cut-Off (MWCO), Sodium Chloride Rejection and Permeability

NF membranes are usually characterized in terms of removal by their permeability, MWCO and their NaCl rejection.

The membrane permeability is determined by the flux of pure water as a function of pressure (equation 2.4) and is dependent on the pore radius, porosity and thickness of the membranes active layer. The permeability determination for four NF membranes is shown in Figure 3.20. Despite the TFC-SR2 being looser than the NF 270, its permeability is the lowest, showing the effect of porosity and thickness in the flux of water through the membrane. The results for different membranes are presented in Table 3.4.

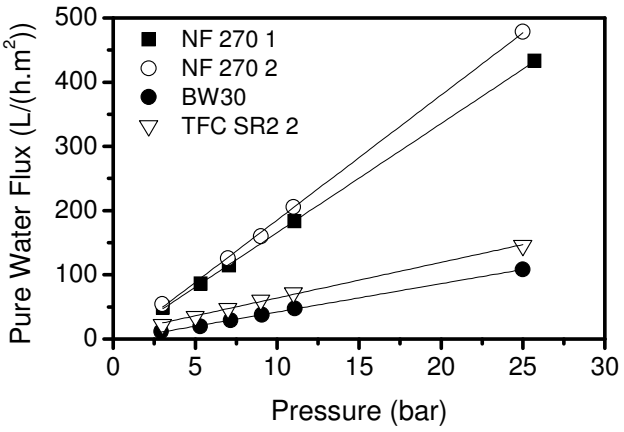

Figure 3.20 Pure water permeability for several NF membranes

The MWCO (in Da or $g.mol^{-1}$) gives the size of the compound that is 90% rejected. The MWCO determination for the NF 270 1 is shown in Figure 3.21. For this membrane, the MWCO was found to be of 180 $g.mol^{-1}$. The MWCO determined for the other membranes in represented in Table 3.4. The membrane TFC-SR 2 is found to have the highest MWCO of 485 $g.mol^{-1}$, meaning the membrane is the loosest one. On the other side of the scale are the NF 90 and BW 30 membranes with a MWCO lower than 90 $g.mol^{-1}$.

Table 3.4 Membranes MWCO, NaCl rejection and permeability (values found in the literature are added in brackets for comparison)

Membrane	**Permeability ($L.h^{-1}.m^{-2}.bar^{-1}$)**	**MWCO at 90% rejection (Da)**	**NaCl Rejection (%) (0.1 M, 10 bar)**
BW30	4.1 ± 0.3 (6.1[233])	88 (98[233])	99.8 (94[233])
NF 90	10.6 ± 1.6 (5.2[233], 6.4 [31])	70 (100[233])	88.7 (92[233], 85 [31])
TFC-SR2 1	12.5 ± 2.3 (15.4 [31])	485	9.8 (9.8 [31])
TFC-SR2 2	7.2 ± 0.6	-	23.4
TFC-SR3	6.7 ± 0.8	167	40.8
NF 270 1	17.0 ± 0.8 (8.5[233], 13.5 [31])	180 (155[233], 170)	52 (59[233], 40 [31])
NF 270 2	19.4 ± 1.0	-	40

NaCl rejection gives the rejection of NaCl yielded by the membrane at a certain pressure. NaCl rejection for the membranes chosen is presented in Table 3.4. In general, rejection decreases with increase of membrane MWCO. Some exceptions are however found, which can be explained by the fact that NaCl rejection is not only achieved by size exclusion, but also by charge repulsion. Differences in membrane surface charge will influence NaCl retention.

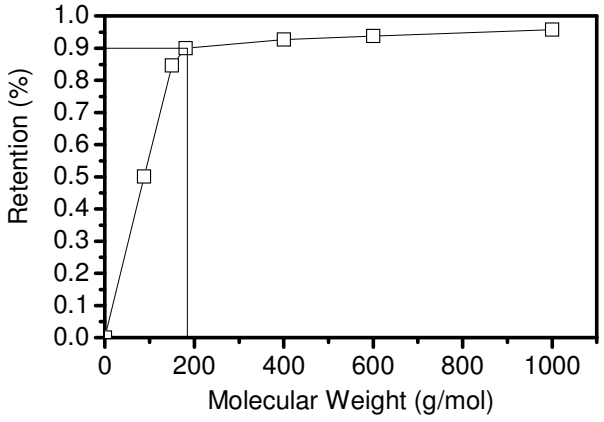

Figure 3.21 MWCO determination for the NF 270 1

In chapter 4, 5 and 7 the NF 270 1 and TFC-SR2 2 membranes were used. In chapter 6 all batches were used as will be identified along the text.

3.5.2 Membrane Morphology

Besides having different permeabilities and removal capacity, membranes also have different surface properties.

Atomic Force Microscopy (AFM) is a tool that can be used to measure the surface roughness of the membranes. This instrument consists of a cantilever with a sharp tip at its extremity, used to scan the surface of the studied material. The cantilever tip is moved along the surface and variations in membrane roughness cause the cantilever to move and bend.

The membranes roughness was measured by AFM (from former Veeco, now Bruker Corporation, USA) with a cantilever Micromask CSC38/AIBS-B. This cantilever uses a resonance frequency of 10 kHz, has a spring constant of 0.03 $N.m^{-1}$ and a size of 350 µm for length, 35 µm width and 1 µm thickness. The uncoated probe tip radius is of 10 nm with a full tip cone angle of 40°. The measurements were carried out with contact mode in liquid and a scan size of 2.0 x 2.0 µm. Two types of roughness were measured: the mean roughness (R_A), which represents the arithmetic average of the deviations from the centre plane and the root mean square roughness (R_{RMS}), which is the standard deviation of the two values within a given area. Results are presented in Table 3.5, along with results found in the literature, for comparison.

Table 3.5 Membranes roughness

Membrane	**R_A (nm)**	**R_{RMS} (nm)**	**R_A literature (nm)**	**R_{RMS} literature (nm)**
TFC SR2	17.9 ± 0.6	23.0 ± 1.3	10[234], 8.13[33]	15.6 [235]
TFC SR3	5.2 ± 0.6	6.8 ± 0.7	-	-
BW 30	67.7 ± 2.4	83.9 ± 3.8	60[234]	61[233], 65 [235], 68.3[236]
NF 90	61.7 ± 2.1	78.5 ± 3.6	70[234], 76.8[33]	108.9 [235], 129.5[236]
NF 270	4.2 ± 0.3	5.5 ± 0.4	5[234], 5.5[237], 8.55[33]	4.6[233], 14.6 [235], 9[236]

The tighter NF 90 and BW 30 have a much higher roughness than any of the other membranes, which is characteristic of dense membranes. The membranes with the lowest roughness are the TFC SR3, the NF 270 and the TFC SR2.

3.5.3 Membrane Layer Thickness

TFC NF membranes are asymmetrical membranes made of three different layers. The bottom support layer is made of polyester and the second support layer is made of polysulphone. These two layers give mechanical support to the active layer but have no resistance to flux and no selectivity towards the removal of compounds. The top layer, which is very dense, is called the active layer and is commonly made of polyamide (Figure 3.22). This layer is the selective layer that presents resistance to the permeate flux and to solute passage. The exact composition of these membranes is however unknown and a property of the manufacturer.

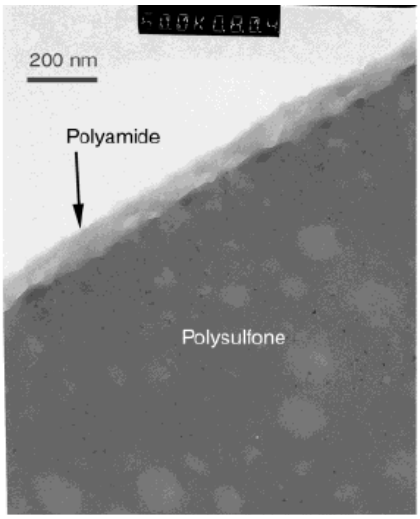

Figure 3.22 Cross-sectional TEM image of an NF membrane [238]

Several studies have reported active layer thicknesses for the TFC membranes ranging from 15 nm up to 400 nm. Their results are presented in Table 3.6. In general, the membranes will have thicker active layers the closer they are to RO properties.

Table 3.6 Active layer thicknesses of membranes from the literature

Membrane	**Average Active Layer Thickness δ (nm)**	**Method**
BW30	200-300 [239]	TEM
NF 90	174 [31, 240, 241]	RBS Spectrum of Sulphur
NF 270	20 [242]; 25 [243]; 15-40 [244]	RBS Spectrum of Sulphur, AFM, SEM

The active layer thicknesses for the studied membranes were obtained from TEM measurements for the TFC-SR2, the NF 270 and the NF 90 membrane [245]. The image results are shown in Figure 3.23. The BW30 thickness was obtained from the literature [239] and since no results are reported in the literature for the TFC-SR3, a thickness of 400 nm (maximum thickness reported for NF membranes) was assumed. References from the literature are provided in Table 3.6 for similar values obtained for the active layer thickness.

Table 3.7 Active layer thicknesses of membranes

Membranes	**Average Active Layer Thickness (nm)**
BW30	233 ± 88
NF90	218 ± 40
TFC-SR2	345 ± 28
TFC-SR3	400 ± 10
NF 270	21 ± 2.4

The average active layer thicknesses and thickness variability (Table 3.7) were determined from the TEM pictures with Image J (version 1.40) as can be seen in Appendix B. For the TFC-SR3, since there are no images available for the thickness, a variability of 10 nm was considered. A similar value as the membrane roughness was chosen since, as can be seen in Table 3.5 and Table 3.7, the variability

obtained in the thickness from the TEM images correlates with the roughness of the active layer.

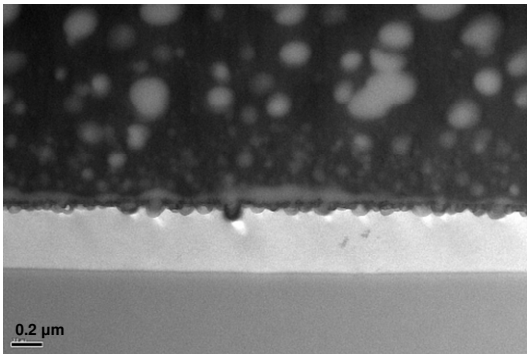

TFC-SR2

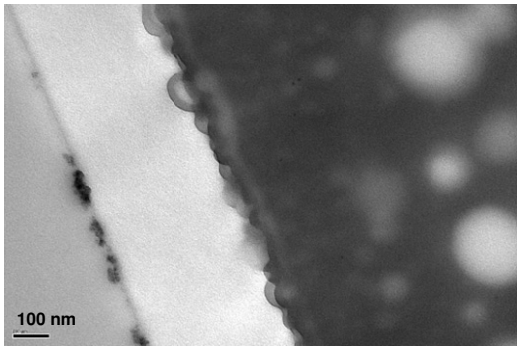

TFC-SR2

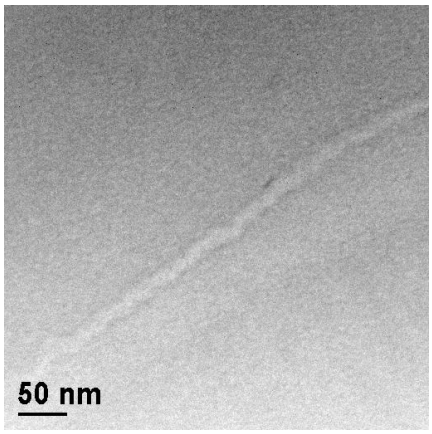

NF 270

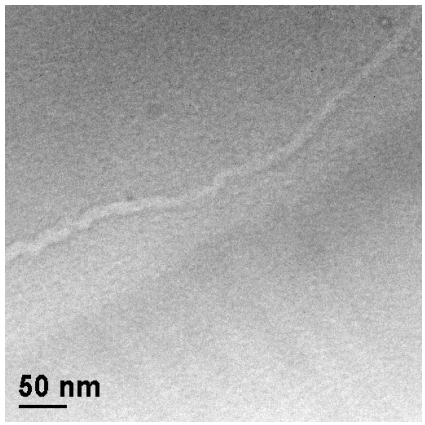

NF 270

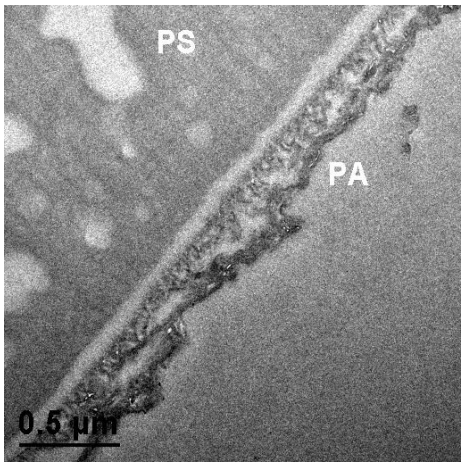

NF 90

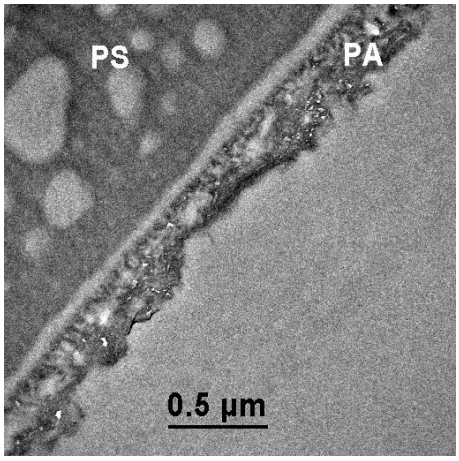

NF 90

Figure 3.23 TEM image of the TFC SR2 [246], the NF 270 and the NF 90 (courtesy of Prof. Polizzi and Dr. Davide Cristofori (University of Ca' Foscari Venezia, Italy))

3.5.4 Membrane Surface Charge

Membranes are known to have surface charge given by streaming potential measurements [32, 41, 157-159]. The membrane surface charge is generally positive up to pH 5, becomes neutral at the isoelectric point (IEP) and then becomes negative at more alkaline pH. Such charge results from chemical modification of polymer surfaces. Actual charge depends on membrane polymer characteristics, functional group content as well as solution chemistry such as pH and ionic strength.

Streaming potential of flat sheet nanofiltration membranes was measured using the electrokinetic analyser EKA, (Anton Paar KG, Gratz, Austria) with an electrolyte solution of 20 mM NaCl, and 1 mM $NaHCO_3$. The isoelectric point (IEP) and the streaming potential values at pH 11 are shown in Table 3.8 along with values found in the literature for comparison purposes. The NF 90 results presented are the ones found in the literature.

As can be seen in Table 3.8, the IEP point for all the membranes varies between 3.6 and 4.3. The Streaming potential values at pH 11 are also very similar, varying from -15 mV to -25 mV. These results show that despite possible functional modifications, membrane surface charge values are similar.

Table 3.8 IEP (pH) and streaming potential (mV) values of the membranes at pH 11

Membrane	**NF 270**	**TFC-SR2**	**TFC-SR3**	**BW 30**	**NF 90[234]**
IEP	3.6	4.3	3.8	4.2	4.0
IEP (Literature)	3.5 – 3.8 [31, 233, 247]	3 [31]	-	3.5 – 5.5 [233, 239, 247]	3.5 – 5.4 [31, 233, 247]
Streaming Potential	-25	-25	-25	-20	-15
Streaming Potential (Literature, pH 10-11)	-26 – -24 [31, 233, 243], -40[247]	-10 [31]	-19 [201]	-22.9 – -5 [233, 239, 247]	-40 – -20 [31, 233, 247]

3.5.5 Membrane Contact Angle

Due to different functional groups present in the NF membranes as a consequence of the manufacturers' chemical surface modification, NF membranes can have different hydrophobicities. Hydrophobicity is a measure of how much a surface will have the tendency to be wet. The more hydrophobic a surface is, the less wet it will become.

Membrane surface hydrophobicity is given by contact angle measurements. The higher the contact angle between a drop of water (placed on the membrane surface) and the membrane surface is, the more hydrophobic the membrane surface will be. Contact angle of the flat sheet membranes was measured with the sessile drop method using the instrument Easy Drop Kruss (model FM40, Germany). Results are shown in Table 3.9.

Whilst TFC-SR2 is the most hydrophobic membrane with a contact angle of 62º, the NF 270 membrane is the more hydrophilic one, with a contact angle of 30º.

Table 3.9 Membranes contact angle

Membrane	**NF-270**	**TFC-SR2**	**TFC-SR3**	**BW30**	**NF 90**
Contact angle (º)	29.1 ± 1.6	61.5 ± 2.5	48.5 ± 1.4	40.3 ± 1.1	47.9 ± 1.7
Literature	14.6-55 [31, 233, 243]	30.7-61.2 [31, 162, 201, 235]	44.6 [201]	43.8-65 [233, 235]	42-54 [31, 233]

3.6. Chemicals

3.6.1 Hormones

Tritium labeled hormones were used due to very low detection limit, small sample volumes required and extremely high accuracy. The radiolabelled hormone [2,4,6,7-^{3}H] estrone (E1) was purchased from Perkin Elmer, UK (3.3 TBq.mmol^{-1}), and the hormone [2,4,6,7-^{3}H] 17β-estradiol (E2) was purchased from GE Healthcare (3.11 TBq.mmol^{-1}), UK and Perkin Elmer (2.59 TBq.mmol^{-1}), UK.

A stock solution of 100 μg.L^{-1} was prepared in methanol from the initial stock. An initial feed concentration of 100 ng.L^{-1} was used in all the experiments, unless otherwise stated. The isotherm experiments were carried out at concentrations varying from 25 ng.L^{-1} to 2 mg.L^{-1} for E2 and 25 ng.L^{-1} to 200 ng.L^{-1} for E1. For concentrations greater than 200 ng.L^{-1}, radiolabelled hormones were mixed with non labeled hormones (98% purity) (Sigma Aldrich, Gillingham, UK).

The hormone chemical properties are found in Table 3.10. The molecular weight (MW) of the hormones is very similar, varying between 270 and 272 g.mol^{-1}. The pK_a shows the acid dissociation constant at which the hormones lose a hydrogen atom in the hydroxyl group of the phenol, and become negatively charged. The hormones that have a phenolic hydroxyl group all dissociate in the same pH range, between 10.2 and 10.4.

The Log K_{OW} parameter measures the hydrophobicity of the hormones by measuring the partitioning of the hormone between octanol and water. As a general rule of thumb, compounds with Log K_{OW}>2.5 are expected to accumulate in solid phases instead of being soluble in the aqueous phase. The Log K_{OW} values for the hormones described in Table 3.10 are above 2.5, indicating a tendency to accumulate in solid phases.

Estrogen solubility in water is reasonably low (3.6 to 147 mg.L^{-1}) with significant variability in published data. Dipole moments give an indication on the polarity of the molecules and vary from 2.2 to 3.36 Debye.

The Stokes-Einstein equation (3.2) was used to calculate the hormones equivalent sphere radius:

$$r_s = \frac{kT}{6\pi\mu D_\infty} \qquad (3.2)$$

where r_s is the hormone radius (m), T is the temperature (K), k is the Boltzman constant (J.K^{-1}), D_∞ (m^2.s^{-1}) is the hormone diffusivity and μ is the solution dynamic viscosity (Pa.s).

The hormones diffusivity D_∞ ($m^2.s^{-1}$) was determined with the Worch equation [248]:

$$D_\infty = 3.595.10^{-14} \frac{T}{\mu \times MW^{0.53}} \quad (3.3)$$

where MW ($g.mol^{-1}$) is the molecular weight.

Table 3.10 Hormone properties

Compound	**Molecular Formula**	**CAS No.**	**Mol Structure**	**MW ($g.mol^{-1}$)**	**Solubility in water ($mg.L^{-1}$)**	**pK_a**	**Log K_{ow}**	**Dipole moment (Debye)**
17- β Estradiol (E2)	$C_{18}H_{24}O_2$	50-28-2	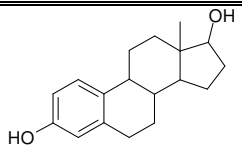	272	3.6, 82 [a,c,h]	10.23 [b]	4.01 [d]	2.2 [e], 2.7 [g]
Estrone (E1)	$C_{18}H_{22}O_2$	53-16-7	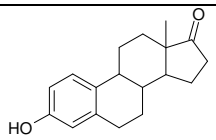	270	13, 147 [c,f,h]	10.34 [b]	3.13 [d]	2.1 [e], 3.4 [g]

[a] [24], [b] [180], [c] [153], [d] [182], [e] [183], [f] [32], [g] [249], [h] [250]

The results obtained for the hormones diffusivity and radius are presented in Table 3.11:

Table 3.11 Estrone (E1) and estradiol (E2) diffusivities and Stokes radius

Hormone	**D_∞ ($m^2.s^{-1}$)**	**r_s (nm)**
estrone E1	$5.87.10^{-10}$	0.396
17-β-estradiol E2	$5.85.10^{-10}$	0.402

3.6.2 Polymers

Several polymers were used to study their adsorption capacity of hormones. A more in depth study on the adsorption with the polymers that constitute the different TFC NF membrane layers was carried out: polyamide (PA), polyethylene teraphtalate (PET), polyethylene naphtalate (PEN) and polysulphone (PSu).

All the polymers were purchased from Goodfellow (Huntingdon, UK) in the form of 2 to 3 mm granules and polysulphone (PSu) and polyvinylidene fluoride (PVDF) were kindly offered from Solvay (Brussels, Belgium) in granular form. Poly(2,6 dimethyl 1,4-phenylene oxide) (PPO), polyacrylate, poly(methyl methacrylate) (PMMA) and cellulose (CEL) were purchased from Sigma Aldrich (UK) in powder form.

Polymers in granular form were ground to a size of 500 μm with a Retsch Ultra Centrifugal Mill ZM 200 (Leeds, UK), in three stages using sieves with 1000, 750 and 500 μm openings. The ground polymer surface area was determined by electron microscopy and analysed with the software Image J (version 1.40), assuming that particles have a spherical shape.

3.6.3 Chemicals and Background Electrolyte

All chemicals were of analytical grade and were purchased from Fisher Scientific (Loughborough, UK). When stated, the feed solution was buffered using 1 mM $NaHCO_3$ with 20 mM NaCl to act as a background electrolyte. In the pH effect studies, pH was adjusted up to pH 11 using 1 M NaOH. Pure water (18.2 $\mu\Omega.cm^{-1}$) was obtained from Elga PURELAB Ultra (High Wycombe, UK). For the desorption of hormone from the membranes pure acetone was used.

For the membrane pore size and MWCO characterisation organic tracers were used: dioxane, dextrose, methanol (Fisher Scientific, UK), xylose (Acros Organics, UK) and PEG 400, 600 and 1000 (Fisher Scientific, UK).

3.7. Analytical Equipment

3.7.1 Scintillation Counter

The radioactivity of the hormones was measured with a Beckman LS 6500 scintillation counter (Fullerton, USA) in disintegrations per minute. A volume of 0.5 mL of sample was placed in 20 mL scintillation vials (Perkin Elmer, UK) with 4 mL of Ultima Gold LLT (Perkin Elmer, UK) and counted in triplicate for 10 minutes each.

The activity of the samples was converted to hormone concentration in $ng.L^{-1}$ based on a calibration curve of hormone concentration up to 1000 $ng.L^{-1}$. The average detection limit of this method is 1 $ng.L^{-1}$ for the hormones studied (See Appendix C).

3.7.2 Total Organic Carbon Analyser

The organic permeate and feed samples used for the membrane pore size and MWCO characterisation were measured using a total organic carbon analyser (TOC-V CPH) in non-purgeable organic carbon (NPOC) mode (Shimadzu, Milton Keyes, UK). Prior to analysis the samples were acidified using 2 M HCl and sparged for 1.5 minutes with N_2 to remove inorganic carbon (See Appendix C).

3.8. Protocols

3.8.1 Hormone Filtration in the Absence of Background Electrolyte

The filtration protocol used in the hormone experiments is described as follows. The membrane coupon was gently washed and stored in MilliQ water for at least 12 hours. The membrane was then placed in the cross-flow cell and compacted for two hours with MilliQ water at 25 bar. The pure water flux was then measured at 25 bar for at least 30 minutes to ensure steady flux followed by flux measurement at the experimental pressure for ten minutes. The system was then drained of the MilliQ

water used and a volume of 1.5 L of fresh MilliQ water was recirculated in the system for one hour at a set hydrodynamic condition by varying pressure (3 to 17 bar) or Re_h number (400 to 1500) to make sure all the process parameters were constant. The Re_h number is changed by varying the feed flow rate or, indirectly, the velocity in the feed channel. For NF spiral-wound membranes the realistic operating range for aqueous solutions varies from 3 to 20 bar for pressure [251] and from 100 to 1000 for Re_h [229].

Feed and permeate samples were taken of the MilliQ water to ensure no hormone contamination of the system occurred. The feed tank was then spiked with hormone solution (0.5 L) to reach the required concentration in the system and mixed well using a mechanic stirrer (200 rpm). The feed and permeate concentrations were measured at regular time intervals (every five minutes for the first half hour and then once every hour) to obtain the transient trend until equilibrium was reached (average of 8 hours). The normalized permeate transient flux (J/J_0) is obtained by dividing the permeate transient flux (J, obtained by weighing the amount of permeate mass collected in one minute) by the pure water flux (J_0) measured before spiking the hormones. The system was operated in recirculation mode. New membranes were used for every experiment with a permeability variation of less than ± 10% (Table 3.4). The transient hormone mass adsorbed was then obtained by mass balance to the feed tank. As a control experiment, adsorption of hormone onto the filtration system in the absence of membrane was investigated. A feed concentration of 100 $ng.L^{-1}$ of E2 was recirculated in the system for 8 hours. A difference in feed concentration of less than 5% was obtained with time showing that for the duration of the experiments, no significant adsorption occurred onto the system.

The feed and permeate pH and conductivity were regularly measured with a pH/Cond 340i meter (WTW, Germany).

Details on the variability of the hormones cross-flow experiments can be found in Appendix D.

3.8.2 Hormone Filtration in the Presence of Background Electrolyte

The previous protocol was followed when studying hormone rejection and adsorption in the presence of background electrolyte except that instead of recirculating MilliQ water for one hour prior to spiking the hormones, 1.5 L of MilliQ water with background electrolyte solution (1 mM $NaHCO_3$ with 20 mM NaCl) was recirculated for one hour before spiking the hormones. This was enough time to reach steady-state of salt rejection. The 0.5 L of hormone solution with the same background electrolyte concentration as the one in the recirculating solution was then spiked to the feed tank and well mixed as before. The feed and permeate pH and conductivity were regularly measured with a pH/Cond 340i meter (WTW, Germany).

3.8.3 Membrane Characterisation and MWCO

The same protocol as the one used for the hormone filtration was adopted in the membrane characterisation, except that the feed solution with 25 $mgC.L^{-1}$ of organics was initially placed in the feed tank and not spiked in the system. For the membrane characterisation experiments with the different PEG, xylose, dioxane, methanol and dextrose the feed flow rate was set to 2 $L.min^{-1}$ (equivalent to a Re_h=1450) to avoid concentration polarization and the pressure was varied every hour between 3 bar and 11 bar. At each pressure 15 mL of feed and permeate samples were taken and analysed in the TOC and the permeate flux was measured.

Additional organic retention experiments with xylose, dioxane and dextrose were carried out in the cross-flow system with the feed flow rate set to 0.6 $L.min^{-1}$ (equivalent to a Re_h=427) and the pressure varying every hour between 3 bar and 11 bar.

3.8.4 Membrane Static Adsorption

The hormones pseudo-first order sorption rate constant for the NF membranes were determined in static mode with an excess of membrane area in order to maximize the contact between the hormone and the membrane surface. Hormone adsorption isotherms were carried out in static mode in glass bottles with 60 mL solution of the relevant hormone concentration with pieces of the membrane (45 cm^2 cut into 5 cm^2 pieces), placed in a Certomat BS-1 UHK-25 shaker (Göttingen, Germany) at 200 rpm and 25ºC.

The same procedure was carried out to determine the different affinities of the hormones onto the different membranes with an excess of hormone, where 2 cm^2 of membrane area was used.

3.8.5 Polymer Static Adsorption

Radiolabelled [2,4,6,7-3H] 17β-estradiol was used to prepare 60 mL of 100 $ng.L^{-1}$ solutions. Several weights of the polymer varying from 0.25 g to 3.1 g were added into separate estradiol solutions and the solutions mixed in a Certomat BS-1 UHK-25 shaker (Göttingen, Germany) at 200 rpm and 25ºC. Samples of 1 mL were taken with 1 mL syringes at certain time intervals and filtered through 0.7 μm glass microfibre filters (Fisher, Loughborough, UK) which were placed in Millipore Swinnex filter supports (Ireland). Based on the results of preliminary experiments where glassfibre filters were chosen due to their lowest sorption of estradiol, after the third sample filtration, the filter reached saturation and the adsorption calculated was due to polymer adsorption. The other filters tested were 0.05 μm cellulose esters (mix of cellulose acetate with cellulose nitrate from Millipore, VMWP02500, UK), 0.1 μm PVDF (Millipore, VVLP04700), 0.45 μm nylon (Whatman 7404-004, UK) and 0.45 μm cellulose acetate (Sartorius Stedim 11106-47-N, UK).

3.8.6 Membrane Desorption

Different desorption experiments of E1 from the NF 270 membrane were carried out:

- Static desorption from a 2×5 cm rectangle of cross-flow pre-saturated membranes at different pressures. The polyester (PE_m) bottom layer was physically separated from the top layers of polyamide and polysulfone (PA_m+PSu_m). These were placed separately in 25 mL of acetone in a Certomat BS-1 UHK-25 (Göttingen, Germany) incubator shaker at 200 rpm and 25ºC for at least 48 hours, when the hormone concentration was measured. Acetone was found to have no influence in the counting process.
- Static desorption experiments from pre-saturated membranes in static mode (no pressure). 15 mm of diameter of membrane pieces were placed in 60 mL of E1 solutions (50, 100 and 500 $ng.L^{-1}$) and left to adsorb in the shaker for at least 48 hours. Once saturation reached steady-state, the membrane pieces were removed from the solutions, left to dry for a few minutes and then placed back in the shaker in 10 mL acetone and left to desorb for at least 48 hours.
- Filtration desorption at 11 bar from a cross-flow pre-saturated membrane (C_{feed} E1=50 ng/L, P=11 bar, Re_h=427). Filtration desorption was first carried out with MilliQ water then with 2% acetone solution.

3.8.7 Diffusion Cell

A diffusion cell was used to measure the adsorption of hormones on the NF 270 membrane PA_m and PSu_m surfaces separately.

The membrane was gently washed with MilliQ water and PA_m+PSu_m was physically peeled from PE_m. The PA_m+PSu_m was then cut to 40 mm of diameter and placed in a diffusion cell of 25 mm diameter. The diffusion cell is made of glass and has two cells of 150 mL each which are constantly stirred with a stirrer (Fisher

Scientific, UK) at 1000 rpm. The membrane is placed between the two cells, tightened with clamps, with each side of the membrane facing a different cell.

A solution of 125 mL of hormone at a determined concentration is placed in each cell for 8 hours. Concentrations of 100 $ng.L^{-1}$ for both hormones, 20 $ng.L^{-1}$ for E1 and 30 $ng.L^{-1}$ for E2 were placed in contact with PA_m and PSu_m to mimic filtration conditions. Hormone samples were taken at regular intervals and measured in the scintillation counter. The amount adsorbed was obtained by mass balance to each feed cell.

4 Hydrodynamics Influence on Adsorption

4.1. Introduction

Trace contaminants such as hormones, pesticides and pharmaceuticals have been found to adsorb on NF and RO polymeric membranes [23, 24, 26-30, 32-36, 142, 155, 160], contributing to the removal of compounds alongside the well established mechanisms of steric exclusion [25-28, 60, 146-150] and charge repulsion [25, 28, 37, 40, 150, 152, 159-162]. Despite adsorption causing a lower retention than would otherwise be expected by NF membranes [23], this mechanism is to date not well understood.

Adsorption of trace contaminants occurring in bench-scale and full-scale applications has several negative implications showing the need to understand the fundamentals of this phenomenon. Firstly, adsorption lowers substantially the retention expected if only steric interactions are considered [23, 160], showing that membrane retention is adsorption dependent. Secondly, adsorption does not occur only in the initial stages of filtration. It has been shown that after each cleaning cycle, adsorbed trace contaminants can be desorbed from the membrane [178, 179], allowing for adsorption to occur again. The adsorption phenomenon is however not understood since studies of adsorbing compounds are usually carried out once the membrane has been pre-saturated with the contaminant [24, 252].

Furthermore, if the study is carried out in a period of time shorter than the required, differing conclusions can be drawn from the results [32, 41]. Whilst a membrane is saturating, the permeate concentration is initially very low, which could lead to the conclusion that the membrane performs well, both in bench-scale [175] and full-scale [176] applications. Bench-scale membrane saturation usually takes a few hours [23, 152] whilst full modules can take more than 4 days [162, 176, 177]. In fact Cornelissen *et al.* [176] did not detect xeno-estrogens in the permeate after 5

days of filtration due to the continuous adsorption onto the membrane module. In the bench-scale study by Steinle-Darling *et al.* [175], no contaminant was detected for 8 hours in the permeate due to adsorption.

The accumulation of contaminants on the polymeric membranes poses a risk since the contaminants can desorb from the membrane during operation or cleaning and contaminate the permeate [152, 178, 179]. A continuous adsorption-desorption phenomenon can occur during operation caused by fluctuations in feed concentration [152, 178]. For example, if the feed concentration increases, due to fluctuations in the membrane plant inlet, this causes the contaminant adsorption and permeation through the membrane [152].

Trace contaminant removal by NF membranes can therefore be difficult to predict due to the occurrence of adsorption, showing the need in understanding what operation parameters affect it. Understanding the mechanisms involved in the removal of adsorbing trace contaminants by NF membranes at bench-scale will contribute to the understanding of the removal of these in full-scale applications, since the same removal mechanisms are involved.

Several studies have shown that parameters such as feed concentration affect the adsorption of hormones onto NF membranes. Adsorption was found to increase linearly with increasing hormone feed concentration up to 1000 $ng.L^{-1}$ in filtration mode [172] and up to 600 $\mu g.L^{-1}$ in static mode (no pressure applied) [152, 172]. This indicates that adsorption is limited by micropollutant availability. However no studies have been carried out at concentrations close to the hormone solubility limit to confirm that the isotherm is linear for a wide hormone concentration range.

In filtration mode, once adsorption reached steady state and pure water was filtered through the membrane, hormone was released from the membrane into the permeate [152]. Release of hormone on the permeate side can occur if the feed concentration varies. It is therefore important to understand what affects adsorption to be able to control it.

Following the connection between feed conditions and micropollutant adsorption onto NF membranes, another study suggested that feed hydrodynamics affect hormone retention and adsorption [36] but no systematic study on the

influence of pressure and Reynolds number (based on channel height Re_h) was carried out. In other studies where different pressures were used [28, 37], membrane saturation was not reached for the studied contaminant. A continuous decrease in the contaminant feed concentration occurred and therefore no conclusions could be drawn on the effect of pressure in the contaminant total mass adsorbed and steady-state retention.

In the work by McCallum *et al.* [152] the influence of three pressures on the transient feed and permeate concentration of estradiol with the NF 270 membrane was studied. It was shown that pressure has an effect in the transient permeate response: the higher the pressure, the quicker the permeate concentration will reach steady-state. However, the estradiol steady-state feed and permeate concentrations were very similar for the three pressures used, showing no effect of pressure on the hormone retention. Furthermore, steady-state mass adsorbed was found not to vary with pressure, as obtained in another study [186]. In contrast, distinct differences in hormone retention when subjected to different pressures have been obtained elsewhere [153]. In this later study, the authors showed that cross-flow velocity has no effect in estrone retention and that increase of pressure decreases retention. The membranes had been pre-saturated in hormone when carrying out this study and hence, the effect of these parameters on the hormone total mass adsorbed and consequent retention for a virgin membrane were not investigated. As previously mentioned membrane retention is adsorption dependent showing the need to elucidate how filtration parameters affect NF adsorption and retention of trace contaminants.

Despite a clear relation between adsorption and lowered retention, understanding of the mechanisms involved in the removal of adsorbing contaminants by NF membranes are not well understood. In fact, studies of adsorbing compounds are usually carried out with the membrane previously pre-saturated with the contaminant [24, 174] and contradictory results have been reported in the literature [41, 153, 156, 252], showing an incomplete understanding of the adsorption phenomenon. For example, in several studies [186, 201, 252, 253] retention increases with permeate flux/pressure whilst other studies show the opposite trend [25, 153, 254].

The focus of this study was to understand how E1 and E2 adsorption and retention in a cross-flow system are affected by operating parameters of NF membrane processes, such as pressure, Reynolds number (Re_h) and feed concentration. These variables are known to contribute to concentration polarization, which has an impact in retention [255] and can therefore have an impact in the adsorption of trace contaminants. This chapter elucidates the mechanisms involved in the adsorption of hormones onto TFC NF membranes as far as membrane filtration operation conditions are concerned.

4.2. Concentration Polarisation Phenomenon

Concentration polarisation is the consequence of the formation of a concentration gradient at the membrane surface due to the accumulation of retained solutes on the feed side of the membrane. This concentration gradient is caused by a diffusive solute flux from the membrane surface to the feed bulk ($-D\frac{dC}{dx}$) which is counter-balanced by a convective flux towards the membrane surface (JC) caused by a pressure difference between the membrane feed side and its permeate side (Figure 4.1). The solute flux that permeates through the membrane is given by JC_p.

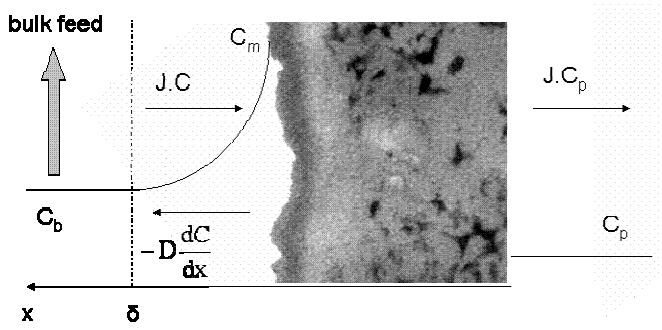

Figure 4.1 Concentration polarisation (picture adapted from Freger [242]); J is the solute flux ($m.s^{-1}$), D is the solute diffusion coefficient ($m^2.s^{-1}$), C is the solute concentration in the concentration boundary layer, C_b is the feed concentration or bulk concentration, C_m is the concentration at the membrane surface and C_p is the solute permeate concentration, (all concentrations are in $kg.m^{-3}$)

At steady-state, a balance between these two fluxes and the permeate flux results in the concentration polarisation equation (equation (4.1)),

$$\frac{C_m - C_p}{C_b - C_p} = \exp\left(\frac{J}{k}\right) \tag{4.1}$$

where C_m, C_p and C_b are the concentrations at the membrane surface, permeate and bulk feed respectively ($ng.L^{-1}$), J is the permeate flux or velocity ($m.s^{-1}$) and k is the mass transfer coefficient ($m.s^{-1}$).

The coefficient k is dependent on the hydrodynamic conditions on the membrane surface and is therefore dependent on the circulating Re_h and Schmidt numbers, which are in turn dependent on the solution characteristics, the solute characteristics and the velocity at the membrane surface.

The Reynolds number based on a slit channel height, Re_h, is given by equation (4.2),

$$Re_h = \frac{\rho v h}{\mu} \tag{4.2}$$

where v is the velocity in the feed channel ($m.s^{-1}$) and is proportional to the feed flow rate, ρ is the solution density ($kg.m^{-3}$), μ is the solution dynamic viscosity (Pa.s) and h is the characteristic flow dimension that, in the present case, is the cross-flow cell height (m). The Schmidt number Sc is given by equation (4.3):

$$Sc = \frac{\mu}{\rho D_\infty} \tag{4.3}$$

where D_∞ is the solute diffusivity ($m.s^{-2}$).

Changes in operational parameters such as pressure or permeate flux, and Re_h number affect the hydrodynamics on the feed channel and membrane surface and hence, have a significant impact on membrane retention because they affect the degree of concentration polarisation development as expressed by equation (4.1).

It is well established that to minimize concentration polarisation and therefore the concentration at the membrane surface (see equation (4.1)), one can either decrease the pressure (or J) or increase the cross-flow velocity by indirectly increasing k. Studies have shown that the higher the concentration at the membrane surface, the lower the retention will be [128, 256, 257].

Since the concentration polarization build-up at the membrane surface has impact on the retention of solutes, its impact on hormone adsorption and retention is assessed herein by studying the effect of hydrodynamic parameters using the cross-flow system described in materials and methods (Chapter 3), the NF 270 (Batch 1, NF 270 1) membrane and the TFC-SR2 membrane (Batch 2, TFC-SR2 2). By varying pressure (or indirectly J), Re_h number (or indirectly k) as well as feed concentration a systematic evaluation of the mechanisms related to the operating conditions that affect the adsorption and removal of E1 and E2 is performed.

4.3. Influence of Hydrodynamics

For NF spiral-wound membranes the operating conditions for aqueous solutions range from 3 to 20 bar for pressure [251] and from 100 to 1000 for the Re_h number [229]. To study the effect of concentration polarisation on the retention and mass adsorbed of hormones by NF membranes, the study of the effect of Re_h number was carried out at a pressure of 11 bar and the study of the effect of pressure was carried out at a Re_h number of 427 to ensure a concentration polarisation build-up at the membrane surface.

4.3.1 Concentration at the Membrane Surface and Polarisation Modulus Determination

For the several operational parameters used (*i.e.* pressure and cross-flow velocity), the initial concentration at the membrane surface was calculated to study the influence of concentration polarisation on the adsorption and retention of hormones by NF membranes. In the first instances of the experiment, the concentration in the permeate is zero, and therefore equation (4.1) simplifies to equation (4.4), the polarisation modulus β [128] at initial conditions of filtration, where $C_m(0)$ and $C_f(0)$ are the initial membrane and feed concentrations, respectively.

$$\beta = \frac{C_m(0)}{C_f(0)} = \exp\left(\frac{J}{k}\right) \tag{4.4}$$

To calculate the initial concentration at the membrane surface $C_m(0)$ in equation (4.4), the parameters used for this equation consider filtration conditions just before the hormones were spiked to the feed tank. The permeate concentration $C_p(0)$ is 0 and J is calculated based on the pure water flux measured before spiking the hormones. The permeate flux J does not vary by more than 5% during the course of the experiments carried out, as will be seen in section 4.3.4. The initial feed concentration $C_f(0)$ is the one measured during the experiment.

The mass transfer coefficient, k, required to calculate $C_m(0)$ in equation (4.4), is calculated based on a Sherwood correlation from the literature determined under the same hydrodynamic conditions as the ones used in this study. Such a Sherwood correlation in a slit channel [258] is expressed by equations (4.5 a) or (4.5 b),

$$Sh = \frac{kd_h}{D_\infty} = 1.195 Re_{dh}^{0.554} Sc^{0.371} \left(\frac{d_h}{L_{cell}}\right)^{0.131} \tag{4.5 a}$$

$$Sh = 1.195\left(\frac{\rho v d_h}{\mu}\right)^{0.554}\left(\frac{\mu}{\rho D_\infty}\right)^{0.371}\left(\frac{d_h}{L_{cell}}\right)^{0.131} \qquad (4.5\ b)$$

where d_h (m) is the hydraulic diameter ($d_h=2\times h$, where h is the slit channel height in m), D_∞ is the solute diffusivity ($m.s^{-2}$), Re_{dh} is the Reynolds number based on hydraulic diameter (-) given by equation (3.1), Sc is the Schmidt number (-) given by equation (4.3), L_{cell} is the cell length (m).

4.3.2 Reynolds Number

The influence of Re_h number in the adsorption and retention of E1 and E2 by the NF 270 and the TFC-SR2 membrane is studied. These two membranes have different permeabilities and NaCl rejections (Table 3.4), with the NF 270 having a permeability four times higher than that of TFC-SR2, despite the lower retention of NaCl by this membrane. Differences in membrane permeabilities will have a different impact on the polarization build up at the membrane surface according to equation (4.4).

The transient feed and permeate concentrations for E1 and E2 and the NF 270 and TFC-SR2 membranes for different Re_h numbers are represented in Figure 4.2.

It is clear from Figure 4.2 that higher Re_h numbers induce a less pronounced decrease with time of the feed concentration for both hormones E1 and E2 and membranes NF 270 and TFC SR2 studied. It is well known that larger Re_h numbers (higher circulating velocities) correspond to higher shear stresses at the membrane surface that have a cleansing effect [259], confirming that the system follows basic principles of chemical engineering. Since the adsorption onto the membrane is intimately related to the hormone concentration at its surface, where a higher surface concentration yields a higher hormone mass adsorbed, a smaller Re_h number will enhance adsorption and, therefore, will increase the hormone permeate

concentration. This implies a reduced "flush" effect of the membrane surface and therefore a reduced performance in the hormones removal.

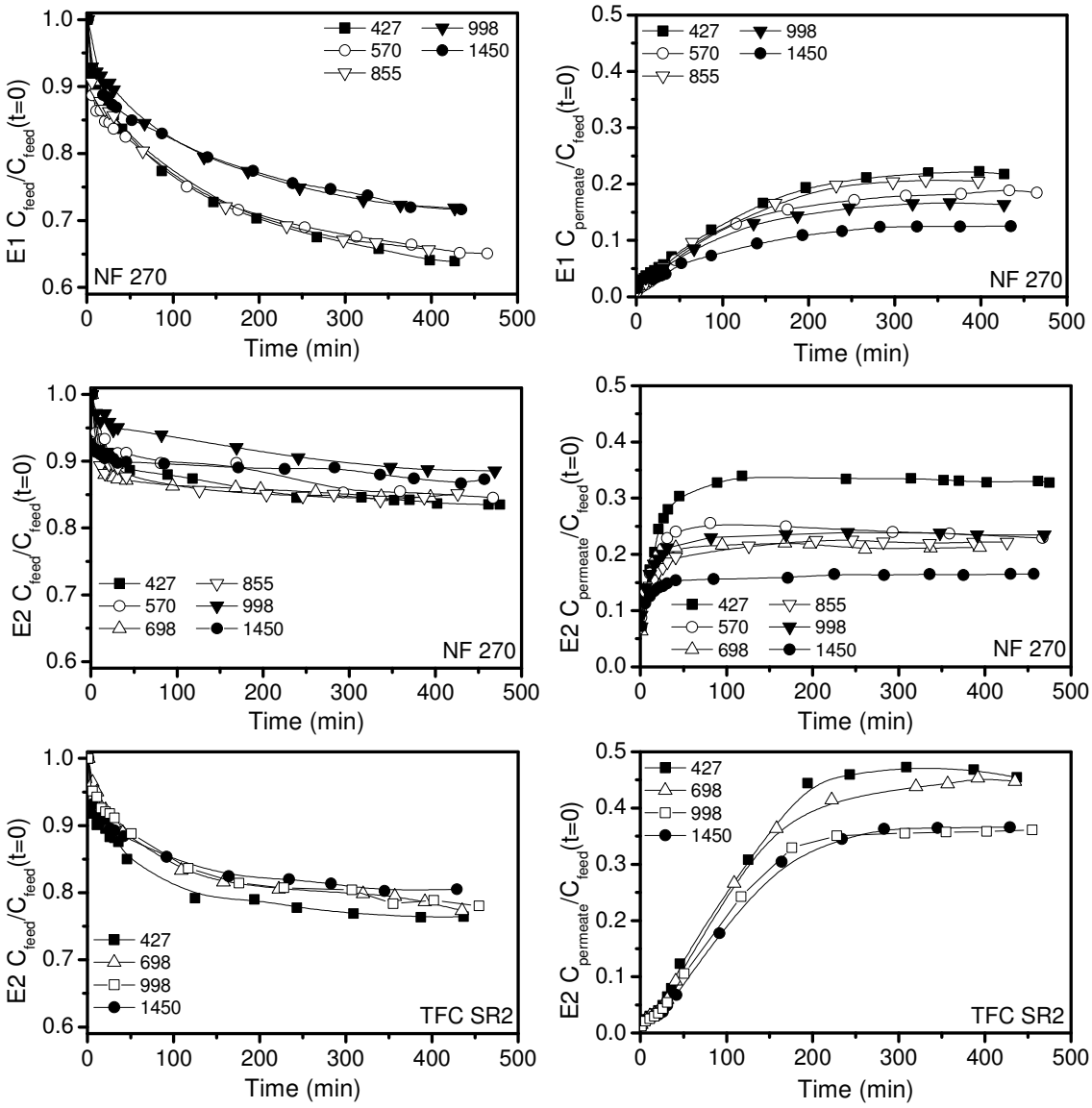

Figure 4.2 Estrone (E1) and estradiol (E2) feed and permeate normalized concentration as a function of time for several Re_h for the NF 270 1 and the TFC-SR2 2 (11 bar, $C_{feed\ initial}$=100 ng.L^{-1}, T=24°C, pH 7)

It is worth noticing that for the NF 270 membrane, larger Re_h numbers (998 and 1450) appear to have a distinct behavior: the feed concentrations at those Re_h

numbers are quite similar. The TFC-SR2 membrane, however, does not show this distinct behaviour for the feed concentration. The feed concentration results are similar for the Re_h number range studied. The difference between these two membranes lies in their surface roughness. In the first case the membrane surface is very smooth and flow instabilities occur for higher Re_h numbers (Re_h=998), whilst for the TFC-SR2, which has a fourfold roughness increase compared to the NF 270 (Table 3.5), flow instabilities occur for lower Re_h numbers (between 427 and 698)..This effect, however, is not directly observable for the permeate concentration results, as they depend also considerably on the membrane morphology.

The total E1 and E2 hormone mass adsorbed and retention once steady-state is reached are represented in Figure 4.3 and Figure 4.4. Retention is calculated using the feed and permeate concentrations once steady-state is reached (equation 2.1), which is achieved after about 250 minutes of experiment.

As can be seen in Figure 4.3 and Figure 4.4, the increase of Re_h causes a decrease in the mass adsorbed and an increase in retention for both hormones and both membranes. When Re_h increases, the concentration polarisation is less pronounced since the mass transfer coefficient increases due to the cleansing effect of the higher shear stress at the membrane surface. Hence, this gives a lower $C_m(0)$ or β calculated by equation (4.4) as shown in Figure 4.3 C and Figure 4.4 B. The lower $C_m(0)$ or β results in lower adsorption and higher retention, showing that adsorption and retention are governed by polarization (or $C_m(0)$ and β) and that they are strongly related. For the NF 270 membrane when the Re_h numbers increased from 427 to 1450, the E2 total mass adsorbed decreased from 0.7 $ng.cm^{-2}$ to 0.5 $ng.cm^{-2}$ and the retention increased from 61% to 81%. When Re_h increases, this causes a lower concentration polarisation to form on the membrane surface. Hence $C_m(0)$ or β given by equation (4.4) are lower (Figure 4.3 C). In fact, the increase of Re_h from 427 to 1450 caused the polarisation modulus to decrease from 1.5 to 1.0.

The same trend was obtained for E1, where an increase of Re_h numbers from 427 to 1450 caused the total mass adsorbed to decrease from 1.5 $ng.cm^{-2}$ to 1.3 $ng.cm^{-2}$ and retention to increase from 69% to 83% accompanied by a polarisation modulus decrease from 1.5 to 1.0. Lower $C_m(0)$ or β results in lower adsorption and

higher retention, showing that adsorption and retention are strongly dependent on $C_m(0)$ or β. The higher the mass adsorbed, the more hormone will permeate through the membrane and give lower retention.

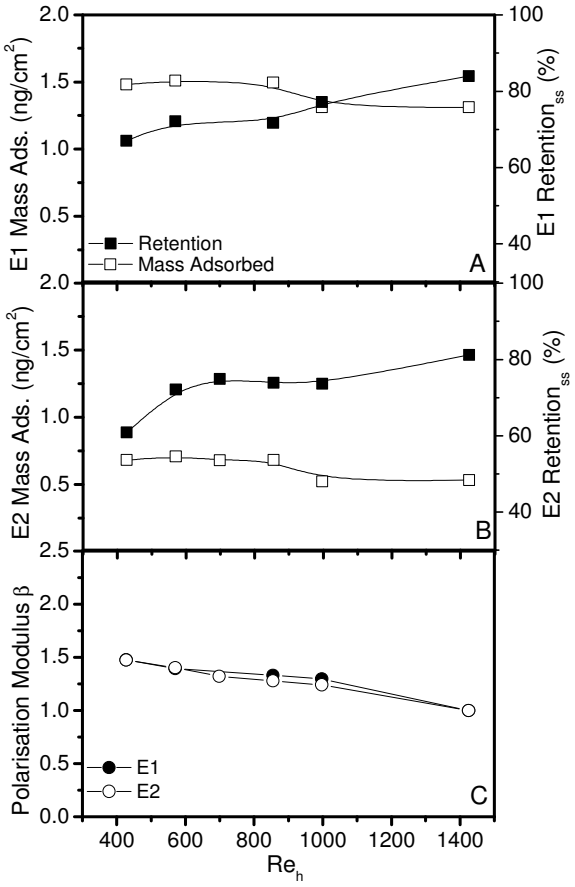

Figure 4.3 Reynolds number (Re_h) influence on **(A)** estrone (E1) and **(B)** estradiol (E2) steady-state retention (Retention $_{ss}$) and adsorption (Mass Ads.) and **(C)** polarisation modulus β (C_{feed} (0)=100 ng.L^{-1}, 11 bar, T=24°C, pH 7) for the NF 270 1

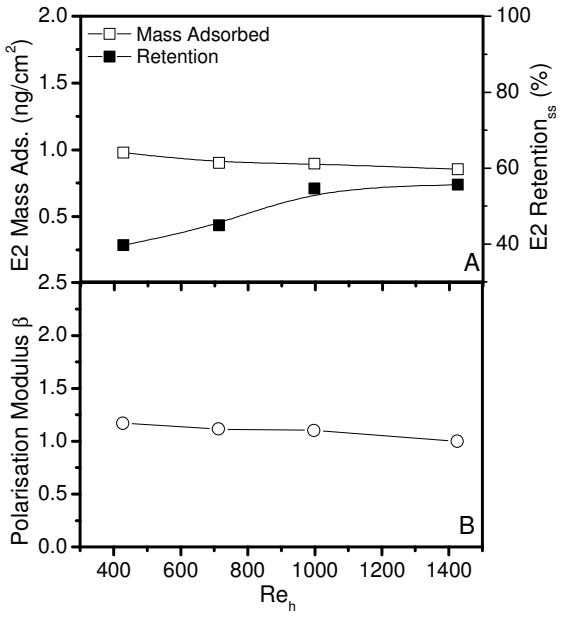

Figure 4.4 Reynolds number (Re_h) influence on **(A)** estradiol (E2) steady-state retention (Retention $_{ss}$) and adsorption (Mass Ads.) and **(B)** polarisation modulus β (C_{feed} (0)=100 ng.L^{-1}, 11 bar, T=24°C, pH 7) for the TFC-SR2 2

When comparing the two membranes, the NF 270 has a more pronounced effect in the mass adsorbed than the TFC SR2. With an increase of Re_h numbers from 427 to 1450, the total mass adsorbed decreased from 1.0 ng.cm^{-2} to 0.85

ng.cm^{-2} and retention increased from 40% to 55% accompanied by a polarisation modulus decrease from 1.2 to 1.0.

The NF 270 with a higher permeability, yields a higher polarization build up at the membrane surface according to equation (4.4), hence a more pronounced variation in β compared to the TFC SR2 membrane (Figure 4.3 C and Figure 4.4 B).

The transitional Re_h for slit channels with hydrodynamically smooth walls reported in the literature varies between 1150 and 1450 [226, 260, 261] but, as can be seen for both hormones, there is no significant change in the mass adsorbed above Re_h=1000 despite a small increase in retention. This suggests that the transition regime might be achieved at a lower Re_h number in this cell due to the membranes roughness as discussed above and to a possible recirculation zone appearing at the cell entrance due to its geometry, where a sudden expansion exists.

As pressure impacts significantly on concentration polarisation, the contribution of pressure was studied systematically to determine the influence of pressure induced changes in $C_m(0)$ and β on adsorption.

4.3.3 Pressure

The effect of pressure on the feed and permeate concentration of E1 and E2 is studied in this section for the NF 270 and the TFC-SR2 membranes. The transient feed and permeate concentrations are displayed in Figure 4.5.

The impact of pressure in the transient feed and permeate concentrations is much more pronounced compared to the effect of the Re_h number previously described. Results from Figure 4.5 show that a higher pressure causes invariably a higher decrease in the feed concentration, translating into higher mass adsorbed, and a higher permeate concentration for both hormones and membranes studied. A higher pressure causes a higher permeate flux through the membrane (J) in equation (4.4) and therefore a more pronounced concentration polarization at the membrane surface. The higher convective transport of hormones towards the membrane surface driven by the higher trans-membrane pressure gradient causes a reduced performance

in the removal of the hormones due to a greater accumulation of hormones at the membrane surface that adsorb and permeate throughout the membrane.

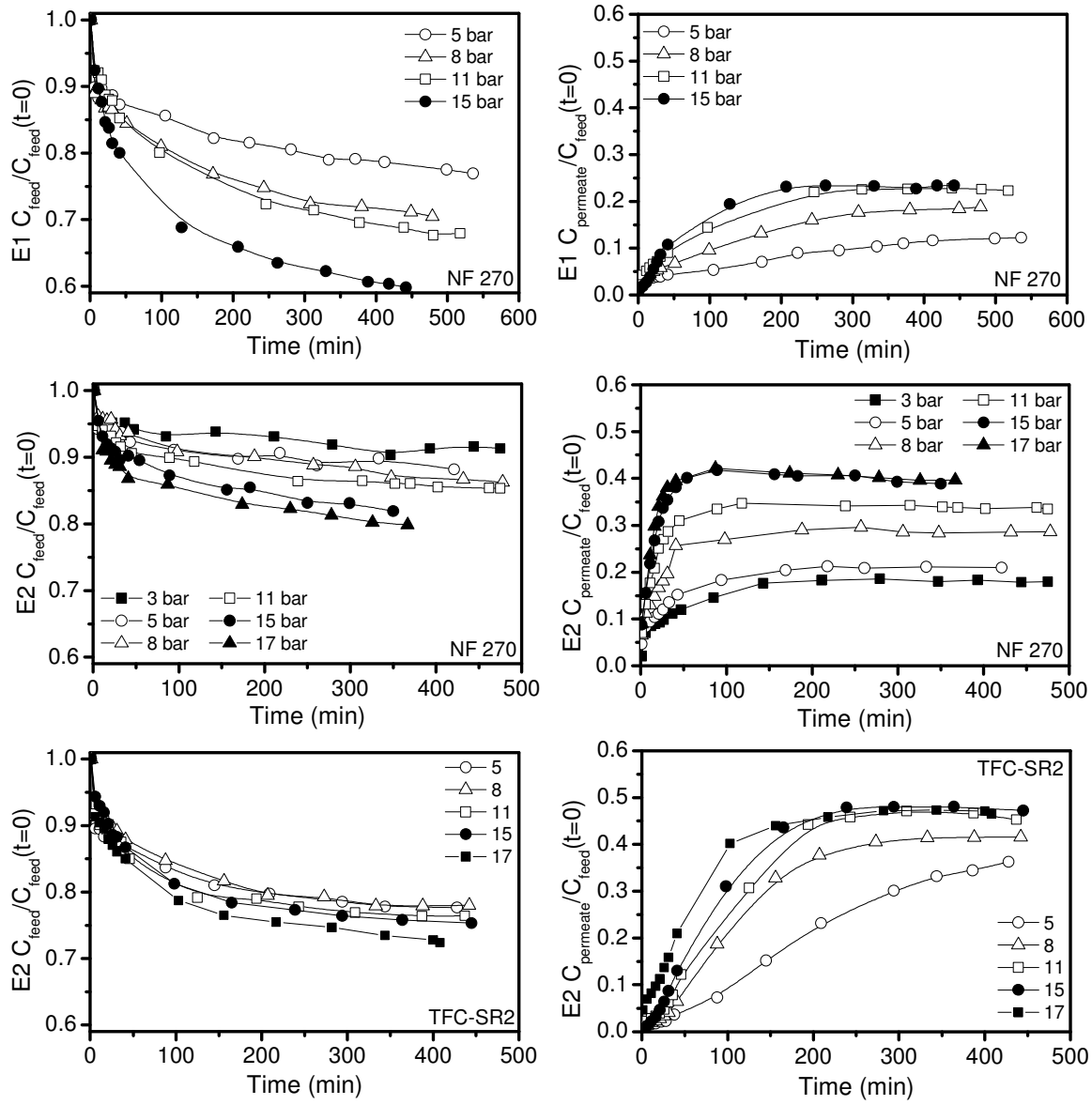

Figure 4.5 Estrone (E1) and estradiol (E2) feed and permeate normalized concentration as a function of time for several pressures for the NF 270 1 and the TFC-SR2 2 (Re_h=427, $C_{feed\ initial}$=100 ng.L^{-1}, T=24°C, pH 7)

Results of the role pressure plays on the total mass adsorbed and retention is depicted in Figure 4.6 and Figure 4.7. Increasing pressure increases flux through

the membrane (J) and therefore causes more severe polarization translated by an increased $C_m(0)$ or β (Figure 4.6 C and Figure 4.7 B). An increase in $C_m(0)$ or β causes an increase in the hormone mass adsorbed and a decrease in retention. When the pressure increased from 3 to 17 bar for the NF 270 membrane, the E2 initial concentration at the membrane surface almost doubled from 100 $ng.L^{-1}$ to 187 $ng.L^{-1}$, causing an increase of the mass adsorbed from 0.4 $ng.cm^{-2}$ to 0.8 $ng.cm^{-2}$. For these same conditions, a decrease of steady-state retention from 80% to 51% was caused by a polarisation modulus increase from 1.1 to 1.9. The same trend was obtained for E1 and the NF 270 membrane, where an increase of pressure from 5 to 15 bar caused a mass adsorbed increase from 1.0 $ng.cm^{-2}$ to 1.8 $ng.cm^{-2}$ and a steady-state retention decrease from 85% to 63%. In comparison, for E2 with the TFC-SR2 membrane, an increase of pressure from 5 to 17 bar caused a mass adsorbed increase from 1.0 $ng.cm^{-2}$ to 1.2 $ng.cm^{-2}$ and a steady-state retention decrease from 57% to 41%.These results confirm that $C_m(0)$ or β indeed have a strong influence on adsorption and retention.

Comparing the impact of Re_h and pressure on the hormone total mass adsorbed and retention (Figure 4.3 and Figure 4.4 *vs* Figure 4.6 and Figure 4.7), Re_h numbers impact less on adsorption or retention compared to pressure. This was expected since, according to equation (4.4), C_m is more sensitive to changes in pressure or permeate velocity (J) than to changes in the circulation velocity v in the feed channel (or Re_h number).

On the other hand, increasing operating pressure and increasing Re_h numbers have opposite effects: pressure increase promotes a growth of concentration polarization by driving hormones by convection towards the membrane surface, that adsorbing, do not back-diffuse in equilibrium with convection, whereas the Re_h number increase yields larger cleansing shear stresses at the membrane surface that impede adsorption partially.

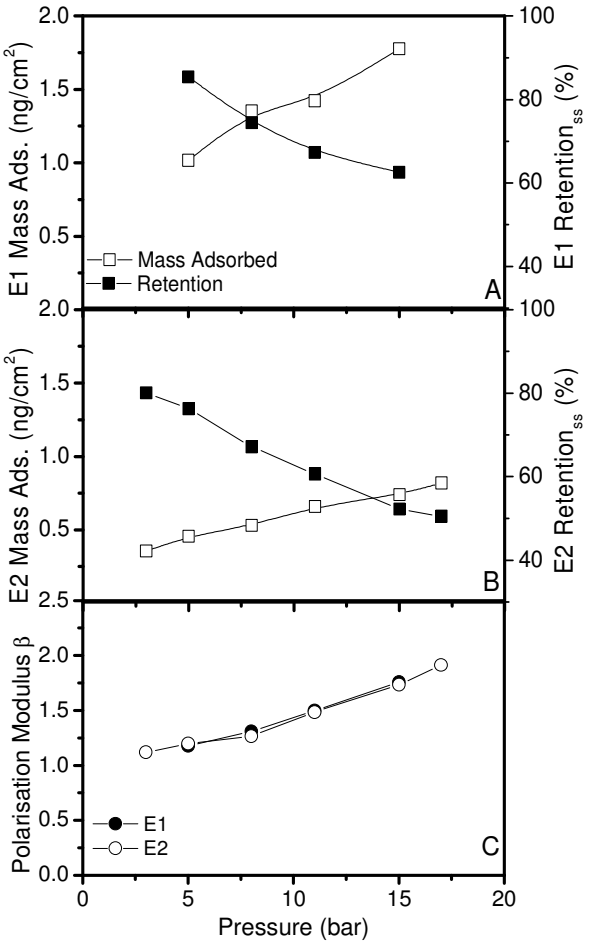

Figure 4.6 Pressure influence on **(A)** estrone (E1) and **(B)** estradiol (E2) steady-state retention (Retention $_{ss}$) and adsorption (Mass Ads.) and **(C)** polarisation modulus β (Re_h=427, $C_{feed\ initial}$=100 ng.L^{-1}, T=24°C, pH 7) for the NF 270 1

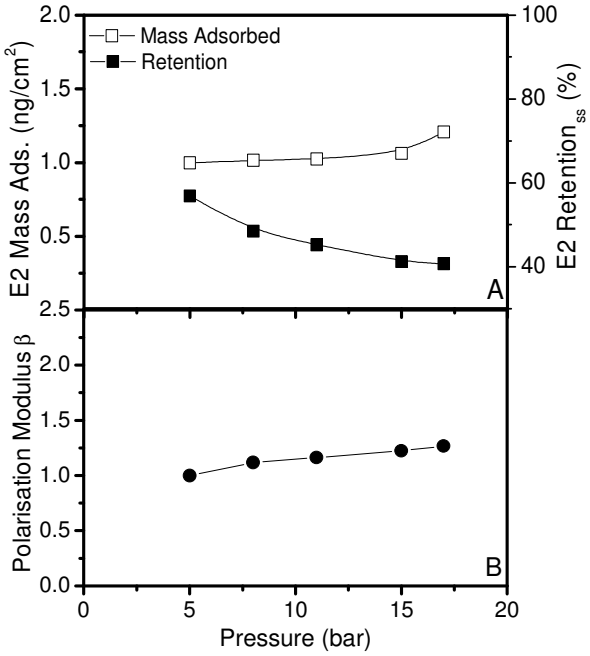

Figure 4.7 Pressure influence on **(A)** estradiol (E2) steady-state retention (Retention $_{ss}$) and adsorption (Mass Ads.) and **(B)** polarisation modulus β (Re_h=427, $C_{feed\ initial}$=100 ng.L^{-1}, T=24°C, pH 7) for the TFC-SR2 2

When comparing the two different membranes used it can be seen that polarization has a higher impact on the tighter NF 270 membrane than the looser TFC-SR2 membrane (Figure 4.6 C and Figure 4.7 B). Despite the latter membrane being more open (lower NaCl retention in Table 3.4), the permeability is much lower and therefore polarization is less severe. The lower the polarization built up at the membrane surface, the lower the impact on adsorption and retention is. Between 5

and 15 bar, E2 adsorption for the NF 270 increases from 0.47 ng.cm^{-2} to 0.74 ng.cm^{-2} whilst for the TFC-SR2 2 adsorption only increases from 1 ng.cm^{-2} to 1.06 ng.cm^{-2}.

The other striking result is that despite the TFC-SR2 being looser than the NF 270, the decrease in retention is much more severe for the NF 270 membrane. Increasing the pressure from 5 bar to 17 bar causes a decrease in E2 retention from 76% to 50% for the NF 270, whilst the TFC-SR2 as a retention decrease from 57% to 41%. Despite the much higher retention obtained for the tightest NF 270 membrane at low pressures, when polarization is severe at high pressures, the mass adsorbed increases substantially. This causes a severe decrease in the E2 retention for the NF 270 membrane, almost down to the same level as the looser membrane TFC-SR2 which suffers a lower impact on polarization.

The previous results suggest that care needs to be taken when choosing a nanofiltration membrane for the removal of trace contaminants. A tight membrane with a high permeability like the NF 270 membrane under certain filtration conditions might perform as well as a looser membrane with a lower permeability like the TFC-SR2 membrane. The existence of an adsorption mechanism contributing to the removal of trace contaminants by NF membranes should therefore be taken into account besides the mechanisms of steric exclusion and charge repulsion.

Variations in hydrodynamic conditions affect the membrane surface concentration which, as previously seen, has an impact in the adsorption mechanism of trace contaminants onto NF membranes.

To elucidate the role of feed concentration at constant hydrodynamic conditions a systematic study of the effect of feed concentration on hormone adsorption and retention was carried out.

4.3.4 Feed Concentration Influence on Adsorption

The hormone isotherms for both membranes were determined both in filtration mode in the cross-flow system and in static mode in the shaker (with no

pressure applied) to confirm that pressure had no influence in the shape of the isotherm. This is important since polarization has an effect on the mass adsorbed by increasing it with the increase of pressure and, in filtration mode, the isotherm might reach a saturation limit which might not be reached in static mode.

The results of E1 and E2 feed concentration variation on adsorption and retention are presented as adsorption isotherms in Figure 4.8 and Figure 4.9 for the NF 270 and TFC-SR2 membranes.

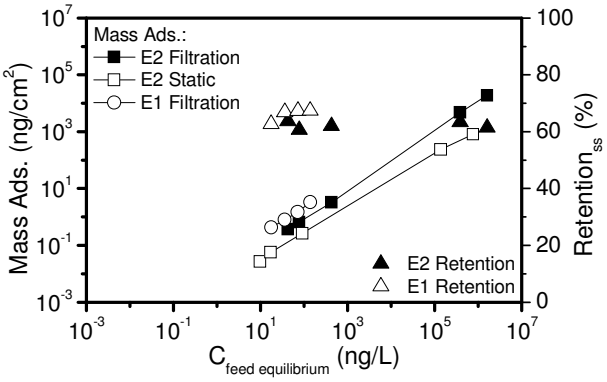

Figure 4.8 Estrone (E1) and estradiol (E2) sorption isotherm in filtration and static mode (E2) and retention at steady state as a function of equilibrium feed concentration (cross-flow filtration conditions: Re_h=427, 11 bar, T=24°C, pH 7; Static conditions: T=24°C, 200 rpm, 46 cm^2) for the NF 270 1 membrane

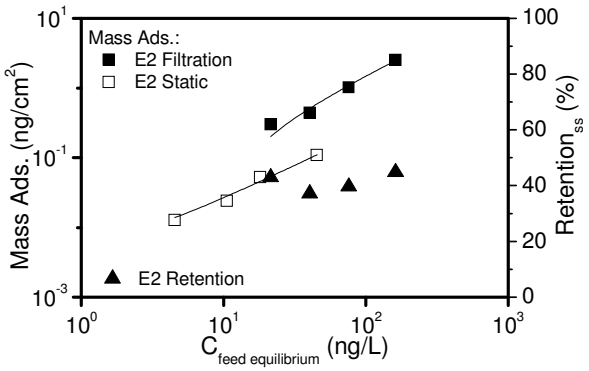

Figure 4.9 Estradiol (E2) sorption isotherm in filtration and static mode and retention at steady state as a function of equilibrium feed concentration (cross-flow filtration conditions: Re_h=427, 11 bar, T=24°C, pH 7; Static conditions: T=24°C, 200 rpm, 46 cm^2) for the TFC-SR2 2 membrane

All hormone isotherms are linear for both filtration and static mode, confirming results of other studies in a lower hormone concentration range [152, 172], showing sorption is limited by the hormone concentration. This suggests that saturation of all the adsorption sites available on the membrane was not reached, not even at the highest E2 concentration (2 $mg.L^{-1}$). However, for this feed concentration, the permeate flux was 15% lower compared to the other concentrations or filtration conditions as shown in Figure 4.10 and Figure 4.11. At the highest feed concentration of 2 $mg.L^{-1}$ and resulting $C_m(0)$ of 3 $mg.L^{-1}$, the

concentration is close to the solubility limit of E2 (Table 3.10), which might precipitate and affect membrane performance by decreasing the permeate flux (Figure 4.11).

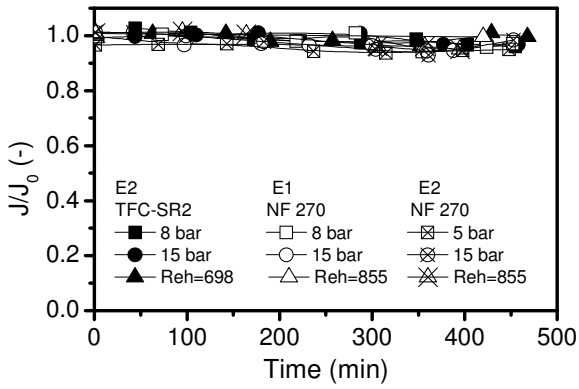

Figure 4.10 Normalized permeate transient flux for several experiments in filtration mode for estrone (E1) and estradiol (E2) and the NF 270 1 and TFC-SR2 2 membranes (T=24°C, pH 7, pure water flux: J_0=17 L/(h.m^2.bar))

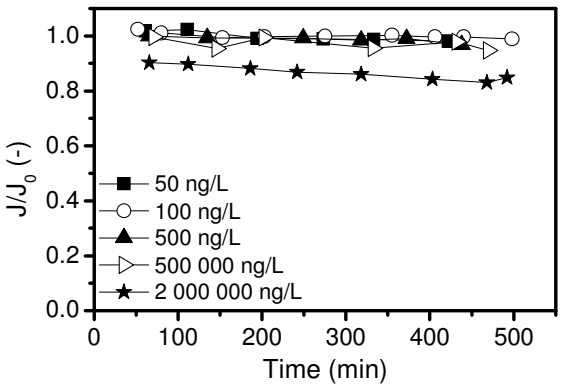

Figure 4.11 Normalized permeate transient flux for the estradiol (E2) isotherm experiments in filtration mode and the NF 270 1 (cross-flow filtration conditions: Re_h=427, 11 bar, T=24°C, pH 7, pure water flux: J_0=17 L/)h.m^2.bar))

As expected, the mass adsorbed as displayed in Figure 4.8 and Figure 4.9 increased with increased feed concentration. This confirms that the total mass adsorbed is proportional to the initial concentration at the membrane surface, $C_m(0)$, which increases with increased hormone feed concentration. However, in Figure 4.8 and Figure 4.9, the retention was practically unchanged with feed concentration variation for both hormones and membranes. When the initial polarization modulus β is calculated for the isotherm experiments, where the pressure and Re_h number are constant, it was found to be constant for both hormones with β_{E1} = 1.44 ± 0.03 and β_{E2} = 1.49 ± 0.03 for the NF 270 membrane and β_{E2} = 1.18 ± 0.02 for the TFC SR2 membrane. It can therefore be inferred that whilst mass adsorbed is dependent on $C_m(0)$, retention is dependent on β.

In reality, when the percentage of hormone mass adsorbed on the membranes is calculated, it does not vary considerably with feed concentration for the same pressure and Re_h numbers as can be seen in Table 4.1, despite the increase in $C_m(0)$ and consequently the increase in mass adsorbed ($ng.cm^{-2}$). This shows that retention at steady-state and the percentage of mass adsorbed are proportional to β, whilst the total mass adsorbed is proportional to $C_m(0)$.

Table 4.1 Percentage of mass adsorbed for estrone (E1) and estradiol (E2) and the NF 270 1 and TFC-SR2 2 membranes for the isotherm experiments (cross-flow filtration conditions: Re_h=427, 11 bar, T=24°C, pH 7)

Feed Concentration ($ng.L^{-1}$)	**TFC-SR2 2 - E2 (% Mass Adsorbed)**	**NF 270 - E2 (% Mass Adsorbed)**	**NF 270 - E1 (% Mass Adsorbed)**
25	26.0	-	36.0
50	21.2	17.6	33.5
100	23.8	16.4	32.2
200	26.4	-	34.8
500	-	15.0	-
Average	24.3 ± 2.4	16.3 ± 1.3	34.1 ± 1.7

The reason why the total mass adsorbed and $Retention_{ss}$ depend on $C_m(0)$ and β, respectively, is explained as follows.

Experiments in static mode and filtration mode evidence that a membrane surface exposed to an increasing initial feed concentration of hormone yield an increase of the mass adsorbed (Figure 4.8 and Figure 4.9). In filtration mode, the total mass adsorbed increases when pressure increases and Re_h decreases (Figure 4.3, Figure 4.4, Figure 4.6 and Figure 4.7), despite the initial feed concentration being the same for both hormones (100 $ng.L^{-1}$). Pressure and Re_h number are known to affect

the concentration at the membrane surface, hence the conclusion that adsorption and retention are governed by the concentration at the membrane surface.

Experimental data further evidences that the higher the initial concentration at the membrane surface $C_m(0)$ (or β) (Figure 4.3, Figure 4.4, Figure 4.6 and Figure 4.7), the higher the total mass adsorbed obtained and the lower the retention. This allows one to infer that adsorption and retention are governed by C_m (0) or β, since it is this concentration that the membrane is in contact with in the first instances of the experiment. The previous inference is corroborated by the following observations and reasoning.

If $C_m(0)$ or β did not govern the process of hormone adsorption and retention, then for similar conditions of $C_m(0)$ or β caused by different combinations of Re_h numbers and pressure, different results of total mass adsorbed and $Retention_{ss}$ should be obtained for the hormones. However, as can be seen in Table 4.2 one can conclude that this is not the case. The same applies for the experimental conditions of 11 bar and 1400 Re_h number, where β=1, and 5 bar and a 427 Re_h number, where β=1.1. This shows that for different filtration conditions that lead to the same C_m (0) or β, the same results of steady-state adsorption and retention are obtained, confirming that it is the initial condition that govern the system.

Moreover the use of $C_m(0)$ or β as the governing parameter for the mass adsorbed and retention is an advantage as this allows the latter two to be predicted, as will be described in Chapter 5.

Table 4.2 Comparison between the estrone (E1) and estradiol (E2) mass adsorbed and retention for different pressure and Re_h numbers combinations for the NF 270 1 (11 bar and a Re_h number of 1000 with the experiment at 8 bar and Re_h number of 427)

Hormone	Experiment	$C_m(0)$ ($ng.L^{-1}$)	β	Mass Adsorbed ($ng.cm^{-2}$)	Retention (%)
E1	11 bar, Re_h=1000	125	1.25	1.3	75
	8 bar, Re_h=427	125	1.25	1.3	73
E2	11 bar, Re_h=1000	125	1.25	0.6	71
	8 bar, Re_h=427	125	1.25	0.6	70

4.3.5 Comparison Between the Two Hormones

It was further noticed that E1 adsorbs twice as much as E2, which is in agreement with findings of Nghiem *et al.* [23]. Despite having similar physical characteristics [262] (Table 3.10), hormones with a ketone group (E1) have been found to bind more to organic matter or activated carbon than hormones with a hydroxyl group (E2) [263, 264]. The ketone group in E1 is very electron-rich (or polarised) compared to the hydroxyl group in E2 and therefore forms stronger hydrogen bonding (H-bond), while other interactions, such as hydrophobicity, may be at play as well. Hydrophobicity, however, does not explain the difference in adsorption between E1 and E2 onto NF membranes since despite E2 being more hydrophobic than E1 (Table 3.10), it adsorbs less. H-bonding has been considered to play a predominant factor in the transport of contaminants in membranes [32, 143, 257, 265-267].

4.4. Conclusions

The previous results illustrated the mechanisms that affect hormone adsorption and retention onto NF membranes, as far as operating conditions are concerned. By studying the effect of hydrodynamics (pressure and Re_h number) and feed concentration on adsorption it was found that concentration polarisation plays a dominant role on adsorption and retention by NF membranes. This means that adsorption is strongly dependent on the concentration at the membrane surface and polarization needs to be taken into account when modeling adsorption and transport of trace contaminants by NF membranes.

This phenomenon has an impact in the design of membranes and operation of membrane processes. To avoid the occurrence of adsorption the concentration at the membrane surface should be minimized either by increasing the Re_h numbers or by introducing spacers. These are in use in spiral-wound modules to minimize polarization by promoting mixing and disrupting cyclically the concentration boundary layer [268]. If the pressure is minimized, polarization will not have a

severe effect on adsorption. This however has a cost as lower product is obtained, *i.e.* permeate.

It was concluded that membranes with low permeability, despite having larger pore radius, have less severe polarization and therefore the variation in mass adsorbed and retention with pressure or Re_h is lower. This shows that a membrane with a larger pore radius but smaller permeability might perform as well as a tighter membrane with a higher permeability in terms of trace contaminant retention.

5 Sorption Model Based on Bulk Flow Properties

5.1. Introduction

In Chapter 4 it was shown that concentration polarization has a relevant impact on hormone adsorption and retention by NF membranes. Mass adsorbed and retention were found to depend on the initial concentration at the membrane surface and the initial polarisation modulus, respectively.

Since membranes have been found to adsorb trace contaminants, they can be treated as an adsorbent phase much in the same way as peat and activated charcoal are. Several studies on adsorption of contaminants onto soils, such as metals and dyes, show a pseudo-first or pseudo-second order kinetics for the cases where an equilibrium concentration is reached [269-274]. Adsorption of E2 and estriol (E3) onto activated carbon has been shown to be described by a pseudo first-order rate reaction [275, 276], whilst adsorption of ethinylestradiol (EE2) onto inactivated sewage sludge was best described by a pseudo-second order model [277].

In membrane processes a few attempts were carried out in describing the adsorption of trace contaminants onto polymeric membranes. Chang *et al.* [141] showed that E1 adsorption onto an MF hollow fibre membrane is described by a pseudo-first order sorption kinetics. In NF, Steinle-Darling *et al.* [175] showed that the transient feed concentration and retention of adsorbing perfluorochemicals can also be described by a pseudo first-order equation by fitting the equation to the experimental results. This work was very important in improving the understanding of adsorption of trace contaminants onto NF membranes. However, further work is necessary to enable the use of the sorption kinetics equation in a predictive rather than a descriptive way.

Following on from the results in Chapter 4, a model based on a first order sorption kinetics is developed in this chapter allowing the prediction of the transient feed and permeate concentrations for E1 and E2 and a wide range of operating pressures (3-17 bar) or Re_h numbers (400-1000) for the NF 270 (Batch 1, NF 270 1) and the TFC-SR2 (Batch 2, TFC-SR2 2) membranes.

For that, the following sequence of steps form the procedure undertaken herein to predict the time-dependent feed and permeate concentrations:

1. Determination of the order of kinetics for mass adsorption onto NF membranes from experimental data and its time dependent equation,
2. From the equation in step 1, determination of the time dependent feed concentration equation obtained from a mass balance to the feed tank of the experimental set-up,
3. Determination of the rate constant k_f of the feed concentration equation in step 2 from static isotherm data,
4. Determination of the relationship between the total mass adsorbed and the initial concentration at the membrane surface at t=0 ($C_m(0)$) from the filtration isotherm experiments,
5. The total mass adsorbed is predicted for several experimental conditions by calculating the expected $C_m(0)$ and using the relationship obtained in step 4,
6. Once the total mass adsorbed is predicted in step 5, determination of the steady-state feed concentration C_{fss} from a mass balance to the recirculating feed solution,
7. From step 3 and 6, prediction of the transient feed concentration for several experimental conditions,
8. Use of experimental filtration experiments to obtain the relationship between steady-state retention or steady-state permeate to feed concentration ratio (C_{pss}/C_{fss}) with the polarization modulus at t=0 (β),
9. Prediction of C_{pss}/C_{fss} for any experimental condition by calculating the expected β and using the relationship obtained in step 8,

10. Determination of the retention rate constant k_{ret} from the isotherm experimental data,
11. From step 8, 9 and 10, determination of the transient permeate concentration for several experimental conditions.

5.2. Kinetics Order of Mass Adsorption

5.2.1 Pseudo-first and pseudo-second order kinetics

Trace contaminant adsorption, more specifically hormone adsorption onto a surface, can be described by equation (5.1) [276],

$$H \xleftrightarrow{k_1 \text{ or } k_2} H^{\bullet} \tag{5.1}$$

where H is the concentration of free hormone in solution ($ng.L^{-1}$), k_1 (s^{-1}) and k_2 ($ng^{-1}.s^{-1}$) are the first order or second order sorption rate constants, respectively, and $H^{\bullet}$ is the adsorbed hormone on the sorbent ($ng.cm^{-2}$).

The Lagergren equation represents the sorption rate equation in liquid/solid systems taking into account the solid adsorption capacity. It describes a pseudo-first order sorption kinetics to an equilibrium, given by equation (5.2),

$$\frac{dq(t)}{dt} = k_1 \left(q_{ss} - q(t)\right) \tag{5.2}$$

where q(t) is the hormone mass adsorbed at time t (ng), q_{ss} is the mass adsorbed once steady-state has been reached (ng) and k_1 is the first-order rate constant. Considering the initial condition (5.3),

$$q(t)=0 \text{ for } t=0 \tag{5.3}$$

equation (5.2) is integrated, and by algebraic manipulation one obtains a linear form given by equation (5.4):

$$\ln(q_{ss} - q(t)) = -k_1 t + \ln(q_{ss}) \tag{5.4}$$

The first order sorption rate constant k_1 can be obtained by the slope of the graphical representation of equation (5.4).

Another possible description of the sorption of hormone in a liquid/solid system might be a pseudo-second order sorption kinetics given in equation (5.5),

$$\frac{dq(t)}{dt} = k_2 \left(q_{ss} - q(t)\right)^2 \tag{5.5}$$

where k_2 is the second-order rate constant ($ng^{-1}.s^{-1}$). By algebraic manipulation, and considering once again the initial condition (5.3), equation (5.5) can be integrated and the linear form given by equation (5.6):

$$\frac{t}{q(t)} = \frac{1}{k_2 q_{ss}^{\ 2}} + \frac{t}{q_{ss}} \tag{5.6}$$

If the hormone mass adsorbed onto NF membranes is found to obey a pseudo-second order sorption kinetics then the mass adsorbed once steady-state is reached q_{ss} can be obtained by the inverse of the slope and the second order rate constant k_2 can be obtained by the intercept of equation (5.6).

5.2.2 Determination of the Sorption Kinetic Order onto the NF Membranes

The first step in describing the adsorption rate of hormones onto NF polymeric membranes is to determine the order of the adsorption kinetics. The best linear fitting of equation (5.4) or equation (5.6) to the experimental hormone mass adsorbed results in the cross-flow system with different feed concentrations will dictate if hormone sorption onto NF membranes is described by a pseudo-first or pseudo-second order sorption kinetic, respectively. The results for the pseudo-first and pseudo-second order fit for E1 with the NF 270 (NF 270 1) membrane are shown in Figure 5.1 and Figure 5.2, respectively, whereas the results of both fitting orders for E2 with the TFC-SR2 (TFC-SR2 2) membrane are shown in Figure 5.3 and Figure 5.4.

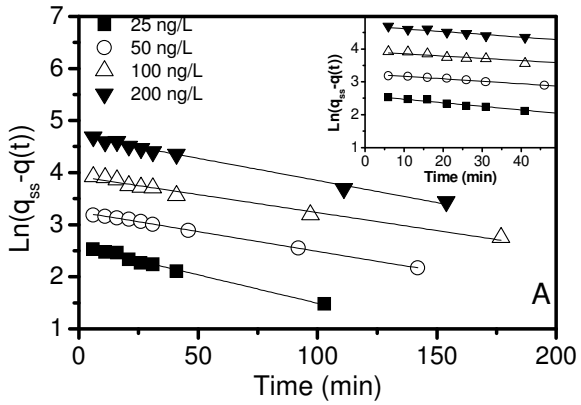

Figure 5.1 First-order sorption kinetics for estrone (E1) and the NF 270 1 membrane for several feed concentrations (Re_h=427, 11 bar, pH 7, T=24°C)

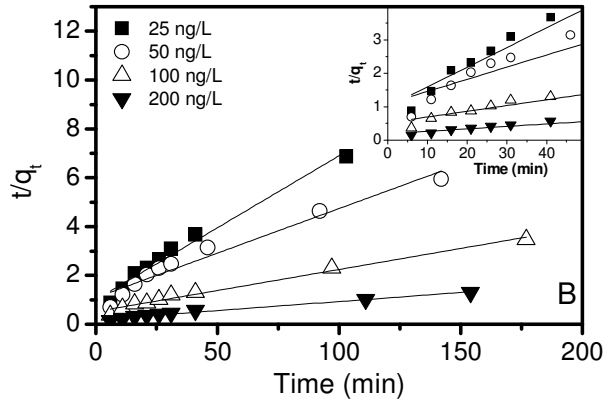

Figure 5.2 Second-order sorption kinetics for estrone (E1) and the NF 270 1 membrane for several feed concentrations (Re_h=427, 11 bar, pH 7, T=24°C)

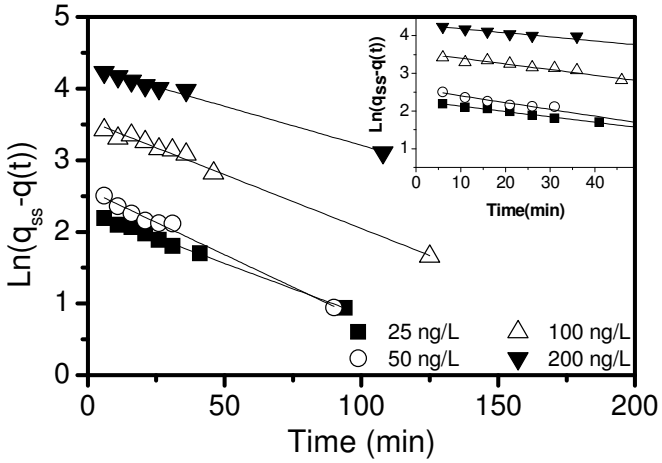

Figure 5.3 First-order sorption kinetics for estradiol (E2) and the TFC-SR2 2 membrane for several feed concentrations (Re_h=427, 11 bar, pH 7, T=24°C)

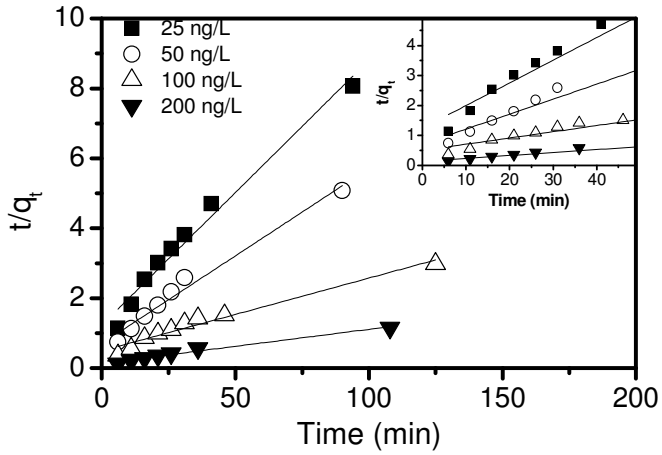

Figure 5.4 Second-order sorption kinetics for estradiol (E2) and the TFC-SR2 2 membrane for several feed concentrations (Re_h=427, 11 bar, pH 7, T=24°C)

Comparing Figure 5.1 with Figure 5.2 and Figure 5.3 with Figure 5.4, one can infer that the best linear fit is given for the pseudo-first order sorption kinetic, since the pseudo-second order kinetic does not describe well the adsorption kinetics, especially in the first 50 minutes of the experiments, where the highest gradient in mass adsorbed with time occurs.

The previous inference can be confirmed by the regression coefficient R^2. The fitting results for such R^2, together with the rate constants k_1 and k_2 and the predicted steady-state mass adsorbed q_{ss} for the second order sorption kinetics are presented in Table 5.1 and Table 5.2.

Table 5.1 First and second order sorption kinetics fitting results for estrone (E1) and the NF 270 1 membrane (total membrane area of 46 cm^2)

C_{feed} ($ng.L^{-1}$)	1st order		2nd order			q_{ss} (ng) experimental
	k_1 (s^{-1})	R^2	k_2 ($ng^{-1}.s^{-1}$)	R^2	q_{ss} (ng)	
25	0.000181	0.9925	$5.79.10^{-5}$	0.9795	16.9	19.4
50	0.000136	0.9988	$2.03.10^{-5}$	0.9601	27.4	32.6
100	0.000115	0.9819	$9.53.10^{-6}$	0.9846	58.0	66.6
200	0.000141	0.9933	$4.85.10^{-6}$	0.9828	135.0	153.4

Table 5.2 First and second order sorption kinetics fitting results for estradiol (E2) and the TFC-SR2 2 (total membrane area of 46 cm^2)

C_{feed} ($ng.L^{-1}$)	1st order		2nd order			q_{ss} (ng) experimental
	k_1 (s^{-1})	R^2	k_2 ($ng^{-1}.s^{-1}$)	R^2	q_{ss} (ng)	
25	0.000239	0.9900	$2.16.10^{-4}$	0.9845	10.1	14.2
50	0.000237	0.9904	$5.94.10^{-5}$	0.9803	20.0	21.7
100	0.000259	0.9913	$9.5.10^{-6}$	0.9625	52.6	47.1
200	0.000181	0.9927	$1.14.10^{-5}$	0.9776	102.9	115.9

The filtration adsorption of hormones onto NF membranes is clearly described by a pseudo-first order sorption kinetics as can be seen in Table 5.1 and Table 5.2. When the prediction of q_{ss} given by the second-order sorption kinetics obtained from the slope of equation (5.6) is compared to the experimental q_{ss} (Table 5.1 and Table 5.2) this parameter is generally underestimated.

It can further be seen that the first order rate constant given by the slopes in Figure 5.1 and Figure 5.3 are similar since the lines are almost parallel, showing that

the rate constant k_1 is independent of feed concentration, contrary to other cases reported in the literature [271].

Once the order rate has been determined as a pseudo-first order sorption kinetic, the next step is to determine the kinetic equation for the feed concentration and its rate constants.

5.3. Feed Concentration Kinetics

5.3.1 Feed Concentration Equation

Due to the proportionality between the mass adsorbed on the membrane and the hormone feed concentration, the latter will either be described by a pseudo-first or a pseudo-second order kinetic, much in the same way as the mass adsorbed is. The relation between the mass adsorbed and the feed concentration and their dependence with time is given by a mass balance to the feed tank as expressed by equation (5.7),

$$\frac{dq(t)}{dt} = -V_{sol}\frac{dC_f(t)}{dt} \qquad (5.7)$$

where V_{sol} is the volume of the hormone solution in the system. In order to obtain the kinetic equation for the feed concentration, equation (5.7) can be integrated with the appropriate initial condition to determine the dependences of q(t) and q_{ss} on the feed concentration. Considering the initial condition (5.8) where $C_f(0)$ is the initial feed concentration ($ng.L^{-1}$):

$$q(t)=0 \text{ for } C_f(t)=C_f(0) \qquad (5.8)$$

one obtains equation (5.9),

$$q(t) = V_{sol}(C_f(0) - C_f(t)) \quad (5.9)$$

If one is interested in establishing the steady-state mass adsorbed, q_{ss} dependency on the feed concentration, from the initial conditions (5.8) and (5.10),

$$q(t=\infty)=q_{ss} \text{ for } C_f(t=\infty)=C_{fss} \quad (5.10)$$

where C_{fss} ($ng.L^{-1}$) is the feed concentration at steady-state conditions, one obtains equation (5.11):

$$q_{ss} = V_{sol}(C_f(0) - C_{f\,ss}) \quad (5.11)$$

Substituting equations (5.7), (5.9) and (5.11) into equation (5.2), one obtains the differential equation describing the pseudo-first order rate of change of the feed concentration as expressed by equation (5.12),

$$-\frac{dC_f(t)}{dt} = k_f\left(C_f(t) - C_{fss}\right) \quad (5.12)$$

with k_f (s^{-1}) replacing k_1 and standing for the pseudo-first order rate constant for exponential decline for the feed concentration.

Solving equation (5.12) considering the initial condition (5.13):

$$C_f(t) = C_f(0) \text{ for } t = 0 \quad (5.13)$$

one obtains equation (5.14) [175], where k_f is dependent on the rate with which the hormone adsorbs onto the membrane surface.

$$C_f(t) = C_{fss} + (C_f(0) - C_{fss})\, e^{-k_f t} \qquad (5.14)$$

With the same reasoning, equations (5.7), (5.8) and (5.11) can be substituted into equation (5.5) in order to obtain the pseudo-second order feed concentration kinetic considering the initial condition (5.10). The hormone sorption kinetics onto NF membranes has however been established in the previous sections as a pseudo-first order, and therefore the feed concentration will also be described by a pseudo-first order kinetic given by equation (5.14).

Once the feed concentration kinetic order has been determined as a pseudo-first-order then the next step is to determine the rate constant k_f for both hormones and membranes.

5.3.2 Feed Concentration Rate Constant k_f

The reaction rate constant k_f can be obtained by fitting equation (5.14) to all the transient feed concentrations in static experiments carried out in the shaker (no pressure) (Chapter 3). An optimization method (Solver, Microsoft Excel) was used, with k_f as the fitting parameter. The fitting results are shown in Figure 5.5. The k_f values for the different hormones and membranes are shown in Table 5.3.

Table 5.3 First order rate constant k_f (s^{-1}) obtained for estrone (E1) and estradiol (E2) and the NF 270 1 and TFC-SR2 2 membranes

Hormone/Membrane	**NF 270 1**	**TFC-SR2 2**
E1	0.00023	-
E2	0.00038	0.00029

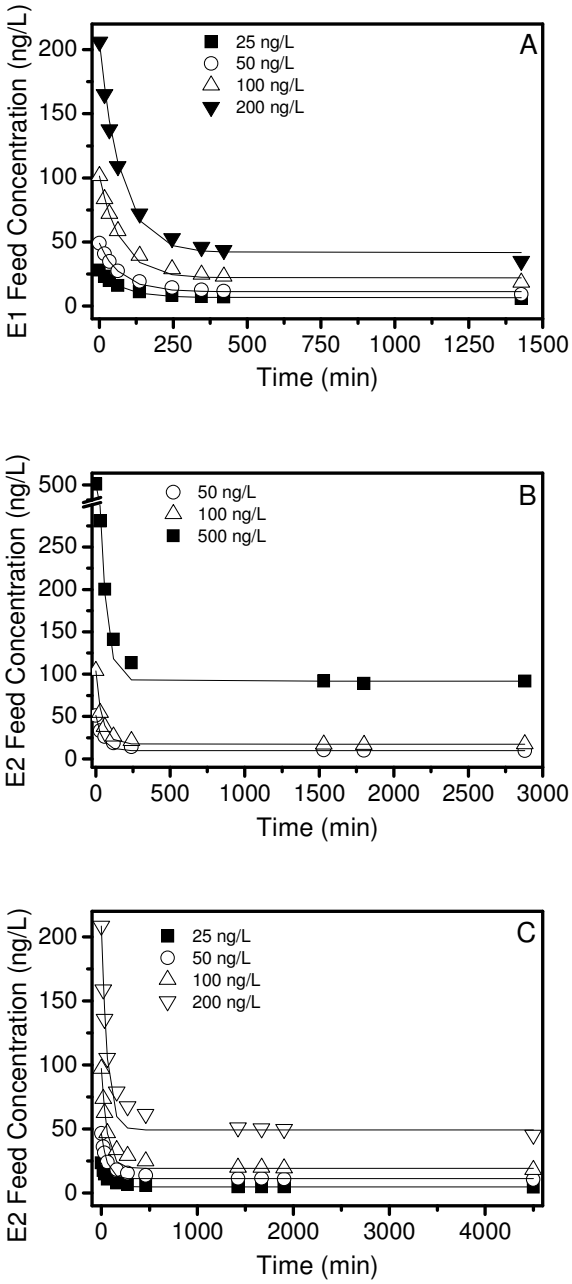

Figure 5.5 First-order concentration kinetics for **(A)** estrone (E1) and **(B)** estradiol (E2) for the NF 270 1 and **(C)** estradiol (E2) for the TFC-SR2 2 membranes for several feed concentrations (pH=7, T=24ºC, 200 rpm)

For the NF 270 the hormone E2 takes 240 minutes to reach 90% of the mass adsorbed, whilst E1 takes 345 minutes (44% more). Since E1 takes longer to reach adsorption steady-state, its reaction rate constant is lower compared to E2. In the case

of E2 with the TFC-SR2, it takes 461 minutes to reach 90% of the total mass adsorbed, explaining the lower constant rate obtained compared to the one obtained for the NF 270 membrane.

5.3.3 Determination of C_{fss}

Once the feed concentration rate constant k_f has been determined, the next step is to find a relationship that allows predicting the feed concentration at steady-state, C_{fss} for any filtration condition.

C_{fss} depends on the total mass adsorbed during filtration and is obtained by performing a mass balance to the feed solution in recirculation mode given by equation (5.15),

$$V_{feed}\ C_f(0) = V_{feed}\ C_{f\,ss} + M_{ads} \qquad (5.15)$$

where V_{feed} is the volume of the feed solution (L), M_{ads} is the total mass adsorbed (ng) until steady state is reached. If the total mass adsorbed can be predicted then C_{fss} will be known by applying equation (5.15). Since it was concluded in Chapter 4 that the total mass adsorbed is dependent on $C_m(0)$, in consequence, $C_m(0)$ is the key parameter to predict adsorption.

The total mass adsorbed for any experimental hydrodynamic condition of pressure and Re_h number is predicted using the relationship between the total mass adsorbed and $C_m(0)$ obtained from the filtration isotherm experiments (Chapter 4). For the filtration isotherm experiments, $C_m(0)$ is calculated according to equation (4.4) and plotted against the total mass adsorbed (M_{ads}) as shown in Figure 5.6. A linear relationship is obtained. The higher the affinity of the compound with the membrane, the larger the slope magnitude of the linear isotherm will be. This is indeed the case with E1 compared to E2 for the NF 270 membrane. For non-linear isotherms such as Freundlich or Langmuir, a non-linear relationship would have to be used.

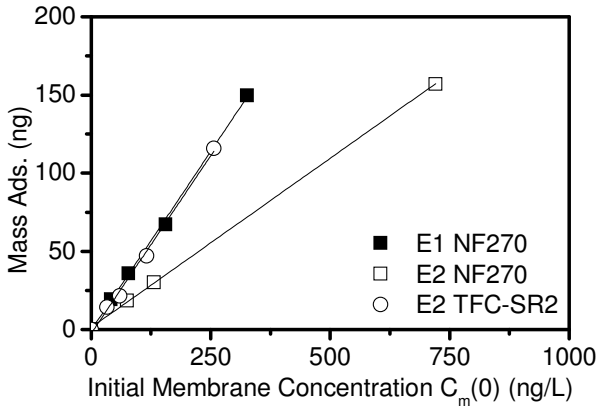

Figure 5.6 Estrone (E1) and estradiol (E2) initial concentration at the membrane surface ($C_m(0)$) as a function of total mass adsorbed (Mass Ads.) for the filtration isotherm experiments for the NF 270 1 and the TFC SR2 2 membranes

5.3.4 Feed Concentration Prediction

For experiments of varying pressure and Re_h number, $C_m(0)$ is calculated according to equation (4.4) and this $C_m(0)$ is used in the linear relationship from Figure 5.6 to predict the total mass adsorbed. With the predicted total mass adsorbed and equation (5.15), C_{fss} is obtained and applied in equation (5.14) in conjunction with the previously determined rate constant k_f.

Figure 5.7, Figure 5.8 and Figure 5.9 show the good prediction and validation of the developed model by applying equation (5.14) to the feed concentration with varying Re_h and pressure for both E1 and E2 and the membranes NF 270 and TFC-SR2. Once the transient feed concentration $C_f(t)$ is predicted, the next step is to predict the transient permeate concentration.

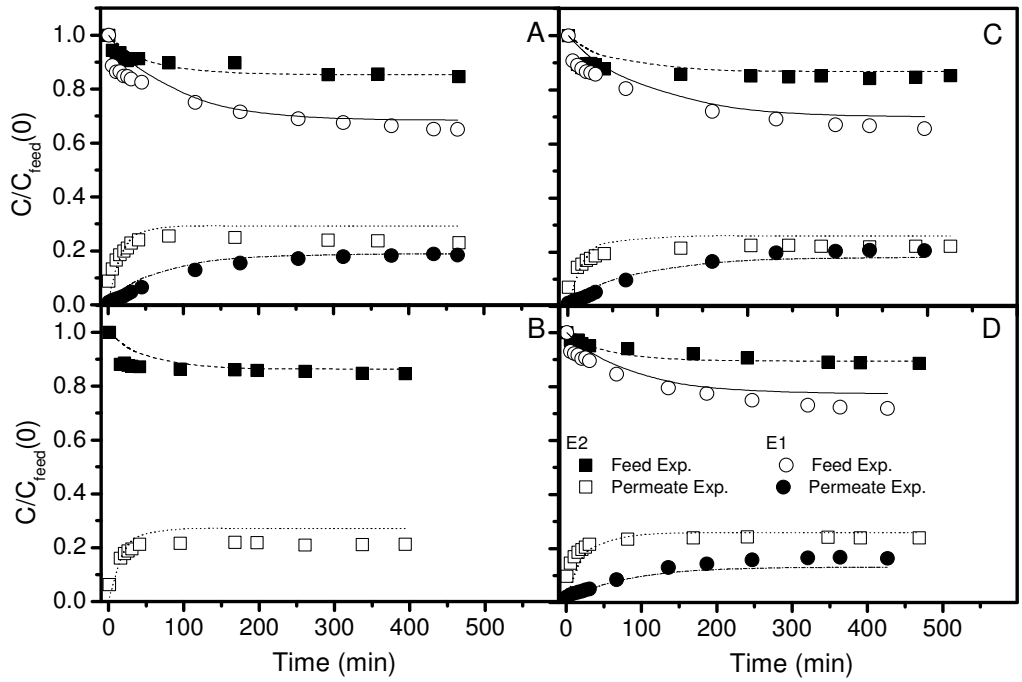

Figure 5.7 Experimental and predicted dimensionless feed and permeate concentration (transient feed and permeate concentration divided by initial feed concentration) for several Reynolds numbers (Re_h) **(A)** 570, **(B)** 698, **(C)** 855 and **(D)** 998 for estrone (E1) and estradiol (E2) and the NF 270 1 ($C_{feed\ initial\ (t=0)}$=100 $ng.L^{-1}$, T=24°C, pH 7, 11 bar)

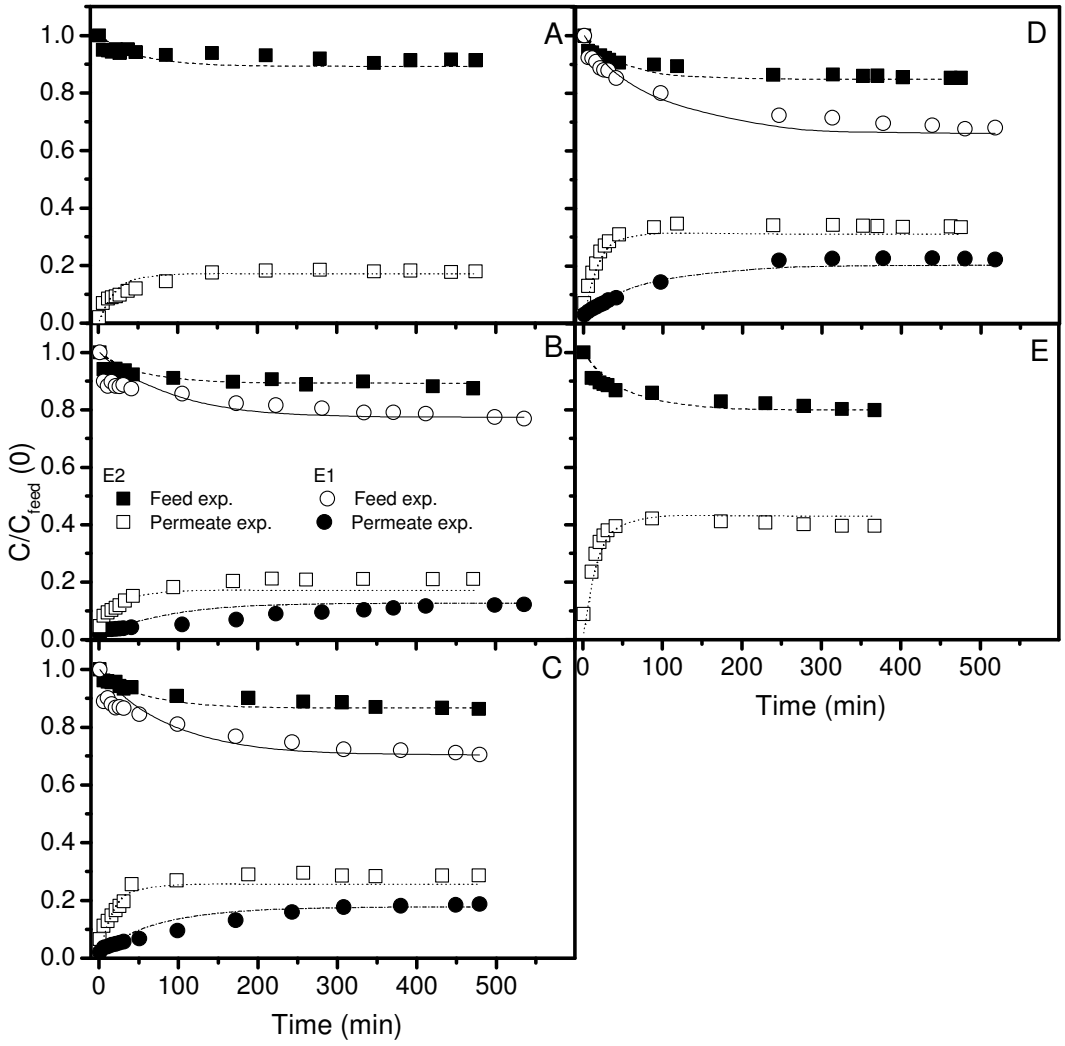

Figure 5.8 Experimental and predicted dimensionless feed and permeate concentration for several pressures **(A)** 3 bar, **(B)** 5 bar, **(C)** 8 bar, **(D)** 11 bar and **(E)** 17 bar for estrone (E1) and estradiol (E2) and the NF 270 1 ($C_{feed\ initial\ (t=0)}$=100 $ng.L^{-1}$, T=24°C, pH 7, Re_h=427)

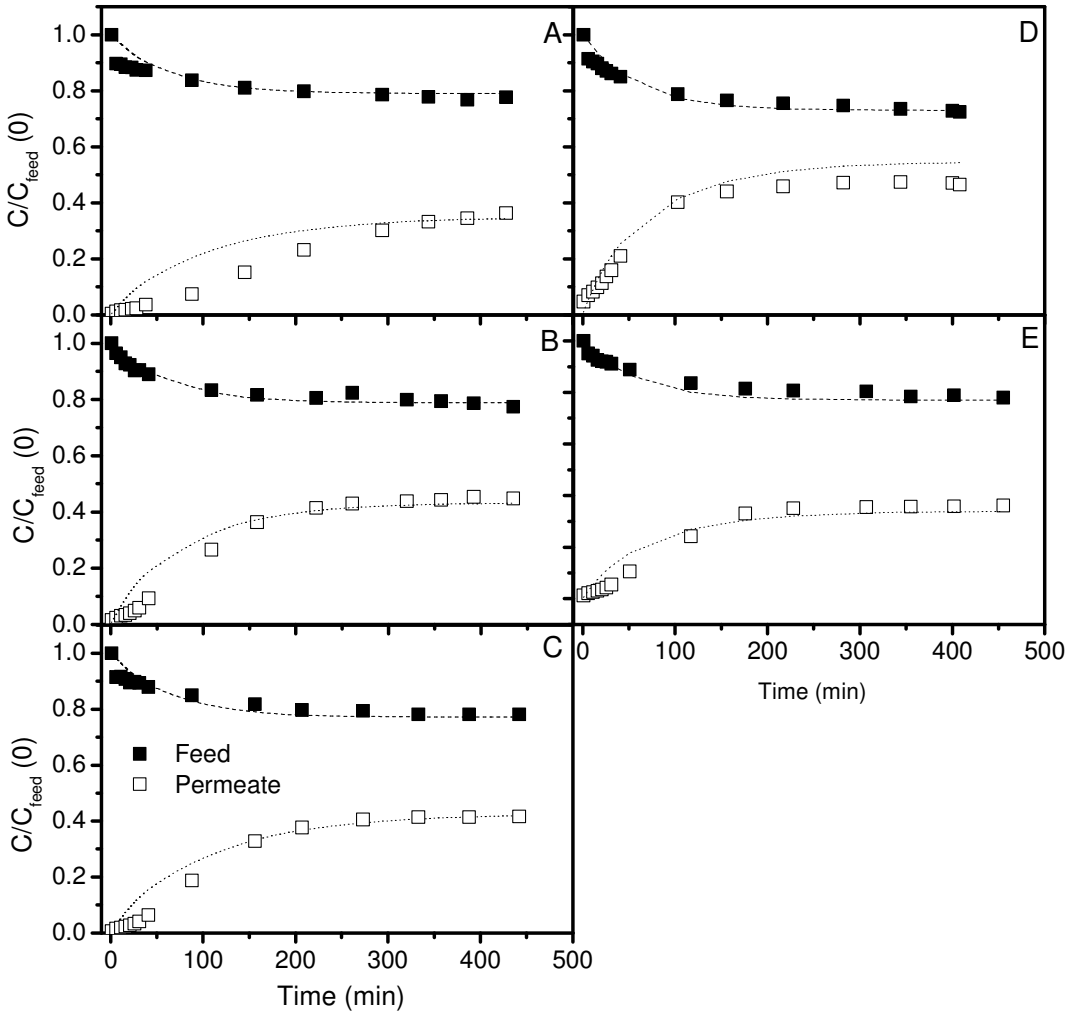

Figure 5.9 Experimental and predicted dimensionless feed and permeate concentration **(A)** 5 bar, **(B)** 8 bar, **(C)** Re_h=698, **(D)** 17 bar and **(E)** Re_h=998 for estradiol (E2) and the TFC-SR2 2 ($C_{feed\ (0)}$=100 ng.L^{-1}, T=24°C, pH 7)

5.4. Permeate Concentration Kinetics

5.4.1 Permeate Concentration Equation

A model capable of predicting the permeate concentration variation with time is developed below. Steinle-Darling *et al.* [175] showed that retention of adsorbing compounds follows the same type of exponential decay as the feed concentration and is given by equation (5.16), where Ret(0) is the retention obtained

in the first instances of filtration (100%), Ret_{ss} is the retention once steady-state is reached, t is time (s) and k_{ret} is a pseudo-first order rate constant (s^{-1}).

$$Ret(t) = Ret_{ss} + (Ret(0) - Ret_{ss}) \cdot e^{-k_{ret}t} \quad (5.16)$$

Using the definition of retention (equation 2.1) in equation (5.16) and after algebraic manipulation, equation (5.17) is obtained, where C_{pss} is the permeate concentration at steady-state ($ng.L^{-1}$).

$$C_p(t) = \frac{C_{p\,ss}}{C_{f\,ss}}\left(1 - e^{-k_{ret}t}\right)C_f(t) \quad (5.17)$$

To determine the transient permeate concentration, the rate constant k_{ret}, C_{pss}/C_{fss} and $C_f(t)$ are required.

5.4.2 C_{pss}/C_{fss} Determination

It was previously concluded (Chapter 4) that Ret_{ss}, and therefore C_{pss}/C_{fss}, depends on the initial polarisation modulus β. Since the isotherm experiments have a constant β, and therefore a constant Ret_{ss} (Figure 4.8 and Figure 4.9), the isotherm data cannot be used to determine this ratio. Experiments with varying β were therefore used as shown in Figure 5.10.

When β is plotted against C_{pss}/C_{fss}, a linear relationship is obtained for both hormones and membranes as shown in Figure 5.10. Once β is calculated for different conditions of pressure and Re_h numbers it can be applied to the relationship in Figure 5.10 and, subsequently, used to predict C_{pss}/C_{fss}, in much the same way as was done for the feed concentration prediction.

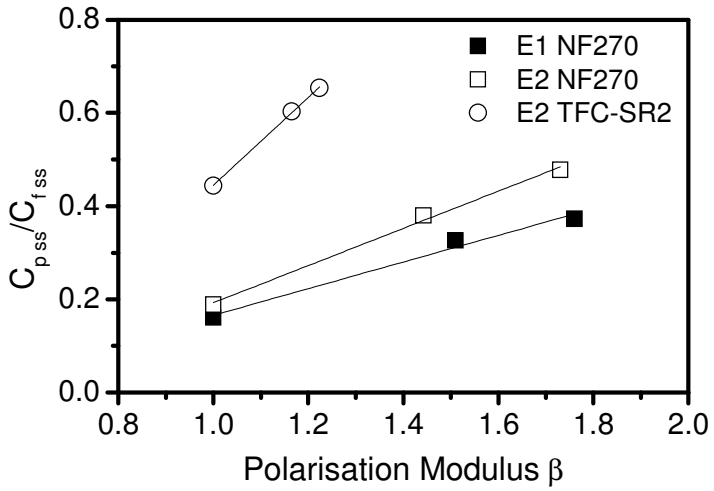

Figure 5.10 C_{pss}/C_{fss} variation with polarisation modulus β for estradiol (E2) and estrone (E1) and the TFC-SR2 2 and NF 270 1 membranes (Re_h=1450, C_{feed}=100 ng.L^{-1}, 11 bar; Re_h=427, C_{feed}=100 ng.L^{-1}, 11 bar; Re_h=427, C_{feed}=100 ng.L^{-1}, 15 bar)

5.4.3 Retention Rate Constant k_{ret}

Constant k_{ret} was determined by fitting equation (5.17) to the filtration isotherm experiments using an optimization method (Solver, Microsoft Excel). The parameter k_{ret} obtained was 2.0×10^{-4} s^{-1} for E1 and 7.2×10^{-4} s^{-1} for E2 with the NF 270 membrane and 1.7×10^{-4} s^{-1} for E2 for the TFC-SR2 membrane. Hormone E1 has a lower first order constant because adsorption, and therefore feed and permeate concentration, take longer to reach steady-state compared to E2.

5.4.4 Permeate Concentration Prediction

Figure 5.7, Figure 5.8 and Figure 5.9 show very good prediction and validation quality of the developed model by applying equation (5.17) for both hormones (E1 and E2) and membranes (NF 270 and TFC-SR2) following the described method for different conditions of pressure and Re_h numbers.

While transient feed and permeate concentrations are well predicted with this model as seen before for most tested operating conditions, that is not the case for all the filtration conditions. In the low pressure range (3 to 5 bar) for E1 and E2 with

the NF 270 and the TFC-SR2 and high Re_h number (998) for E1 with the NF 270 and E2 with the TFC-SR2 the predictions did not fit the experimental results as well. Concentration polarisation is not very pronounced at these conditions. In fact the mass adsorbed and the Ret_{ss} for these three conditions are similar to that obtained with a Re_h number in the transient regime, where polarisation is minimized (Chapter 4). Therefore, the use of the relationship of Figure 5.6 and Figure 5.10 with $C_m(0)$ is prone to overestimate the predicted mass adsorbed and the parameter C_{pss}/C_{fss}. Using the initial condition $C_f(0)$ instead of $C_m(0)$ in Figure 5.6 and Figure 5.10, where no concentration polarisation is considered, the prediction is more accurate, as can be seen in Figure 5.11. These results confirm the inference of Chapter 4 on the cleansing effect (larger shear stresses at the membrane surface of larger Re_h numbers).

The transient permeate trend provides information on the transport mechanisms of hormones. Since adsorption for E1 is much higher than for E2, the permeate concentration transient response is slower and therefore takes longer to reach steady-state. Because more mass is adsorbed inside the membrane, it also takes longer to obtain a breakthrough curve. Due to the higher sorption of E1 compared to E2 this is more emphasized for E1. Compounds that sorb in high quantities onto the membrane have a very low permeate concentration for a long time [175], sometimes giving 100% retention for the initial stages of filtration (first 8 hours).

The lower the concentration at the membrane surface (low pressures and high Re_h numbers), the higher is the retention and the slower is the breakthrough curve. This occurs because the pressure driving force for the compound to permeate through is smaller and therefore there is less adsorption on the membrane.

When comparing the different membranes used, TFC-SR2 is seen to adsorb larger quantities of E2 than NF 270 (Figure 5.6), showing that adsorption is not only dependent on the hydrodynamics at the membrane surface, but also on the membrane morphological characteristics.

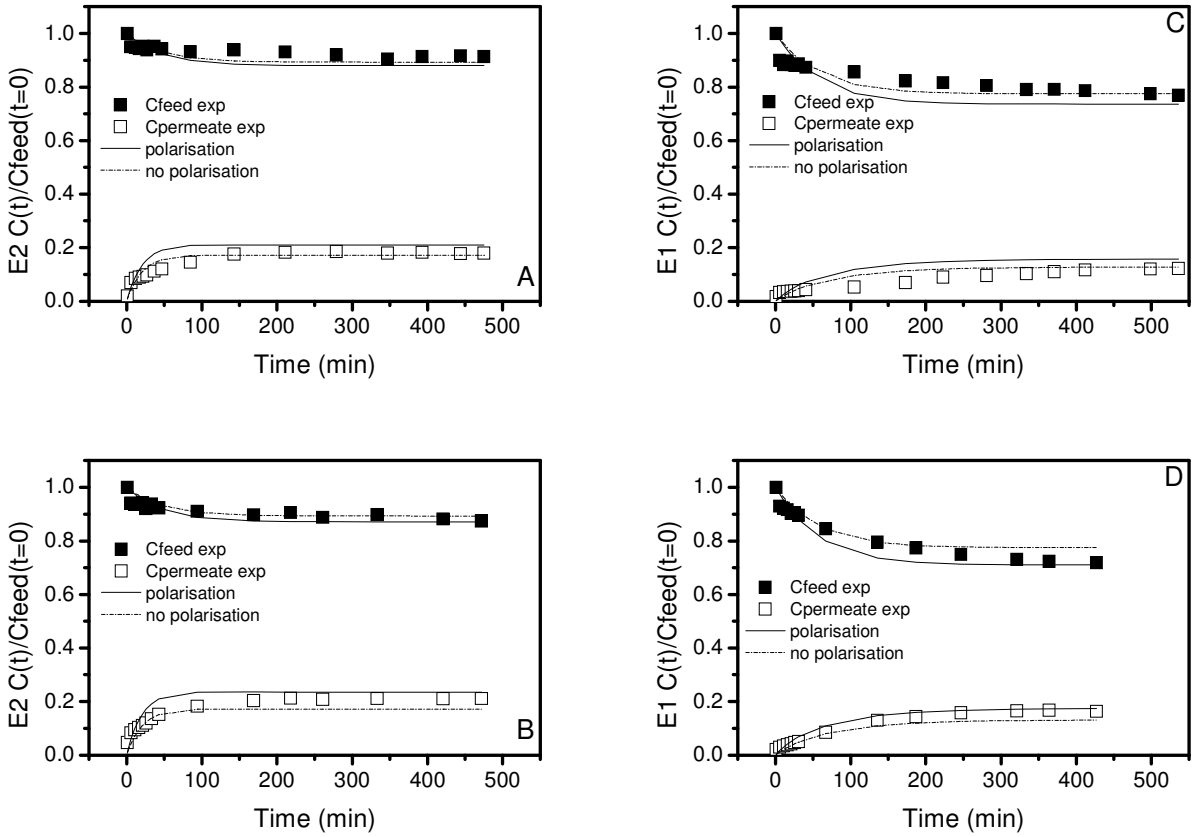

Figure 5.11 Experimental and predicted dimensionless feed and permeate concentration in the presence or absence of polarisation for estradiol (E2) **(A)** 3 bar, **(B)** 5 bar, and E1 **(C)** 5 bar and **(D)** Re_h=998 ($C_{feed\ initial}$ (t=0)=100 ng.L^{-1}, T=24°C, pH 7, 11 bar, NF 270 1)

5.5. Model Validation with Background Electrolyte

It has been argued that when salts present in background electrolyte are found in solution, they shield the membrane charge and therefore affect the removal of trace contaminants if they are charged or polar [32, 40, 164, 166, 167]. In the study by Nghiem *et al.* [153] the effect of cross-flow velocity and pressure onto E1 retention with background electrolyte on a pre-saturated membrane was carried out. It was found that cross-flow velocity had no effect, and that the pressure increase caused a decrease in retention. This, however, does not provide any information of

the effect of pressure and Re_h number on the adsorption of hormones in the presence of background electrolyte.

When background electrolyte is present in solution, the permeate flux is lower when compared to the pure water flux (J_s/J_0) due to osmotic pressure difference between the feed side and the permeate side. In Figure 5.12 the osmotic pressure affects the permeate flux in the same proportion for several pressures, causing a decrease of up to 20% in the permeate flux when compared to the situation where electrolyte is absent ($J/J_0 \approx 1$). This is accompanied by a decrease in the salt retention. When the Re_h number effect is studied, its results depicted in Figure 5.13 show that the permeate flux decreases less for higher Re_h numbers when compared to the situation where electrolyte is absent ($J/J_0 \approx 1$) because there is less polarization, causing an increase in the salt retention.

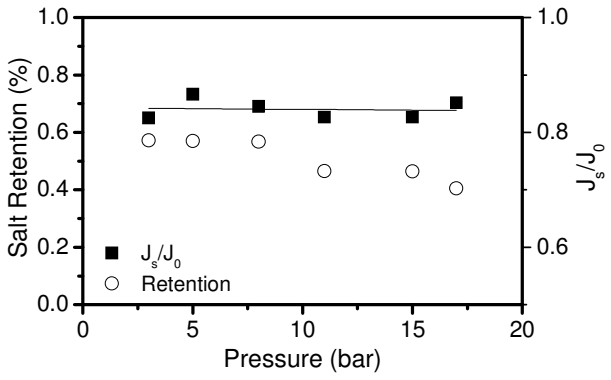

Figure 5.12 Steady-state background retention and normalized flux as a function of pressure for the NF 270 1 ($C_{feed\ E2}$ (t=0)=100 ng.L^{-1}, T=24°C, pH 7, Re_h=427, 1mM $NaHCO_3$, 20 mM NaCl)

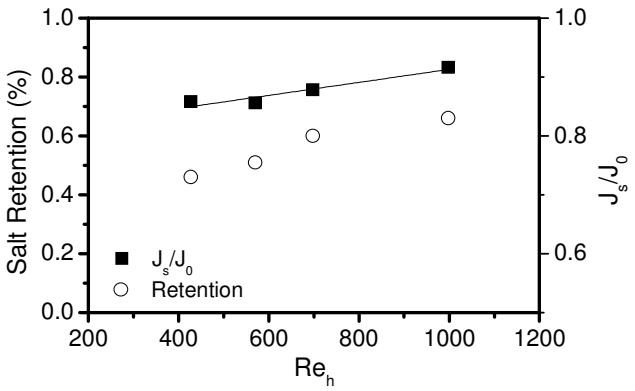

Figure 5.13 Steady-state background retention and normalized flux as a function of Re_h for the NF 270 1 ($C_{feed\ E2}$ (t=0)=100 ng.L^{-1}, T=24°C, pH 7, 11 bar, 1mM $NaHCO_3$, 20 mM NaCl)

When background electrolyte is present two types of initial polarization modulus can be determined for the hormones:

- the one that would be expected in the absence of salts and previously defined as β (equation 4.4), which is calculated based on the pure water flux J_0 measured before spiking the hormones, and

- the polarization modulus in the presence of salts, calculated based on the decrease in pure water flux J_{s0} caused by the osmotic pressure difference between feed and permeate before spiking the hormones (equation (5.18)),

$$\beta_s = \frac{C_{ms}(0)}{C_f(0)} \tag{5.18}$$

where $C_{ms}(0)$ is the initial hormone concentration at the membrane surface in the presence of salt by taking into account the decrease in permeate flux caused by osmotic pressure and $C_f(0)$ is the initial feed concentration.

When background electrolyte is present, the same effect of pressure and Re_h is obtained: the mass adsorbed increases with increase of pressure and decrease of Re_h (Figure 5.14 and Figure 5.15). However, the total mass adsorbed in the presence of salt is smaller than that in the absence of salt, especially when polarization is more severe, *i.e.* for higher pressures and lower Re_h numbers (Figure 5.14 A and Figure 5.15 A). Whenever polarization is minimized, the differences between the total mass adsorbed in the presence or absence of background electrolyte are much less pronounced.

When the different initial polarization modulus β_s and β are compared with each other in Figure 5.14 B and Figure 5.15 B, it can be seen that the presence of salts lowers the initial polarization modulus, therefore explaining the lower mass adsorbed obtained.

The osmotic pressure difference between the feed (membrane surface) and permeate can be calculated based on the feed and permeate salt concentrations, given by equation (5.19):

$$\Delta\pi = \pi_{membrane} - \pi_{permeate} \tag{5.19}$$

where the osmotic pressure is calculated with equation (5.20):

$$\pi = iCRT \qquad (5.20)$$

In the previous equation i is the number of ions produced by the salt dissociation (assumed only as NaCl, which is present in much higher concentrations compared to $NaHCO_3$), C is the salt concentration either on the membrane surface or in the permeate ($mol.L^{-1}$), R is the gas constant ($L.bar.mol^{-1}.K^{-1}$) and T is the temperature (K).

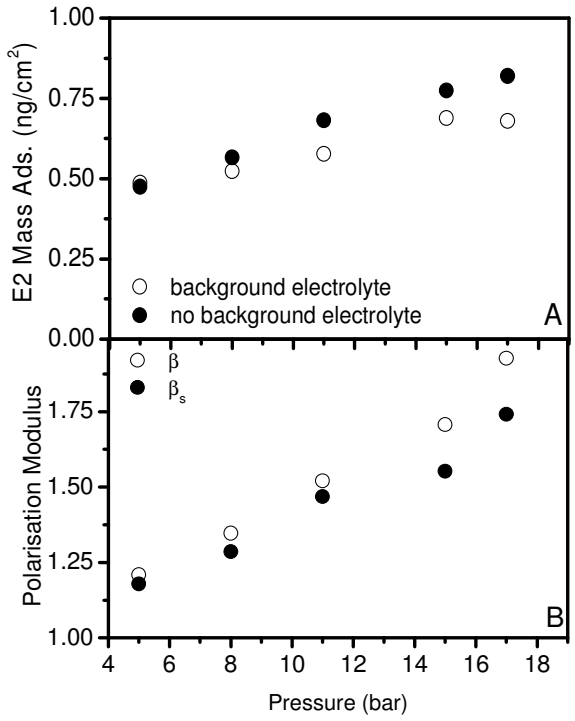

Figure 5.14 Pressure influence on estradiol (E2) steady-state **(A)** adsorption (Mass Ads.) and **(B)** polarisation modulus β (Re_h=427, $C_{feed\ initial}$=100 $ng.L^{-1}$, T=24°C, pH 7, presence and absence of 1 mM $NaHCO_3$, 20 mM NaCl) for the NF 270 1

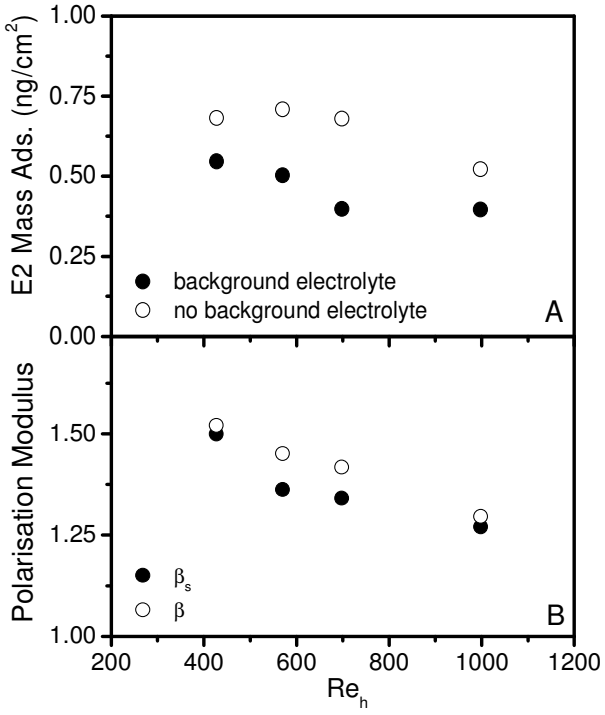

Figure 5.15 Re_h influence on estradiol (E2) steady-state **(A)** adsorption (Mass Ads.) and **(B)** polarisation modulus β (11 bar, $C_{feed\ initial}$=100 $ng.L^{-1}$, T=24°C, pH 7, presence and absence of 1 mM $NaHCO_3$, 20 mM NaCl) for the NF 270 1

The salt concentration at the membrane surface is calculated through the use of the concentration polarization theory (equation 4.4) where J is substituted by the permeate flux obtained in the presence of salts, J_{s0}, and the Sherwood correlation used in Chapter 4 (equation 4.5 b).

The permeate flux in the presence of salts can then be calculated by taking the osmotic pressure into account as expressed by equation (5.21),

$$J_{s0} = L_p(\Delta P - \Delta\pi) \qquad (5.21)$$

where J_{s0} is the permeate flux in the presence of salts (L. $h^{-1}.m^{-2}$), ΔP is the applied pressure (bar) and $\Delta\pi$ is the osmotic pressure (bar) calculated by equation (5.19).

Since in the present case the osmotic pressure is much smaller than the applied pressure ($\Delta\pi << \Delta P$), the prediction is expected to be good. The results of the permeate flux calculated for several pressures according to equation (5.21), are shown in Figure 5.16 and compared against the experimental results. They exhibit very similar values, confirming the osmotic pressure phenomena caused by the presence of background electrolyte.

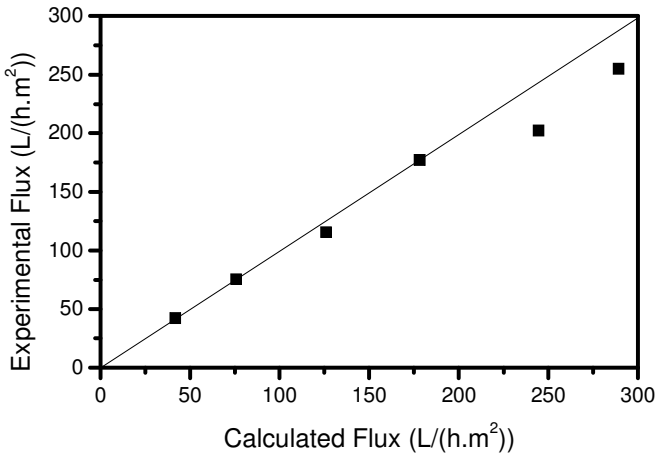

Figure 5.16 Experimental and calculated flux for several pressures for estradiol (E2) for the NF 270 1 ($C_{feed\ initial}$ (t=0)=100 ng.L^{-1}, T=24°C, pH 7, Re_h=427, 1mM $NaHCO_3$, 20 mM NaCl, 3, 5, 8, 11 and 17 bar)

As previously discussed, the presence of salts decreases the permeate flux due to osmotic pressure. The presence of background electrolyte therefore decreases the polarization modulus and consequently the mass adsorbed. The decrease in flux affects the hydrodynamics by decreasing the hormone concentration at the membrane surface, or β and, consequently, decreasing the mass adsorbed.

To confirm this hypothesis, the previous sorption model was applied for E2 by using the rate constants and relationships obtained for the NF 270 in Figure 5.6, Figure 5.10 and Table 5.3 (*i.e.* in the absence of background electrolyte) for several experimental conditions with background electrolyte. The hormone initial concentration at the membrane surface $C_m(0)$ is calculated with equation (4.4). In this case, the permeate flux used was the experimental one J_{s0} measured in the presence of background electrolyte before spiking the hormones. This $C_m(0)$ is then used in the relationships obtained from Figure 5.6 and Figure 5.10 to predict the transient feed and permeate concentrations where the yielded results are shown in Figure 5.17 for several Re_h numbers, Figure 5.18 for several pressures and Figure 5.19 for several feed concentrations.

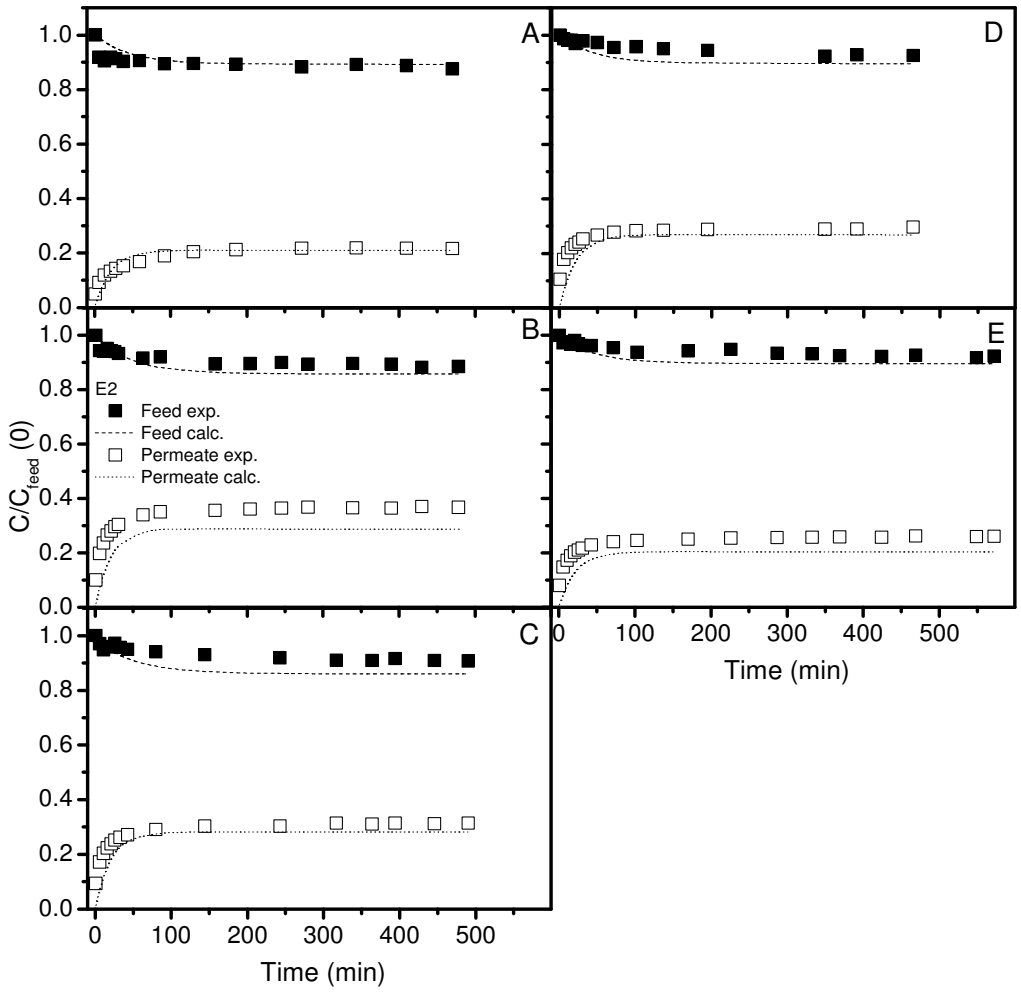

Figure 5.17 Experimental and predicted dimensionless feed and permeate concentration for several Reynolds numbers (Re_h) **(A)** 427, **(B)** 570, **(C)** 698, **(D)** 998 and **(E)** 1211 for estradiol (E2) and the NF 270 1 membrane ($C_{feed\ initial}$ (t=0)=100 $ng.L^{-1}$, T=24°C, pH 7, 11 bar, 1 mM $NaHCO_3$, 20 mM NaCl)

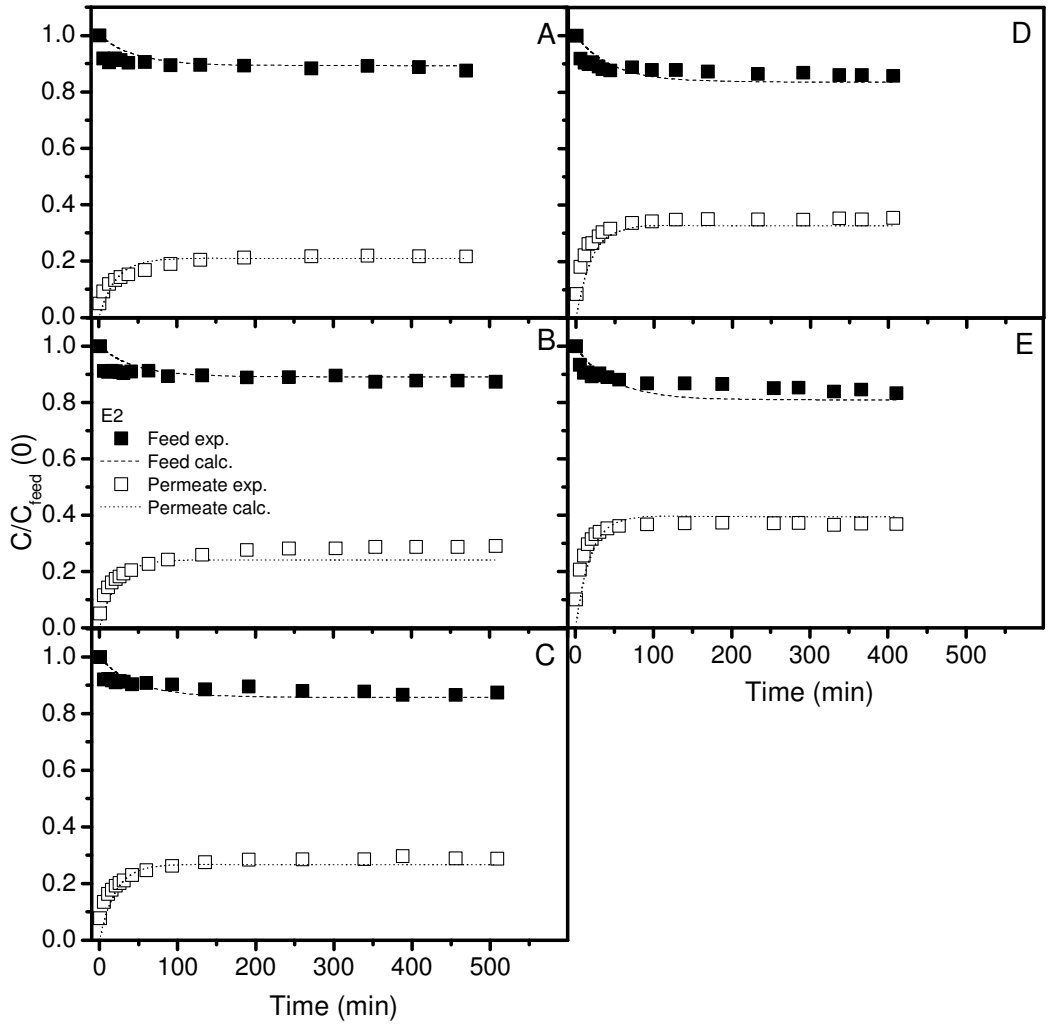

Figure 5.18 Experimental and predicted dimensionless feed and permeate concentration for several pressures **(A)** 3 bar, **(B)** 5 bar, **(C)** 8 bar, **(D)** 11 bar and **(E)** 17 bar for estradiol (E2) and the NF 270 1 membrane ($C_{feed\ initial}$ (t=0)=100 ng.L^{-1}, T=24°C, pH 7, Re_h=427, 1 mM $NaHCO_3$, 20 mM NaCl)

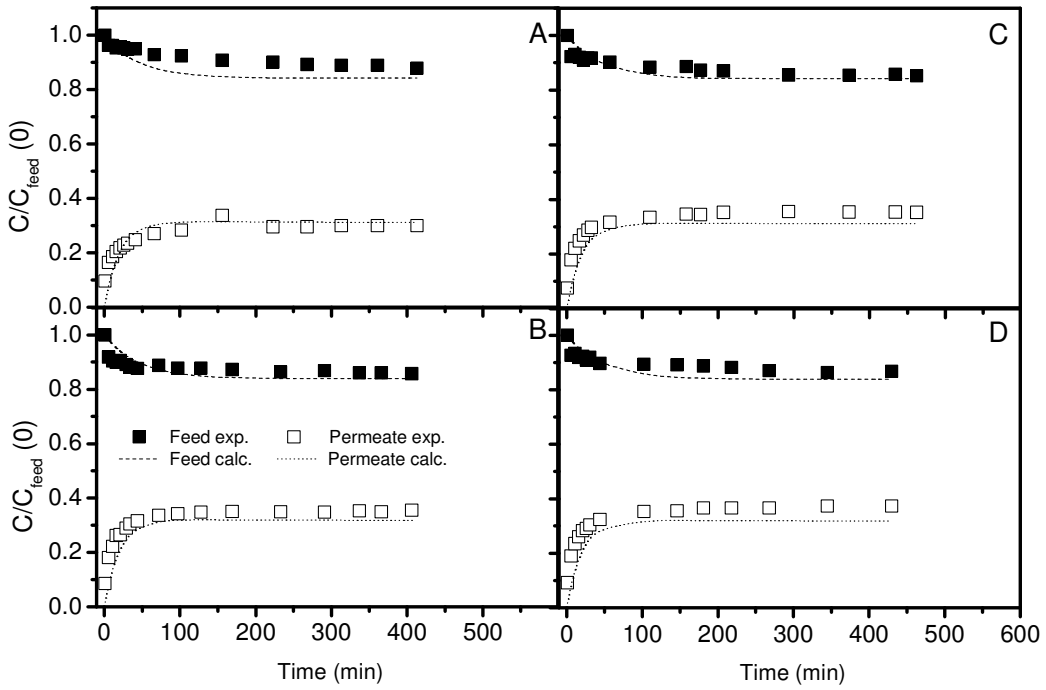

Figure 5.19 Experimental and predicted dimensionless feed and permeate concentration for several feed concentrations **(A)** 50 ng.L^{-1}, **(B)** 100 ng.L^{-1}, **(C)** 500 ng.L^{-1}, **(D)** 1000 ng.L^{-1} for estradiol (E2) and the NF 270 1 membrane (11 bar, T=24°C, pH 7, Re_h=427, 1 mM $NaHCO_3$, 20 mM NaCl)

As can be seen from those figures, the model predicts well the time dependent feed and permeate concentrations in the presence of background electrolyte. This confirms that the differences obtained in the presence of background electrolyte are not caused by solute characteristics such as polarity, but by changes in the hydrodynamics caused by the salt osmotic pressure.

5.6. Conclusions

The mechanisms that affect hormone adsorption and retention onto NF membranes have been elucidated, as far as the permeation operating conditions are concerned. By studying the impact of hydrodynamics (pressure and Re_h number) and feed concentration it was found that concentration polarisation has a strong influence

on adsorption. Adsorption is therefore dependent on the concentration at the membrane surface.

Adsorption of hormones onto NF membranes, the hormone transient feed concentration and retention were found to be described by a pseudo-first order sorption kinetics. Based on this equation and on the knowledge that adsorption is dependent on the concentration polarization, the transient feed and permeate concentration can be predicted for any experimental condition with the developed model.

Furthermore, the presence of background electrolyte was found to increase the osmotic pressure, hence decreasing the permeate flux. This permeate flux decrease lowered the hormone concentration at the membrane surface, causing a lower mass adsorbed and a higher retention by the NF membrane. The model developed to predict the transient feed and permeate concentration was validated in the presence of background electrolyte, where the occurrence of osmotic pressure was taken into account.

This model can be further applied to other adsorbing trace contaminants onto NF membranes. However, one needs to firstly check the adsorption order of kinetics and then experimentally determine the necessary rate constants. Once these are determined, the membrane performance in terms of contaminant rejection can be predicted for several hydrodynamic conditions.

6 Influence of Membrane and Solute Characteristics in Adsorption

6.1. Introduction

In Chapter 4 the influence of the membrane filtration parameters, *i.e.* hydrodynamic conditions and feed concentration, on adsorption and retention was studied. This allowed for the development of a predictive model in Chapter 5 based on a pseudo-first order sorption kinetics. The membranes were, however, treated as black boxes in that study leaving a gap in the understanding of the effect of different membrane characteristics such as the pore radius and the membrane material in adsorption. Understanding the effect of these parameters is a crucial further step in understanding the transport and removal of hormones by NF membranes.

The effect of pore radius on trace contaminant adsorption and retention by NF membranes is important since it allows determining if steric exclusion (*i.e.* solute to pore radius ratio) need to be taken into account when modelling adsorption onto NF membranes. In general, retention increases with increase of compound molecular weight [26, 28, 150] showing a size exclusion mechanism. Nghiem *et al.* [23, 160], however, showed that the occurrence of hormone adsorption onto NF membranes caused a lower retention than would be expected if only steric interactions were considered. Hormone adsorption was found to be higher for two NF membranes compared to an RO membrane, suggesting a pore radius effect in hormone adsorption and retention by polymeric membranes [172].

Several studies [41, 278] have suggested the occurrence of internal adsorption on the NF active layer. Kimura *et al.* [37] obtained lower contaminant extraction in static mode from membranes saturated under pressure (40%-60%) compared to membranes saturated under static conditions (100%). McCallum *et al.* [152] on the other hand obtained 100% extraction efficiency when carrying out the

desorption under pressure of a pre-saturated membrane. All these studies indicate that membrane adsorption occurs inside the active layer. If this is the case, then pore radius might not be the only parameter affecting adsorption and retention of trace contaminants by NF membranes: internal surface area might play a role as well. A systematic study showing the contribution of internal surface area needs to be carried out.

Adsorption of trace contaminants onto different types of polymeric membranes has been reported in the literature [26, 29, 35, 37]. Adsorption of 100 $ng.L^{-1}$ estrone to two NF membranes made of cellulose acetate and polyamide active layer resulted in a decrease in feed concentration caused by sorption of 20% and 65%, respectively [173]. A higher decrease in feed concentration caused by adsorption was also obtained between 4-phenylphenol and a polyamide membrane compared to a cellulose acetate one [24]. Adsorption of estrone by a polypropylene MF membrane and estradiol in a UF polyimide membrane has been obtained [141, 142]. Determining where trace contaminant adsorption occurs in TFC NF membranes is necessary to understand and model the removal of trace contaminants. According to Ben-David *et al.* [279] adsorption is thought to be caused by the partitioning of trace organics onto the NF polyamide active layer. Several authors have carried out static adsorption experiments with membrane coupons of the polysulfone (PSu) support with and without the polyamide (PA) active layer. Williams *et al.* [192] and Steinle-Darling *et al.* [175] obtained much higher adsorption of phenolic compounds and perfluorochemicals, respectively, onto PA+PSu compared to just PSu. McCallum *et al.* [152] results showed that hormone adsorption onto PA+PSu was slightly higher than PSu only. Polyester (PET), the third material of TFC membranes, was shown not to adsorb any hormones. These results give a good indication of the affinity of the contaminant with the different materials. However, it is difficult to determine the affinity of the contaminant for each material independently. The affinity with PA is carried out in the presence of PSu since these two layers are not possible to separate and competition between the two layers might occur. A systematic study for the separate polymers is therefore necessary to properly establish the differences in affinity between the hormone and the polymeric materials.

The relevant membrane characteristics needed to understand and model transport of adsorbing hormones through NF membranes are determined in this chapter. Understanding how these membrane characteristics affect adsorption and retention of hormones by NF membranes is a first step for modelling development as it allows deciding as to which approach is the most appropriate to characterise the transport of adsorbing hormones through NF membranes.

The affinity of the hormones onto the different raw polymeric materials that constitute the TFC membranes is established, by ensuring access to the same surface area. The adsorption of hormones onto the polyamide and polysulfone layers for the NF 270 membrane is also independently quantified.

Several TFC NF membranes are characterised in terms of pore radius and active layer thickness to porosity ratio to study the effect of pore radius in hormone adsorption and retention. The effect of the internal surface area was further considered in this study.

6.2. Hormone Adsorption on Different Polymeric Materials

The first step in determining the different affinities the hormones have with the different polymeric materials consists in performing adsorption experiments with E2 and ground polymeric materials with a determined and known area.

6.2.1 Adsorption on Different Filters

Several filters of different materials are tested in order to choose the most appropriate one to separate the polymeric material in solution from the freely dissolved E2. This allows determining the E2 mass adsorbed onto the polymeric material by mass balance. A feed concentration of 100 $ng.L^{-1}$ of E2 was permeated through these filters 10 times (*i.e.* total of 10 mL) to check for E2 adsorption on the filter material, with the results presented in Figure 6.1 and the total mass adsorbed presented in Figure 6.2. In Figure 6.1 the feed concentration of 100 $ng.L^{-1}$ is represented as a horizontal line. In Figure 6.2 the total mass permeated through the filters was 1 ng and is also represented as a horizontal line.

The filter made of glass material was found to adsorb the lowest mass of E2. After the third permeation, the permeate concentration is the same as the feed one and the total mass adsorbed is 0.02 ng. The PVDF filter, despite a low first permeate concentration, also adsorbed low amount of E2. The total mass adsorbed was 0.07 ng and the filter saturated after 3 filtrations, in the same way as the glass fibre filter.

In comparison, PA, which constitutes the material used in the active layer of TFC NF membranes, was found to adsorb the highest mass compared to any other material, with the permeate concentration never exceeding 15 $ng.L^{-1}$, even after 10 permeations. The filter adsorbed a total mass of 0.9 ng of E2, which represents 90% of the total E2 mass filtered. These results show the high interaction that exists between hormones and polyamide-based materials. The filters made of CA and CE adsorbed about half of the total mass permeated and did not reach saturation after 10 filtrations, with permeate concentration values less than 80 $ng.L^{-1}$ for CE and 60 $ng.L^{-1}$ for CA.

These results show the different degrees of interaction that occur between hormones and different polymeric materials. PA is found to adsorb higher mass of hormone compared to any other of the filters tested. These results further have an obvious impact in the pre-treatment of environmental samples for analysis. The pre-filtration of these samples might cause the loss of analytes, as previously suggested by Peta *et al.* [280] where hormones can be lost due to interaction with the filter. Care needs therefore to be taken when choosing the filter material to be used in sample pre-treatment.

Despite giving a preliminary idea of the different degrees of interaction between the hormones and different polymeric materials, these filters will have different thicknesses, pore radius (section 2.8.5. in Chapter 3) and, therefore, different surface areas available that may impact on adsorption. To be able to compare the hormone adsorption capacity of the different materials, these need to be subjected to the same conditions of hormone concentration and surface area.

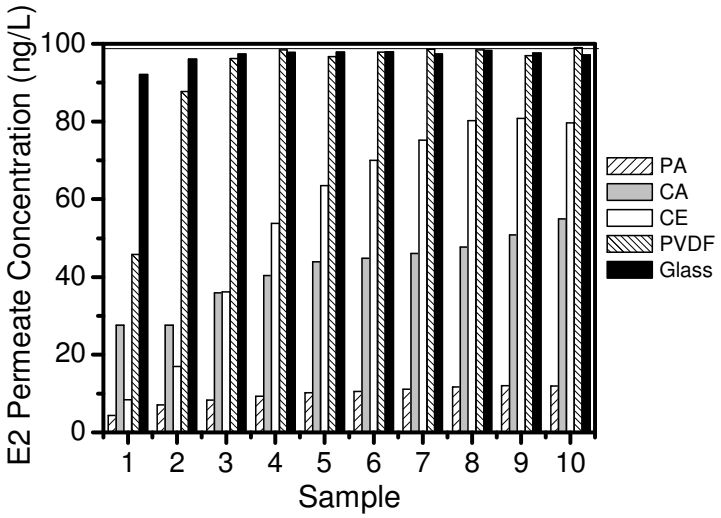

Figure 6.1 Permeate concentrations of several filters ($C_{feed\ E2}$=100 ng.L^{-1})

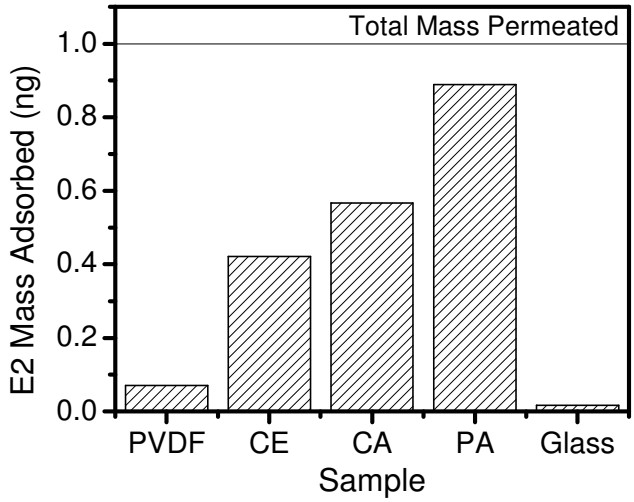

Figure 6.2 Total filter estradiol (E2) mass adsorbed after 10 filtrations ($C_{feed\ E2}$=100 ng.L^{-1})

6.2.2 Adsorption on Different Polymeric Materials

Several polymers ground and with known surface area (as described in section 3.8.5) are tested for E2 adsorption under the same conditions of E2 feed concentration. The polymer properties are presented in Table 6.1. These polymers are commonly used in MF, UF, NF and RO polymeric membranes. The results of the performed experiments of E2 adsorption are displayed in Figure 6.3.

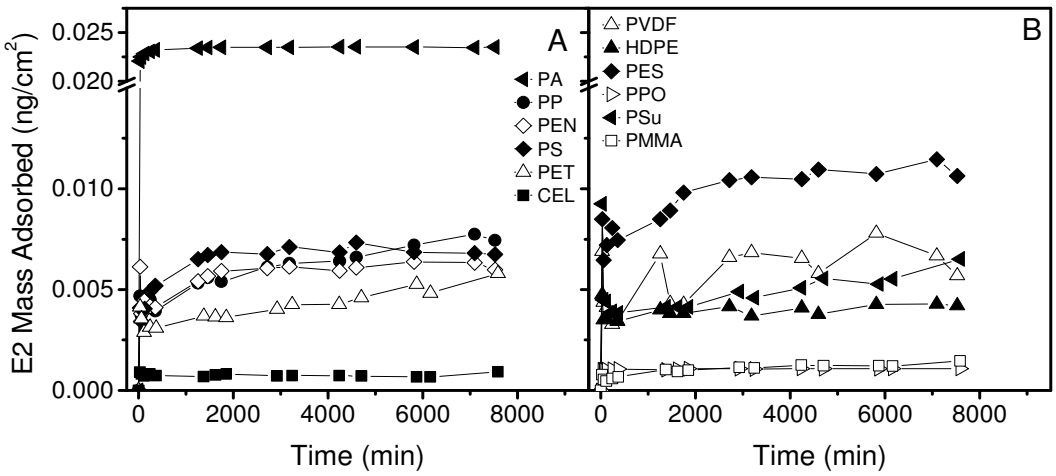

Figure 6.3 Estradiol (E2) adsorption on different polymeric materials

As can be seen from the different polymer adsorption results (Figure 6.3), PA has once again been found to adsorb the highest mass of hormone, reaching almost 0.025 ng.cm^{-2} compared to values less than 0.010 ng.cm^{-2} for all other polymers tested. Moreover, the total mass of adsorbed on PA is greater than 95% of the available E2 initial mass.

The polymer PES was the second polymer that adsorbed the most (0.010 ng.cm^{-2}), with adsorption values below half of those that PA adsorbs, despite PA being one of the least hydrophobic polymers (Table 6.1).

The polymers that adsorbed the least were CEL, PPO and PMMA. None of these three polymers have highly polarised groups that can exchange a hydrogen atom to form hydrogen bonding. In comparison, cellulose ester for example is a modified cellulose molecule, where highly polarised functional groups are inserted in the molecule. This may explain the much greater adsorption values obtained in the filters displayed in Figure 6.2 as compared to the much smaller ones obtained with cellulose in Figure 6.3.

All the other polymers studied adsorbed similar quantities, around 0.005 ng.cm^{-2}, where differences in affinity between the hormone E2 and the polymeric material are difficult to discern.

Table 6.1 Polymer type, supplier, and selected characteristics of polymers

Polymer Name	**Supplier**	**Structure**	**Monomer MW ($g.mol^{-1}$)**	**Contact Angle (º)**
Polysulphone (PSu), (PSu UDEL)	Solvay	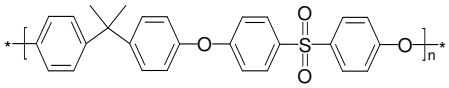	442	84 [281]
Polyester; Polyethylene Teraphthalate (PET)	Goodfellow	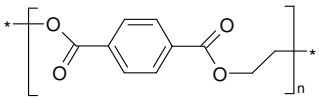	192	70 -81 [282-284]
Polyester; Polyethylene Naphthalate (PEN)	Goodfellow	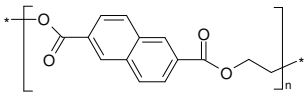	242	80 [282]
Polyamide Nylon, 6 (PA)	Goodfellow	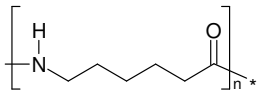	113	69.2-70 [284, 285]
Polyethersulphone (PES)	Goodfellow	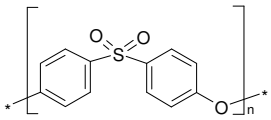	232	56-72 [282, 286]
Polyvinylidene fluoride (PVDF)	Solvay	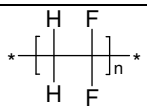	64	71 [287]
Polystyrene (PS)	Goodfellow	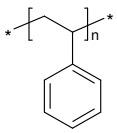	104	91 [284]
Polypropylene (PP)	Goodfellow	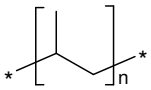	42	95 [282]
Polyethylene (HDPE)	Goodfellow	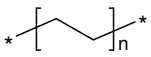	28	93-94 [282]
Poly(2,6 dimethyl 1,4-phenylene oxide) (PPO)	Sigma	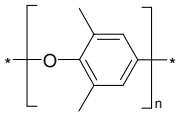	120	88 [288]
Polyacrylate; Poly(methyl methacrylate) (PMMA)	Sigma	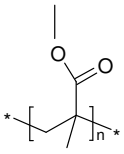	100	73 [282]
Cellulose (CEL)	Sigma	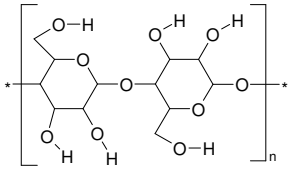	324	24 [289]

The polymers that constitute the TFC NF membranes, PSu, PET and PEN were found to adsorb less than 35% of the total initial mass available in the feed solution. However, a more in depth study with different polymer or surface area is necessary to permit the comparison of the degree of interaction between the different polymers and the hormone. To determine where the bulk of the adsorption occurs on commercial polymeric TFC NF membranes, such more in depth study is carried out for PA, PET, PEN and PSu.

6.2.3 Adsorption on the Polymers Composing TFC NF

TFC NF membranes are made of three layers of different materials. Polyester PE (PET or PEN) and PSu support layers that do not have any role in the separation under filtration conditions, and a PA dense active layer that acts as the separation layer. These three layers have different thicknesses and porosities and in filtration they are in contact with different hormone concentrations (Figure 6.4): the PA layer is in contact with the concentration at the membrane surface, which is much higher than the permeate concentration; in turn, the permeate concentration is in contact with the PSu and PE layers.

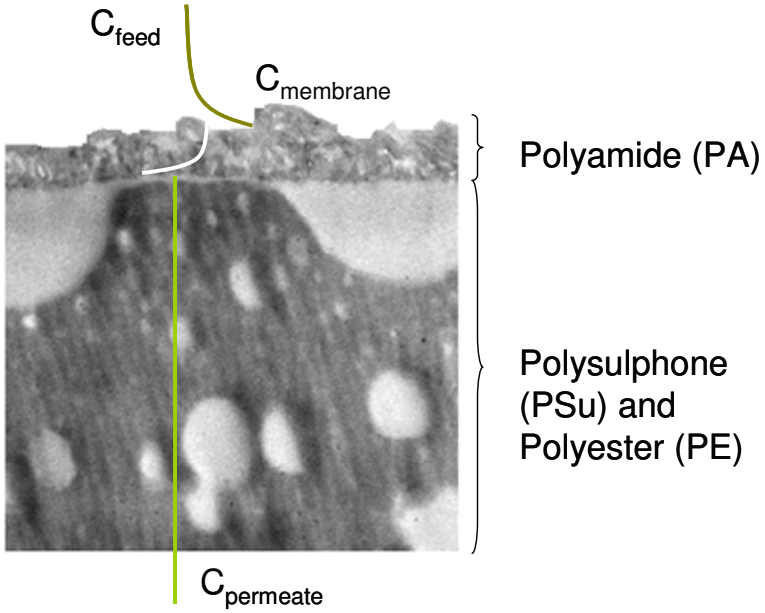

Figure 6.4 Concentration profile for TFC membranes (adapted from [238])

To determine the affinity of a hormone with a polymeric material, these need to be tested independently with a known surface area, which is different from that occurring in filtration, where the different layers have different characteristics and are in contact with different hormone concentrations, as previously seen.

Hormone adsorption experiments onto the powder polymeric materials that constitute commercial TFC NF membranes (PA, PSu, PET and PEN) is carried out to determine which material preferentially adsorbs the hormones. The adsorption isotherms for the different materials are presented in Figure 6.5 A.

The isotherms are clearly not linear. They convex upwards, indicating a Freundlich type of isotherm (Figure 6.5 A). The Freundlich isotherm equation is given by equation (6.1),

$$M_{ads} = K_f C_{equilibrium}^{1/n_i} \quad (6.1)$$

where M_{ads} is the mass adsorbed ($ng.m^{-2}$), K_f is the Freundlich capacity factor related to the adsorption capacity of the sorbent ($ng^{(1-1/ni)}.m^{(3/ni-2)}$), $C_{equilibrium}$ is the hormone concentration in solution at equilibrium ($ng.m^{-3}$) and n_i is the Freundlich exponent, related to the energy of adsorption. The logarithmic form of equation (6.1) yields equation (6.2):

$$Log(M_{ads}) = \frac{1}{n_i} Log(C_{equilibrium}) + log(K_f) \quad (6.2)$$

To confirm if the isotherm is of the Freundlich type, the data in Figure 6.5 A is represented in logarithmic form (Figure 6.5 B) and the linear fitting provides the Freundlich coefficients according to equation (6.2).

The correlation coefficient R^2 and the isotherm coefficients are presented in Table 6.2. The slope $1/n_i$ obtained from Figure 6.5 B dictates the type of free energy involved in the sorption. Since $1/n_i>1$ for all the polymers (Table 6.2), the isotherm is convex upwards (Figure 6.5 B). This means that more sorbate (*i.e.* hormone) present in the sorbent (*i.e.* polymeric material) enhances the free-energy of further sorption [290]. It is thought that sorbed molecules lead to a modification of the sorbent

surface properties, enhancing further sorption. Estradiol is a hydrophobic compound (Table 3.10) and possibly causes the material surface to become more hydrophobic when adsorbing onto it.

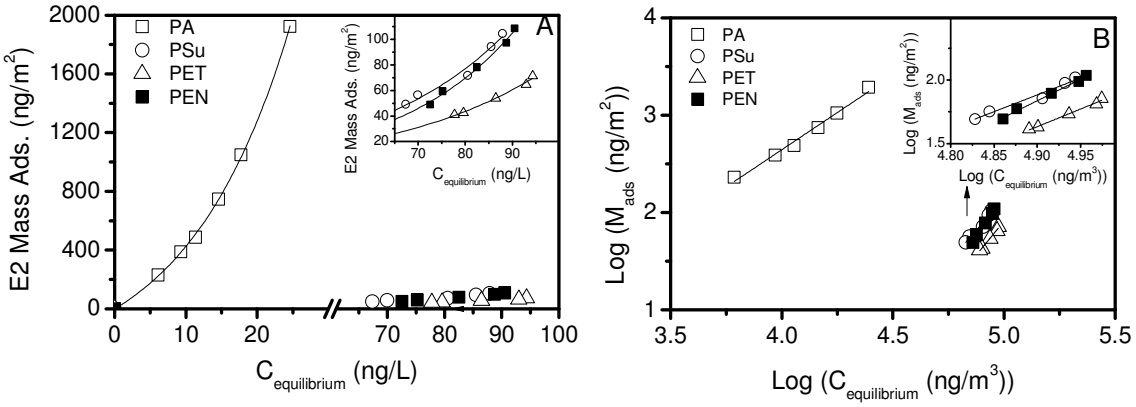

Figure 6.5 Estradiol (E2) static adsorption **(A)** isotherm onto different polymers (PA, PSu, PET and PEN, C_{feed}=100 ng.L^{-1}, 200 rpm, 25ºC) and **(B)** linear regression of the logarithmic form of the Freundlich isotherm

The coefficient K_f can give an indication of the affinity of the hormone with the polymer. A higher K_f equates to a greater hormone adsorption capacity. The highest K_f was obtained for PA, followed by much smaller values for PSu and PET. This confirms the higher affinity of the hormones with PA compared to the other polymers. As can be seen in Figure 6.5 A, PA adsorbs greater mass compared to any of the other polymers. In fact, PA adsorbs more than twice at the lowest E2 concentration of that adsorbed by the other polymers at the highest E2 concentration.

Table 6.2 Freundlich isotherm coefficients

Polymer	**R^2**	**$1/n_i$**	**K_f**
PA	0.99	1.5	3.5×10^{-4}
PSu	0.97	2.7	7.6×10^{-12}
PET	0.99	2.8	1.0×10^{-12}
PEN	0.99	3.4	1.8×10^{-15}

The striking difference in adsorption between the hormone and the different materials still needs further understanding. Hydrophobic interactions for example, do

not explain the difference in interaction of E2 with PA compared to the other polymers. In fact, from Table 6.1 one can see that PA is the least hydrophobic polymer and PSu the most hydrophobic one, despite PA adsorbing much larger mass of E2. Hydrophobicity does not explain therefore adsorption of hormones onto these polymers. As previously seen in Figure 2.10, the hormones' hydrophobicity does not explain adsorption either.

Since hydrophobic interactions do not give a satisfactory answer, other types of interactions are at play. Adsorption of hormones onto the different polymers can be explained by different types of interactions that occur due to their molecular structure, such as hydrogen bonding (H-bond) and π-π interactions (Figure 6.6).

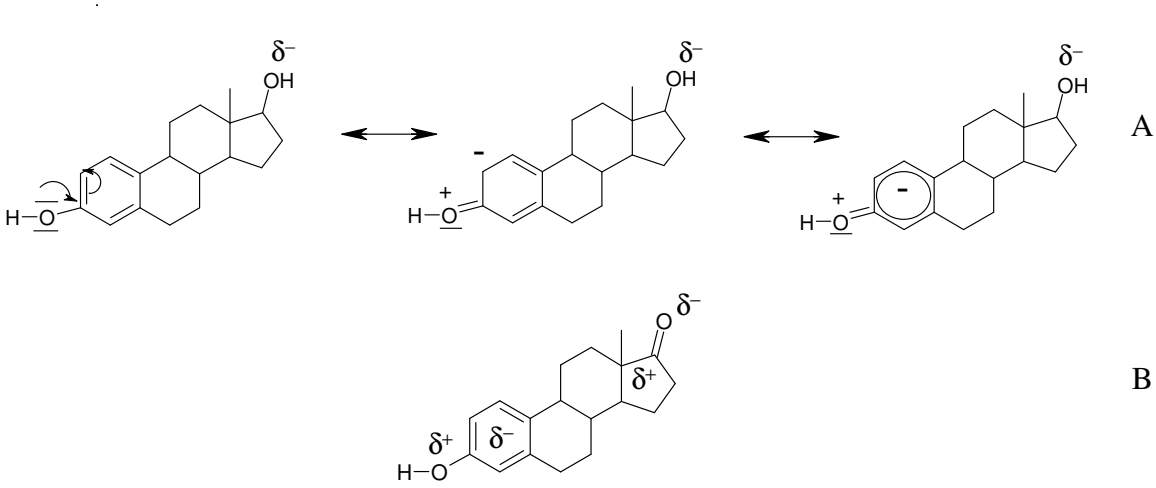

Figure 6.6 Electron density and resonance structures of **(A)** estradiol (E2) and **(B)** estrone (E1)

The hormones E1 and E2 have several functional groups that interact with several functional groups of the polymers [291]. The benzene ring in the E1 and E2 phenol group is electron rich by resonance, caused by delocalization of electrons within the benzene molecule, as can be seen in detail in Figure 6.6 A. The hormone E1 will have the same delocalization of electrons in the phenol group. This allows, in principle, for π-π stacking with an electron poor benzene ring of another molecule [292]. Ji *et al.* [293], for example, proposed that π-π interactions are responsible for the sorption of electron rich benzene groups in sulphonamide antibiotics on multiwalled carbon nanotubes.

The hydroxyl group in the E1 and E2 phenol can be H-bond donor or receiver (Figure 6.6 A and B). In fact, due to the previously mentioned resonance stabilisation in the phenol, the H in this group is more acidic ($pK_a \approx 10$) and therefore more available for H-bonding than a regular hydroxyl group ($pK_a > 15$) [291].

The hormones have another functional group that can form H-bonding. In E2, the hydroxyl group in the pentane ring is electron rich and available for H-bonding acting both as a donor or a receiver. In E1, the ketone group in the pentane is very electron rich and therefore a strong H-bond acceptor.

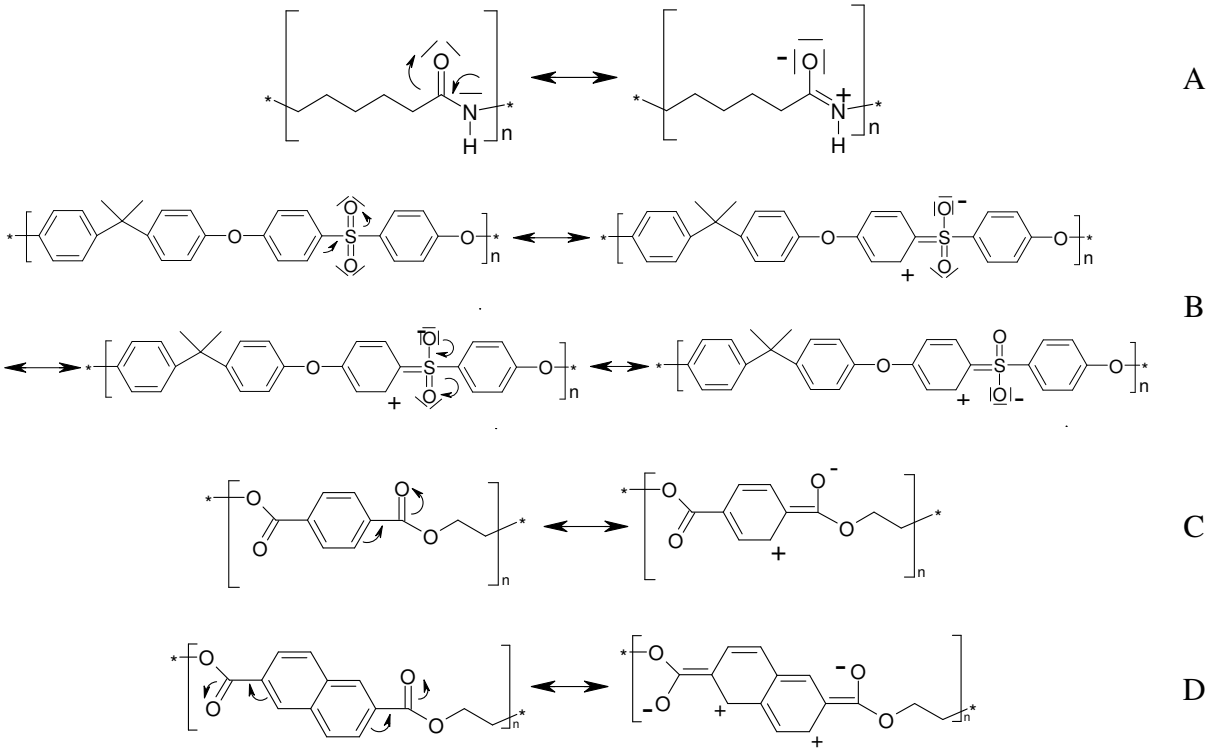

Figure 6.7 Electron density and resonance structures of **(A)** PA, **(B)** PSu, **(C)** PET and **(D)** PEN

The polymers further have functional groups that play a role in the interaction with the hormones. PA is capable of forming very strong H-bonds: the resonance structure shown in Figure 6.7 A originates a very polarised molecule, with a positively charged amine and negatively charged oxygen [291] which can form H-bonds with other molecules. These two groups, which are known to form strong H-

bonds, interact with the hormones. Furthermore, H-bond can also be formed through the H atom in the amine group of the PA polymer.

The polymers PSu, PET and PEN, on the other hand, have a resonance structure shown in Figure 6.7 B, C and D, respectively. PET and PEN have ester groups and PSu has sulfonyl groups linked to benzene rings, which due to their electronegativity withdraw electrons from the benzene ring making them poor in electrons. This would allow the formation of π-π stacking with the electron rich benzene groups of the hormones previously mentioned. However these latter resonance structures in PSu, PET and PEN are known to result in poorly polarised groups and therefore poorly polarised benzene groups [291]. In consequence, these would form very weak interactions with the hormones compared to the H-bonding formed between the hormones and PA.

The material PA was found to adsorb much larger quantities of hormones than PSu or PET and PEN and interactions are explained by H-bonding and not hydrophobic interactions. These experimental results lead to the conclusion that when it comes to adsorption, PA will adsorb much larger quantities of hormones than the other materials under the same conditions. As concluded in the study of Ben-David *et al.* [279], the usage of polyamide NF membranes in water treatment poses a problem in the removal of trace contaminants due to the interaction of these with the active layer. From the results presented here, hormones that have a high endocrine potency are included in this family of contaminants.

In reality, as already mentioned, the different layers of the TFC NF membranes are in contact with solutions with different concentrations in filtration conditions, with the PA active layer contacting the concentration at the membrane surface (Chapter 4) and the support layers a much lower concentration, *i.e.* the permeate concentration. This indicates that the bulk of the hormone adsorption in filtration occurs on the active layer. TFC NF membranes are, however, not made of these pure polymers, and surface modifications which are propriety of the manufacturer have been reported.

6.2.4 Adsorption on NF TFC membranes

As reported above, TFC NF membranes are made of three different layered materials (PA_m, PSu_m and PE_m), which are impossible to physically separate from each other. Furthermore, they are propriety of the manufacturer and there is no information on how these polymers are modified with additives [239], especially as far as the active layer is concerned.

It is however possible to have an indication of which layer adsorbs the highest mass by physically peeling the active PA_m and support PSu_m layer from the PE_m layer of the NF 270 membrane and putting the PA_m+PSu_m layers in a diffusion cell. This allows exposing the PA_m and PSu_m layers separately to a determined concentration. The results are presented in Figure 6.8.

Despite possible surface chemistry modifications, PA_m is found to adsorb much higher amounts of E1 and E2 than the support PSu_m layer, confirming a higher affinity of the hormone with the polyamide active layer. When exposed to the same concentrations, PA_m adsorbs at least 3 times more than PSu_m for both hormones. For 100 $ng.L^{-1}$ of E1 and E2, PA_m adsorbed 3.6 ng and 3 ng, respectively, whilst PSu_m adsorbed 1.3 ng and 1 ng, respectively.

In reality, the active layer in filtration mode is in contact with a higher concentration (>100 $ng.L^{-1}$), compared to the PSu_m layer (20 $ng.L^{-1}$ for E1 and 30 $ng.L^{-1}$ for E2 as seen in Chapter 4). At these concentration conditions, PA_m adsorbs 14 and 10 times higher mass than PSu_m for E1 and E2, respectively. Whilst PA_m adsorbed 3.6 ng of E1 and 3 ng of E2 at 100 $ng.L^{-1}$, PSu_m adsorbed 0.23 ng of E1 at 20 $ng.L^{-1}$ and 0.29 ng of E2 at 30 $ng.L^{-1}$. This confirms the higher affinity and mass adsorption of hormone on PA_m compared to the PSu_m layer.

Firstly, it was found that PA naturally adsorbs much larger quantities of hormone than any of the other polymers studied (Figure 6.5). Secondly, in filtration, the PA_m active layer is in contact with a higher concentration adsorbing therefore larger quantities compared to the other layers, confirming that the bulk of the hormone adsorption occurs in the active layer (Figure 6.8).

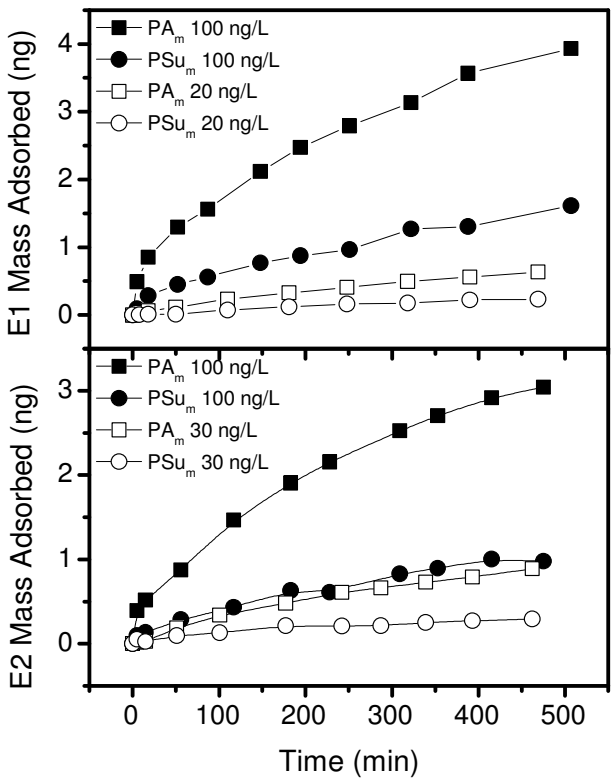

Figure 6.8 Estrone (E1) and estradiol (E2) adsorption onto the PA and PSu sides of the NF 270 1 membrane tested in a diffusion cell (pH 7, 1000 rpm, $C_{feed\ E1\text{-}PA}$= 100 and 20 ng.L^{-1}, $C_{feed\ E1\text{-}PSu}$=100 and 20 ng.L^{-1}, $C_{feed\ E2\text{-}PA}$=100 and 30 ng.L^{-1}, $C_{feed\ E2\text{-}PSu}$=100 and 30 ng.L^{-1}, 4.9 cm^2 membrane area, 125 ml of volume in each cell)

The results presented in the previous sections clearly indicate that the bulk of the adsorption of hormones occurs on the PA active layer. This material has been shown to adsorb larger mass compared to the other ones either when under the same concentration or when under the concentrations measured in filtration mode.

Once it has been established that the bulk of the adsorption occurs on the active layer, the next step is to study the influence of the active layer characteristics in the retention and adsorption of hormones by NF membranes.

6.3. Pore Size Effect on Retention and Adsorption

Nanofiltration membranes have been frequently characterised in terms of average pore radius (r_p) and active layer thickness divided by porosity (δ/ε) [197,

198, 294]. This is possible to quantify by applying the hydrodynamic model that considers only steric interactions between the membrane and the solute [43]. The membrane pores are considered as cylindrical capillary tubes with an average pore radius r_p and length δ. To study the effect of pore radius in the adsorption and retention of hormones several membranes were characterised for r_p and δ/ε.

The theoretical real retention, given by equation (6.3), is fitted to the experimental real retention, given by equation (6.4), to obtain the value of r_p and δ/ε using an optimization method (Solver Microsoft Excel). The experimental real retention R_r in equation (6.4) is calculated from the experimental results of the observed retention R_0 as a function of pressure, or permeate flux J, for selected organics.

$$R_r = 1 - \frac{\Phi K_c}{1 - \exp(-Pe)(1 - \Phi K_c)} \tag{6.3}$$

$$\ln\frac{1-R_r}{R_r} = \ln\frac{1-R_0}{R_0} - \frac{J}{k_f} \tag{6.4}$$

where in equation (6.3), Pe is the Peclet number given by equation (6.5), where δ/ε is one of the fitting parameters:

$$Pe = \frac{K_c J}{K_d D_\infty}\frac{\delta}{\varepsilon} \tag{6.5}$$

In these equations the following parameters are defined: Φ is the partition coefficient given by $\Phi=(1-\lambda)^2$, with $\lambda=r_s/r_p$, where r_s (m) is the solute radius determined with the Stokes Einstein equation (equation (6.6)) and r_p (m) is the membrane average pore radius, one of the fitting parameters.

$$r_s = \frac{kT}{6\pi\mu D_\infty} \tag{6.6}$$

where in the previous equation k is the Boltzman constant, T is the temperature (K) and μ is the solution viscosity (Pa.s).

The partition coefficient takes into account the partitioning that exists between the feed solution and pore entrance and between the permeate solution and pore exit. The coefficients K_c and K_d, which depend only on λ, are the diffusion and convective hindrance factors, respectively, calculated using the Bungay and Brenner coefficients reviewed by Deen [43]. J is the permeate flux ($m.s^{-1}$) and D_∞ ($m^2.s^{-1}$) is the organic diffusion coefficient in the liquid medium (in this case water).

The parameter k_f is the mass transfer coefficient determined with the Sutkover method [295] with 0.1 M NaCl and a Re_h of 1450 (minimal polarisation) and two different pressures (7 and 11 bar). The mass transfer coefficient for each organic was corrected in relation to the NaCl one using equation (6.7) [294]:

$$k_s = k_{NaCl}\left(\frac{D_\infty}{D_{NaCl}}\right)^{0.7} \qquad (6.7)$$

For the TFC-SR2, the Sutkover method is not applicable due to an increase in permeate flux when salt is present compared to the pure water flux at the same pressure. The Deissler Sherwood [296] correlation in cases of minimised polarisation was therefore applied in this case

Several organics that are neutrally charged and do not adsorb on the membrane were used to characterise the membranes. Their physical properties are shown in Table 6.3. The organics solute radius was obtained with the Stokes-Einstein equation (6.6).

Table 6.3 Tracer organics characteristics

Compound	**MW ($g.mol^{-1}$)**	**D_∞ ($m^2.s^{-1}$)**	**r_s (nm)**
dioxane	88.11	9.82×10^{-10}	0.24
xylose	150.13	7.50×10^{-10} [297, 298]	0.31
dextrose	180.16	6.80×10^{-10} [299-301]	0.34
methanol	32	1.5×10^{-9}	0.13

The organics' diffusivities were either obtained from the literature (Table 6.3), calculated with the Worch equation [248] as was the case of methanol or calculated with the Wilke & Chang equation (equation 6.8) [302] for dioxane with the necessary parameters obtained from Perry's Handbook [302].

$$D_{\infty} = 7.4\times10^{-8}\frac{\sqrt{\Psi_B M_B}T}{\mu V_A^{0.6}} \qquad (6.8)$$

Results for the theoretical real retention calculated with equation (6.3) were fitted to the experimental real retention given by equation (6.4) by optimizing r_p and δ/ε. The characterisation results of the NF 270 and TFC-SR2 membranes are shown in Figure 6.9. NF 270 having a smaller pore radius shows higher retentions for all the organic compounds.

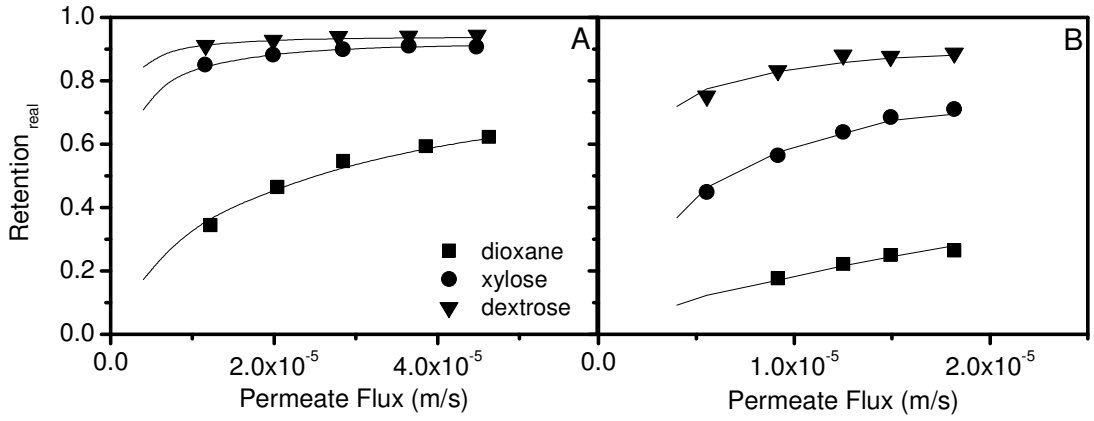

Figure 6.9 Real retention as a function of permeate water flux for the different organic tracers for the **(A)** NF 270 1 and **(B)** TFC-SR2 2 (Cross-flow conditions: C_{feed}=25 mgC.L^{-1}, Re_h= 1450, pH 7, 24°C)

The results of r_p and δ/ε obtained for these two membranes are presented in Table 6.4 and Table 6.5. For comparison and modelling purposes the membrane average pore radius were given with two decimal points.

Table 6.4 Estimated pore radii (r_p) and active layer thickness to porosity ratio (δ/ε) for the TFC SR2 2 membrane

Compound	**r_p (nm)**	**δ/ε (m)**
dioxane	0.45	1.16×10^{-6}
xylose	0.47	1.01×10^{-6}
dextrose	0.46	1.08×10^{-6}
average	0.46 ± 0.01	$1.09\times10^{-6} \pm 7.50\times10^{-8}$

Table 6.5 Estimated pore radii (r_p) and active layer thickness to porosity ratio (δ/ε) for the NF 270 1 membrane

Compound	**r_p (nm)**	**δ/ε (m)**
dioxane	0.40	1.06×10^{-6}
xylose	0.42	1.01×10^{-6}
dextrose	0.44	1.08×10^{-6}
average	0.42 ± 0.02	$1.05\times10^{-6} \pm 3.65\times10^{-8}$

Once the parameters r_p and δ/ε are obtained, the porosity ε can be calculated using values of δ for each membrane (Table 6.6). With ε, the total area available for adsorption is estimated considering the pores as perfect cylinders of height δ and pore radius r_p. After algebraic manipulation the total effective interfacial area of the active layer (*i.e.* membrane surface A_{sm} and internal pore area A_p) is obtained with equation (6.9),

$$A_{total} = A_{sm} + A_p = WL(1-\varepsilon) + \frac{2WL\varepsilon\delta}{r_p} \qquad (6.9)$$

where W (m) and L (m) are the membrane width and length, A_{total} (m^2) is the total effective interfacial surface area available for adsorption, A_{sm} (m^2) is the membrane surface area and A_p (m^2) is the total pore area inside the active layer. Results for the membrane characterisation are presented in Table 6.6. The method used to obtain the effective interfacial area and porosity variability presented in Table 6.6 are explained in Appendix E.

The effective interfacial area of the active layer is dependent on the active layer pore radius, porosity and active layer thickness (equation 6.9). It increases with membrane thickness and porosity increase and decreases with pore radius increase. The NF 270 membrane has the smallest effective interfacial area because of a small thickness and large pore radius. In contrast, the TFC-SR2 2 has the highest effective interfacial area despite having larger pores than the NF 270 1. This is due to its very thick active layer.

Table 6.6 Membranes characteristics (the effective interfacial area is given for a membrane area of 46 cm^2)

Membrane	**Average Pore Radius R_p (nm)**	**Active Layer Thickness Porosity Ratio δ/ε (μm)**	**Average Active Layer Thickness δ (nm)** (Table 3.7)	**Effective Interfacial Area of Active Layer (cm^2/ cm^2 membrane)**	**Porosity**
BW30	0.32 ± 0.01	5.4 ± 1.5	233 ± 88	64 ± 39	0.04 ± 0.02
NF 90	0.34 ± 0.04	0.8 ± 0.2	218 ± 40	336 ± 146	0.26 ± 0.08
TFC-SR2 1	0.52 ± 0.03	2.5 ± 0.1	345 ± 28	185 ± 33	0.14 ± 0.01
TFC-SR2 2	0.46 ± 0.01	1.1 ± 0.1	345 ± 28	467 ± 69	0.32 ± 0.03
TFC-SR3	0.38 ± 0.01	1.60 ± 0.04	400 ± 10	518 ± 38	0.25 ± 0.01
NF 270 1	0.42 ± 0.02	1.10 ± 0.04	21 ± 2.4	2.9 ± 0.4	0.020 ± 0.002

In this work the tortuosity of the pores and the surface roughness were not considered in the calculation of the surface and internal area available for sorption. Tortuosity has not been determined for NF membranes due to the lack of analytical tools which makes this task impossible to determine at this moment.

In regards to the surface roughness, there is no available direct relationship between this and the membrane surface area. AFM has however been used to estimate the surface area of membranes taking the roughness into account. It was estimated that a projection area of 100 μm^2 gave areas between 150 and 180 μm^2 for an average surface roughness between 40 and 85 nm [303]. For the roughest

membranes used in this study, the BW 30 and the NF 90, the internal pore area estimated is at least 70 times higher than the surface area. In that case, the increase of surface area caused by the membrane roughness has a very small impact in the effective interfacial area of the active layer. Considering double the surface area caused by a roughness of 60 nm (Table 3.5), the total membrane area estimated would be of 2996 cm^2 for BW30 and 15472 cm^2 for the NF 90 membrane instead of 2953 cm^2 and 15439 cm^2 (Table 6.6), respectively. The other membranes used have a very low roughness which will have a minimal impact on the membrane effective interfacial area.

The effect of pore radius in the adsorption and retention of E2 is shown in Figure 6.10. Increasing the pore radius r_p leads to a decrease in the steric exclusion capacity of the membrane causing a decrease in retention and increase in mass adsorbed (Figure 6.10 A and B at pH 7): the more hormones partition inside the membrane pores the more adsorb. This trend is especially pronounced for membranes with r_p>0.42 nm where the hormone has a radius of r_{E2}≈0.4 nm [32] (Table 3.11). A similar trend was obtained by Nghiem *et al.* [172] where RO membranes adsorbed less than NF membranes.

It could be argued that because the NF 90 has a higher flux and therefore a higher concentration polarisation, then adsorption would be higher (Chapter 4). However, when comparing membranes with similar fluxes such as the TFC-SR2 2, the TFC-SR3 and the BW30 and the membranes NF 90 and TFC-SR2 1 (Table 3.4), the trend shows an increase with pore radius (Figure 6.10 B). Moreover, since the experiments were carried out at conditions of minimised polarisation (Re_h=1450), the previous reasoning is hardly applicable.

Differences in membrane materials caused by additives [239] or differences in membrane characteristics such as roughness may influence adsorption: surface roughness of the NF 90, 70 nm, is much larger than that of the NF 270 membrane, 5 nm (Table 3.5), for example.

To confirm the effect of pore radius without the influence of the membrane material and characteristics such as surface roughness, the study of hormone retention and adsorption for two batches of the NF 270 membranes is carried out (Figure 6.11, NF 270 Batch 1 and 2).

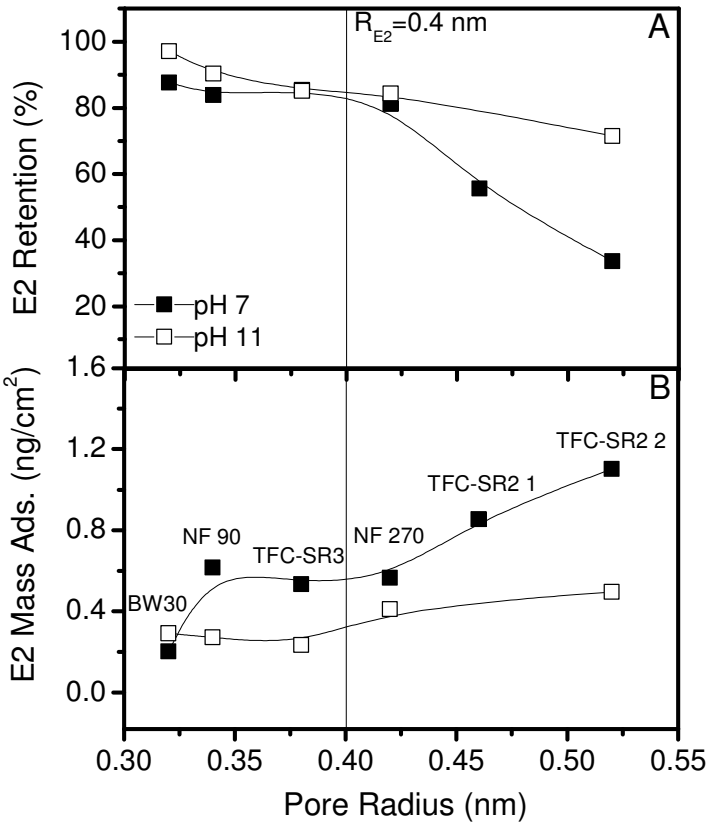

Figure 6.10 Estradiol (E2) **(A)** retention and **(B)** mass adsorbed (Mass Ads.) per membrane surface area (ng.cm^{-2}) with increasing effective pore radius; membranes used are presented in Table 6.6 (Cross-flow conditions: $C_{feed\ initial}$=100 ng.L^{-1}, 24°C, 11 bar, Re_h=1450, and pH 7 and 11)

The NF 270 batch 1 membrane with smallest pore radius exhibits lower mass adsorbed, showing that access to internal surface area is compromised by steric exclusion, decreasing therefore the access to area available to adsorb onto.

The same effect of pressure and Re_h is obtained for both membranes. Increase of pressure and decrease of Re_h increases the concentration at the membrane surface and therefore increases adsorption and decreases retention (Chapter 4).

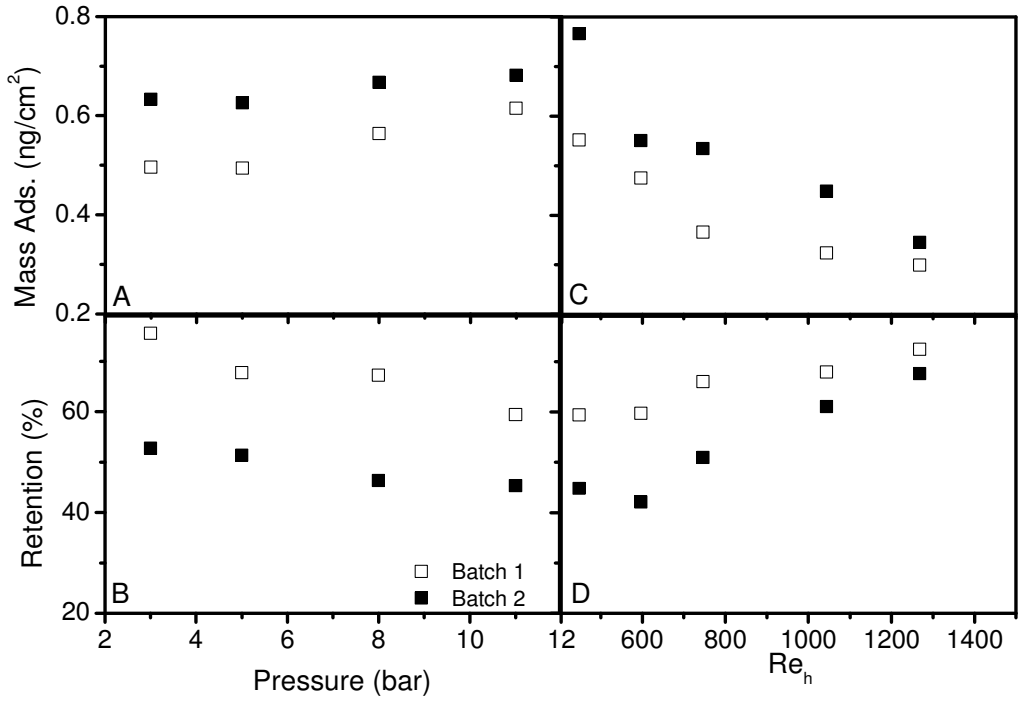

Figure 6.11 Comparison of estradiol (E2) mass adsorbed (A and C) and retention (B and D) for NF 270 1 and 2 as a function of pressures and Re_h ($C_{feed\ initial}$=100 ng.L^{-1}, 24ºC, 1 mM $NaHCO_3$, 20 mM NaCl)

For the membrane with a pore radius r_p=0.34 nm (NF 90), the mass adsorbed is much higher, 0.64 ng.cm^{-2}, compared to the membrane with a similar pore radius r_p=0.32 nm (BW 30), 0.17 ng.cm^{-2} (Figure 6.10). Besides the pore radius effect on adsorption and retention, two other effects might be at play which might affect adsorption onto NF membranes: hormone-membrane affinity and internal surface area.

By analysing the static isotherms obtained for E2 with the NF 90 and the BW 30 membranes, one can see that the hormone affinity for these two membranes is very similar (Figure 6.12), thus not explaining the higher adsorption obtained for the NF 90 membrane. Membrane roughness could also impact in adsorption. However, as can be seen in Table 3.5, the NF 90 and the BW 30 membranes have very similar surface roughness, thus not explaining the difference in adsorption.

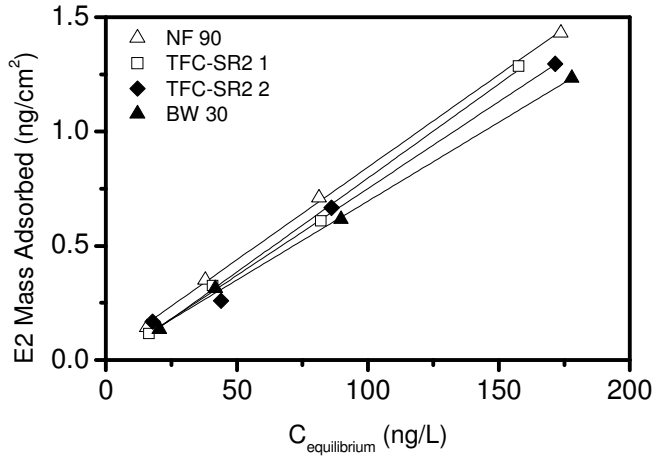

Figure 6.12 Estradiol (E2) static isotherm for the NF 90, the BW 30 and the TFC-SR2 1 and 2 membranes ($C_{feed\ initial}$=24, 50, 100 and 200 ng.L^{-1}, 24°C, 200 rpm and pH 7)

The hormone static isotherm with the two batches of the TFC-SR2 membranes (1 and 2) is very similar to the ones obtained for the NF 90 and BW 30 (Figure 6.12). Furthermore, the first membranes have a much lower roughness than the later two, not explaining the higher adsorption for the first ones (Table 3.5). The difference in mass adsorption obtained in Figure 6.10 is thus likely caused by a pore size effect and the internal area available for sorption.

If the effective interfacial area of the active layer is taken into account (Table 6.6), in general an increase of the total effective interfacial surface area increases the hormone mass adsorbed, showing that internal surface area plays a role in adsorption (Figure 6.13):

- The BW30 and the NF 90 membranes have similar pore radius (0.32 and 0.34 nm, respectively - Table 6.6), but since the NF 90 has a higher surface area of 15439 cm^2 compared to 2953 cm^2 for the BW 30 it adsorbs more E2.
- The NF 270, NF 90 and TFC-SR3 adsorb similar E2 mass (around 0.55 ng.cm^{-2} - Figure 6.10) despite the NF 270 membrane having a bigger pore radius 0.42 nm compared to 0.34 nm for the NF 90 and 0.38 nm for the TFC-SR3 (Table 6.6). These later two have a much higher internal surface area (15439 cm^2 for

the NF 90 and 23817 cm^2 for the TFC-SR3) compared to the NF 270 membrane (134 cm^2) compensating for a smaller pore radius.

- The TFC-SR2 1 and 2 have higher surface area and pore radius than the NF 270 membrane and therefore adsorb more.

Hormone filtration by NF membranes at neutral pH indicates penetration and internal pore sorption. However, at alkaline pH, when the hormone is dissociated the occurrence of charge repulsion might interfere in the hormone adsorption mechanism.

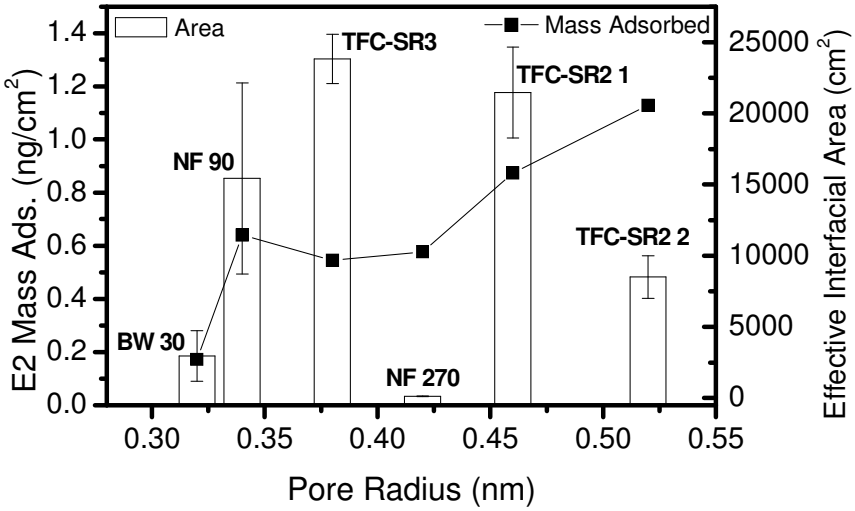

Figure 6.13 Estradiol (E2) mass adsorbed (Mass Ads.) ($ng.cm^{-2}$) and membrane effective interfacial area A_{total} (cm^2) with increasing effective pore radius (Cross-flow conditions: $C_{feed\ initial}$=100 $ng.L^{-1}$, 24°C, 11 bar, Re_h=1450, pH 7). The variability in A_{total} is presented as error bar.

At pH 11 when charge repulsion occurs between the membrane and the dissociated hormone ($pK_{aE1,E2}$ = 10.4 in Table 3.10) less hormone adsorbs and a higher retention is obtained (Figure 6.10). Similar trends were obtained by other authors [41, 152, 185]. Although the hormone phenol group is negatively charged at pH 11 (Figure 6.6 A and B) and charge repulsion by the membrane occurs, the hormone is still able to form hydrogen bonding with the membrane through the ketone group for E1 and the hydroxyl group for E2 (Table 3.10). At pH 11 the effect of pore radius is not very pronounced when compared to that occurring at pH 7,

suggesting that adsorption occurs on the surface. At pH 7, both partitioning and penetration occur on the membrane, suggesting once again internal adsorption on the active layer.

In Figure 6.14 adsorption kinetics is represented for a tight (NF 90) and a loose (TFC-SR2 batch 1) membrane at pH 7 and 11. At pH 7 adsorption increases gradually with time until it reaches steady-state. Saturation is attained quicker for the loosest membrane: it takes 100 minutes for the looser membrane (TFC-SR2 batch 1) to reach 80% of the total mass adsorbed compared to 200 minutes for the tighter membrane (NF 90). A slower penetration and consequent slower adsorption is likely to occur on the tighter membrane. This shows the importance of reaching full saturation of the membrane during the experiment.

At pH 11 adsorption increases sharply in the first 5 minutes attaining steady-state quickly: adsorption is probably occurring mainly at the membrane surface with some penetration occurring for the loosest membrane due to the difference between the hormone size (0.4 nm) and the pore size (0.52 nm). Steinle-Darling *et al.* [278] also found that charged compounds reached adsorption saturation quickly while uncharged ones took several days to reach saturation.

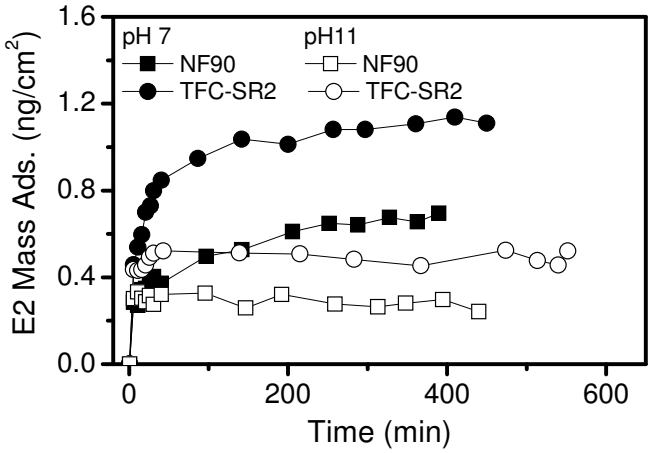

Figure 6.14 Estradiol (E2) mass adsorbed (Mass Ads.) for the NF 90 and the TFC-SR2 1 membrane for pH 7 and 11. (Cross-flow conditions: $C_{feed\ initial}$=100 ng.L^{-1}, Re_h=1450, 11 bar, 24°C)

To confirm in depth adsorption in the active layer, E1 desorption experiments from membranes saturated in filtration mode at different pressures are carried out. Results are presented in Figure 6.15.

The percentage of E1 static extraction from pressure experiments decreases from 100% in static experiment (no pressure applied) down to less than 20% for 15 bar pressure. Kimura *et al.* [37] obtained lower extraction of trace contaminants from pressure experiments (40%-60% recovery) when compared to static experiments (around 100% recovery). Extraction efficiency decreases with increase of pressure used to saturate the membrane (Figure 6.15) because the higher the pressure, the higher the concentration at the membrane surface is (Chapter 4) and, therefore the more partitions inside the membrane active layer, causing a higher adsorption to occur there. Since internal access for extraction in static mode is difficult, the extraction efficiency decreases with increase of pressure.

When filtered extraction at 11 bar is carried out with MilliQ water, a much higher extraction is obtained (82%) when compared to the static extraction (25%), because filtered MilliQ water has access to hormones adsorbed in the membrane pores inside the active layer. Subsequent filtration with 2% acetone allowed recovering a further 7% of E1, showing internal adsorption on the active layer. McCallum *et al.* [152] also obtained high recoveries under MilliQ water filtration mode.

The PE layer that had been separated from the other two layers, consistently desorbed less than 2% of the total hormone mass adsorbed, showing a low adsorption onto such a layer, confirming previous results of polymer adsorption.

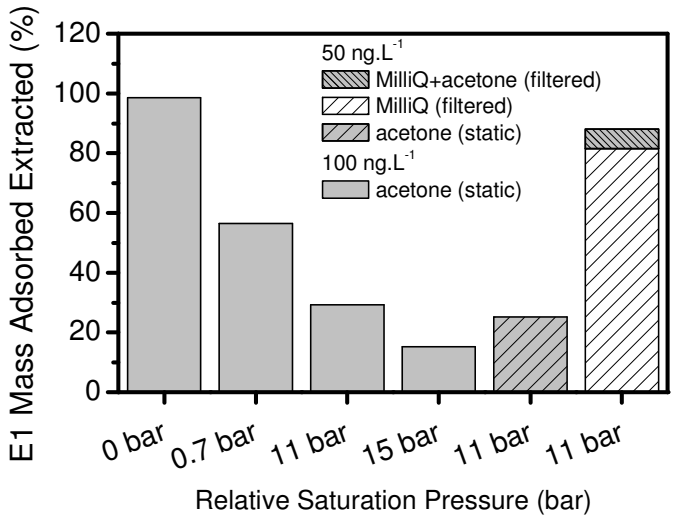

Figure 6.15 Estrone (E1) mass extracted from the NF 270 1 membrane (filtered extraction in cross-flow: T=24ºC, Re_h=427, 11 bar, MilliQ water, then MilliQ+acetone solution (2%); static extraction: T=24ºC, 200 rpm, acetone)

To better understand the effect of pore radius and internal surface area, a simple conceptual schematic is shown in Figure 6.16. For a membrane of same pore radius r_{p1} but increased active layer thickness ($\delta_1>\delta_2$), a higher internal area is available, increasing hormone adsorption (Figure 6.16 A). For a membrane with the same active layer thickness δ_2 but increased pore radius $r_{p2}> r_{p1}$, the bigger the pore radius, the more hormone partitions inside the pore, and therefore the higher the concentration inside the membrane will be, increasing the adsorption (Figure 6.16 B), since adsorption is linearly proportional to concentration (Figure 4.8 and Figure 4.9). This very simplistic approach gives an idea of the actual phenomenon, where the membranes have different pore radius and active layer thicknesses. Thus a combination of the effect of pore radius, or partitioning, and internal surface area play a role in trace contaminant adsorption onto NF membranes.

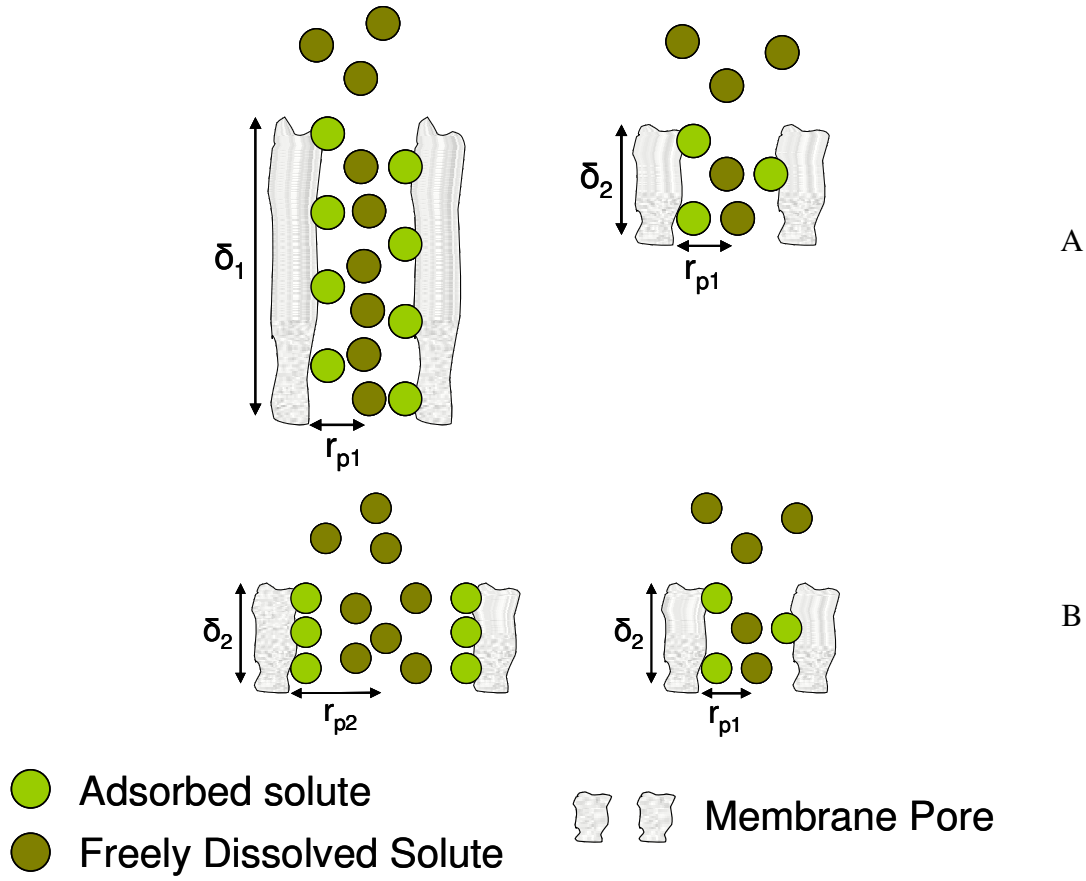

Figure 6.16 Conceptual schematic of the effect of **(A)** internal surface area and **(B)** pore radius r_p in hormone adsorption in the active layer. Note: for schematic purposes the pores are shown wider relative to the hormone molecule size. In reality they are of similar size.

Pore size has been shown to be an important parameter in the transport of adsorbing compounds through the active layer when the hormone is not dissociated. Steric exclusion plays an important role in adsorption since it allows or prevents access to the internal surface area. These results indicate that internal area is an important parameter in modelling hormone adsorption on NF membranes.

6.4. Conclusions

To be able to understand the transport of adsorbing trace contaminants through TFC NF membranes it is firstly necessary to determine where the adsorption occurs. It was shown in this study that the bulk of the hormone adsorption occurs in

the polyamide active layer of the TFC NF membranes. Hormone adsorption is negligible in the other polymeric materials that constitute these membranes. As concluded in the study of Ben-David *et al.* [279], the usage of polyamide NF membranes in water treatment poses a problem in the removal of trace contaminants due to the interaction of these with the active layer. From the results presented here, hormones which have a high endocrine potency are included in this family of contaminants. Other materials should therefore be considered in the making of NF and RO membranes, justifying future work focusing on the interaction between trace contaminants and different polymeric materials.

The active layer characteristics, such as pore radius and internal surface area, were found to affect the total mass that adsorbs and therefore permeates through the membrane.

Steric exclusion determines the amount of hormone that penetrates (*i.e.* partitions) inside the membranes. The bigger the pore radius the higher the mass of hormone that penetrates inside the membrane pores, and therefore the higher the concentration inside the pore will be. As a consequence, the more will adsorb inside the membrane.

At the same time, since the hormones were found to penetrate and adsorb internally at pH 7, the internal surface area of the membrane further contributes to hormone adsorption. The higher the internal surface area, the more will adsorb inside the membrane.

To model the transport of adsorbing hormones through NF membranes, only the characteristics of the active layer need to be taken into account.

These results have obvious repercussions in the membrane design depending on the desired outcome. If adsorption is to be avoided, the tighter (*i.e.* low permeability and small pore radius) and thinner the membrane PA active layer is, the less will adsorb and therefore the less will permeate through. Another possibility would be to substitute the polyamide active layer by a different polymeric material such as cellulose or PMMA, that adsorbs very little, as previously shown.

However, if adsorption is to be used as another removal mechanism, then the thicker the membrane is the more will adsorb. However, the thicker the active layer, the more resistance to water permeation will be encountered.

7 Integration of Sorption on Transport of Hormones by NF Membranes: Modelling

7.1. Introduction

Trace contaminants, such as hormones, have been found to adsorb onto polymeric membranes, including NF and RO membranes. However, few studies have been carried out in modelling the transport of adsorbing compounds by NF membranes. In fact, in some of these studies problems were encountered due to the adsorption of these contaminants in the membrane polymer.

Modelling the retention of several contaminants in NF membranes has been carried out without considering adsorption [176]. However, for some of these contaminants, such as xeno-estrogens, high membrane adsorption occurred and, in consequence, no permeate concentration was measurable. Hence, adsorption may prevent the application of a developed model for solutes that interact with the membranes if not taken into account. In comparison, for other solutes, diffusion-only transport closely matched the measured retention. In another study the irreversible thermodynamic model was used as a basis to understand whether convection or diffusion is the predominant contributor to the solute permeate flux (DBP and halogenated solvents) for NF and RO membranes [256]. Again, the application of this model proved to be problematic for adsorbing compounds. The membranes had to be pre-saturated to achieve steady-state and apply the model. However, reaching steady-state proved to be impossible for some contaminants as for the case of trichloroethene, and no conclusions could be drawn from the study. In a study by Verliefde *et al.* [252], the interaction existing between adsorbing contaminants and the membrane was incorporated in the hydrodynamic model for NF using an affinity concept. Although retention was predicted well and increased with permeate flux for the adsorbing contaminants, for other contaminants such as hormones, retention

decreased with increase of flux/pressure [153]. Furthermore, as in other studies, the predictions were carried out for the membrane saturated with trace contaminants.

It was shown in Chapter 4 that the total mass of hormones adsorbed will vary with filtration conditions, giving different values of retention. Adsorption should, therefore, be a mechanism to be considered as it determines the retention once steady-state is reached.

Adsorption has previously been considered in a modified sorption-diffusion model for RO by assuming a sorption induced flux decline [192]. Results confirm flux decline through specific adsorption of the organic compounds on the membrane polymer such as hydrogen bonding. Organics may compete with water for adsorption sites and decrease water content on the membrane and, consequently, cause a decrease in permeate flux. This model described the transient permeate concentration behaviour more adequately than considering steady state conditions of water and solute flux across the membrane by assuming adsorption-diffusion transport of organics in the membrane polymer. Shortfalls of this model remain (i) the inapplicability to NF due to a missing convection transport term, and (ii) the common absence of a flux reduction element in NF due to contaminant sorption [192, 205]. This outlines the need for retention models that are solute specific and consider possible solute-membrane interactions. Some attempts have been made in this direction using artificial neural networks. The principal component analysis method (quantitative structure relations or QSR) has been developed to obtain a model that describes retention as a function of the contaminants most important variables, such as molecular width and depth, by NF membranes [174, 304] and the NF membrane characteristics such as roughness or active layer thickness [305]. Limitations of such models lie in the validity for certain boundary conditions, and while simple in nature, they cannot replace the understanding of fundamental mechanisms.

It is clear from the previous studies discussion that transport of adsorbing contaminants by NF membranes is not well understood. Moreover the occurrence of adsorption hinders the application of certain models and theories making it impractical.

In Chapter 4 it was concluded that polarisation needs to be taken into account when modelling the adsorption of trace contaminants by NF membranes. Pressure, Re_h numbers and feed concentration were therefore found to influence adsorption. In Chapter 5, a model that predicts the transient feed and permeate concentration for several filtration conditions was developed. Finally, in Chapter 6 it was shown that hormone adsorption occurs mainly in the PA active layer and that the active layer pore radius and internal surface area are important in modelling transport of adsorbing trace contaminants by NF membranes. The studies carried out in the previous chapters lead in this study to the development and validation of a new transport model for adsorbing contaminants in the removal by NF membranes. Conclusions are withdrawn as to what influences adsorption and how adsorption influences the transport of contaminants through NF membranes. Understanding the fundamental mechanisms of trace contaminant removal will enlighten and contribute to the design of new membranes and an optimization of the design of the membrane process.

As will be seen below, the time-dependent solute transport inside the membrane with adsorption is governed by the following differential equation that has no analytical solution:

$$-K_i \frac{\partial C_A}{\partial z} + D_i \frac{\partial^2 C_A}{\partial z^2} = \frac{\partial C_A}{\partial t} \qquad (7.1)$$

The first and second term on the left hand side of equation (7.1) correspond to a convective and diffusion term, respectively, and the term on the right-hand side of the equation corresponds to an accumulation term caused by adsorption on the membrane.

Because there is no analytical solution, a numerical method has to be developed and used to obtain its solution. In this work, the finite-difference method was used. To do so, the following steps are followed.

1. Since the differential transport equation of solutes inside the NF membranes pores, comprising a convection-diffusion balance, has an analytical solution, this solution served as a validation benchmark for the numerical method

itself. The excellent prediction results obtained (error below 10^{-6} for grids comprising more than 100 grid nodes and a second order rate of convergence of the numerical scheme) encouraged one to proceed to predictions of more complex phenomena with adsorption playing a role (unsteady-state).

2. Before proceeding to the model predictions with adsorption, and taking advantage of the previously-mentioned excellent results, a parametric study of the Peclet number (convection/diffusion transport ratio) effect on the solute profiles along the membrane thickness was performed in order to determine the relevance of convection transport in NF membranes. This study allowed confirmation of the necessity to keep the convective term in equation (7.1).
3. The numerical model to solve equation (7.1) with adsorption is developed and applied to different pressure operating conditions, different hormones (E1 and E2) and different membranes (NF 270 batch 1 and TFC-SR2 batch 2), in order to analyse the results and identify the mechanisms at play for each set of conditions. In particular, the role of convection (that has been frequently disregarded) in the hormones' transport inside NF pores when adsorption is present is to be assessed.
4. The model is then validated by comparing time-dependent predicted values of hormone mass adsorbed against the corresponding experimental values.

7.2. Solute Transport in NF Membranes Without Adsorption

The transport of uncharged solutes in a pore can be described by the hydrodynamic model [43] where the pores are described as straight cylindrical pores of identical radius, while solutes are considered as spherical. This model has been widely applied in the characterisation of NF membranes and/or the description of transport of charged [23, 197, 198] and uncharged [23, 197] solutes in NF membranes.

For non-adsorbing and uncharged solutes, which is the case for most trace contaminants at neutral pH, the solute flux is constant at steady-state conditions (equation (7.2)) and is expressed by a diffusion and convection term, given by

equation (7.3). Note that the transport of solutes in NF pores is considered as one-dimensional, *i.e.* along the membrane depth, due to the small differences between the pore size and the solute size that allows one to consider uniform conditions in the radial direction.

$$\frac{dJ_A}{dz} = 0 \tag{7.2}$$

$$J_A = VC_p = -K_d D_\infty \frac{dC_A}{dz} + K_c V C_A \tag{7.3}$$

In the previous equations J_A is the solute flux ($kg.m^{-2}.s^{-1}$), K_d and K_c are the diffusion and convection hindrance coefficients, respectively, and are dependent on the hydrodynamic coefficients, the dimensionless radial position and the potential describing long range interactions (*e.g.* electrostatic) between the solute and the membrane, D_∞ is the solute diffusion coefficient in the solution ($m^2.s^{-1}$), C_A is the solute concentration in the pore ($kg.m^{-3}$), V is the unperturbed fluid velocity far upstream or downstream of the solute ($m.s^{-1}$) and considered as the average velocity inside the pore, and z is the spatial dimension from the pore entrance to the pore exit, *i.e.* along the membrane active layer thickness or membrane depth.

Substituting equation (7.3) into equation (7.2) gives the concentration dependence with z, where equation (7.4) is obtained with the corresponding boundary conditions.

$$\begin{aligned} &\frac{d^2C_A}{dz^2} - \frac{K_j}{D_j}\frac{dC_A}{dz} = 0 \\ &z = 0 \Rightarrow C_A = \Phi' C_{Am} \\ &z = \delta \Rightarrow C_A = \Phi' C_{Ap} \end{aligned} \tag{7.4}$$

In the previous equations, C_{Am} is the concentration at the membrane surface and C_{Ap} is the permeate concentration. K_j is the hindrance convection contribution (*i.e.* K_cV) and D_j is the hindrance diffusion contribution (*i.e.* K_dD_∞) in the transport equation,

Φ' is the partition coefficient of the solute between the solution and the pore on the feed side and on the permeate side and δ is the membrane active layer thickness.

The equation for the real retention (equation 6.3), which is the observed retention considering polarisation effects, can be obtained from equation (7.4) and its boundary conditions. The focus herein is on the transport of contaminants in NF membrane pores and, therefore, on the concentration profile in the membrane pore, obtained by solving equation (7.4).

Assuming a fully developed flow inside the pore (with a parabolic profile of the Hagen-Poiseuille type), the hindrance factor coefficients K_c and K_d are calculated for a centreline approach (*i.e* solute is transported in the pore centre and its position does not vary with pore radius) by using equations (7.5) and (7.6) [306], respectively, where λ is the solute to pore radius ratio (r_s/r_p). These equations are frequently used for contaminant removal by NF membranes assuming a continuous medium [197, 252, 253, 307]:

$$K_d = 1.0 - 2.30\lambda + 1.154\lambda^2 + 0.224\lambda^3 \qquad (7.5)$$

$$K_c = (2 - \Phi)(1.0 - 0.054\lambda - 0.988\lambda^2 + 0.441\lambda^3) \qquad (7.6)$$

The steric partition coefficient Φ represents the pure steric interaction at play caused by the difference between the solute and the membrane pore sizes and is given by equation (7.7) [43]:

$$\Phi = (1 - \lambda)^2 \qquad (7.7)$$

However, for solutes that interact with the membrane polymer as the cases studied here, a different partition coefficient has been proposed for the membrane entrance and exit [252], given by equation (7.8),

$$\Phi' = \frac{C_{mp}}{C_{mf}} = \frac{C_{pp}}{C_p} = (1 - \lambda)^2 \exp\left(-\frac{\Delta G_i}{kT}\right) = \Phi\, B \qquad (7.8)$$

where ΔG_i (J) is the Gibbs energy of interaction between the solute and the membrane in the water phase.

The concentration profile of the hormone inside the membrane governed by equation (7.4) at steady-state conditions, *i.e.* once adsorption has reached steady-state can be solved analytically, and such an analytical solution is presented next. This is an advantage since this analytical solution constitutes a benchmark to validate numerical methods that are required for the solution of more complex differential equations, as it will be seen later on for adsorbing conditions.

7.2.1 Analytical Solution of the Solute Transport Equation in a Pore Without Adsorption

7.2.1.1 The Equation

Equation (7.4) is a homogeneous second order linear differential equation with constant coefficients that can be analytically solved, having the following characteristic equation:

$$r^2 - \frac{K_j}{D_j} r = 0 \tag{7.9}$$

The roots of equation (7.9) are $r_1=0$ and $r_2=K_j/D_j$, which determines the solution of the differential equation (7.4) as:

$$C(z) = C_1 e^{r_1 z} + C_2 e^{r_2 z} = C_1 e^{\frac{K_j}{D_j} z} + C_2 \tag{7.10}$$

Considering the boundary conditions in equation (7.4) and defining the Peclet number as $Pe=\delta K_j/D_j$, after some algebra (7.10) becomes:

$$C(z) = \Phi' C_{Am} e^{\frac{K_j}{D_j} z} - \frac{\Phi' C_{Ap} - \Phi' C_{Am} e^{Pe}}{1 - e^{Pe}} e^{\frac{K_j}{D_j} z} + \frac{\Phi' C_{Ap} - \Phi' C_{Am} e^{Pe}}{1 - e^{Pe}} \tag{7.11}$$

Or:

$$C(z) = C_1 e^{\frac{K_j}{D_j} z} + C_2 \qquad (7.12)$$

With:

$$C_1 = \Phi' C_{Am} - \frac{\Phi' C_{Ap} - \Phi' C_{Am} e^{Pe}}{1 - e^{Pe}} \qquad (7.13\ a)$$

$$C_2 = \frac{\Phi' C_{Ap} - \Phi' C_{Am} e^{Pe}}{1 - e^{Pe}} \qquad (7.14\ b)$$

Equation (7.11) provides the solute concentration profile along the membrane active layer thickness for a defined membrane and solute. The membrane characteristics used for this study can be found in Table 6.6 and the solute characteristics can be found in Table 3.10 and Table 3.11.

7.2.1.2 Partition Coefficient Φ'

To apply equation (7.11) and obtain the concentration profile along any membrane pore for a solute that interacts with the membrane polymer, the parameter B in equation (7.8) needs to be determined.

The determination of this parameter is carried out for the hormones E1 and E2 and the membranes studied, NF 270 1 and TFC-SR2 2 due to the interaction between the hormones and the polyamide active layer material.

The parameter B in equation (7.8) is evaluated by fitting the hydrodynamic model with the modified partition coefficient to the experimental results of the hormone real retention as a function of the permeate flux [252]. Retention is determined once the membrane saturates with the hormone, to avoid contribution of adsorption in the removal mechanism, and at conditions of minimum concentration

polarisation to avoid its contribution. Results are presented in Figure 7.1. The values obtained for the parameter B are presented in Table 7.1.

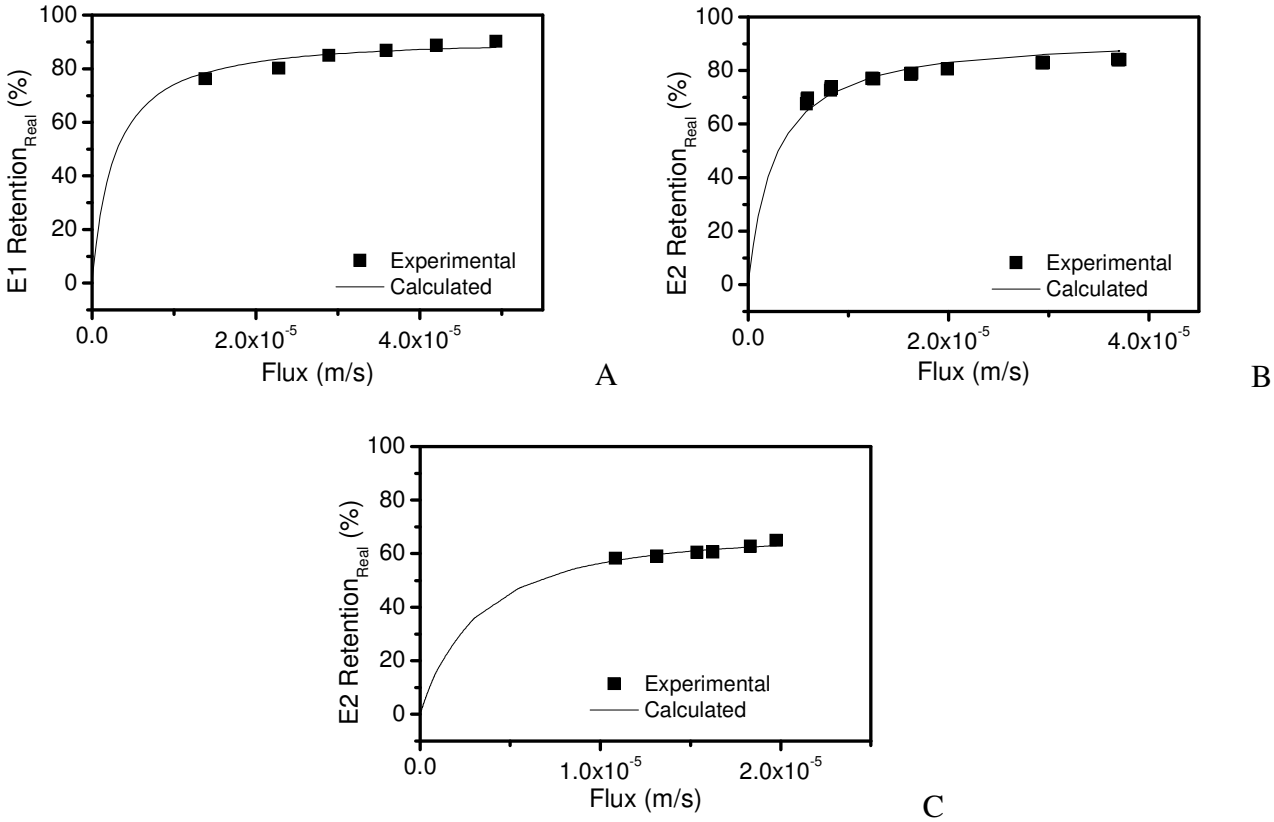

Figure 7.1 Determination of the solute-affinity constant B for **(A)** estrone (E1) and the NF 270 1 membrane **(B)** estradiol (E2) and the NF 270 1 membrane and **(C)** estradiol (E2) and the TFC-SR2 2 membrane (C_{feed}=50 ng.L^{-1}, Re_h=1450, T=24°C)

Table 7.1 Parameter B determination for the hormones estrone (E1) and estradiol (E2) and the NF 270 1 and TFC-SR2 2 membranes

Hormone - Membrane	**Parameter B**
Estrone – NF 270	35.0
Estradiol – NF 270	38.4
Estradiol – TFC SR2 2	15.6

7.2.1.3 Peclet Number Study

One of the fundamental studies that can be done using equation (7.11) is the influence of the Peclet number (that provides the ratio between the convective and diffusive transport of mass) on the concentration profile inside the membrane. Considering the same active layer thickness, the higher the permeate flux (or V), the higher Pe will be. Generally speaking, for small Peclet numbers Pe<<1, diffusion dominates the solute transport and the profile becomes linear. For large Peclet numbers, Pe>>1, convection dominates the solute transport, and the profile becomes curved tending to a constant value for high enough Pe numbers. Figure 7.2 gives the influence of several Peclet numbers varying from 0.001 to 37 on the E2 concentration profile inside the NF 270 membrane for a saturated membrane in the cross-flow system, *i.e.* for steady-state conditions.

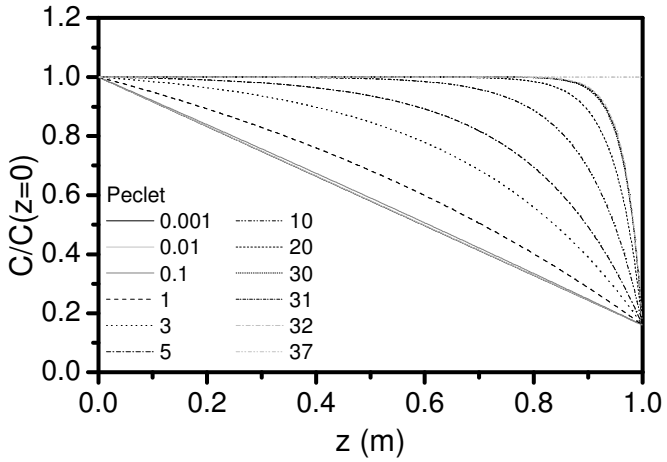

Figure 7.2 Peclet number influence in the normalized concentration profile of a saturated NF 270 1 membrane (estradiol (E2), 3 bar, $C_{feed\ initial}(t=0)=100$ ng.L^{-1}, $Re_h=427$) (z=0 corresponds to the membrane surface)

For 0.001<Pe<0.1 the solute transport inside the pore is diffusion-dominated since the concentration profiles are linear (which corresponds to the trivial solution of equation (7.4) where K_i/D_i is close to zero), while for higher Pe, convection contributes increasingly to the transport of solutes inside the NF membrane. For Pe≥37 the concentration inside the membrane is constant because convection dominates completely the transport of solutes inside the membrane and, diffusion

being negligible, no concentration gradients appear (which corresponds to the trivial solution of equation (7.4) when K_i/D_i is very large). This case is expected to occur for MF and UF membranes but not for NF membranes.

7.2.2 Numerical Solution with the Finite-Difference Method

To solve a partial differential equation as the one given in (7.4), or, as it will be seen later, the one governing time-dependent transport of solute in the membrane pore with adsorption, the finite difference approach can be applied in order to solve it numerically. For that, the physical domain is discretized into a finite number of elements (usually called nodes) through the use of a grid, so that the dependent variables are calculated only at discrete points (the nodes). The continuous problem domain is hence replaced with a finite-difference grid containing a finite number of grid-points (nodes) as represented in Figure 7.3, where Ψ can be a two-dimensional function.

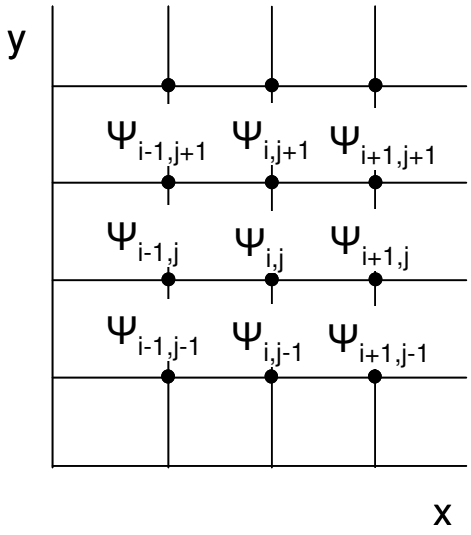

Figure 7.3 Typical finite-difference grid

The derivative expressions such as the ones in equation (7.4) are replaced with approximated equivalent difference quotients given by the Taylor's series expansion.

Considering a differentiable function Ψ (x,y) and applying Taylor's theorem for *x* near the point x_0 yields,

$$\Psi(x_0+\Delta x, y_0) = \Psi(x_0, y_0) + \left.\frac{\partial \Psi}{\partial x}\right|_{x0} \frac{\Delta x}{1!} + \left.\frac{\partial^2 \Psi}{\partial x^2}\right|_{x0} \frac{\Delta x^2}{2!} + \ldots + \left.\frac{\partial^n \Psi}{\partial x^n}\right|_{x0} \frac{\Delta x^n}{n!} + R_n(x) \quad (7.15)$$

where $R_n(x)$ is called the remainder.

The first derivative of the function Ψ can be given by rearranging equation (7.15) in what is called the "forward" difference given by equation (7.16) – see Figure 7.3:

$$\left.\frac{\partial \Psi}{\partial x}\right|_{x_0,y_0} = \frac{\Psi(x_0+\Delta x, y_0) - \Psi(x_0, y_0)}{\Delta x} + O(\Delta x) \quad (7.16)$$

or

$$\left.\frac{\partial \Psi}{\partial x}\right|_{i,j} = \frac{\Psi_{i+1,j} - \Psi_{i,j}}{\Delta x} + O(\Delta x) \quad (7.17)$$

O(Δx) is the truncation error that gives the difference between the partial derivative and its finite-difference representation.

Several other representations for the first derivative can be used:

i) the "backward" representation (in the negative *x* direction of Figure 7.3)

$$\left.\frac{\partial \Psi}{\partial x}\right|_{i,j} = \frac{\Psi_{i,j} - \Psi_{i-1,j}}{\Delta x} + O(\Delta x) \quad (7.18)$$

which originates from the Taylor expansion in the negative x direction:

$$\Psi(x_0-\Delta x, y_0) = \Psi(x_0, y_0) - \left.\frac{\partial \Psi}{\partial x}\right|_{x0} \frac{\Delta x}{1!} + \left.\frac{\partial^2 \Psi}{\partial x^2}\right|_{x0} \frac{\Delta x^2}{2!} - \left.\frac{\partial^3 \Psi}{\partial x^3}\right|_{x0} \frac{\Delta x^3}{3!} + \ldots \quad (7.19)$$

ii) or the "central" difference which originates from subtracting equation (7.19) from (7.15):

$$\left.\frac{\partial \Psi}{\partial x}\right|_{i,j} = \frac{\Psi_{i+1,j} - \Psi_{i-1,j}}{2\Delta x} + O(\Delta x)^2 \qquad (7.20)$$

where the truncation error is of second order, and therefore smaller than that of the "forward" or "backward" differencing, and the numerical result gives a more accurate representation of the solution.

The representation for the second derivative of Ψ is obtained by adding equations (7.19) and (7.15) yielding a truncation error of second order:

$$\left.\frac{\partial^2 \Psi}{\partial x^2}\right|_{i,j} = \frac{\Psi_{i+1,j} - 2\Psi_{i,j} + \Psi_{i-1,j}}{\Delta x^2} + O(\Delta x)^2 \qquad (7.21)$$

A finite-difference representation is consistent if the difference between the partial derivative and its finite-difference representation, *i.e.* truncation error, vanishes as the mesh is refined (*i.e.* $\Delta x \rightarrow 0$), as will be seen in the next section.

Equations (7.20) and (7.21) applied for the pore concentration take the form of equations (7.22 a) and (7.22 b):

$$\left.\frac{\partial C_A}{\partial z}\right|_{i} = \frac{C_{A,i+1} - C_{A,i-1}}{2\delta z} + O(\delta z)^2 \qquad (7.22\ a)$$

$$\left.\frac{\partial^2 C_A}{\partial z^2}\right|_{i} = \frac{C_{A,i+1} - 2C_{A,i} + C_{A,i-1}}{(\delta z)^2} + O(\delta z)^2 \qquad (7.22\ b)$$

where C_A is the solute concentration, *z* is the entrance-exit direction inside the pore, i is a grid node with i-1 and i+1 being, respectively, the upstream and downstream neighboring grid nodes, each of them distancing δz from the node i.

Applying the discretization method (equations 7.22 a and 7.22 b) that uses central differencing to equation (7.4) yields equation (7.23 a):

$$K_i \frac{C_{A,i+1} - C_{A,i-1}}{2(\delta z)} - D_i \frac{C_{A,i+1} - 2C_{A,i} + C_{A,i-1}}{(\delta z)^2} = 0 \qquad (7.23\ a)$$

Rearranging equation (7.23 a) by separating the concentrations in the different nodes gives equation (7.23 b):

$$C_{A,i}\underbrace{\left[\frac{2D_i}{(\delta z)^2}\right]}_{\alpha} + C_{A,i+1}\underbrace{\left[\frac{K_i}{2(\delta z)} - \frac{D_i}{(\delta z)^2}\right]}_{\beta} + C_{A,i-1}\underbrace{\left[-\frac{K_i}{2(\delta z)} - \frac{D_i}{(\delta z)^2}\right]}_{\gamma} = 0 \qquad (7.23\ b)$$

Writing the previous equation (7.23 b) for each node, from node 1 to node k, and considering the boundary conditions in (7.4) applied for node 1 and node k, one obtains the following set of equations:

i=1 $\quad \alpha C_1 + \beta C_2 = -\gamma \Phi' C_{membrane}$ (7.24 a)

i=2 $\quad \gamma C_1 + \alpha C_2 + \beta C_3 = 0$ (7.24 b)

i=3 $\quad \gamma C_2 + \alpha C_3 + \beta C_4 = 0$ (7.24 c)

(…) (…)

i=k $\quad \gamma C_{k-1} + \alpha C_k = -\beta \Phi' C_{permeate}$ (7.24 d)

The set of equations to be solved is given in matrix form in equation (7.25), with the matrix sizes identified:

$$\underbrace{\begin{bmatrix} \alpha & \beta & 0 & 0 & 0 & 0 & \dots & 0 \\ \gamma & \alpha & \beta & 0 & 0 & 0 & \dots & 0 \\ 0 & \gamma & \alpha & \beta & 0 & 0 & \dots & 0 \\ \dots & \dots & \dots & \dots & \dots & \dots & \dots & \dots \\ 0 & 0 & 0 & 0 & 0 & \dots & \gamma & \alpha \end{bmatrix}}_{k \times k} \times \underbrace{\begin{bmatrix} C_1 \\ C_2 \\ C_2 \\ \dots \\ C_k \end{bmatrix}}_{k \times 1} = \underbrace{\begin{bmatrix} -\gamma \Phi' C_{membrane} \\ 0 \\ 0 \\ \dots \\ -\beta \Phi' C_{permeate} \end{bmatrix}}_{k \times 1} \qquad (7.25)$$

A comparison between the numerical solution for a different number of nodes and the analytical solution is given in the next section, allowing determination of the accuracy of the numerical solution.

7.2.3 Comparison Between the Numerical and Analytical Solutions of Equation (3)

Comparing the analytical solution of equation (7.4), given by equation (7.11) with the numerical solution of the same equation obtained with different number of nodes (equation 7.25) allows quantifying the results accuracy and determining the grid independent solution.

For several grids comprising of 25, 50, 100, 200, 400, 800, 1600 and 3200 nodes, the concentration profiles are practically coincident as depicted in Figure 7.4, which indicates the high accuracy of the numerical results.

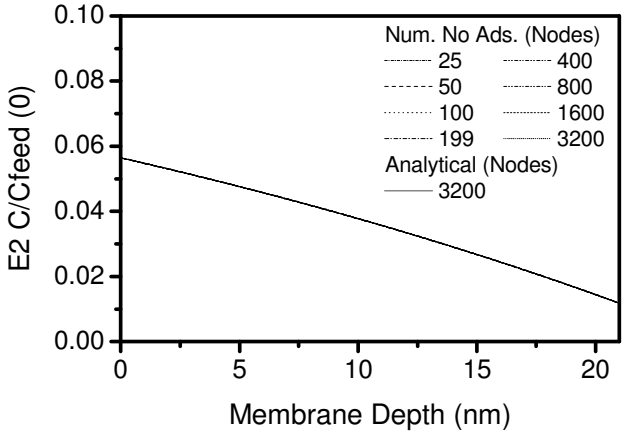

Figure 7.4 Comparison between the analytical solution and the numerical solutions of equation (7.4) (with no adsorption) with different grid sizes (estradiol (E2), 5 bar, $C_{feed}(0)$=100 ng.L^{-1}, Re_h=427 and the NF 270 1 membrane at equilibrium conditions)

When the exact solution of the studied partial differential equations is not known, a classical estimator of the order p of the convergence of the numerical

scheme (the method order of convergence) is given by the Richardson formula [308-310],

$$p = \frac{1}{\ln(n)} \ln\left(\frac{E(nh)}{E(h)}\right) \quad (7.26a)$$

$$E(nh) = \left\| \Phi_{n^2h} - \Phi_{nh} \right\| \quad (7.26b)$$

$$E(h) = \left\| \Phi_{nh} - \Phi_{h} \right\| \quad (7.26c)$$

where Φ is the calculated variable on grids of mesh sizes h, nh, and n^2h.

In the present work n = 2 and, therefore, the previous equations become:

$$p = \frac{1}{\ln(2)} \ln\left(\frac{E(2h)}{E(h)}\right) \quad (7.27\ a)$$

$$E(2h) = \left\| \Phi_{4h} - \Phi_{2h} \right\| \quad (7.27\ b)$$

$$E(h) = \left\| \Phi_{2h} - \Phi_{h} \right\| \quad (7.27\ c)$$

From the previous equations it is straightforward to conclude that the order p of convergence is the magnitude of the slope of the straight line connecting the points $(h, E(h)),\ (2h, E(2h))$ in the bi-logarithmic scale plot.

However, when there is an analytical solution, to ascertain the grid independence of the numerical solution the average error is calculated as the sum of the absolute differences between the numerical and the analytical concentrations at each grid node divided by the total number of nodes. The results are shown in Figure 7.5. As can be seen, this error decreases with the grid refinement. Moreover, grids comprising more than 100 nodes yield a similar error (below 10^{-6} ng.L^{-1}), which means that the solution is no longer dependent on the grid refinement.

By plotting the results errors yielded by equations (7.27) in Figure 7.6, the absolute value of the slope p gives 2, confirming the second order of convergence of the method [310].

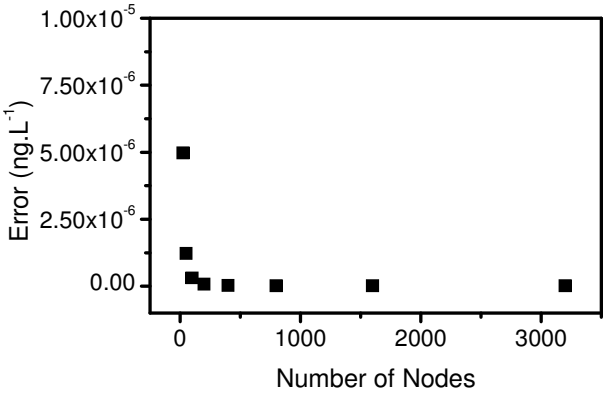

Figure 7.5 Errors between analytical and numerical solutions for different grid sizes

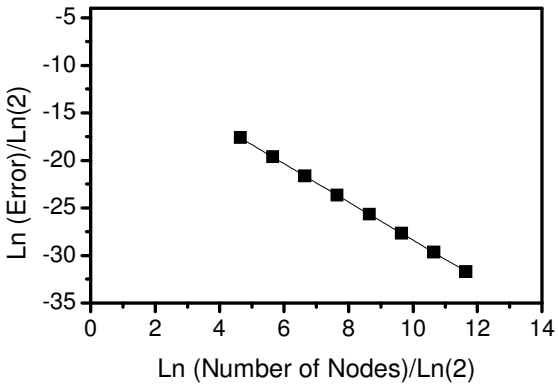

Figure 7.6 Ln (Errors)/ln(2) *vs* Log (Number of Nodes) between analytical and numerical solutions for different grid sizes

7.3. Adsorbing and Non-Adsorbing Compounds

Experiments to study the retention of neutral and non-adsorbing organic solutes of different molecular weights (MW) are carried out with the NF 270 membrane. The retention of the hormones E1 and E2 for the same filtration conditions is also included in the results plot. Two different Re_h numbers are studied to see the effect of concentration polarisation, as presented in Figure 7.7.

For both Re_h numbers, the organics retention increases with MW (Figure 7.7 A). In the laminar regime (Re_h=457) retention is always smaller due to concentration polarisation, which is more noticeable for compounds with MW smaller than the membrane MWCO.

For adsorbing compounds such as E1 and E2, retention is lower than expected by size exclusion, when compared with the retention obtained for the other solutes with similar MW. The higher adsorption obtained at Re_h=457 (E1: 1.5 $ng.cm^{-2}$ and E2: 0.7 $ng.cm^{-2}$) compared to Re_h=1450 (E1: 1.3 $ng.cm^{-2}$ and E2: 0.5 $ng.cm^{-2}$), causes a decrease in retention, from about 80% to 60% for both hormones (Figure 7.7 A). Hormones are found to behave differently than non-adsorbing neutral organics when subjected to the same operational conditions.

The experimental study of the effect of pressure in the observed retention of the hormones is also carried out, for a Re_h= 457 (Figure 7.7 B). As can be seen, it decreases with increase of pressure, which is opposite to the expected behaviour if no adsorption was at play [164, 167, 196, 199]. It could be argued that this decrease is caused by the presence of concentration polarisation, which might cause the observed retention to decrease with pressure and the real retention to increase with pressure. However, when the dioxane retention is measured at different pressures under the same conditions as the hormones, dioxane retention increases with pressure, despite being smaller than the pore radius ($\lambda_{dioxane}=r_s/r_p=0.24/0.42=0.57$).

Adsorption is found to affect membrane performance and, consequently, the transport of hormones through NF membranes. The models that describe transport of solutes through NF membranes are not applicable for adsorbing hormones while adsorption is occurring, *i.e.* in the transient phase. Hence, a new transport model needs to be developed.

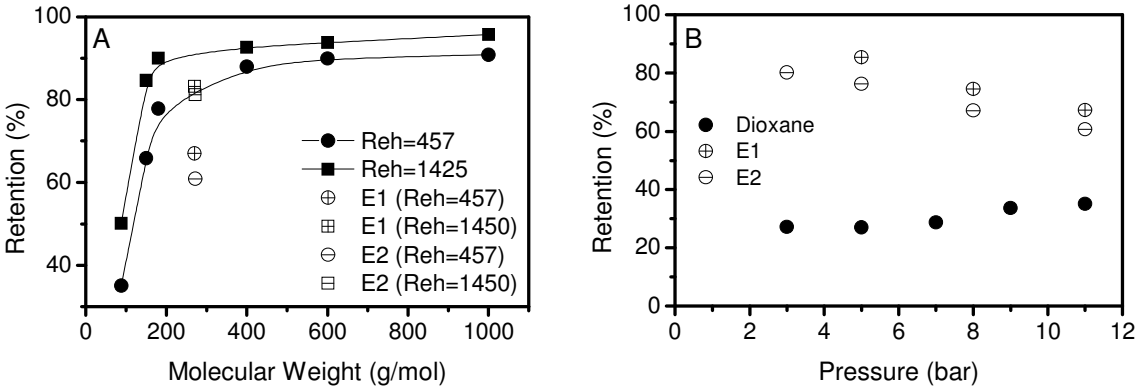

Figure 7.7 Experimental results for NF 270 1 retention **(A)** as a function of molecular weight for two Re_h numbers ($C_{feed\ organics}$= 25 mgC.L^{-1}, $C_{feed\ hormone}$=100 ng.L^{-1}, 24°C, pH 7, 11 bar, Re_h=457 and Re_h=1450) and **(B)** as a function of pressure for estrone (E1), estradiol (E2) and dioxane ($C_{feed\ dioxane}$= 25 mgC.L^{-1}, $C_{feed\ hormone}$=100 ng.L^{-1}, 24°C, pH 7, Re_h=457)

7.4. Integration of Sorption onto Solute Transport by NF Membranes

The mathematical model describing the transport of adsorbing solutes through NF membranes is described next.

7.4.1 Concentration Polarisation

When an adsorbing trace contaminant encounters the membrane surface it can either adsorb on it, be rejected or be transported through the membrane pore onto which it can either adsorb or permeate (Figure 7.8 A). As shown in Chapter 4, concentration polarisation needs to be taken into account when modelling adsorption and retention of hormones in NF membranes. This phenomenon causes an increase in solute concentration at the membrane surface, originating a concentration gradient from the bulk feed (C_{fb}) to the membrane surface (C_{mf}) as depicted in Figure 7.8 B. The more pronounced the polarisation is, the more solute will adsorb on the membrane and the less will be retained.

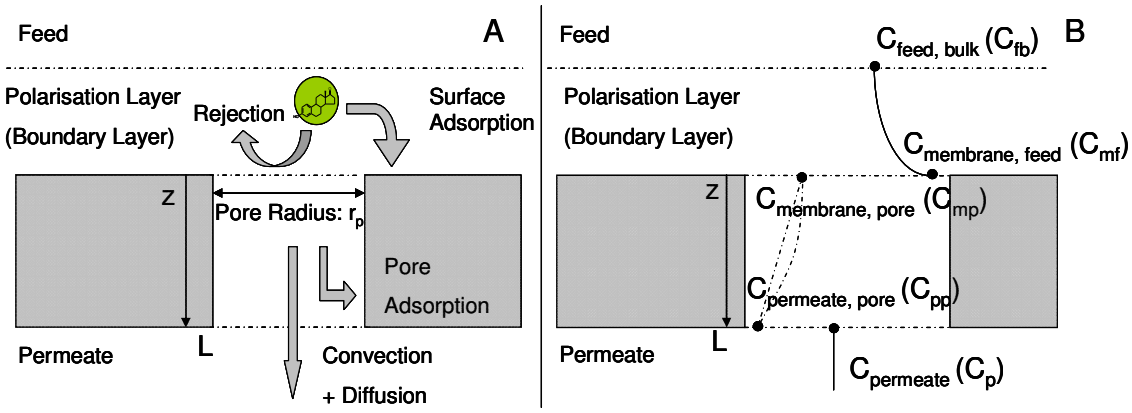

Figure 7.8 Physical phenomena occurring in the filtration of adsorbing compounds onto NF membrane active layer with an effective pore radius r_p **(A)** mass adsorbed and transport mechanisms and **(B)** concentration profiles

7.4.2 Transport Equation through NF Membranes with Adsorption

In Chapter 6, it was found that the ratio solute radius to pore radius (r_s/r_p) and the internal available surface area of the active layer are parameters that need to be taken into account in the modelling of adsorption and, hence, transport of hormones in NF membranes. The solution-diffusion model, for example, that considers the membrane to be dense and excludes the internal surface area, for adsorption, is not appropriate to be used for that purpose. Furthermore, if the transport was caused by diffusion only, then the total mass adsorbed on the membrane and the retention at steady-state would not increase and decrease, respectively, with increase of pore radius but they would be dependent on the concentration at the membrane surface, hence permeability (Chapter 6), and on the number of pores available for diffusion.

The hydrodynamic model reviewed by Deen [43] was chosen to describe the transport of adsorbing hormones in NF membranes. This model takes into account the ratio between the solute and membrane pore size (r_s/r_p) and, by considering the membrane as having perfectly cylindrical pores with an average pore radius r_p, allows using the internal surface area as a parameter in modelling hormone adsorption on NF pores.

The membrane pores are considered as perfect cylindrical capillary tubes all having the same radius and the solute molecule is assumed to be a spherical particle. Once the solute is transported to the pore entrance and exit it partitions in the feed and permeate side as shown in Figure 7.8 B with C_{mp} and C_{mf} and C_{pp} and C_p.

Performing a mass balance on a solute A inside the membrane pores for a time interval δt and a thickness of δz yields equation (7.28), where the solute flux (convective and diffusive) is balanced by an adsorption term and a time accumulation term.

$$\left(j_A\big|_z - j_A\big|_{z+\Delta z}\right)A_a\delta t - \left(\Omega\big|_t - \Omega\big|_{t+\Delta t}\right)n_p P_p \delta z = \left(C_A\big|_{t+\Delta t} - C_A\big|_t\right)A_a\delta z \qquad (7.28)$$

In the previous equation, C_A is the concentration of free species A inside the pore ($kg.m^{-3}$), j_A is the flux of A through the membrane ($m.s^{-1}$), Ω is the mass adsorption

of A on the membrane ($kg.m^{-2}$), t is time (s), z is the membrane active layer depth or thickness (m) and has the direction from the pore entrance to the pore exit, A_a is the open area to permeation (m^2) and P_p is the pore perimeter (m) that multiplied by the pore length or membrane thickness gives the internal area in which the solute A can adsorb inside the membrane wall. The pore perimeter is given by $P_p = 2\pi r_p$ where r_p is the pore radius (m).

By making δt and δz infinitesimal one obtains:

$$-A_a \frac{\partial j_A}{\partial z} - P_p \frac{\partial \Omega}{\partial t} = A_a \frac{\partial C_A}{\partial t} \tag{7.29}$$

In equation (7.29) it is assumed that the flux j_A does not vary with time and reaches the steady-state instantaneously. This means that changes in the concentration profile inside the membrane with time are only due to adsorption on the membrane surface and membrane pores. This can be assumed as a first approximation considering that permeate and feed concentration for non-adsorbing species do not vary with time and the steady-state is quickly reached when only steric interactions are involved [159]. Furthermore, the flux of species A is considered one-dimensional (membrane pores are very tight compared to pore length and species A size).

As previously discussed, the flux in a NF membrane pore is given by equation (7.3), as the sum of hindered convection and diffusion caused by the finite pore size [43].

Substituting equation (7.3) into equation (7.29) and after some algebraic manipulation one obtains the transport equation of the solute inside the pore with adsorption:

$$-K_c V \frac{\partial C_A}{\partial z} + K_d D_\infty \frac{\partial^2 C_A}{\partial z^2} = \frac{\partial C_A}{\partial t} + \frac{P_p}{A_a} \frac{\partial \Omega}{\partial t} \tag{7.30}$$

The last term on the right hand side of equation (7.30) takes into account experimental evidence: the membrane adsorption isotherm for both hormones is linear (Figure 4.8 and Figure 4.9) and given by equation (7.31),

$$\Omega = \chi C_A \tag{7.31}$$

with χ standing for the straight line slope (m). The time variation of equation (7.31) is therefore given by equation (7.32):

$$\frac{\partial \Omega}{\partial t} = \chi \frac{\partial C_A}{\partial t} \tag{7.32}$$

Equation (7.32) can be substituted into equation (7.30), assuming that sorption in the membrane surface pore is faster compared to the diffusion in the pore [311, 312]. Static adsorption of E1 and E2 on the membrane surface in Chapter 5 proved to be a very fast process. In comparison, the tighter the membrane, the longer the diffusion process through the membrane will take as seen in Chapter 6. After algebraic manipulation one obtains equation (7.33):

$$-K_i \frac{\partial C_A}{\partial z} + D_i \frac{\partial^2 C_A}{\partial z^2} = \frac{\partial C_A}{\partial t} \tag{7.33}$$

In the previous equation K_i and D_i are given by equations (7.34 a) and (7.34 b), respectively:

$$Di = \frac{K_d D_\infty}{(1 + \frac{P_p}{A_a}\chi)} \tag{7.34 a}$$

$$Ki = \frac{K_c V}{(1 + \frac{P_p}{A_a}\chi)} \tag{7.34 b}$$

7.4.3 Boundary and Initial Conditions

Due to the time dependence of equation (7.33), an initial condition in addition to the two spatial boundary conditions used previously in the absence of adsorption is necessary. The initial and boundary conditions used are presented in equations (7.35 a, b and c):

$$C_A = 0\,,\ t = 0,\ 0<z<L \qquad (7.35\ a)$$

$$C_A = C_{mf}\,\Phi',\ z = 0,\ \forall t \qquad (7.35\ b)$$

$$C_A = C_p\Phi',\ z=L,\ \forall t \qquad (7.35\ c)$$

When the hormone is spiked in the system, in the first instance the concentration inside the membrane pore is zero. For the spatial boundary conditions, the concentration at the pore entrance (or feed side) is equal to the concentration at the membrane surface multiplied by the steric partitioning coefficient modified for interaction between the solute and the membrane. The same spatial boundary condition is applied on the permeate side.

7.5. The Numerical Model Build-Up

There is no analytical solution for the unsteady-state partial differential equation (7.33) with the boundary conditions expressed by equations (7.35 a, b and c). There are very particular situations that allow equation (7.33) to be solved analytically. For example, transport in porous media with adsorption expressed similarly to equation (7.33) can be analytically solved considering the media as infinite with a nil concentration there [313], that is $C_A=0$ for $z=\infty$. For the case of NF membranes with a few nanometres of thickness this approach cannot be used. Furthermore, in hormone NF permeation there is some solute present in the permeate side in the first instances (Chapter 4), increasing with time, contrary to packed beds, where there is no solute measured in the exit side for some considerable time.

The previous reasoning leads to the conclusion that the solution of equation (7.33) requires a numerical method. In this work the finite difference method is applied, as previously described. A grid is built to discretize the physical domain so that the dependent variables are calculated at discrete points: the grid nodes. The spatial derivative expressions are replaced by finite differences obtained by Taylor's series expansion. Both first and second derivatives are calculated by the second order central differencing scheme (equations (7.22 a) and (7.22 b)), which has a truncation error $O(\delta z)^2$, to ensure higher results accuracy [314].

The unsteady character of equation (7.33) (*i.e.* dependency on time) was dealt with the full implicit method, which is of first order in time $O(\delta t)$. This scheme is unconditionally stable as opposed to the explicit scheme. Therefore, no time step (δt) limitations are required [314].

Applying the central differencing and the full implicit schemes to equation (7.33) for the generic i grid node, and denoting superscripts n and n+1 as two consecutive moments separated by the time step δt, one obtains the algebraic equation (7.36):

$$\frac{C_{A,i}^{n+1} - C_{A,i}^{n}}{\delta t} = D_i \frac{C_{A,i+1}^{n+1} - 2C_{A,i}^{n+1} + C_{A,i-1}^{n+1}}{(\delta z)^2} - K_i \frac{C_{A,i+1}^{n+1} - C_{A,i-1}^{n+1}}{2\delta z} \qquad (7.36)$$

Equation (7.36) must be written for each grid node, which leads to a set of n equations to n unknowns (the concentration at the n nodes), n being the number of grid nodes. The first and last nodes of the grid, those nearest the pore entrance and exit respectively, must include the boundary conditions expressed by equations (7.35 b) and (7.35 c), where the experimental results measured for the feed and permeate concentrations are used.

The set of equations is solved by a matrix algorithm in Matlab to obtain the concentration profile along the pore for different times. In the present case the tridiagonal matrix algorithm (TDMA) was used [314]. The work of Matthieu Foucher in developing the first version of the Matlab code to apply the matrix algorithm resolution is acknowledged.

7.5.1 Solving the Equation with Adsorption

Using the discretization implicit method with central differencing for node i yields the following equation (7.37) and, with some algebra, the equations (7.38) and (7.39):

$$\frac{C_i^{n+1} - C_i^n}{\delta t} = D_i \frac{C_{i+1}^{n+1} - 2C_i^{n+1} + C_{i-1}^{n+1}}{(\delta z)^2} - K_i \frac{C_{i+1}^{n+1} - C_{i-1}^{n+1}}{2\delta z} \qquad (7.37)$$

$$C_i^{n+1} - C_i^n = \frac{Di\delta t}{(\delta z)^2}\left[C_{i+1}^{n+1} - 2C_i^{n+1} + C_{i-1}^{n+1}\right] - \frac{K_i \delta t}{2\delta z}\left[C_{i+1}^{n+1} - C_{i-1}^{n+1}\right] \qquad (7.38)$$

$$C_{i-1}^{n+1}\underbrace{\left[-\frac{Di\delta t}{(\delta z)^2} - \frac{Ki\delta t}{2\delta z}\right]}_{\gamma} + C_i^{n+1}\underbrace{\left(1 + \frac{2Di\delta t}{(\delta z)^2}\right)}_{\alpha} + C_{i+1}^{n+1}\underbrace{\left[-\frac{Di\delta t}{(\delta z)^2} + \frac{Ki\delta t}{2\delta z}\right]}_{\beta} - C_i^n = 0 \qquad (7.39)$$

Writing the same equation for all the k nodes covering the entire membrane pore thickness one obtains:

i=1 $\quad \gamma\Phi' C_{membrane}^{n+1} + \alpha C_1^{n+1} + \beta C_2^{n+1} - C_1^n = 0 \qquad (7.40\ a)$

i=2 $\quad \gamma C_1^{n+1} + \alpha C_2^{n+1} + \beta C_3^{n+1} - C_2^n = 0 \qquad (7.40\ b)$

i=3 $\quad \gamma C_2^{n+1} + \alpha C_3^{n+1} + \beta C_4^{n+1} - C_3^n = 0 \qquad (7.40\ c)$

(…) $\quad$ (…) $\quad$ (…)

i=k $\quad \gamma C_{k-1}^{n+1} + \alpha C_k^{n+1} + \beta\Phi' C_{permeate}^{n+1} - C_k^n = 0 \qquad (7.40\ d)$

Rewriting the previous equations by separating the independent terms corresponding to the boundary condition, one obtains:

i=1 $\quad \alpha C_1^{n+1} + \beta C_2^{n+1} + \underbrace{\left(\gamma\Phi' C_{membrane}^{n+1} - C_1^n\right)}_{\text{independent term}} = 0 \qquad (7.41\ a)$

i=2 $$\gamma C_1^{n+1} + \alpha C_2^{n+1} + \beta C_3^{n+1} + \underbrace{\left(-C_2^n\right)}_{\text{independent term}} = 0 \quad (7.41\text{ b})$$

i=3 $$\gamma C_2^{n+1} + \alpha C_3^{n+1} + \beta C_4^{n+1} + \underbrace{\left(-C_3^n\right)}_{\text{independent term}} = 0 \quad (7.32.\text{c})$$

(…) (…) (…)

i=k $$\gamma C_{k-1}^{n+1} + \alpha C_k^{n+1} + \underbrace{\left(\beta\Phi' C_{permeate}^{n+1} - C_k^n\right)}_{\text{independent term}} = 0 \quad (7.41\text{ d})$$

In the form of a matrix product (tridiagonal matrix), the set of equations to be solved can be expressed as:

$$\begin{bmatrix} A_{11} & A_{12} & 0 & 0 & 0 & 0 & ... & 0 \\ A_{21} & A_{22} & A_{23} & 0 & 0 & 0 & ... & 0 \\ 0 & A_{32} & A_{33} & A_{34} & 0 & 0 & ... & 0 \\ ... & ... & ... & .. & ... & ... & ... & ... \\ 0 & 0 & 0 & 0 & 0 & ... & A_{i,k-1} & A_{i,k} \end{bmatrix} \times \begin{bmatrix} C_1^{n+1} \\ C_2^{n+1} \\ C_3^{n+1} \\ ... \\ C_i^{n+1} \end{bmatrix} + \begin{bmatrix} TI_1 \\ TI_2 \\ TI_3 \\ ... \\ TI_i \end{bmatrix} = 0 \quad (7.42)$$

where, i is the node and k the matrix row:

$$\begin{aligned} &A_{i,k} = \alpha \quad (k = i) \\ &A_{i,k} = \beta \quad (k = i+1) \\ &A_{i,k} = \gamma \quad (k = i-1) \\ &TI_i \rightarrow \text{independent term} \end{aligned} \quad (7.43)$$

The initial condition is given by:

$$t = 0 \rightarrow C_i^0 = 0 \quad (7.44)$$

7.5.2 Model Coefficients

The solution of equation (7.33) requires the determination of several membrane and solute characteristics. These are determined next.

7.5.2.1 Determining χ

The parameter χ in equations (7.35 a) and (7.35 b) needs to be determined so that the solution of equation (7.33) can be obtained. The parameter χ is determined by fitting the results of the solution of the transport equation (7.33) to the experiments of varying feed concentration. The parameter χ gives a direct proportion between the hormone mass adsorbed and a concentration for a known surface area and concentration at a determined point. In filtration mode the membrane is subjected to different concentrations: the membrane surface concentration at the feed side and the pore concentration that varies along the pore. Hence, a single value of χ cannot be obtained. Each pair solute-membrane has its own χ value.

For the case of E1-NF 270, E2-NF 270 and E2-TFC-SR2, the fitting results are shown in Figure 7.9, Figure 7.10 and Figure 7.11, respectively. The values obtained are: $\chi_{TFC\text{-}SR2\text{-}E2}$=0.0013±0.0002 m, $\chi_{NF270\text{-}E2}$=0.17±0.02 m, $\chi_{NF270\text{-}E1}$=0.21±0.02 m. This value is a measure of the affinity of the hormone to the membrane used.

These different affinities can be explained by the differences in the isotherms obtained in the shaker and displayed in Figure 7.12. E1 and E2 have similar affinities with the NF 270, with E1 being slightly higher, which is in accordance with the χ values obtained. The affinity of the E2 with the NF 270 is higher compared to the TFC-SR2 which is mirrored in the χ values obtained.

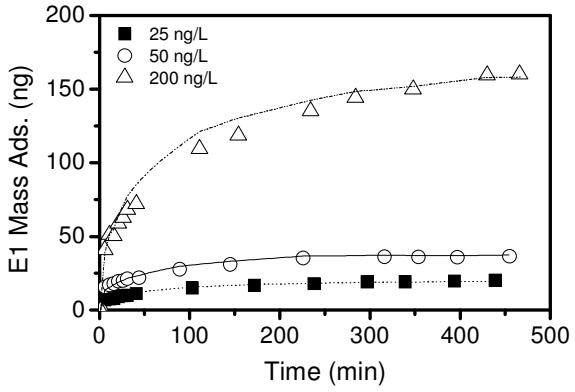

Figure 7.9 Model fitting to feed concentration experiments for estrone (E1) and the NF 270 1 (C_{feed}=25, 50 and 200 ng.L^{-1}, 11 bar, Re_h=427, T=24°C, pH 7)

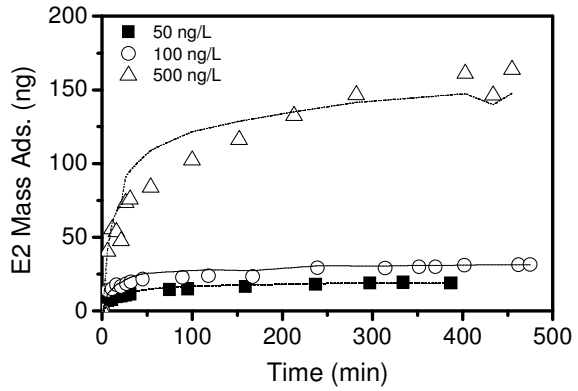

Figure 7.10 Model fitting to feed concentration experiments for estradiol (E2) and the NF 270 1 (C_{feed}=50, 100 and 500 ng.L^{-1}, 11 bar, Re_h=427, T=24°C, pH 7)

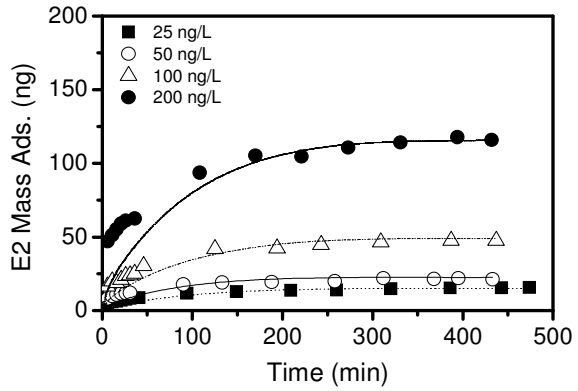

Figure 7.11 Model fitting to feed concentration experiments for estradiol (E2) and the TFC-SR2 2 (C_{feed}=25, 50, 100 and 200 ng.L^{-1}, 11 bar, Re_h=427, T=24°C, pH 7)

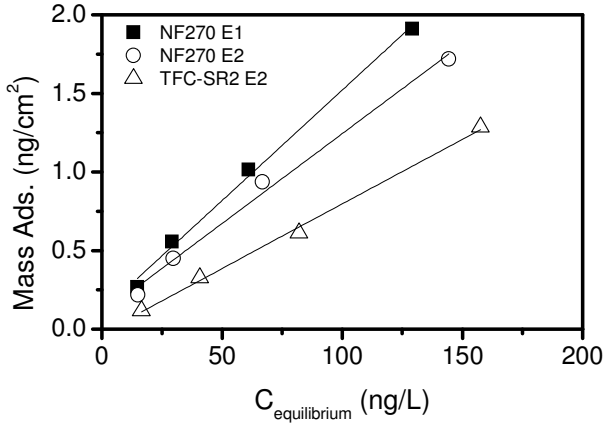

Figure 7.12 Shaker isotherm experiments for estrone (E1) and estradiol (E2) and the NF 270 1 and estradiol (E2) and the TFC-SR2 2 (C_{feed}=25, 50, 100, 200 ng.L^{-1}, T=24°C, 200 rpm)

The comparison between the constant χ obtained from static experiments and from model fitting is given in Table 7.2.

Table 7.2 Comparison between χ obtained from static experiments and from model fitting

Hormone/Membrane	χ Fitted (m)	χ from Static Isotherm (m)
TFC-SR2 E2	0.0013	0.08
NF 270 E2	0.17	0.13
NF 270 E1	0.21	0.16

As can be seen in Table 7.2, there is a difference between the χ obtained from the numerical model fitting and from the static isotherm for the TFC-SR2 2 membrane (active layer thickness of 345 nm). The model assumption of perfect cylindrical pores is probably more adequate for the NF 270 1 membrane, with a thin active layer of 21 nm (Table 3.7) which supports the likely absence of tortuosity.

7.5.2.2 Membrane and Solute Characteristics

The membrane characteristics needed to solve equation (7.33) were estimated as described in Chapter 6. The membrane average pore radius and the thickness to porosity ratio are those given in Table 6.6.

With the average value of the membrane active layer thicknesses for the NF 270 and the measured thickness for the TFC-SR2 presented in Table 6.6, the porosity was obtained. With the porosity and pore radius several parameters can be estimated such as the pore perimeter, the membrane permeation area, the average velocity inside the pore, etc., as discussed in Chapter 6.

7.5.2.3 Determination of the Concentration at the Membrane Surface

The transient concentration at the membrane surface C_{mf} is given by the concentration polarisation and film theory and is calculated with the transient feed and permeate experimental results.

The mass transfer coefficient k is calculated using the Sherwood for the same hydrodynamic conditions, a correlation that was previously used in Chapter 4 [258]:

$$Sh = \frac{kd_h}{D_\infty} = 1.195\,Re^{0.554}\,Sc^{0.371}\left(\frac{d_h}{L_{cell}}\right)^{0.131} \qquad (7.45)$$

7.5.3 Concentration Profile and Mass Adsorbed

7.5.3.1 Surface Mass Adsorbed

The mass adsorbed on the membrane surface was found to be linearly proportional to the concentration at equilibrium (Chapter 4, isotherm figures). To calculate the mass adsorbed on the membrane surface, the same linearity between mass adsorbed and concentration at the membrane surface is assumed, where the variation of the mass adsorbed and membrane concentration with time is considered as a succession of quasi-equilibrium states. As seen in Chapter 6 and in the study by McCallum *et al.* [152], the adsorption process is reversible when MilliQ water is filtered through the membrane, where the initial conditions of filtration are recovered showing that the assumption of a succession of quasi-equilibrium states can be used.

Due to the adsorption of hormone onto the membrane, the membrane surface concentration decreases with time. The relationship between the mass adsorbed on the surface and the concentration at the membrane surface is given by equation (7.46):

$$\frac{dM_{ads\ surface}}{dt} = A_{surface}\frac{d\Omega_{surface}}{dt} = -A_{surface}\chi\frac{dC_m}{dt} \qquad (7.46)$$

Solving equation (7.46) with the initial and boundary conditions: t=0, $M_{ads\ surface}$=0 and C_m=$C_m(0)$, yields equation (7.47):

$$M_{ads\ surface} = A_{surface}\chi(C_m(0) - C_m(t)) \qquad (7.47)$$

7.5.3.2 Pore Surface Mass Adsorbed

The hormone concentration profile inside the pore is obtained by solving equation (7.33) with the boundary conditions expressed by equations (7.35 a, b and c). To verify if the numerical model with sorption describes the problem well one can compare the results obtained with the adsorption numerical model at equilibrium conditions (Num. Ads. at Steady-State in Figure 7.4) with the analytical solution given by equation (7.11) using the same boundary conditions as the ones used for the numerical model at steady-state. As can be seen in Figure 7.13, that exhibits this comparison, they coincide showing the good accuracy of the solution of the numerical model. The error $\varepsilon = \frac{1}{N}\sum_{i=1}^{N}\left|AS_i - NS_i\right|$, where N is the number of nodes, AS_i is the analytical solution for node i and NS_i is the numerical solution for node i, for a grid comprising of 190 nodes was of the order of 10^{-6} ng.L^{-1}. Moreover, tests of grid independence showed that a grid comprising of 190 nodes was found enough for the solution to be grid independent.

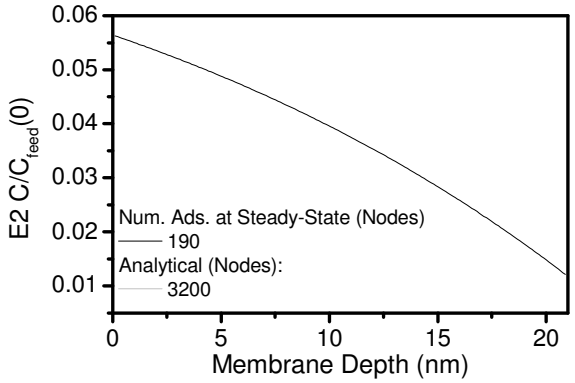

Figure 7.13 Comparison between the analytical solution and the numerical solutions with adsorption at equilibrium (estradiol (E2), 5 bar, 100 ng.L^{-1}, Re_h=427 and NF 270 1 membrane at equilibrium conditions)

7.6. Pore Concentration Profiles

The solute concentration profiles inside the pore obtained from the model describe precisely a whole series of experiments and, therefore, clarify the dominating transport mechanisms of adsorbing trace contaminants inside the NF membrane, which has always been the focus of much discussion. The membrane has been either considered dense and, hence, no pores are present, which means that no convection term is included, or the membrane has been considered porous and a convection term has to be considered. Although the inclusion of a convective term makes the solution of equation (7.33) much more complex, demanding numerical methods of second order of accuracy, it will bring some insight as to when the transport of solutes inside the membrane is diffusion-dominated or convection-dominated. Assuming as a starting point that a convection term is not to be included is much too limited in describing the problem for NF membranes [256].

Figure 7.14 E and F exhibit the transient concentration profiles for E2 at pressures of 5 and 15 bar. Figure 7.14 B and C shows the same results for E1. For comparison purposes, Figure 7.14 A and D shows the concentration profiles of E2 and E1, respectively, that would be obtained at 5 bar if no adsorption was considered. The same boundary conditions as the ones considered for adsorption were used. Figure 7.15 shows the E2 concentration profile at 5 bar and 15 bar for the TFC-SR2 membrane.

Comparing Figure 7.14 A with Figure 7.14 B (or Figure 7.14 D with Figure 7.14 E), the effect of adsorption on the concentration profile of the solute inside the pore becomes evident: adsorption starts at the pore entrance region making, for the first instances, the solute concentration to decrease along the membrane depth (in fact, the curve concavity is reverted in those instances). Then, adsorption spreads out along the membrane depth and, with time, the profile shape approaches that without adsorption.

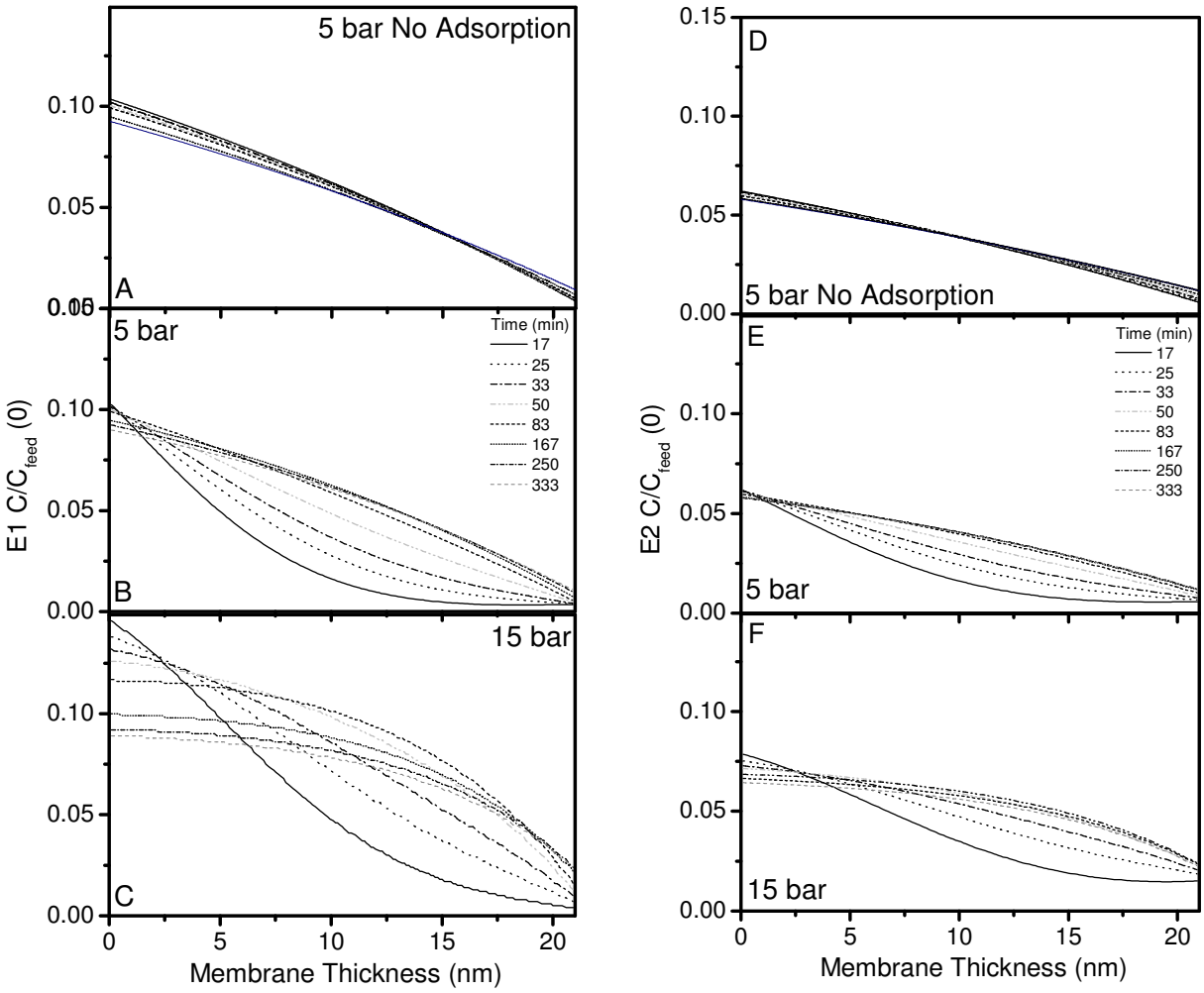

Figure 7.14 Predicted pore concentration profiles for estradiol (E2) and estrone (E1) as a function of time for the NF 270 1 membrane (Re_h=427; C_{feed} =100 ng.L^{-1}); E1: **(A)** 5 bar, **(B)** 15 bar and **(C)** with no adsorption at 5bar; E2: **(D)** 5 bar, **(E)** 15 bar and **(F)** with no adsorption at 5 bar

When adsorption occurs at lower pressures (5 bar, Figure 7.14 B and E), the hormone concentration reduces considerably along the pore length (*i.e.* membrane depth) at the beginning of the experiment, particularly downstream the entrance region. This means high adsorption rates at the pore entrance region at the beginning of permeation.

A higher pressure causes higher concentrations along the pore as can be seen by comparing Figure 7.14 B and E with Figure 7.14 C and F, therefore yielding more adsorption. This trend is particularly noticeable at the pore centre and exit and is a consequence of the higher concentration polarisation yielded by higher pressures.

For the highest pressure (15 bar, Figure 7.14 C and F), convection increases in importance: the profile shifts from linear (diffusion-dominated transport) to curve (convection-dominated transport) showing that convection cannot be ignored in the transport of solutes by NF membranes, particularly at high pressures. Although present at all instants in Figure 7.14 C and F, this effect of the convective transport is particularly noticeable when steady-state is approached and adsorption becomes negligible.

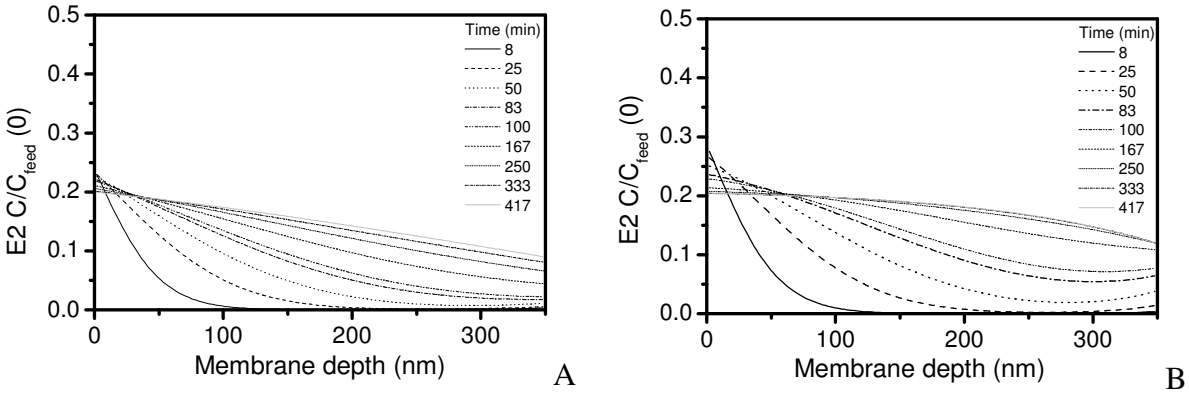

Figure 7.15 Predicted pore concentration profiles for estradiol (E2) as a function of time for the TFC-SR2 2 membrane (Re_h=427; $C_{feed\ initial}$(t=0)=100 ng.L^{-1}); E2: **(A)** 5 bar, **(B)** 15 bar

There is a difference in the mass partitioned into the membrane of E1 compared to E2 (*e.g.* Figure 7.14 B and E): the solute radius to pore radius ratio, λ, is closer to 1 for E2, compared to E1 and therefore partitions less. E1 is likely to adsorb more because the concentrations inside the membrane are higher.

Interestingly, the concentration of E1 and E2 in the results for the NF 270 membrane at the pore exit are very similar when reaching steady-state, despite the higher permeate concentrations obtained for E2 compared to E1 (Chapter 4) that were used as boundary condition values for the predictions. This is caused by the small differences in the molecule size of E1 and E2. The closer the solute size is to the pore size, as is the case of E2, the smaller the partition coefficient Φ' will be and therefore, the smaller the concentration inside the membrane on the permeate side will be.

Comparing the E2 concentration profiles of the TFC-SR2 and the NF 270 membranes, one can see that the partitioning of E2 inside the membrane SR2 is much higher than the NF 270 membrane because the SR2 has larger pores than the NF 270 membrane (Table 6.6). On the other hand, the SR2 having a much thicker active layer compared to the NF 270 membrane has a much slower breakthrough curve in the permeate side (Chapter 4), which originates bigger differences in the concentration profiles inside the membrane. This thicker active layer also causes the diffusive transport to be more relevant at 15 bar after steady-state is attained, when compared to the profile obtained for the NF 270 membrane at this same pressure, where diffusion is much less relevant.

7.7. Model Validation

Once the pore concentration profile is obtained, the pore mass adsorbed is estimated by numerically integrating the concentration profile along the pore and considering the linear relationship between the mass adsorbed and the concentration given by equation (7.31). The pore mass adsorbed is then summed to the surface mass adsorbed for each time and compared to the experimental results obtained for each hormone.

The model predicted results are compared with the corresponding experimental ones for several experimental conditions for E1 and E2 in Figure 7.16 for the NF 270 membrane and Figure 7.17 for the TFC-SR2 one.

The model predicts well the total mass of hormone adsorbed in the NF membranes when the hydrodynamic model considers both the surface and internal sorption.

The variability of the model predictions obtained for the hormone mass adsorbed as a function of the variability of its parameters, such as membrane average pore radius and solute radius, amongst others, is described in Appendix F.

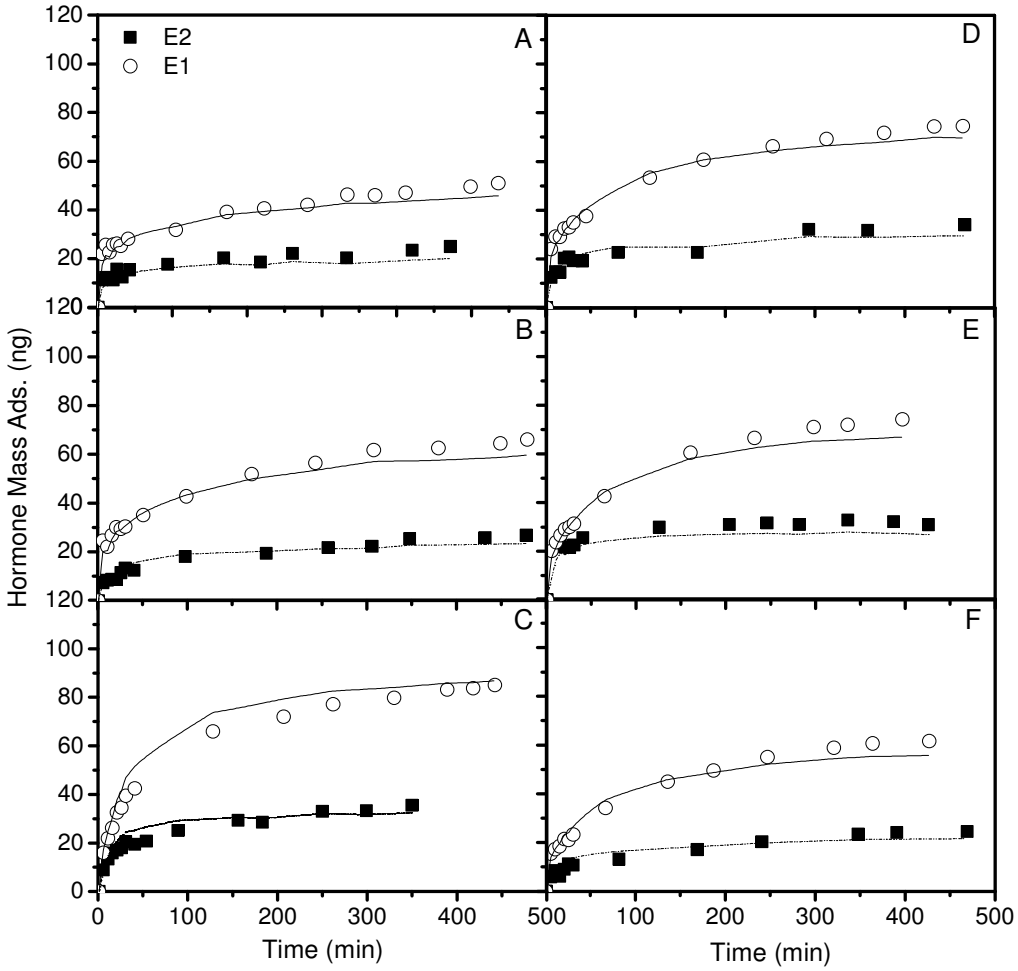

Figure 7.16 Comparison between experimental and model results of the estrone (E1) and estradiol (E2) mass adsorbed for the NF 270 1 membrane (C_{feed}=100 ng.L^{-1}, T=24°C, pH 7): Re_h=457 **(A)** P=5bar, **(B)** P=8 bar, **(C)** P=15 bar; P=11 bar **(D)** Re_h=570, **(E)** Re_h=855, **(F)** Re_h=991

As can be seen in Figure 7.16, E1 adsorbs much higher mass than E2 for the same filtration conditions. When E1 adsorption in static mode is compared to E2, a higher affinity between E1 and the membrane is obtained (Figure 7.12), confirming the higher adsorption for E1. However, the difference in adsorption between E1 and E2 in static mode is 20% (Figure 7.12) not explaining the differences obtained in filtration mode. This is however explained by the higher partitioning of E1 inside the pore compared to E2. This example illustrates well how similar molecules can behave differently when one partitions more inside the membrane pore.

Because E1 adsorbs more than E2 this causes more pronounced changes in the time-varying profiles of E1 (Figure 7.14 D and E) than those observed for the E2 profiles (Figure 7.14 A and B). These differences are more noticeable, as expected, at higher pressures, since larger concentration polarisation occurs.

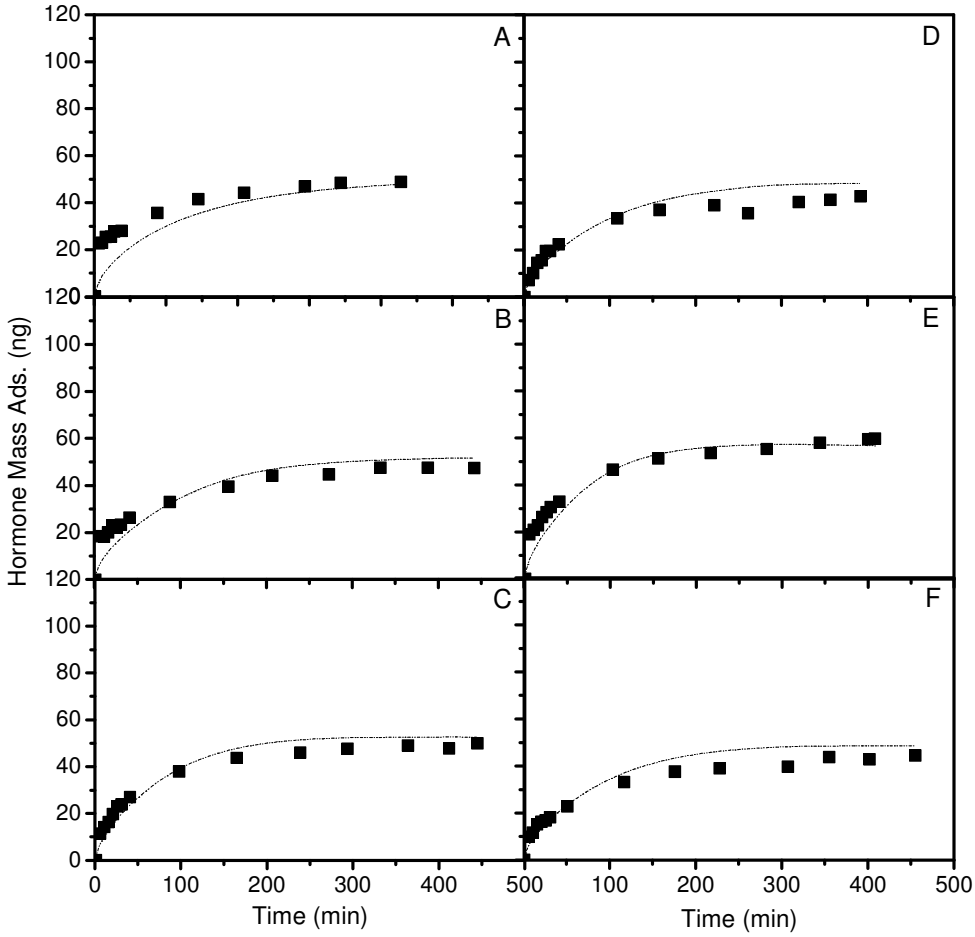

Figure 7.17 Comparison between experimental and model results of the estradiol (E2) mass adsorbed for the TFC-SR2 2 membrane (C_{feed}=100 ng.L^{-1}, T=24°C, pH 7): Re_h=457 **(A)** P=5bar, **(B)** P=8 bar, **(C)** P=15 bar; **(D)** P=17 bar, P=11 bar **(E)** Re_h=712, **(F)** Re_h=991

7.8. Conclusions

Hormones adsorb onto NF polymeric membranes causing a lower retention than would be expected by purely steric interactions.

The relationship between solute and pore size is important. The highest r_s/r_p is the better the removal will be by steric exclusion. However, this factor is not the only one playing a role in the removal of trace contaminants by NF membranes. The interaction with the membrane polymer may overcome this steric exclusion factor leading to high rates of adsorption. The lower the interaction of trace contaminants with the membrane (Φ') the less will they partition inside the membrane and, therefore, less will adsorb in the pores. This has an impact on the design of membrane materials. On the other hand, the more internal surface area the membrane has, the more will adsorb in it and the more will permeate through the membrane.

A new model taking into account adsorption inside the membrane polymeric active layer was developed and describes precisely a whole series of experiments, allowing understanding the different mechanisms taking place in the transport of these components inside the membrane pores that depend on the operating conditions. The developed sorption model which takes transport by convection into account in the NF process describes well the experimental data. Therefore it makes sense to take convection transport into account, especially at pressures higher than 11 bar, commonly used pressure in NF.

Further attention needs to be taken when studies of adsorbing compounds are carried out. As previously mentioned, erroneous conclusions can be taken from studies with the transport of adsorbing trace contaminants in unsaturated membranes, because while adsorption occurs, the permeate concentration will be low for highly adsorbing contaminants such as E1 with the NF 270 and E2 for the TFC-SR2. These results might lead to the conclusion of a diffusion-dominated transport, when in fact it makes sense to consider convection, as is the case for the NF 270 membrane at 15 bar.

8 Conclusions and Future Work

8.1. Conclusions

Trace contaminants are present in untreated, treated and natural waters. This problem has led to the application of membrane processes in water treatment and water reclamation. A higher water quality compared to that obtained with currently established treatment processes is obtained. However, the occurrence of adsorption of some of these contaminants onto the membranes contributes to the lack of understanding and control of the mechanisms involved in their removal by NF and RO membranes. Consequently, understanding the fundamental mechanisms involved in the removal of these contaminants by NF membranes is essential. Within this scope, the main objectives of this thesis were:

- To understand what filtration parameters affect adsorption and how they affect it, and consequently, how retention of hormones by NF membranes is affected;

- To understand how membrane and solute characteristics affect adsorption, and, consequently, how retention of hormones by NF membranes is affected;

- To use the knowledge acquired to attain the previous objectives in developing a new predictive transport model for the removal of adsorbing trace contaminants by NF membranes.

In Chapter 4 it was shown how filtration parameters, such as pressure, circulating Reynolds number and feed concentration affect adsorption and retention of hormones by NF membranes. This study clearly showed for the first time that the adsorbed mass to the membrane is directly dependent on the initial concentration at the membrane surface. Thus, concentration polarisation proved to have a dominant role in the adsorption of hormones by NF membranes. Retention was found to be governed by the initial polarisation modulus β that expresses the ratio of the initial

membrane surface to the feed concentration: the higher the β value is, the lower the retention that is obtained. Furthermore, the higher the adsorption obtained on the membrane for a certain hormone is, the more permeates through the membrane. That, in turn, increases with the increase of the operating pressure and hormone feed concentration and with the decrease of the circulating Reynolds number.

This adsorption phenomenon has an impact in the design of membranes and operation of membrane processes. To avoid the negative impact on adsorption the concentration at the membrane surface should be minimized either by increasing the Reynolds numbers or by introducing spacers, which are in use in spiral-wound modules to minimize concentration polarization. Moreover, if the pressure is minimized, concentration polarization will not have a severe effect on adsorption. This, however, has a cost since less product (clean water) is obtained.

When two different membranes were compared, it was concluded that membranes with higher permeate flux have more severe concentration polarisation, which has a higher impact on adsorption and retention of trace contaminants. This occurred despite the larger pores of the membrane with a lower flux. In fact, for pressures between 11 and 17 bar, E2 retention for the NF 270 membrane (r_p=0.42 nm) was only slightly higher (10%) compared to the looser membrane TFC-SR2 (r_p=0.46). Concentration polarisation was much more severe for the NF 270 membrane, which has a permeability of 17 $L.h^{-1}.m^{-2}.bar^{-1}$, than for the TFC-SR2 one, which has a permeability of 7.2 $L.h^{-1}.m^{-2}.bar^{-1}$.

From the experimental results of hormone permeation, adsorption and retention obtained in Chapter 4, a new sorption model was developed in Chapter 5 for the prediction of the transient hormone feed and permeate concentrations. The hormones were shown to adsorb according to pseudo-first order sorption kinetics, as was the transient feed concentration and retention. Based on this kinetics equation and on the experimental evidence that adsorption is dependent on the concentration polarization, the transient feed and permeate concentration could be predicted by the developed model for all tested experimental conditions. In fact, this developed model predicted very well those concentrations for both hormones E1 and E2 and both the TFC-SR2 and NF 270 membranes.

Further work on this model may be performed to understand the physical grounds supporting some of the constants used in the model. For example, the pseudo-first order sorption constant k_f for the feed concentration was experimentally determined by measuring the adsorption rate in static experiments (no pressure applied). The constant was then successfully applied to describe the transient feed concentration in filtration mode. However, for the case of the permeate prediction, the first order rate constant k_{ret}, for example, was determined by fitting the developed model to the isotherm filtration experiments. Further understanding of the physical grounds supporting this constant, leading to the prediction of this parameter instead of obtaining it through a fitting procedure might be useful to obtain a fully predictive model.

The presence of background electrolyte was found to increase the osmotic pressure that had as consequence the decrease of the permeate flux. This permeate flux decrease lowers the initial hormone concentration at the membrane surface, causing a smaller mass adsorbed and a higher retention by the NF membrane. The model developed to predict the transient feed and permeate concentration was validated with good accuracy in the presence of background electrolyte, taking into account the presence of an osmotic pressure. These results show that the presence of background electrolyte only affects the hydrodynamics at the membrane surface. No occurrence of charge shielding or polarity effects take place in the removal of hormones by NF membranes in the presence of background electrolyte.

The previous modelling treated the membranes as black boxes. However, to understand at a more fundamental level the mechanisms of adsorption and retention of hormones by NF membranes it is necessary to study the effect of the membrane characteristics on such mechanisms. In Chapter 6, the effect of the membrane material and pore radius were experimentally studied. It was shown that hormone adsorption is much higher for the polyamide material when compared to any other polymer tested, including polyesters, polysulphone and cellulose.

Furthermore, the bulk of the hormone adsorption on TFC NF membranes was found to occur mainly in the polyamide active layer. These results evidenced that the active layer characteristics, such as pore radius and internal surface area affect the total mass that adsorbs and, consequently, permeates through the

membrane. The larger the pore radius and the more internal surface area the membrane has, the more adsorbs internally. This constitutes a new result, which allowed to conclude that the modelling of the transport of adsorbing hormones through NF membranes require only the characteristics of the active layer.

With the findings from the previous chapters a new transport model for the hormones in NF membranes was developed as described in Chapter 7, allowing understanding the different mechanisms taking place in the transport of such pollutants inside the membrane pores. Despite much debate on the subject, hormones' transport by convection cannot be ignored in NF processes, especially at pressures above 11 bar, commonly used in NF, as was clearly shown in this thesis. Furthermore, the relationship between solute and pore size is most important. The highest the value of the solute to pore radius ratio is, the better the removal will be by steric exclusion. However, this factor is not the only one playing a role in the removal of trace contaminants by NF membranes. The present work showed that the interaction with the membrane polymer may overcome this steric exclusion factor leading to high rates of adsorption. The lower the interaction of trace contaminants with the membrane is, the less will be the hormone partitioned inside the membrane and, therefore, the less will their concentration inside the membrane be. This will cause less hormone to adsorb inside the pores. On the other hand, the more internal surface area the membrane has, the more will adsorb in it and the more will permeate through the membrane.

8.2. Future Work

The sorption numerical model developed provides the hormone concentration profiles inside the membrane by predicting the transient mass adsorbed for a particular membrane. Further work in the model development would be valuable. To start with, it would be important to determine experimentally the parameter χ, which gives the proportion between the mass adsorbed and the freely dissolved hormone concentration. As mentioned in Chapter 7, this parameter cannot be obtained from the filtration isotherm because the membrane is in contact with different concentrations of the hormone rather than a single concentration value,

which is a requirement to determine the constant χ. Furthermore, the model assumes a membrane with perfectly cylindrical pores with an average pore radius, when in reality a pore size distribution exists [315, 316]. The use of a pore size distribution would be an interesting work for the future in order to evaluate its effects on the prediction, as is the usage of pore tortuosity. Another assumption used by the model is that the contaminant is perfectly spherical, when in reality it can have a different shape, such as cylindrical or ellipsoid [317]. Further work on this issue might bring some interesting results. Despite the previous assumptions, which are most common in this type of model, the model developed in this thesis predicts very well the transient mass adsorbed.

Moreover, the work carried out in this thesis has elucidated the mechanisms involved in the removal of adsorbing trace contaminants by NF membranes, where all the relevant parameters involved in the filtration process were taken into account. Once these mechanisms have been established and elucidated, the next step is to pursue understanding of the removal mechanisms of adsorbing trace contaminants in more complex water matrixes, such as the presence of organic matter.

Hormones are known to bind with organic matter [184, 318] which may affect their removal mechanisms by NF and RO membranes. Due to the complexity of the system when organic matter is present, opposite results have been reported in the literature. When NOM is present in solution enhanced retention is generally obtained for trace contaminants [26, 139, 153, 160, 162, 169, 173, 179] due to partitioning of the contaminant into the retained NOM [34, 204]. Agbekodo *et al.* [179] showed that increasing organic carbon concentration from 2 to 2.8 $mg.L^{-1}$ increases pesticide removal from 67% to 90%. However, certain types of NOM, *e.g.* surfactants, are found not to affect trace contaminants retention [25, 153, 173], showing that the nature of NOM plays a fundamental role in NOM-contaminant interaction and consequent retention by the membrane. According to Neale *et al.* [184] estradiol binds less to surfactants because partitioning is expected to occur through weak H-bonding with the hydrophilic surfactant head in contrast with other types of NOM, such as humic acid, which form stronger H-bonding.

Besides the interactions that may occur between the trace contaminants and the organic matter in solution, the occurrence of organic matter fouling or scaling

(*i.e.* inorganic precipitation) will further affect the removal mechanisms of organic trace contaminants. Once again, opposite results on the effect of organic matter fouling can be found in the literature.

Fouling by NOM modifies the membrane surface and pore properties and affects the retention of small compounds [161, 204], and this phenomenon is particularly acute for NF membranes when compared to RO [151]. NOM can block the membrane pores or change the membrane surface properties enhancing contaminant removal by steric exclusion and charge repulsion [33, 34, 149, 151, 152, 168, 173, 185, 319]. A decrease in trace contaminant retention as a consequence of fouling can also occur. NOM adsorption and increase in membrane negative surface charge increases the MWCO of the membrane due to charge repulsion between the functional groups on the membrane [161] and resulting in lower rejection of ionic solutes. Colloidal fouling also causes a decrease in trace contaminants retention by NF and RO membranes [36, 185]. Due to the cake formed on the membrane surface, back diffusion to the feed is hindered, and this hindrance causes accumulation of matter on the membrane surface and consequent diffusion through the membrane polymer [33, 265, 319]. Other types of foulant decrease the membrane surface charge when adsorbed, decreasing the repulsion between the membrane and the trace contaminant [168, 319].

When NOM is present two main trends are found in the trace contaminant adsorption mechanism on membranes. On one hand, higher adsorption of the contaminant is obtained, possibly on both membrane and NOM layer that is formed on the membrane surface [41, 155, 161, 173, 179]. In the case of hydrophobic HA presence for example, it renders the membrane more hydrophobic, enhancing estrone adsorption [41, 173]. Jin *et al.* [173] found that estrone interaction with NOM depends on the NOM specific functional groups, such as the presence of phenolic groups, which enhance estrone retention by partitioning into the NOM, but do not seem to readily affect estrone adsorption on the membrane. On the other hand, a decrease in trace contaminants adsorption also occurs when there is competition between the NOM and the contaminant for adsorbing sites [33, 35, 39, 142, 152, 185, 204]. Competition for adsorption between different trace contaminants also take

place [29, 204] decreasing the retention when compared to a single trace contaminant solution.

Complexity of natural waters renders the removal prediction of trace contaminants difficult due to all the different interactions that take place between the trace contaminant, the compounds in water (*e.g.* NOM) and the membrane. Removal mechanisms are to date poorly understood.

The previous section focused on process parameters. However, another branch of membrane technology is affected by the occurrence of adsorption of trace contaminants by NF and RO membranes: new membrane designs and materials. Understanding the fundamental mechanisms involved in the removal of trace contaminants by NF membranes can lead to the development of new membrane designs capable of avoiding the occurrence of adsorption. As shown in this work, the tighter and thinner the NF membrane active layer is, the less will adsorb and, as a consequence, the less will permeate through. Furthermore, the design of spiral-wound modules with spacers that have a high adsorption capacity for trace contaminants could further be considered. The spacers would minimise the concentration polarisation and, therefore, the adsorption on the membrane, but the adsorption on the spacers might further avoid adsorption on the membrane.

On the other hand, new materials to substitute the polyamide active layer by a different polymeric material that adsorbs very little (such as cellulose or PMMA as shown in this study) would be another possibility to minimise hormones adsorption onto the membranes. These materials however need to comply with certain requirements: have a high permeability [320], be able to endure high pressures and avoid fouling. This clearly shows that more work on the interactions between trace contaminants and different polymeric materials is justified and needed in the near future.

Finally, adsorption onto the membrane polymeric materials presents a few further challenges. Firstly, the accumulation of contaminants on the polymeric membranes poses a risk since the contaminants can desorb from the membrane during operation or cleaning and contaminate the cleaning solution and the permeate line [152, 178, 179]. Furthermore, the membrane cleaning might degrade the membrane polymeric material and affect trace contaminant and inorganic removal by

NF membranes [234, 321, 322]. Secondly, the polymer itself will have adsorbed trace contaminants posing a waste disposal issue [178]. Thirdly, the concentrate will also have considerable trace contaminant concentrations. Issues of waste disposal have recently arisen and very little research on this has been performed [323, 324].

The need to obtain safe drinking water is increasing at an alarming rate, not only due to climate change, independently of its anthropogenic source or other, but also due to the constant human and industrial waste discharged in our natural resources, either ground, water or air. Since water treatment is such an interdisciplinary subject, it has brought together different branches of science, from engineering, to chemistry, to material science, amongst others, in order to solve this pressing problem. More research at fundamental and applied levels is necessary due to the complexity of the problem: there are many different types of water sources with many different types of contaminants (organic trace contaminants, heavy metals, organic matter, etc.) and interactions occurring between them, where they behave differently and finding a sustainable treatment process for all of them is an immense challenge.

REFERENCES

[1] D.W. Kolpin, E.T. Furlong, M.T. Meyer, E.M. Thurman, S.D. Zaugg, L.B. Barber, H.T. Buxton, Pharmaceuticals, hormones, and other organic wastewater contaminants in U.S. streams, 1999-2000: a national reconnaissance, Environmental Science & Technology, 36 (2002) 1202-1211.

[2] R.J. Williams, A.C. Johnson, J.J.L. Smith, R. Kanda, Steroid estrogens profiles along river stretches arising from sewage treatment works discharges, Environmental Science & Technology, 37 (2003) 1744-1750.

[3] M. Clara, B. Strenn, O. Gans, E. Martinez, N. Kreuzinger, H. Kroiss, Removal of selected pharmaceuticals, fragrances and endocrine disrupting compounds in a membrane bioreactor and conventional wastewater treatment plants, Water Research, 39 (2005) 4797-4807.

[4] T. Heberer, Tracking persistent pharmaceutical residues from municipal sewage to drinking water, Journal of Hydrology, 266 (2002) 175-189.

[5] M. Huerta-Fontela, M.T. Galceran, F. Ventura, Stimulatory drugs of abuse in surface waters and their removal in a conventional drinking water treatment plant, Environmental Science & Technology, 42 (2008) 6809-6816.

[6] K. Kümmerer, Antibiotics in the aquatic environment - A review - Part I, Chemosphere, 75 (2009) 417-434.

[7] F.C. Cabello, Heavy use of prophylactic antibiotics in aquaculture: a growing problem for human and animal health and for the environment, Environmental Microbiology, 8 (2006) 1137-1144.

[8] N. Kemper, Veterinary antibiotics in the aquatic and terrestrial environment, Ecological Indicators, 8 (2008) 1-13.

[9] A.K. Sarmah, M.T. Meyer, A.B.A. Boxall, A global perspective on the use, sales, exposure pathways, occurrence, fate and effects of veterinary antibiotics (VAs) in the environment, Chemosphere, 65 (2006) 725-759.

[10] C.G. Daughton, T.A. Ternes, Pharmaceuticals and personal care products in the environment: agents of subtle change? Environmental Health Perspectives, 107 (1999) 907-938.

[11] P.K. Jjemba, Excretion and ecotoxicity of pharmaceutical and personal care products in the environment, Ecotoxicology and Environmental Safety, 63 (2006) 113-130.

[12] B. Kasprzyk-Hordern, R.M. Dinsdale, A.J. Guwy, The occurrence of pharmaceuticals, personal care products, endocrine disruptors and illicit drugs in surface water in South Wales, UK, Water Research, 42 (2008) 3498.

[13] D.J. Ecobichon, Pesticide use in developing countries, Toxicology, 160 (2001) 27-33.

[14] E.C. Voldner, Y.-F. Li, Global usage of selected persistent organochlorines, Science Of The Total Environment, 160-161 (1995) 201-210.

[15] P.C. Abhilash, N. Singh, Pesticide use and application: an Indian scenario, Journal of Hazardous Materials, 165 (2009) 1-12.

[16] G.-G. Ying, R.S. Kookana, Y.-J. Ru, Occurrence and fate of hormone steroids in the environment, Environment International, 28 (2002) 545-551.

[17] A.L. Batt, M.S. Kostich, J.M. Lazorchak, Analysis of ecologically relevant pharmaceuticals in wastewater and surface water using selective solid-phase extraction and UPLC-MS/MS, Analytical Chemistry, 80 (2008) 5021-5030.

[18] M. Rabiet, A. Togola, F. Brissaud, J.-L. Seidel, H. Budzinski, F. Elbaz-Poulichet, Consequences of treated water recycling as regards pharmaceuticals and drugs in surface and ground waters of a medium-sized mediterranean catchment, Environmental Science & Technology, 40 (2006) 5282-5288.

[19] D.M. Fry, Reproductive effects in birds exposed to pesticides and industrial chemicals, Environmental Health Perspectives, 103 (1995) 165-171.

[20] J.P. Sumpter, Endocrine disrupters in the aquatic environment: an overview, Acta Hydrochimica Et Hydrobiologica, 33 (2005) 9-16.

[21] S.A. Ahmed, The immune system as a potential target for environmental estrogens (endocrine disrupters): a new emerging field, Toxicology, 150 (2000) 191-206.

[22] H. Inadera, The immune system as a target for environmental chemicals: xenoestrogens and other compounds, Toxicology Letters, 164 (2006) 191-206.

[23] L.D. Nghiem, A.I. Schäfer, M. Elimelech, Removal of natural hormones by nanofiltration membranes: measurement, modeling, and mechanisms, Environmental Science & Technology, 38 (2004) 1888-1896.

[24] K. Kimura, S. Toshima, G. Amy, Y. Watanabe, Rejection of neutral endocrine disrupting compounds (EDCs) and pharmaceutical active compounds (PhACs) by RO membranes, Journal of Membrane Science, 245 (2004) 71-78.

[25] P. Berg, G. Hagmeyer, R. Gimbel, Removal of pesticides and other micropollutants by nanofiltration, Desalination, 113 (1997) 205-208.

[26] I. Koyuncu, O.A. Arikan, M.R. Wiesner, C. Rice, Removal of hormones and antibiotics by nanofiltration membranes, Journal of Membrane Science, 309 (2008) 94-101.

[27] G. Ducom, C. Cabassud, Interests and limitations of nanofiltration for the removal of volatile organic compounds in drinking water production, Desalination, 124 (1999) 115-123.

[28] K. Kimura, G. Amy, J.E. Drewes, T. Heberer, T.-U. Kim, Y. Watanabe, Rejection of organic micropollutants (disinfection by-products, endocrine disrupting compounds, and pharmaceutically active compounds) by NF/RO membranes, Journal of Membrane Science, 227 (2003) 113-121.

[29] Y. Kiso, Y. Nishimura, T. Kitao, K. Nishimura, Rejection properties of non-phenylic pesticides with nanofiltration membranes, Journal of Membrane Science, 171 (2000) 229-237.

[30] E.S.K. Chian, W.N. Bruce, H.H.P. Fang, Removal of pesticides by reverse osmosis, Environmental Science & Technology, 9 (1975) 52-59.

[31] L.D. Nghiem, Removal of emerging trace organic contaminants by nanofiltration and reverse osmosis, PhD, University of Wollongong, Wollongong, 2005.

[32] A.I. Schäfer, L.D. Nghiem, T.D. Waite, Removal of the natural hormone estrone from aqueous solutions using nanofiltration and reverse osmosis, Environmental Science & Technology, 37 (2003) 182-188.

[33] L.D. Nghiem, D. Vogel, S. Khan, Characterising humic acid fouling of nanofiltration membranes using bisphenol A as a molecular indicator, Water Research, 42 (2008) 4049-4058.
[34] W. Pronk, H. Palmquist, M. Biebow, M. Boller, Nanofiltration for the separation of pharmaceuticals from nutrients in source-separated urine, Water Research, 40 (2006) 1405-1412.
[35] Y. Zhang, C. Causserand, P. Aimar, J.P. Cravedi, Removal of bisphenol A by a nanofiltration membrane in view of drinking water production, Water Research, 40 (2006) 3793-3799.
[36] H.Y. Ng, M. Elimelech, Influence of colloidal fouling on rejection of trace organic contaminants by reverse osmosis, Journal of Membrane Science, 244 (2004) 215-226.
[37] K. Kimura, G. Amy, J. Drewes, Y. Watanabe, Adsorption of hydrophobic compounds onto NF/RO membranes: an artifact leading to overestimation of rejection, Journal of Membrane Science, 221 (2003) 89-101.
[38] A.M. Comerton, R.C. Andrews, D.M. Bagley, P. Yang, Membrane adsorption of endocrine disrupting compounds and pharmaceutically active compounds, Journal of Membrane Science, 303 (2007) 267-277.
[39] Y. Yoon, P. Westerhoff, S.A. Snyder, E.C. Wert, Nanofiltration and ultrafiltration of endocrine disrupting compounds, pharmaceuticals and personal care products, Journal of Membrane Science, 270 (2006) 88-100.
[40] L.D. Nghiem, A.I. Schäfer, M. Elimelech, Role of electrostatic interactions in the retention of pharmaceutically active contaminants by a loose nanofiltration membrane, Journal of Membrane Science, 286 (2006) 52-59.
[41] J.Y. Hu, X. Jin, S.L. Ong, Rejection of estrone by nanofiltration: influence of solution chemistry, Journal of Membrane Science, 302 (2007) 188-196.
[42] C.D. Metcalfe, T.L. Metcalfe, Y. Kiparissis, B.G. Koenig, C. Khan, R.J. Hughes, T.R. Croley, R.E. March, T. Potter, Estrogenic potency of chemicals detected in sewage treatment plant effluents as determined by in vivo assays with Japanese medaka (Oryzias latipes), Environmental Toxicology and Chemistry, 20 (2001) 297-308.
[43] W.M. Deen, Hindered transport of large molecules in liquid-filled pores, AIChE Journal, 33 (1987) 1409-1425.
[44] E. Zuccato, D. Calamari, M. Natangelo, R. Fanelli, Presence of therapeutic drugs in the environment, Lancet, 355 (2000) 1789-1790.
[45] M.M. Schultz, E.T. Furlong, Trace analysis of antidepressant pharmaceuticals and their select degradates in aquatic matrixes by LC/ESI/MS/MS, Analytical Chemistry, 80 (2008) 1756-1762.
[46] W. Körner, U. Bolz, W. Süßmuth, G. Hiller, W. Schuller, V. Hanf, H. Hagenmaier, Input/output balance of estrogenic active compounds in a major municipal sewage plant in Germany, Chemosphere, 40 (2000) 1131-1142.
[47] C. Baronti, R. Curini, G. D'Ascenzo, A. Di Corcia, A. Gentili, R. Samperi, Monitoring natural and synthetic estrogens at activated sludge sewage treatment plants and in a receiving river water, Environmental Science & Technology, 34 (2000) 5059-5066.
[48] A.C. Johnson, J.P. Sumpter, Removal of endocrine-disrupting chemicals in activated sludge treatment works, Environmental Science & Technology, 35 (2001) 4697-4703.

[49] J. Heidler, R.U. Halden, Meta-analysis of mass balances examining chemical fate during wastewater treatment, Environmental Science & Technology, 42 (2008) 6324-6332.

[50] M. Carballa, F. Omil, J.M. Lema, Calculation methods to perform mass balances of micropollutants in sewage treatment plants. Application to pharmaceutical and personal care products (PPCPs), Environmental Science & Technology, 41 (2007) 884-890.

[51] J. Radjenovic, M. Petrovic, D. Barcelo, Analysis of pharmaceuticals in wastewater and removal using a membrane bioreactor, Analytical And Bioanalytical Chemistry, 387 (2007) 1365-1377.

[52] H. Chapman, Removal of endocrine disruptors by tertiary treatments and constructed wetlands in subtropical Australia, Water Science and Technology, 47 (2003) 151-156.

[53] Z.-h. Liu, Y. Kanjo, S. Mizutani, Removal mechanisms for endocrine disrupting compounds (EDCs) in wastewater treatment - physical means, biodegradation, and chemical advanced oxidation: A review, Science Of The Total Environment, 407 (2009) 731-748.

[54] A.C. Johnson, A. Belfroid, A. Di Corcia, Estimating steroid oestrogen inputs into activated sludge treatment works and observations on their removal from the effluent, Science Of The Total Environment, 256 (2000) 163-173.

[55] T.A. Ternes, M. Stumpf, J. Mueller, K. Haberer, R.D. Wilken, M. Servos, Behavior and occurrence of estrogens in municipal sewage treatment plants - I. Investigations in Germany, Canada and Brazil, Science Of The Total Environment, 225 (1999) 81-90.

[56] S. Zorita, L. Mårtensson, L. Mathiasson, Occurrence and removal of pharmaceuticals in a municipal sewage treatment system in the south of Sweden, Science Of The Total Environment, 407 (2009) 2760-2770.

[57] M. Auriol, Y. Filali-Meknassi, R.D. Tyagi, C.D. Adams, R.Y. Surampalli, Endocrine disrupting compounds removal from wastewater, a new challenge, Process Biochemistry, 41 (2006) 525-539.

[58] W.A. Mitch, A.C. Gerecke, D.L. Sedlak, A N-Nitrosodimethylamine (NDMA) precursor analysis for chlorination of water and wastewater, Water Research, 37 (2003) 3733-3741.

[59] W.A. Mitch, J.O. Sharp, R.R. Trussel, R.L. Valentine, L. Alvarez-Cohen, D.L. Sedlak, N-Nitrosodimethylamine (NDMA) as a drinking water contaminant: a review, Environmental Engineering Science, 20 (2003) 389-404.

[60] S.D. Kim, J. Cho, I.S. Kim, B.J. Vanderford, S.A. Snyder, Occurrence and removal of pharmaceuticals and endocrine disruptors in South Korean surface, drinking, and waste waters, Water Research, 41 (2007) 1013-1021.

[61] C. Desbrow, E.J. Routledge, G.C. Brighty, J.P. Sumpter, M. Waldock, Identification of estrogenic chemicals in STW effluent. 1. Chemical fractionation and in vitro biological screening, Environmental Science & Technology, 32 (1998) 1549-1558.

[62] A. Joss, H. Andersen, T. Ternes, P.R. Richle, H. Siegrist, Removal of estrogens in municipal wastewater treatment under aerobic and anaerobic conditions: consequences for plant optimization, Environmental Science & Technology, 38 (2004) 3047-3055.

[63] K. Barel-Cohen, L.S. Shore, M. Shemesh, A. Wenzel, J. Mueller, N. Kronfeld-Schor, Monitoring of natural and synthetic hormones in a polluted river, Journal of Environmental Management, 78 (2006) 16-23.

[64] A.C. Belfroid, A. Van der Horst, A.D. Vethaak, A.J. Schäfer, G.B.J. Rijs, J. Wegener, W.P. Cofino, Analysis and occurrence of estrogenic hormones and their glucuronides in surface water and waste water in The Netherlands, Science Of The Total Environment, 225 (1999) 101-108.

[65] H.M. Kuch, K. Ballschmiter, Determination of endocrine-disrupting phenolic compounds and estrogens in surface and drinking water by HRGC-(NCI)-MS in the picogram per liter range, Environmental Science & Technology, 35 (2001) 3201-3206.

[66] P. Labadie, H.l.n. Budzinski, Determination of steroidal hormone profiles along the Jalle d'Eysines River (near Bordeaux, France), Environmental Science & Technology, 39 (2005) 5113-5120.

[67] S. Cathum, H. Sabik, Determination of steroids and coprostanol in surface water, effluent and mussel using gas chromatography-mass spectrometry, Chromatographia, 53 (2001) S394-S399.

[68] M. Camusso, S. Galassi, D. Vignati, Assessment of river Po sediment quality by micropollutant analysis, Water Research, 36 (2002) 2491-2504.

[69] U. Dmitruk, M. Piaščik, B. Taboryska, J. Dojlido, Persistent organic pollutants (POPs) in bottom sediments of the Vistula River, Poland, CLEAN – Soil, Air, Water, 36 (2008) 222-229.

[70] J. Fu, B. Mai, G. Sheng, G. Zhang, X. Wang, P.a. Peng, X. Xiao, R. Ran, F. Cheng, X. Peng, Z. Wang, U. Wa Tang, Persistent organic pollutants in environment of the Pearl River Delta, China: an overview, Chemosphere, 52 (2003) 1411-1422.

[71] S.J. Kalkhoff, D.W. Kolpin, E.M. Thurman, I. Ferrer, D. Barcelo, Degradation of chloroacetanilide herbicides: the prevalence of sulfonic and oxanilic acid metabolites in Iowa groundwaters and surface waters, Environmental Science & Technology, 32 (1998) 1738-1740.

[72] Z.L. Zhang, H.S. Hong, J.L. Zhou, J. Huang, G. Yu, Fate and assessment of persistent organic pollutants in water and sediment from Minjiang River Estuary, Southeast China, Chemosphere, 52 (2003) 1423-1430.

[73] M.A. Tisseau, N. Fauchon, J. Cavard, T. Vandevelde, Pesticide contamination of water resources: a case study - the rivers in the Paris region, Water Science and Technology, 34 (1996) 147-152.

[74] T.S.S. Dikshith, R.B. Raizada, S.N. Kumar, M.K. Srivastava, S.K. Kulshrestha, U.N. Adholia, Residues of DDT and HCH in major sources of drinking water in Bhopal, India, Bulletin of Environmental Contamination and Toxicology, 45 (1990) 389-393.

[75] A.M. Soto, J.M. Calabro, N.V. Prechtl, A.Y. Yau, E.F. Orlando, A. Daxenberger, A.S. Kolok, L.J. Guillette Jr, B. le Bizec, I.G. Lange, C. Sonnenschein, Androgenic and estrogenic activity in water bodies receiving cattle feedlot effluent in Eastern Nebraska, USA, Environmental Health Perspectives, 112 (2004) 346-352.

[76] T.A. Hanselman, D.A. Graetz, A.C. Wilkie, Manure-borne estrogens as potential environmental contaminants: a review, Environmental Science & Technology, 37 (2003) 5471-5478.

[77] P. Matthiessen, D. Arnold, A.C. Johnson, T.J. Pepper, T.G. Pottinger, K.G.T. Pulman, Contamination of headwater streams in the United Kingdom by oestrogenic hormones from livestock farms, Science Of The Total Environment, 367 (2006) 616-630.

[78] E.P. Kolodziej, T. Harter, D.L. Sedlak, Dairy wastewater, aquaculture, and spawning fish as sources of steroid hormones in the aquatic environment, Environmental Science & Technology, 38 (2004) 6377-6384.

[79] A.K. Sarmah, G.L. Northcott, F.D.L. Leusch, L.A. Tremblay, A survey of endocrine disrupting chemicals (EDCs) in municipal sewage and animal waste effluents in the Waikato region of New Zealand, Science Of The Total Environment, 355 (2006) 135-144.

[80] M. Younes, Specific issues in health risk assessment of endocrine disrupting chemicals and international activities, Chemosphere, 39 (1999) 1253-1257.

[81] C.R. Tyler, S. Jobling, J.P. Sumpter, Endocrine disruption in wildlife: a critical review of the evidence, Critical Reviews in Toxicology, 28 (1998) 319-361.

[82] S.H. Safe, Endocrine disruptors and human health: is there a problem? An update, Environmental Health Perspectives, 108 (2000) 487-493.

[83] S. Jobling, M. Nolan, C.R. Tyler, G. Brighty, J.P. Sumpter, Widespread sexual disruption in wild fish, Environmental Science & Technology, 32 (1998) 2498-2506.

[84] E.J. Routledge, D. Sheahan, C. Desbrow, G.C. Brighty, M. Waldock, J.P. Sumpter, Identification of estrogenic chemicals in STW effluent. 2. In vivo responses in trout and roach, Environmental Science & Technology, 32 (1998) 1559-1565.

[85] L.J. Guillette Jr., T.S. Gross, G.R. Masson, J.M. Matter, H.F. Percival, A.R. Woodward, Developmental abnormalities of the gonad and abnormal sex hormone concentrations in juvenile alligators from contaminated and control lakes in Florida, Environmental Health Perspectives, 102 (1994) 680-688.

[86] S. Jobling, J.P. Sumpter, Detergent components in sewage effluent are weakly oestrogenic to fish: An in vitro study using rainbow trout (Oncorhynchus mykiss) hepatocytes, Aquatic Toxicology, 27 (1993) 361-372.

[87] F. Pomati, S. Castiglioni, E. Zuccato, R. Fanelli, D. Vigetti, C. Rossetti, D. Calamari, Effects of a complex mixture of therapeutic drugs at environmental levels on human embryonic cells, Environmental Science & Technology, 40 (2006) 2442-2447.

[88] J.M. Smeets, I. van Holsteijn, J.P. Giesy, W. Seinen, M. van den Berg, Estrogenic potencies of several environmental pollutants, as determined by vitellogenin induction in a carp hepatocyte assay, Toxicological Sciences, 50 (1999) 206-213.

[89] M. Petrovic, E. Eljarrat, M.J. Lopez de Alda, D. Barceló, Endocrine disrupting compounds and other emerging contaminants in the environment: a survey on new monitoring strategies and occurrence data, Analytical And Bioanalytical Chemistry, 378 (2004) 549-562.

[90] J.P. Sumpter, A.C. Johnson, Lessons from endocrine disruption and their application to other issues concerning trace organics in the aquatic environment, Environmental Science & Technology, 39 (2005) 4321-4332.

[91] J. Gao, L. Liu, X. Liu, J. Lu, H. Zhou, S. Huang, Z. Wang, P.A. Spear, Occurrence and distribution of organochlorine pesticides - lindane, p,p'-DDT, and heptachlor epoxide - in surface water of China, Environment International, 34 (2008) 1097-1103.

[92] A. Verliefde, E. Cornelissen, G. Amy, B. Van der Bruggen, H. van Dijk, Priority organic micropollutants in water sources in Flanders and the Netherlands and assessment of removal possibilities with nanofiltration, Environmental Pollution, 146 (2007) 281-289.

[93] O. Braga, G.A. Smythe, A.I. Schäfer, A.J. Feitz, Steroid estrogens in ocean sediments, Chemosphere, 61 (2005) 827-833.

[94] N. Minh, T. Minh, N. Kajiwara, T. Kunisue, A. Subramanian, H. Iwata, T. Tana, R. Baburajendran, S. Karuppiah, P. Viet, B. Tuyen, S. Tanabe, Contamination by persistent organic pollutants in dumping sites of asian developing countries: implication of emerging pollution sources, Archives of Environmental Contamination and Toxicology, 50 (2006) 474-481.

[95] B. Kasprzyk-Hordern, R.M. Dinsdale, A.J. Guwy, The occurrence of pharmaceuticals, personal care products, endocrine disruptors and illicit drugs in surface water in South Wales, UK, Water Research, 42 (2008) 3498-3518.

[96] T. Agarwal, P. Khillare, V. Shridhar, PAHs contamination in bank sediment of the Yamuna River, Delhi, India, Environmental Monitoring and Assessment, 123 (2006) 151-166.

[97] G.R. Boyd, H. Reemtsma, D.A. Grimm, S. Mitra, Pharmaceuticals and personal care products (PPCPs) in surface and treated waters of Louisiana, USA and Ontario, Canada, Science Of The Total Environment, 311 (2003) 135-149.

[98] G. Bremle, L. Okla, P. Larsson, Uptake of PCBs in fish in a contaminated river system: bioconcentration factors measured in the field, Environmental Science & Technology, 29 (1995) 2010-2015.

[99] R.-a. Doong, Y.-t. Lin, Characterization and distribution of polycyclic aromatic hydrocarbon contaminations in surface sediment and water from Gao-Ping River, Taiwan, Water Research, 38 (2004) 1733-1744.

[100] I.K. Konstantinou, D.G. Hela, T.A. Albanis, The status of pesticide pollution in surface waters (rivers and lakes) of Greece. Part I. Review on occurrence and levels, Environmental Pollution, 141 (2006) 555-570.

[101] J. Japenga, W.J. Wagenaar, W. Salomons, L.D. Lacerda, S.R. Patchineelam, C.M.L. Filho, Organic micropollutants in the Rio de Janeiro coastal region, Brazil, Science Of The Total Environment, 75 (1988) 249-259.

[102] T.I. Moiseenko, N.A. Gashkina, Y.N. Sharova, L.P. Kudryavtseva, Ecotoxicological assessment of water quality and ecosystem health: a case study of the Volga River, Ecotoxicology and Environmental Safety, 71 (2008) 837-850.

[103] J. Rwetabula, F.D. Smedt, M. Rebhun, F. Mwanuzi, Transport of micropollutants and phosphates in Simiyu River (tributary Lake Victoria), Tanzania, The First International Conference on Environmental Science and Technology, New Orleans, Louisiana, USA,2005.

[104] B. Quémerais, C. Lemieux, K.R. Lum, Temporal variation of PCB concentrations in the St. Lawrence river (Canada) and four of its tributaries, Chemosphere, 28 (1994) 947-959.

[105] R.A. van Steenderen, S.J. Theron, A.J. Hassett, The occurrence of organic micropollutants in the Vaal River between Grootdraai Dam and Parys, Water Sa, 13 (1987) 209-214.
[106] Y. Wang, W. Hu, Z. Cao, X. Fu, T. Zhu, Occurrence of endocrine-disrupting compounds in reclaimed water from Tianjin, China, Analytical And Bioanalytical Chemistry, 383 (2005) 857-863.
[107] M. Stumpf, T.A. Ternes, R.-D. Wilken, R. Silvana Vianna, W. Baumann, Polar drug residues in sewage and natural waters in the state of Rio de Janeiro, Brazil, Science Of The Total Environment, 225 (1999) 135-141.
[108] M.J. Focazio, D.W. Kolpin, K.K. Barnes, E.T. Furlong, M.T. Meyer, S.D. Zaugg, L.B. Barber, M.E. Thurman, A national reconnaissance for pharmaceuticals and other organic wastewater contaminants in the United States - II) Untreated drinking water sources, Science Of The Total Environment, 402 (2008) 201-216.
[109] H.-R. Buser, M.D. Muller, N. Theobald, Occurrence of the pharmaceutical drug clofibric acid and the herbicide mecoprop in various Swiss lakes and in the North Sea, Environmental Science & Technology, 32 (1998) 188-192.
[110] C. Tixier, H.P. Singer, S. Oellers, S.R. Muller, Occurrence and fate of carbamazepine, clofibric acid, diclofenac, ibuprofen, ketoprofen, and naproxen in surface waters, Environmental Science & Technology, 37 (2003) 1061-1068.
[111] J. Nogueira, B. Simplício, M. Floréncio, A. Bettencourt, Levels of tributyltin in sediments from Tagus estuary nature reserve, Estuaries and Coasts, 26 (2003) 798-802.
[112] D. Azevedo, E. Gerchon, E.O. dos Reis, Monitoring of pesticides and polycyclic aromatic hydrocarbons in water from Paraíba do Sul River, Brazil, Journal of the Brazilian Chemical Society, 15 (2004) 292-299.
[113] S. Lacorte, P. Viana, M. Guillamon, R. Tauler, T. Vinhas, D. Barcelo, Main findings and conclusions of the implementation of Directive 76/464/CEE concerning the monitoring of organic pollutants in surface waters (Portugal, April 1999–May 2000), Journal of Environmental Monitoring, 3 (2011) 475-482.
[114] A.A. Ansari, I.B. Singh, H.J. Tobschall, Organotin compounds in surface and pore waters of Ganga Plain in the Kanpur-Unnao industrial region, India, Science Of The Total Environment, 223 (1998) 157-166.
[115] C. Turgut, The contamination with organochlorine pesticides and heavy metals in surface water in Küçük Menderes River in Turkey, 2000-2002, Environment International, 29 (2003) 29-32.
[116] G.W. Ware, H.N. Nigg, D.R. Doerge, R. Barra, J.C. Colombo, G. Eguren, N. Gamboa, W.F. Jardim, G. Mendoza, Persistent organic pollutants (POPs) in eastern and western South American countries, in: L.A. Albert, C.P. Gerba, J. Giesy, O. Hutzinger, J.B. Knaak, J.T. Stevens, R.S. Tjeerdema, P. Voogt, G.W. Ware (Eds.) Reviews of Environmental Contamination and Toxicology, Springer New York, 2006.
[117] T.W. Assmuth, T. Strandberg, Ground water contamination at Finnish landfills, Water, Air, & Soil Pollution, 69 (1993) 179-199.
[118] S. Baran, P. Oleszczuk, A. Lesiuk, E. Baranowska, Trace metals and polycyclic aromatic hydrocarbons in surface sediment samples from the

Narew River (Poland), Polish Journal of Environmental Studies, 11 (2002) 299-305.
[119] A. Oren, Z. Aizenshtat, B. Chefetz, Persistent organic pollutants and sedimentary organic matter properties: a case study in the Kishon River, Israel, Environmental Pollution, 141 (2006) 265-274.
[120] K. Booij, M.T.J. Hillebrand, R.F. Nolting, J.v. Ooijen, Nutrients, trace metals, and organic contaminants in Banten Bay, Indonesia, Marine Pollution Bulletin, 42 (2001) 1187-1190.
[121] F. Carvalho, J.-P. Villeneuve, C. Cattini, I. Tolosa, C. Bajet, M. Navarro-Calingacion, Organic contaminants in the marine environment of Manila Bay, Philippines, Archives of Environmental Contamination and Toxicology, 57 (2009) 348-358.
[122] A.J. Jafari, R.P. Abasabad, A. Salehzadeh, Endocrine disrupting contaminants in water resources and sewage in Hamadan City of Iran, Iranian Journal of Environmental Health, Science and Engineering, 6 (2009) 89-96.
[123] O. Mahjoub, M. Leclercq, M. Bachelot, C. Casellas, A. Escande, P. Balaguer, A. Bahri, E. Gomez, H. Fenet, Estrogen, aryl hydrocarbon and pregnane X receptors activities in reclaimed water and irrigated soils in Oued Souhil area (Nabeul, Tunisia), Desalination, 246 (2009) 425-434.
[124] I. Monirith, D. Ueno, S. Takahashi, H. Nakata, A. Sudaryanto, A. Subramanian, S. Karuppiah, A. Ismail, M. Muchtar, J. Zheng, B.J. Richardson, M. Prudente, N.D. Hue, T.S. Tana, A.V. Tkalin, S. Tanabe, Asia-Pacific mussel watch: monitoring contamination of persistent organochlorine compounds in coastal waters of Asian countries, Marine Pollution Bulletin, 46 (2003) 281-300.
[125] J.L. Sericano, T.L. Wade, T.J. Jackson, J.M. Brooks, B.W. Tripp, J.W. Farrington, L.D. Mee, J.W. Readmann, J.P. Villeneuve, E.D. Goldberg, Trace organic contamination in the Americas: an overview of the US national status & trends and the international 'Mussel Watch' programmes, Marine Pollution Bulletin, 31 214-225.
[126] T.M. Williams, J.G. Rees, D. Setiapermana, Metals and trace organic compounds in sediments and waters of Jakarta Bay and the Pulau Seribu complex, Indonesia, Marine Pollution Bulletin, 40 (2000) 277-285.
[127] A.I. Schäfer, A.G. Fane, T.D. Waite, Elsevier, Oxford, 2005.
[128] M. Mulder, Basic Principles of Membrane Technology, 2nd Edition, Kluwer Academic Publishers, Dordrecht, 1996.
[129] A.I. Schäfer, Natural organic matter removal using membranes: principles, performance and cost, CRC Press, Boca Raton, 2001.
[130] C. Anselme, E.P. Jacobs, Ultrafiltration, in: J. Mallevialle, P.E. Odendaal, M.R. Wiesner (Eds.) Water Treatment Membrane Processes, McGraw-Hill, New York, 1996.
[131] J. Manem, R. Sanderson, Membrane bioreactors, in: J. Malleviale, P.E. Odendaal, M.R. Wiesner (Eds.) Water Treatment Membrane Processes, McGraw-Hill, New York, 1996.
[132] P. Aptel, C.A. Buckley, Categories of membrane operations, in: J. Mallevialle, P.E. Odendaal, M.R. Wiesner (Eds.) Water Treatment Membrane Processes, McGraw-Hill, 1996.

[133] A. Higuchi, B.O. Yoon, T. Kaneko, M. Hara, M. Maekawa, T. Nohmi, Separation of endocrine disruptors from aqueous solutions by pervaporation: dioctylphthalate and butylated hydroxytoluene in mineral water, Journal of Applied Polymer Science, 94 (2004) 1737-1742.

[134] A. Higuchi, B.-O. Yoon, T. Asano, K. Nakaegawa, S. Miki, M. Hara, Z. He, I. Pinnau, Separation of endocrine disruptors from aqueous solutions by pervaporation, Journal of Membrane Science, 198 (2002) 311-320.

[135] T.Q. Nguyen, K. Nobe, Extraction of organic contaminants in aqueous solutions by pervaporation, Journal of Membrane Science, 30 (1987) 11-22.

[136] Y. Wu, Y. Kong, J. Liu, J. Zhang, J. Xu, An experimental study on membrane distillation-crystallization for treating waste water in taurine production, Desalination, 80 (1991) 235-242.

[137] J.L. Cartinella, T.Y. Cath, M.T. Flynn, G.C. Miller, K.W. Hunter, A.E. Childress, Removal of natural steroid hormones from wastewater using membrane contactor processes, Environmental Science & Technology, 40 (2006) 7381-7386.

[138] Y. Yoon, P. Westerhoff, S.A. Snyder, E.C. Wert, J. Yoon, Removal of endocrine disrupting compounds and pharmaceuticals by nanofiltration and ultrafiltration membranes, Desalination, 202 (2007) 16-23.

[139] E.C. Devitt, P.C. Ducellier, P. Cote, M.R. Wiesner, Effects of natural organic matter and the raw water matrix on the rejection of atrazine by pressure-driven membranes, Water Research, 32 (1998) 2563-2568.

[140] A.I. Schäfer, M. Mastrup, R.L. Jensen, Particle interactions and removal of trace contaminants from water and wastewaters, Desalination, 147 (2002) 243-250.

[141] S. Chang, T.D. Waite, A.I. Schäfer, A.G. Fane, Adsorption of the endocrine-active compound estrone on microfiltration hollow fiber membranes, Environmental Science & Technology, 37 (2003) 3158-3163.

[142] Y. Yoon, P. Westerhoff, J. Yoon, S.A. Snyder, Removal of 17 β–estradiol and fluoranthene by nanofiltration and ultrafiltration, Journal of Environmental Engineering, 130 (2004) 1460-1467.

[143] S. Lyko, T. Wintgens, T. Melin, Estrogenic trace contaminants in wastewater - possibilities of membrane bioreactor technology, Desalination, 178 (2005) 95-105.

[144] A.I. Schäfer, L.D. Nghiem, N. Oschmann, Bisphenol A retention in the direct ultrafiltration of greywater, Journal of Membrane Science, 283 (2006) 233-243.

[145] S. Hajibabania, A. Verliefde, J.A. McDonald, S.J. Khan, P. Le-Clech, Fate of trace organic compounds during treatment by nanofiltration, Journal of Membrane Science, 373 130.

[146] O. Raff, R.-D. Wilken, Removal of dissolved uranium by nanofiltration, Desalination, 122 (1999) 147-150.

[147] M.J. Rosa, M.N. de Pinho, The role of ultrafiltration and nanofiltration on the minimisation of the environmental impact of bleached pulp effluents, Journal of Membrane Science, 102 (1995) 155-161.

[148] S. Weber, M. Gallenkemper, T. Melin, W. Dott, J. Hollender, Efficiency of nanofiltration for the elimination of steroids from water, Water Science and Technology, 50 (2004) 9-14.

[149] K. Kosutic, D. Dolar, D. Asperger, B. Kunst, Removal of antibiotics from a model wastewater by RO/NF membranes, Separation and Purification Technology, 53 (2007) 244-249.

[150] B. Van der Bruggen, J. Schaep, D. Wilms, C. Vandecasteele, Influence of molecular size, polarity and charge on the retention of organic molecules by nanofiltration, Journal of Membrane Science, 156 (1999) 29-41.

[151] A.M. Comerton, R.C. Andrews, D.M. Bagley, C. Hao, The rejection of endocrine disrupting and pharmaceutically active compounds by NF and RO membranes as a function of compound and water matrix properties, Journal of Membrane Science, 313 (2008) 323-335.

[152] E.A. McCallum, H. Hyung, T.A. Do, C.-H. Huang, J.-H. Kim, Adsorption, desorption, and steady-state removal of 17β-estradiol by nanofiltration membranes, Journal of Membrane Science, 319 (2008) 38-43.

[153] L.D. Nghiem, A. Manis, K. Soldenhoff, A.I. Schäfer, Estrogenic hormone removal from wastewater using NF/RO membranes, Journal of Membrane Science, 242 (2004) 37-45.

[154] L.D. Nghiem, J. McCutcheon, A.I. Schäfer, M. Elimelech, The role of endocrine disrupters in water recycling – risk or mania? Water Science and Technology, 50 (2004) 215-220.

[155] L.D. Nghiem, A.I. Schäfer, T.D. Waite, Adsorption of estrone on nanofiltration and reverse osmosis membranes in water and wastewater treatment, Water Science and Technology, 46 (2002) 265-272.

[156] L.D. Nghiem, A.I. Schäfer, T.D. Waite, Membrane filtration in water recycling: removal of natural hormones, Water Science and Technology: Water Supply, 3 (2003) 155-160.

[157] A.E. Childress, M. Elimelech, Effect of solution chemistry on the surface charge of polymeric reverse osmosis and nanofiltration membranes, Journal of Membrane Science, 119 (1996) 253-268.

[158] M. Elimelech, W.H. Chen, J.J. Waypa, Measuring the zeta (electrokinetic) potential of reverse osmosis membranes by a streaming potential analyzer, Desalination, 95 (1994) 269-286.

[159] L.D. Nghiem, A.I. Schäfer, M. Elimelech, Pharmaceutical retention mechanisms by nanofiltration membranes, Environmental Science & Technology, 39 (2005) 7698-7705.

[160] L.D. Nghiem, A.I. Schäfer, M. Elimelech, Nanofiltration of hormone mimicking trace organic contaminants, Separation Science and Technology, 40 (2005) 2633-2649.

[161] P. Xu, J.E. Drewes, T.-U. Kim, C. Bellona, G. Amy, Effect of membrane fouling on transport of organic contaminants in NF/RO membrane applications, Journal of Membrane Science, 279 (2006) 165-175.

[162] P. Xu, J.E. Drewes, C. Bellona, G. Amy, T.-U. Kim, M. Adam, T. Heberer, Rejection of emerging organic micropollutants in nanofiltration/reverse osmosis membrane applications, Water Environment Research, 77 (2005) 40-48.

[163] C. Bellona, J.E. Drewes, The role of membrane surface charge and solute physico-chemical properties in the rejection of organic acids by NF membranes, Journal of Membrane Science, 249 (2005) 227-234.

[164] A. Seidel, J.J. Waypa, M. Elimelech, Role of charge (Donnan) exclusion in removal of arsenic from water by a negatively charged porous nanofiltration membrane, Environmental Engineering Science, 18 (2001) 105-113.
[165] A.L. Ahmad, L.S. Tan, S.R. Abd. Shukor, The role of pH in nanofiltration of atrazine and dimethoate from aqueous solution, Journal of Hazardous Materials, 154 (2008) 633-638.
[166] A. Favre-Reguillon, G. Lebuzit, J. Foos, A. Guy, M. Draye, M. Lemaire, Selective concentration of uranium from seawater by nanofiltration, Industrial & Engineering Chemistry Research, 42 (2003) 5900-5904.
[167] A. Favre-Reguillon, G. Lebuzit, D. Murat, J. Foos, C. Mansour, M. Draye, Selective removal of dissolved uranium in drinking water by nanofiltration, Water Research, 42 (2008) 1160-1166.
[168] S.G.J. Heijman, A.R.D. Verleifde, E.R. Cornelissen, G. Amy, J.C. van Dijk, Influence of natural organic matter (NOM) fouling on the removal of pharmaceuticals by nanofiltration and activated carbon filtration, Water Science and Technology: Water Supply, 7 (2007) 17-23.
[169] J. Radjenovic, M. Petrovic, F. Ventura, D. Barceló, Rejection of pharmaceuticals in nanofiltration and reverse osmosis membrane drinking water treatment, Water Research, 42 (2008) 3601-3610.
[170] B. Van der Bruggen, J. Schaep, W. Maes, D. Wilms, C. Vandecasteele, Nanofiltration as a treatment method for the removal of pesticides from groundwaters, Desalination, 117 (1998) 139-147.
[171] M. Gallenkemper, T. Wintgens, T. Melin, Nanofiltration of endocrine disrupting compounds, Water Science and Technology: Water Supply, 3 (2003) 321-327.
[172] L.D. Nghiem, A.I. Schäfer, Adsorption and transport of trace contaminant estrone in NF/RO membranes, Environmental Engineering Science, 19 (2002) 441-451.
[173] X. Jin, J. Hu, S.L. Ong, Influence of dissolved organic matter on estrone removal by NF membranes and the role of their structures, Water Research, 41 (2007) 3077-3088.
[174] V. Yangali-Quintanilla, A. Sadmani, M. McConville, M. Kennedy, G. Amy, A QSAR model for predicting rejection of emerging contaminants (pharmaceuticals, endocrine disruptors) by nanofiltration membranes, Water Research, 44 (2010) 373-384.
[175] E. Steinle-Darling, E. Litwiller, M. Reinhard, Effects of sorption on the rejection of trace organic contaminants during nanofiltration, Environmental Science & Technology, 44 (2010) 2592-2598.
[176] E.R. Cornelissen, J. Verdouw, A.J. Gijsbertsen-Abrahamse, J.A.M.H. Hofman, A nanofiltration retention model for trace contaminants in drinking water sources, Desalination, 178 (2005) 179-192.
[177] A.R.D. Verliefde, S.G.J. Heijman, E.R. Cornelissen, G. Amy, B. Van der Bruggen, J.C. van Dijk, Influence of electrostatic interactions on the rejection with NF and assessment of the removal efficiency during NF/GAC treatment of pharmaceutically active compounds in surface water, Water Research, 41 (2007) 3227-3240.

[178] L.D. Nghiem, A.I. Schäfer, Critical risk points of nanofiltration and reverse osmosis processes in water recycling applications, Desalination, 187 (2006) 303-312.
[179] K.M. Agbekodo, B. Legube, S. Dard, Atrazine and simazine removal mechanisms by nanofiltration: influence of natural organic matter concentration, Water Research, 30 (1996) 2535-2542.
[180] J.H. Kwon, H. Liljestrand, L.E. Katz, Partitioning of moderately hydrophobic endocrine disruptors between water and synthetic membrane vesicles, Environmental Toxicology and Chemistry, 25 (2006) 1984-1992.
[181] T.A. Ternes, A. Joss, Human Pharmaceuticals, Hormones and Fragrances: the Challenge of Micropollutants in Urban Water Management, IWA, London, 2006.
[182] C. Hansch, A. Leo, D. Hoekman, Exploring QSAR: hydrophobic, electronic, and steric constants, American Chemical Society, Washington, DC., 1995.
[183] C. Kubli-Garfias, Comparative study of the electronic structure of estradiol, epiestradiol and estrone by ab initio theory, Journal of Molecular Structure: THEOCHEM, 452 (1998) 175-183.
[184] P.A. Neale, B.I. Escher, A.I. Schäfer, Quantification of solute-solute interactions using negligible-depletion solid-phase microextraction: measuring the affinity of estradiol to bulk organic matter, Environmental Science & Technology, 42 (2008) 2886-2892.
[185] L.D. Nghiem, P.J. Coleman, NF/RO filtration of the hydrophobic ionogenic compound triclosan: transport mechanisms and the influence of membrane fouling, Separation and Purification Technology, 62 (2008) 709-716.
[186] F.J. Benítez, J.L. Acero, F.J. Real, C. García, Nanofiltration processes applied to the removal of phenyl-ureas in natural waters, Journal of Hazardous Materials, 165 (2009) 714.
[187] K. Goss, P. Schwarzenbach, Rules of thumb for assessing equilibrium partitioning of organic compounds: successes and pitfalls, Journal of Chemical Education, 80 (2003) 450-455.
[188] M. Dudziak, M. Bodzek, Selected factors affecting the elimination of hormones from water using nanofiltration, Desalination, 240 (2009) 236-243.
[189] I. Ikeda, Y. Tomari, M. Sugano, Interrelated Effects of Dietary Fiber and Fat on Lymphatic Cholesterol and Triglyceride Absorption in Rats, Journal of Nutrition, 119 (1989) 1383-1387.
[190] O.E. Sundaravalli, K.S. Shurpalekar, M.N. Rao, Effects of dietary cellulose supplements on the body composition and cholesterol metabolism of albino rats, Journal of Agriculture Food Cehmistry, 19 (1971) 116-118.
[191] P.A. Neale, Influence of solute-solute interactions on membrane filtration, University of Edinburgh, Edinburgh, 2009.
[192] M.E. Williams, J.A. Hestekin, C.N. Smothers, D. Bhattacharyya, Separation of organic pollutants by reverse osmosis and nanofiltration membranes: mathematical models and experimental verification, Industrial & Engineering Chemistry Research, 38 (1999) 3683-3695.
[193] K.S. Spiegler, O. Kedem, Thermodynamics of hyperfiltration (reverse osmosis): criteria for efficient membranes, Desalination, 1 (1966) 311-326.

[194] N.A. Peppas, D.L. Meadows, Macromolecular structure and solute diffusion in membranes: an overview of recent theories, Journal of Membrane Science, 16 (1983) 361-377.
[195] J.G.A. Bitter, Transport Mechanisms in Membrane Separation Processes, Plenum Press, New York, 1991.
[196] W.R. Bowen, J.S. Welfoot, Modelling the performance of nanofiltration membranes, in: A.I. Schäfer, A.G. Fane, T.D. Waite (Eds.) Nanofiltration: Principles and Applications, Elsevier, Oxford, 2005.
[197] W.R. Bowen, A.W. Mohammad, N. Hilal, Characterisation of nanofiltration membranes for predictive purposes - use of salts, uncharged solutes and atomic force microscopy, Journal of Membrane Science, 126 (1997) 91-105.
[198] C. Combe, C. Guizard, P. Aimar, V. Sanchez, Experimental determination of four characteristics used to predict the retention of a ceramic nanofiltration membrane, Journal of Membrane Science, 129 (1997) 147-160.
[199] M.N. de Pinho, V. Semião, V. Geraldes, Integrated modeling of transport processes in fluid/nanofiltration membrane systems, Journal of Membrane Science, 206 (2002) 189-200.
[200] F.J. Benitez, J.L. Acero, F.J. Real, C. Garcia, Removal of phenyl-urea herbicides in ultrapure water by ultrafiltration and nanofiltration processes, Water Research, 43 (2009) 267-276.
[201] M.A. Zazouli, H. Susanto, S. Nasseri, M. Ulbricht, Influences of solution chemistry and polymeric natural organic matter on the removal of aquatic pharmaceutical residuals by nanofiltration, Water Research, 43 (2009) 3270-3280.
[202] W.R. Bowen, H. Mukhtar, Characterisation and prediction of separation performance of nanofiltration membranes, Journal of Membrane Science, 112 (1996) 263-274.
[203] L. Braeken, B. Van der Bruggen, C. Vandecasteele, Flux decline in nanofiltration due to adsorption of dissolved organic compounds: model prediction of time dependency, The Journal of Physical Chemistry B, 110 (2006) 2957-2962.
[204] K.V. Plakas, A.J. Karabelas, T. Wintgens, T. Melin, A study of selected herbicides retention by nanofiltration membranes - the role of organic fouling, Journal of Membrane Science, 284 (2006) 291-300.
[205] E. Steinle-Darling, Rejection of trace organics - nitrosamines, perfluorochemicals, and others - via reverse osmosis and nanofiltration, PhD, Stanford University, Palo Alto, 2008.
[206] V. Yangali-Quintanilla, A. Sadmani, M. McConville, M. Kennedy, G. Amy, Rejection of pharmaceutically active compounds and endocrine disrupting compounds by clean and fouled nanofiltration membranes, Water Research, 43 (2009) 2349-2362.
[207] L. Braeken, K. Boussu, B. Van der Bruggen, C. Vandecasteele, Modeling of the adsorption of organic compounds on polymeric nanofiltration membranes in solutions containing two compounds, ChemPhysChem, 6 (2005) 1606-1612.
[208] B. Cyna, G. Chagneau, G. Bablon, N. Tanghe, Two years of nanofiltration at the Méry-sur-Oise plant, France, Desalination, 147 (2002) 69-75.

[209] C. Ventresque, V. Gisclon, G. Bablon, G. Chagneau, An outstanding feat of modern technology: the Méry-sur-Oise nanofiltration Treatment plant (340,000 m3/d), Desalination, 131 (2000) 1-16.
[210] Sindicat des Eaux d'Ile de France, Bilan de la qualité des eaux brutes, produites et distribuées en 2007, 2007, Accessed on: March 17 2009, http://www.sedif.com/le_sedif/iso_album/bilan_qualite_des_eaux_2007.pdf.
[211] P. Singapore Public Utilities Board, Singapore water reclamation study - expert panel review and findings, 2002, Accessed on: March 17 2009, http://www.pub.gov.sg/newater/AboutNEWater/Documents/review.pdf.
[212] Orange County Water District - Groundwater Authority, Orange County Water District takes a proactive stance on contaminants of concern, 2002, Accessed on: March 17, 2009, http://www.ocwd.com/_html/_pr/_pr02/pr02_0129_dioxane.htm.
[213] C.D.o.P. Health, A brief history of NDMA findings in drinking water, 2006, Accessed on: March 17, 2009, http://www.cdph.ca.gov/certlic/drinkingwater/Pages/NDMAhistory.aspx.
[214] M.H. Plumlee, M. López-Mesas, A. Heidlberger, K.P. Ishida, M. Reinhard, N-nitrosodimethylamine (NDMA) removal by reverse osmosis and UV treatment and analysis via LC-MS/MS, Water Research, 42 (2008) 347-355.
[215] Groundwater Replenishment System, Orange County's historic water factory 21 stops producing highly purified water, 2004, Accessed on: March 17, 2009, http://www.gwrsystem.com/news/releases/040121.html.
[216] Orange County Water District, OCWD set to build advanced water quality assurance laboratory, 2007, Accessed on: March 17, 2009, http://www.ocwd.com/fv-98.aspx.
[217] Sindicat des Eaux d'Ile de France, Rapport annuel, 2007, Accessed on: March 17 2009, http://www.sedif.com/le_sedif/iso_album/sedif_rap_annuel_2007.pdf.
[218] M. Wilf, (1998), Advanced membrane technology for water reclamation, Hydranautics, a Nitto Denko Corporation, Accessed on: May 11 2011, http://www.membranes.com/docs/papers/18_watertech.pdf.
[219] L. Braeken, B. Bettens, K. Boussu, P. Van der Meeren, J. Cocquyt, J. Vermant, B. Van der Bruggen, Transport mechanisms of dissolved organic compounds in aqueous solution during nanofiltration, Journal of Membrane Science, 279 (2006) 311-319.
[220] A.R.D. Verliefde, E.R. Cornelissen, S.G.J. Heijman, J.Q.J.C. Verberk, G.L. Amy, B. Van der Bruggen, J.C. van Dijk, The role of electrostatic interactions on the rejection of organic solutes in aqueous solutions with nanofiltration, Journal of Membrane Science, 322 (2008) 52-66.
[221] J.M. Jackson, D. Landolt, About the mechanism of formation of iron hydroxide fouling layers on reverse osmosis membranes, Desalination, 12 (1973) 361-378.
[222] C. Ventresque, G. Bablon, The integrated nanofiltration system of the Méry-sur-Oise surface water treatment plant (37 mgd), Desalination, 113 (1997) 263-266.
[223] K. Boussu, C. Vandecasteele, B. Van der Bruggen, Relation between membrane characteristics and performance in nanofiltration, Journal of Membrane Science, 310 (2008) 51-65.

[224] A.M. Comerton, R.C. Andrews, D.M. Bagley, The influence of natural organic matter and cations on the rejection of endocrine disrupting and pharmaceutically active compounds by nanofiltration, Water Research, 43 (2009) 613-622.
[225] A.R.D. Verliefde, E.R. Cornelissen, S.G.J. Heijman, I. Petrinic, T. Luxbacher, G.L. Amy, B. Van der Bruggen, J.C. van Dijk, Influence of membrane fouling by (pretreated) surface water on rejection of pharmaceutically active compounds (PhACs) by nanofiltration membranes, Journal of Membrane Science, 330 (2009) 90-103.
[226] F.M. White, Fluid Mechanics, International Student Edition, McGraw-Hill, Tokyo, London, 1979.
[227] R.B. Bird, W.E. Stewart, E.N. Lightfoot, Transport phenomena, John Wiley & Sons, 1960.
[228] V. Geraldes, V. Semião, M.N. de Pinho, Flow and mass transfer modelling of nanofiltration, Journal of Membrane Science, 191 (2001) 109-128.
[229] G. Schock, A. Miquel, Mass transfer and pressure loss in spiral wound modules, Desalination, 64 (1987) 339-352.
[230] N.M. Al-Bastaki, A. Abbas, Improving the permeate flux by unsteady operation of a RO desalination unit, Desalination, 123 (1999) 173-176.
[231] N.M. Al-Bastaki, A. Abbas, Periodic operation of a reverse osmosis water desalination unit, Separation Science and Technology, 33 (1998) 2531-2540.
[232] S. Jacob, M.Y. Jaffrin, Purification of brown cane sugar solutions by ultrafiltration with ceramic membranes: investigation of membrane fouling, Separation Science and Technology, 35 (2000) 989-1010.
[233] K. Boussu, Y. Zhang, J. Cocquyt, P. Van der Meeren, A. Volodin, C. Van Haesendonck, J.A. Martens, B. Van der Bruggen, Characterization of polymeric nanofiltration membranes for systematic analysis of membrane performance, Journal of Membrane Science, 278 (2006) 418-427.
[234] A. Simon, L.D. Nghiem, P. Le-Clech, S.J. Khan, J.E. Drewes, Effects of membrane degradation on the removal of pharmaceutically active compounds (PhACs) by NF/RO filtration processes, Journal of Membrane Science, 340 (2009) 16-25.
[235] D. Norberg, S. Hong, J. Taylor, Y. Zhao, Surface characterization and performance evaluation of commercial fouling resistant low pressure RO membranes, Desalination, 202 (2007) 45-52.
[236] C.Y. Tang, Q.S. Fu, C.S. Criddle, J.O. Leckie, Effect of flux (transmembrane pressure) and membrane properties on fouling and rejection of reverse osmosis and nanofiltration membranes treating perfluorooctane sulfonate containing wastewater, Environmental Science & Technology, 41 (2007) 2008-2014.
[237] Q. Li, M. Elimelech, Synergistic effects in combined fouling of a loose nanofiltration membrane by colloidal materials and natural organic matter, Journal of Membrane Science, 278 (2006) 72-82.
[238] V. Freger, Nanoscale heterogeneity of polyamide membranes formed by interfacial polymerization, Langmuir, 19 (2003) 4791-4797.
[239] C.Y. Tang, Y.-N. Kwon, J.O. Leckie, Probing the nano- and micro-scales of reverse osmosis membranes - a comprehensive characterization of physiochemical properties of uncoated and coated membranes by XPS, TEM,

ATR-FTIR, and streaming potential measurements, Journal of Membrane Science, 287 (2007) 146-156.

[240] J.O. Abitoye, P. Mukherjee, K. Jones, Ion implantation: effect on flux and rejection properties of NF membranes, Environmental Science & Technology, 39 (2005) 6487-6493.

[241] H. Saidani, N.B. Amar, J. Palmeri, A. Deratani, Interplay between the transport of solutes across nanofiltration membranes and the thermal properties of the thin active layer, Langmuir, 26 (2009) 2574-2583.

[242] V. Freger, Swelling and morphology of the skin layer of polyamide composite membranes: an atomic force microscopy study, Environmental Science & Technology, 38 (2004) 3168-3175.

[243] K. Boussu, J.D. Baerdemaeker, C. Dauwe, M. Weber, K. G. Lynn, D. Depla, S. Aldea, I. F. J. Vankelecom, V. Carlo, B.V.d. Bruggen, Physico-chemical characterization of nanofiltration membranes, ChemPhysChem, 8 (2007) 370-379.

[244] M. Mänttäri, T. Pekuri, M. Nyström, NF270, a new membrane having promising characteristics and being suitable for treatment of dilute effluents from the paper industry, Journal of Membrane Science, 242 (2004) 107-116.

[245] S. Polizzi, D. Cristofori, A.J.C. Semião, A.I. Schäfer, Nanofiltration Membrane Characteristics, Journal of Membrane Science, in preparation (2011)

[246] H.M.A. Rossiter, Remote community drinking water supply - mechanisms of uranium retention and adsorption by ultrafiltration, nanofiltration and reverse osmosis, University of Edinburgh, Edinburgh, 2011.

[247] C.Y. Tang, Y.N. Kwon, J.O. Leckie, Characterization of humic acid fouled reverse osmosis and nanofiltration membranes by transmission electron microscopy and streaming potential measurements, Environmental Science & Technology, 41 (2007) 942-949.

[248] E. Worch, Eine neue Gleichung zur Berechnung von Diffusionskoeffizienten gelöster Stoffe, Vom Wasser, 81 (1993) 289-297.

[249] C.W. Lim, S.-i. Fujiwara, F. Yamashita, M. Hashida, Prediction of human skin permeability using a combination of molecular orbital calculations and artificial neural network, Biological & Pharmaceutical Bulletin, 25 (2002) 361-366.

[250] A. Bhandari, Surampalli, R. Y., Adams, C. D., Champagne, P., Ong, S. K., Tyagi, R. D. & Zhang, T. C., Contaminants of Emerging Environmental Concern, ASCE, 2009.

[251] T. Thorsen, H. Fløgstad, (2006), Nanofiltration in drinking water treatment, Techneau, Accessed on: May 2011, http://www.techneau.org/fileadmin/files/Publications/Publications/Deliverables/D5.3.4b.pdf.

[252] A.R.D. Verliefde, E.R. Cornelissen, S.G.J. Heijman, E.M.V. Hoek, G.L. Amy, B.V.d. Bruggen, J.C. van Dijk, Influence of solute-membrane affinity on rejection of uncharged organic solutes by nanofiltration membranes, Environmental Science & Technology, 43 (2009) 2400-2406.

[253] A.R.D. Verliefde, E.R. Cornelissen, S.G.J. Heijman, J.Q.J.C. Verberk, G.L. Amy, B. Van der Bruggen, J.C. van Dijk, Construction and validation of a

full-scale model for rejection of organic micropollutants by NF membranes, Journal of Membrane Science, 339 (2009) 10-20.

[254] V. Uyak, I. Koyuncu, I. Oktem, M. Cakmakci, I. Toroz, Removal of trihalomethanes from drinking water by nanofiltration membranes, Journal of Hazardous Materials, 152 (2008) 789-794.

[255] D. Vogel, A. Simon, A.A. Alturki, B. Bilitewski, W.E. Price, L.D. Nghiem, Effects of fouling and scaling on the retention of trace organic contaminants by a nanofiltration membrane: The role of cake-enhanced concentration polarisation, Separation and Purification Technology, 73 256.

[256] T.-U. Kim, J.E. Drewes, R. Scott Summers, G.L. Amy, Solute transport model for trace organic neutral and charged compounds through nanofiltration and reverse osmosis membranes, Water Research, 41 (2007) 3977-3988.

[257] T.U. Kim, G. Amy, J.E. Drewes, Rejection of trace organic compounds by high-pressure membranes, Water Science and Technology, 51 (2005) 335-344.

[258] S. Lee, G. Amy, J. Cho, Applicability of Sherwood correlations for natural organic matter (NOM) transport in nanofiltration (NF) membranes, Journal of Membrane Science, 240 (2004) 49-65.

[259] V. Geraldes, V. Semiao, M. Norberta de Pinho, The effect on mass transfer of momentum and concentration boundary layers at the entrance region of a slit with a nanofiltration membrane wall, Chemical Engineering Science, 57 (2002) 735-748.

[260] T.W. Kao, C. Park, Experimental investigations of the stability of channel flows. Part 1. Flow of a single liquid in a rectangular channel, Journal of Fluid Mechanics, 43 (1970) 145-164.

[261] V.C. Patel, M.R. Head, Some observations on skin friction and velocity profiles in fully developed pipe and channel flows, Journal of Fluid Mechanics, 38 (1969) 181-201.

[262] A.I. Schäfer, I. Akanyeti, A.J.C. Semião, Micropollutant sorption to membrane polymers: a review of mechanisms for estrogens, Advances in Colloid and Interface Science, doi:10.1016/j.cis.2010.09.006 (2010)

[263] P.A. Neale, B.I. Escher, A.I. Schäfer, pH dependence of steroid hormone-organic matter interactions at environmental concentrations, Science Of The Total Environment, 407 (2009) 1164-1173.

[264] T. Fukuhara, S. Iwasaki, M. Kawashima, O. Shinohara, I. Abe, Adsorbability of estrone and 17 β-estradiol in water onto activated carbon, Water Research, 40 (2006) 241-248.

[265] K.O. Agenson, T. Urase, Change in membrane performance due to organic fouling in nanofiltration (NF)/reverse osmosis (RO) applications, Separation and Purification Technology, 55 (2007) 147-156.

[266] Y.-L. Lin, P.-C. Chiang, E.E. Chang, Removal of small trihalomethane precursors from aqueous solution by nanofiltration, Journal of Hazardous Materials, 146 (2007) 20-29.

[267] A.M. Urmenyi, A.A. Poot, M. Wessling, M.H.V. Mulder, Affinity membranes for hormone removal from aqueous solutions, Journal of Membrane Science, 259 (2005) 91-102.

[268] V. Geraldes, V. Semiao, M. Norberta de Pinho, Concentration polarisation and flow structure within nanofiltration spiral-wound modules with ladder-type spacers, Computers & Structures, 82 (2004) 1561-1568.
[269] S.M. Dal Bosco, R.S. Jimenez, W.A. Carvalho, Removal of toxic metals from wastewater by Brazilian natural scolecite, Journal of Colloid and Interface Science, 281 (2005) 424-431.
[270] Y.-S. Ho, Second-order kinetic model for the sorption of cadmium onto tree fern: a comparison of linear and non-linear methods, Water Research, 40 (2006) 119-125.
[271] Y.S. Ho, G. McKay, The sorption of lead(II) ions on peat, Water Research, 33 (1999) 578-584.
[272] Y.S. Ho, G. McKay, Sorption of dye from aqueous solution by peat, Chemical Engineering Journal, 70 (1998) 115-124.
[273] Y.S. Ho, G. McKay, The kinetics of sorption of basic dyes from aqueous solution by sphagnum moss peat, The Canadian Journal of Chemical Engineering, 76 (1998) 822-827.
[274] Y.S. Ho, G. McKay, Pseudo-second order model for sorption processes, Process Biochemistry, 34 (1999) 451-465.
[275] A.K. Kumar, S.V. Mohan, P.N. Sarma, Sorptive removal of endocrine-disruptive compound (estriol, E3) from aqueous phase by batch and column studies: kinetic and mechanistic evaluation, Journal of Hazardous Materials, 164 (2009) 820-828.
[276] M. Fuerhacker, A. Dürauer, A. Jungbauer, Adsorption isotherms of 17β-estradiol on granular activated carbon (GAC), Chemosphere, 44 (2001) 1573-1579.
[277] Y. Feng, Z. Zhang, P. Gao, H. Su, Y. Yu, N. Ren, Adsorption behavior of EE2 (17 α-ethinylestradiol) onto the inactivated sewage sludge: kinetics, thermodynamics and influence factors, Journal of Hazardous Materials, 175 (2010) 970-976.
[278] E. Steinle-Darling, M. Reinhard, Nanofiltration for trace organic contaminant removal: structure, solution, and membrane fouling effects on the rejection of perfluorochemicals, Environmental Science & Technology, 42 (2008) 5292-5297.
[279] A. Ben-David, S. Bason, J. Jopp, Y. Oren, V. Freger, Partitioning of organic solutes between water and polyamide layer of RO and NF membranes: correlation to rejection, Journal of Membrane Science, 281 (2006) 480-490.
[280] P.A. Neale, A.I. Schäfer, W. Pronk, Influence of pH on losses of analyte estradiol in sample pre-filtration, Environmental Engineering Science, 26 (2009) 1157-1161.
[281] E. Bormashenko, R. Pogreb, G. Whyman, Y. Bormashenko, R. Jager, T. Stein, A. Schechter, D. Aurbach, The reversible giant change in the contact angle on the polysulfone and polyethersulfone films exposed to UV irradiation, Langmuir, 24 (2009) 5977-5980.
[282] A. Fujinami, D. Matsunaka, Y. Shibutani, Water wettability/non-wettability of polymer materials by molecular orbital studies, Polymer, 50 (2009) 716-720.

[283] D. Li, A.W. Neumann, Contact angles on hydrophobic solid surfaces and their interpretation, Journal of Colloid and Interface Science, 148 (1992) 190-200.
[284] A.H. Ellison, W.A. Zisman, Wettability studies on nylon, polyethylene terephthalate and polystyrene, The Journal of Physical Chemistry, 58 (1954) 503-506.
[285] C.W. Extrand, Water Contact Angles and Hysteresis of Polyamide Surfaces, Journal of Colloid and Interface Science, 248 (2002) 136-142.
[286] J. Pieracci, J.V. Crivello, G. Belfort, Photochemical modification of 10 kDa polyethersulfone ultrafiltration membranes for reduction of biofouling, Journal of Membrane Science, 156 (1999) 223-240.
[287] M.D. Duca, C.L. Plosceanu, T. Pop, Surface modifications of polyvinylidene fluoride (PVDF) under rf Ar plasma, Polymer Degradation and Stability, 61 (1998) 65-72.
[288] M. Khayet, J.P.G. Villaluenga, M.P. Godino, J.I. Mengual, B. Seoane, K.C. Khulbe, T. Matsuura, Preparation and application of dense poly(phenylene oxide) membranes in pervaporation, Journal of Colloid and Interface Science, 278 (2004) 410-422.
[289] J.M. Joubert, G.J.R. Krige, K. Borgin, Evidence for a Hydrate of Cellulose from Studies of its Surface Properties, Nature, 184 (1959) 1561-1562.
[290] R.P. Schwarzenbach, P.M. Gschwend, D.M. Imboden, Environmental Organic Chemistry, 2nd Edition, Wiley-Interscience, 2003.
[291] G.M. Loudon, Organic Chemistry, 2nd Edition, The Benjamin/Cummings Publishing Company, Inc., 1988.
[292] J.W. Steed, J.L. Atwood, Supramolecular chemistry, 2nd Edition, Wiley, 2009.
[293] L. Ji, W. Chen, S. Zheng, Z. Xu, D. Zhu, Adsorption of sulfonamide antibiotics to multiwalled carbon nanotubes, Langmuir, 25 (2009) 11608-11613.
[294] M.J. Rosa, M.N. de Pinho, Separation of organic solutes by membrane pressure-driven processes, Journal of Membrane Science, 89 (1994) 235-243.
[295] I. Sutzkover, D. Hasson, R. Semiat, Simple technique for measuring the concentration polarization level in a reverse osmosis system, Desalination, 131 (2000) 117-127.
[296] V. Gekas, B. Hallström, Mass transfer in the membrane concentration polarization layer under turbulent cross flow: I. Critical literature review and adaptation of existing sherwood correlations to membrane operations, Journal of Membrane Science, 30 (1987) 153-170.
[297] H. Uedaira, H. Uedaira, Sugar-water interaction from diffusion measurements, Journal of Solution Chemistry, 14 (1985) 27-34.
[298] H. Uedaira, H. Uedaira, Diffusion coefficients of xylose and maltose in aqueous solution, Bulletin of the Chemical Society of Japan, 42 (1969) 2140-2142.
[299] D.R. Lide, CRC Handbook of Chemistry and Physics, 87th Edition, CRC Press, 2008-2009.
[300] I.M.J.J. van de Ven-Lucassen, P.J.A.M. Kerkhof, Diffusion coefficients of ternary mixtures of water, glucose, and dilute ethanol, methanol, or acetone

by the Taylor dispersion method, Journal of Chemical & Engineering Data, 44 (1998) 93-97.
[301] E.M. Renkin, Filtration, diffusion, and molecular sieving through porous cellulose membranes, Journal of General Physiology, 38 (1954) 225-243.
[302] D.W. Green, R.H. Perry, Perry's Chemical Engineers' Handbook, 8th, 2007.
[303] S.-Y. Kwak, D. Woo Ihm, Use of atomic force microscopy and solid-state NMR spectroscopy to characterize structure-property-performance correlation in high-flux reverse osmosis (RO) membranes, Journal of Membrane Science, 158 (1999) 143-153.
[304] V. Yangali-Quintanilla, A. Verliefde, T.U. Kim, A. Sadmani, M. Kennedy, G. Amy, Artificial neural network models based on QSAR for predicting rejection of neutral organic compounds by polyamide nanofiltration and reverse osmosis membranes, Journal of Membrane Science, 342 (2009) 251-262.
[305] D. Libotean, J. Giralt, R. Rallo, Y. Cohen, F. Giralt, H.F. Ridgway, G. Rodriguez, D. Phipps, Organic compounds passage through RO membranes, Journal of Membrane Science, 313 (2008) 23-43.
[306] W.R. Bowen, A.O. Sharif, Transport through microfiltration membranes - particle hydrodynamics and flux reduction, Journal of Colloid and Interface Science, 168 (1994) 414-421.
[307] W.R. Bowen, A.W. Mohammad, Diafiltration by nanofiltration: prediction and optimization, AIChE Journal, 44 (1998) 1799-1812.
[308] I. Ginzburg, D. d'Humieres, Multireflection boundary conditions for lattice Boltzmann models, Physical Review E, 68 (2003) 066614-066611-066614-066630.
[309] C.-L. Lin, Y.G. Lai, Lattice Boltzmann method on composite grids, Physical Review E, 62 (2000) 2219-2225.
[310] M.B. Reider, J.D. Sterling, Accuracy of discrete-velocity BGK models for the simulation of the incompressible Navier-Stokes equations, Computers and Fluids, 24 (1995) 459-467.
[311] P. Grathwohl, Diffusion in natural porous media - contaminant transport, sorption/desorption and dissolution kinetics, Kluwer Academic Publishers, Dordrecht, 1998.
[312] G.S. Committee, G.R. Forum, N.R. Council, Groundwater Contamination, National Academy Press, Washington D.C., 1984.
[313] C.W. Fetter, Contaminant Hydrogeology, Prentice-Hall, Upper Saddle River, 1992.
[314] R.H. Pletcher, W.J. Mincowycz, E.M. Sparrow, G.E. Schneider, Overview of Basic Numerical Methods, in: W.J. Mincowycz, E.M. Sparrow, G.E. Schneider, R.H. Pletcher (Eds.) Handbook of Numerical Heat Transfer, John Wiley & Sons, New York, 1988.
[315] K. Kosutic, D. Dolar, B. Kunst, On experimental parameters characterizing the reverse osmosis and nanofiltration membranes' active layer, Journal of Membrane Science, 282 (2006) 109-114.
[316] W.R. Bowen, J.S. Welfoot, Modelling of membrane nanofiltration--pore size distribution effects, Chemical Engineering Science, 57 (2002) 1393.
[317] J.L.C. Santos, P. de Beukelaar, I.F.J. Vankelecom, S. Velizarov, J.G. Crespo, Effect of solute geometry and orientation on the rejection of uncharged

compounds by nanofiltration, Separation and Purification Technology, 50 (2006) 122.
[318] H. Yamamoto, H.M. Liljestrand, Y. Shimizu, M. Morita, Effects of physical-chemical characteristics on the sorption of selected endocrine disruptors by dissolved organic matter surrogates, Environmental Science & Technology, 37 (2003) 2646-2657.
[319] L.D. Nghiem, S. Hawkes, Effects of membrane fouling on the nanofiltration of pharmaceutically active compounds (PhACs): mechanisms and role of membrane pore size, Separation and Purification Technology, 57 (2007) 176-184.
[320] A. Ben-David, R. Bernstein, Y. Oren, S. Belfer, C. Dosoretz, V. Freger, Facile surface modification of nanofiltration membranes to target the removal of endocrine-disrupting compounds, Journal of Membrane Science, 357 (2010) 152-159.
[321] G.-D. Kang, C.-J. Gao, W.-D. Chen, X.-M. Jie, Y.-M. Cao, Q. Yuan, Study on hypochlorite degradation of aromatic polyamide reverse osmosis membrane, Journal of Membrane Science, 300 (2007) 165-171.
[322] N.P. Soice, A.C. Maladono, D.Y. Takigawa, A.D. Norman, W.B. Krantz, A.R. Greenberg, Oxidative degradation of polyamide reverse osmosis membranes: Studies of molecular model compounds and selected membranes, Journal of Applied Polymer Science, 90 (2003) 1173-1184.
[323] M.M. Nederlof, J.A.M. van Paassen, R. Jong, Nanofiltration concentrate disposal: experiences in The Netherlands, Desalination, 178 (2005) 303-312.
[324] B. Van der Bruggen, L. Lejon, C. Vandecasteele, Reuse, treatment, and discharge of the concentrate of pressure-driven membrane processes, Environmental Science & Technology, 37 (2003) 3733-3738.